UNIVERSITÀ DEGLI STUDI DI NAPOLI FEDERICO II

DOTTORATO DI RICERCA IN

MEDICINA CLINICA E SPERIMENTALE

CURRICULUM IN SCIENZE ODONTOSTOMATOLOGICHE

XXXV Ciclo
(Anni 2019-2022)

Coordinatore: Prof. Francesco Beguinot

TESI DI DOTTORATO

TECNOLOGIE DIGITALI E MATERIALI CORRELATI IN PROTESI DENTARIA

RELATORE

Chiar.mo Prof. Fernando Zarone

CORRELATORE

Chiar.mo Prof. Roberto Sorrentino

CANDIDATO

Dott. Gennaro Ruggiero

UNIVERSITY OF NAPLES FEDERICO II

PH.D. PROGRAM IN

CLINICAL AND EXPERIMENTAL MEDICINE

CURRICULUM IN ODONTOSTOMATOLOGICAL SCIENCES

XXXV Cycle
(Years 2019-2022)

Chairman: Prof. Francesco Beguinot

PH.D. THESIS

DIGITAL TECHNOLOGIES AND LINKED MATERIALS IN PROSTHODONTICS

TUTOR

Prof. Fernando Zarone

CO-TUTOR

Prof. Roberto Sorrentino

PH.D. STUDENT

Dr. Gennaro Ruggiero

The present thesis was the result of a Ph.D. program attended at the Department of Neurosciences, Reproductive and Odontostomatological Sciences, Division of Prosthodontics and Digital Dentistry, University of Naples “Federico II”, Naples, Italy.

CONTENTS

1. INTRODUCTION

SUMMARY:

1.1 DIGITAL TECHNOLOGY AND LINKED MATERIALS: AN OVERVIEW

Digital dentistry is a rapidly growing field based on advanced technologies to improve the accuracy and efficiency of dental procedures [1]. These technologies include computer-aided design and computer-aided manufacturing (CAD/CAM) systems, 3D imaging, and digital impression systems [2].

The first step in the CAD/CAM process is the image acquisition of the three-dimensional morphology of the dental arches.

The following phase includes the designing process, which will be made by using Computer Aided Design (CAD) software. A wide variety of designs, including copings and fixed partial denture (FPD) frameworks, full anatomical crowns and FPD, inlays, onlays, veneers, etc., may be made.

The last step is defined as "Computer Aided Manufacturing" (CAM). It involves making the restoration into a physical part from the CAD model, which may then go through processing, finishing, and polishing before its delivery [3-4].

The variety of restorations that may now be manufactured by CAD/CAM appears to have no bounds, from simple inlays to fully digitally designed and fabricated complete dentures, study models, implant-related components, orthodontic appliances, braces, retainers, and both basic and elaborate surgical guides [5-6]. Using 3D printing technology, dentists can create appliances that are tailored to the specific shape and alignment of an individual's teeth, resulting in improved comfort and effectiveness [1].

Digital dentistry has also been shown to improve patient communication and education [1, 7]. By using 3D imaging and visualization, dentists can more effectively explain dental conditions and treatment options to patients, leading to better understanding and compliance. In particular, a key aspect of digital dentistry is the ability to share and collaborate on digital dental records and images. With the use of electronic health records (EHRs), dentists can securely access and share patient information with other members of the dental care team, enabling more coordinated and effective treatment [1, 7-8]. In addition, the use of 3D imaging can help dentists identify and diagnose problems earlier, enabling earlier intervention and treatment [1, 7-8].

Nowadays, it is possible to use a full digital workflow from the previsualization of potential surgical and restorative results to the delivery of accurate, biocompatible, and highly esthetic restorations, going to new restorative frontiers and operating with the so-called "virtual patient." [9-11]

In recent years, the field of digital dentistry has seen the development of several materials that are helping to improve the accuracy, efficiency, and affordability of dental care [12-13]. These materials, which are used in a variety of dental applications, are enabling dentists to create more precise and comfortable restorations, as well as streamlining the manufacturing process [12-13].

Intraoral scanners and fabrication systems such as CAD/CAM and 3D printing have enabled for enhancement of advanced metal-free dental materials, giving the opportunity to replace traditional metal frameworks and improving the biomimetic and esthetic results of restorations [9-11]. Additionally, by reinterpreting the surgical method in a more conservative manner, dentists have been able to minimize the biological sacrifice of bone and tooth tissues due to the extraordinary mechanical properties of these new-generation materials [9-11, 14].

Some innovative and advanced materials in digital dentistry are lithium disilicate, zirconia, and zirconia-reinforced lithium silicate, types of ceramic materials that are increasingly being used in digital dentistry [15-16]. These materials offer several advantages over traditional ceramics, making them an increasingly popular choice for dental restorations [15-18].

One of their key advantages is the strength and durability, in particular for zirconia. These materials are much stronger than traditional ceramics, such as porcelain, making they ideal for use in dental restorations [12-14].

Another advantage is their natural-looking appearance. Unlike traditional porcelain-fused-to-metal restorations, monolithic restorations made of these innovative materials have not the typical grey appearance due to the absence of a metal core. This makes they even more useful in the fabrication of crowns and bridges, as they provide a more natural-looking result [12-16].

In addition to the strength and natural-looking appearance, zirconia is also highly biocompatible [17-19].

The development of these manufacturing technologies has allowed to manufacture prostheses using a fully digital workflow [9-11]. In effect, the introduction of novel restorative materials has given the application of advanced technologies (such as CAD/CAM, laser sintering/melting, and

3D printing) a synergistic boost, and these advancements have greatly expanded the clinical options available for prosthetic treatments for both teeth and implants [9-11].

Digital-related materials, such as lithium disilicate, zirconia, and zirconia-reinforced lithium silicate offer several advantages in the field of digital dentistry. Their strength, durability, natural-looking appearance, and biocompatibility make them interesting materials for use in the making of dental restorations.

As technology continues to advance, it is likely that digital dentistry and the related restoration materials will play an even more important role in the practice of dentistry.

References

1. Mangano F, Gandolfi A, Luongo G, Logozzo S. Intraoral scanners in entistry: a review of the current literature. BMC Oral Health 2017;17:149.
2. Schweiger J, Edelhoff D, Güth JF. 3D Printing in Digital Prosthetic Dentistry: An Overview of Recent Developments in Additive Manufacturing. J Clin Med. 2021;10:2010.
3. Ubale D, Uddanwadiker RV. Latest trends in Digital Dentistry : A Review. Int J S Res Sci Engg Tech 2018;4:533-539
4. Duret F, Blouin JL, Duret B. CAD-CAM in dentistry. J Am Dent Assoc 1988;117:715-20.
5. Rekow ED. Digital dentistry: The new state of the art - Is it disruptive or destructive? Dent Mater. 2020;36:9-24.
6. Jabri MA, Wu S, Pan Y, Wang L. An overview on the veracity of intraoral digital scanning system and utilization of iTero scanner for analyzing orthodontic study models both In-Vivo and Ex-Vivo. Niger J Clin Pract. 2021;24:1-7.
7. Bilgin MS, Baytaroğlu EN, Erdem A, Dilber E. A review of computer-aided design/computer-aided manufacture techniques for removable denture fabrication. Eur J Dent. 2016;10:286-291.
8. Janett RS, Yeracaris PP. Electronic Medical Records in the American Health System: challenges and lessons learned. Cien Saude Colet. 2020;25:1293-1304.
9. Spagnuolo G, Sorrentino R. The Role of Digital Devices in Dentistry: Clinical Trends and Scientific Evidences. J Clin Med. 2020;9:1692.
10. Joda T., Zarone F., Ferrari M. The complete digital workflow in fixed prosthodontics: A systematic review. BMC Oral Health. 2017;17:124.
11. Joda T., Ferrari M., Gallucci G.O., Wittneben J.G., Brägger U. Digital technology in fixed implant prosthodontics. Periodontol. 2000. 2017;73:178–192.
12. Sulaiman TA. Materials in digital dentistry-A review. J Esthet Restor Dent. 2020;32:171-181.
13. Blatz MB, Conejo J. The Current State of Chairside Digital Dentistry and Materials. Dent Clin North Am. 2019;63:175-197.
14. Zarone F., Ferrari M., Mangano F.G., Leone R., Sorrentino R. “Digitally Oriented Materials”: Focus on Lithium Disilicate Ceramics. Int. J. Dent. 2016;2016:9840594.
15. Sorrentino R, Ruggiero G, Di Mauro MI, Breschi L, Leuci S, Zarone F. Optical behaviors, surface treatment, adhesion, and clinical indications of zirconia-reinforced lithium silicate (ZLS): A narrative review. J Dent. 2021;112:103722.

16. Zarone F, Ruggiero G, Leone R, Breschi L, Leuci S, Sorrentino R. Zirconia-reinforced lithium silicate (ZLS) mechanical and biological properties: A literature review. J Dent. 2021;109:103661.
17. Zhang Y, Lawn BR. Novel Zirconia Materials in Dentistry. J Dent Res. 2018;97:140-147.
18. Shelar P, Abdolvand H, Butler S. On the behaviour of zirconia-based dental materials: A review. J Mech Behav Biomed Mater. 2021;124:104861.
19. Chopra D, Jayasree A, Guo T, Gulati K, Ivanovski S. Advancing dental implants: Bioactive and therapeutic modifications of zirconia. Bioact Mater. 2021;13:161-178.

1.2 AIMS AND OBJECTIVES

In the present thesis, there are several studies aimed at using intraoral scanner systems on typodonts of a totally edentulous upper jaw. In particular, the digitizations performed with intraoral scanners versus laboratory scanners and the digitizations of impressions in several materials are compared. Furthermore, different scanning strategies with intraoral scanners on an edentulous maxilla were evaluated, and both the role of natural and artificial landmarks were tested. Moreover, there is an excerpt regarding the use of digital technologies for the rehabilitation of jaw defects in maxillofacial patients. Besides, a study comparing two different intraoral scanners in the case of different geometries of subgingival tooth preparation was presented.

Some of the most innovative materials used in prosthodontics and related to the digital workflow are analyzed through several reviews on lithium disilicate, zirconia, and zirconia-reinforced lithium silicate. Besides, there is an experimental study about the exposure of dentin in the case of different tooth preparation geometries for laminate veneers. Also, there is a clinical study regarding cement-retained implant-supported CAD/CAM monolithic zirconia single crowns in posterior areas. In addition, it is possible to find an excerpt from a literature review regarding the procedures to be performed for the management and control of the risk of contagion of COVID-19 during prosthodontics clinical procedures.

.

1.3 PUBLICATIONS AS PART OF THE RESEARCH

The following list of scientific papers were published by the author of the present Ph.D. thesis and are part of it.

1. Zarone F, Di Mauro MI, Ausiello P, Ruggiero G, Sorrentino R. Current status on lithium disilicate and zirconia: a narrative review. BMC Oral Health. 2019 Jul 4;19(1):134. doi: 10.1186/s12903-019-0838-x.

2. Ruggiero G, Bocca N, Magrini G, D'Addona A, Carossa M, Gassino G. Surgical procedures performed to improve the prosthetic prognosis in case of maxillary defects: a review of the literature. J Osseointegr 2019;11(4):519-524. https://doi.org/10.23805/JO.2019.11.03.09

3. Zarone F, Ruggiero G, Di Mauro MI, Spagnuolo G, Ferrari M, Sorrentino R. Accuracy of Three Impression Materials on the Totally Edentulous Maxilla: In Vitro/In Silico Comparative Analysis. Materials 2020;13:515. https://doi.org/10.3390/ma13030515

4. Ruggiero G, Bocca N, Carossa M, Gassino G. Alterations in surgical interventions to improve the prosthetic prognosis in patients with mandibular defects: a review of the literature. J Osseointegr 2020:12(4):161-71. https://doi.org/10.23805/10.23805/JO.2020.12.03.4

5. Zarone F, Ruggiero G, Ferrari M, Mangano F, Joda T, Sorrentino R. Accuracy of a chairside intraoral scanner compared with a laboratory scanner for the completely edentulous maxilla: An in vitro 3-dimensional comparative analysis. J Prosthet Dent 2020;124:767. https://doi.org/10.1016/j.prosdent.2020.07.018

6. Zarone F, Ruggiero G, Ferrari M, Mangano F, Joda T, Sorrentino R. Comparison of different intraoral scanning techniques on the completely edentulous maxilla: An in vitro 3-dimensional comparative analysis. J Prosthet Dent 2020;124:768.https://doi.org/10.1016/j.prosdent.2020.07.017

7. Zarone F, Ruggiero G, Leone R, Breschi L, Leuci S, Sorrentino R. Zirconia-reinforced lithium silicate (ZLS) mechanical and biological properties: A literature review. J Dent. 2021;109:103661. doi: 10.1016/j.jdent.2021.103661

8. Sorrentino R, Ruggiero G, Di Mauro MI, Breschi L, Leuci S, Zarone F. Optical behaviors, surface

treatment, adhesion, and clinical indications of zirconia-reinforced lithium silicate (ZLS): A narrative review. J. Dent. 2021;103722. https://doi.org/10.1016/j.jdent.2021.103722

9. Sorrentino R, Ruggiero G, Leone R, Ferrari M, Zarone F. Area accuracy gradient and artificial markers: a three-dimensional analysis of the accuracy of IOS scans on the completely edentulous upper jaw. J Osseointegr 2021;13(4):S256-S263. https://doi.org/10.23805/JO.2021.13.S04.1

10. Sorrentino R, Ruggiero G, Zarone F. Laser systems for gingival retraction in fixed prosthodontics: A narrative review. J Osseointegr 2022;14(1):1-5. https://doi.org/10.23805/JO.2022.14.9

11. Sorrentino R, Ruggiero G, Borelli B, Barlattani A, Zarone F. Dentin Exposure after Tooth Preparation for Laminate Veneers: A Microscopical Analysis to Evaluate the Influence of Operators' Expertise. Materials. 2022; 15(5):1763. https://doi.org/10.3390/ma15051763.

12. Sorrentino R, Basilicata M, Ruggiero G, Mauro MID, Leone R, Bollero P, Zarone F. A Review on Risk Management of Coronavirus Disease 19 (COVID-19) Infection in Dental Practice: Focus on Prosthodontics and All-Ceramic Materials. Prosthesis.2022; 4(3):338-352. https://doi.org/10.3390/prosthesis4030028

13. Sorrentino R, Ruggiero G, Toska E, Leone R, Zarone F. Clinical Evaluation of Cement-Retained Implant-Supported CAD/CAM Monolithic Zirconia Single Crowns in Posterior Areas: Results of a 6-Year Prospective Clinical Study. Prosthesis 2022;4:383-393. https://doi.org/10.3390/prosthesis4030031

The other studies present in this manuscript, and not included in the list, have not been published yet but are *in press* or *submission* phase as of January 15, 2023.

2. DIGITAL DEVICES IN REMOVABLE PROSTHODONTICS

In the first part of this chapter, the accuracy was compared among 3 different impression materials, such as polyether, polyvinylsiloxane and polysulfide on a completely edentulous maxilla, using an innovative protocol based on a comparison by surfaces between the made impressions and a reference model. To do this, digitizations of the impressions were carried out, then inverted in order to compare each digital surface to the reference model.

Secondly, a comparative analysis was performed between the accuracy of impressions made by traditional procedure, i.e., with polysulphide and impressions made with the use of an intraoral scanner on a totally edentulous maxilla. The aim was to assess if there was a significant difference between the accuracy of the impressions made with the intraoral scanner and the ones made in the traditional way.

In the third phase, in vitro/in silico analyses were performed to identify the most accurate scanning strategy with an intraoral scanner on a completely edentulous maxilla. Moreover, the level of accuracy of the scans was also evaluated in either presence or absence of natural landmarks on the edentulous arches (i.e., absence of palatine rugae and flattened ridges).

A further study presented in the chapter had the aim of evaluating the accuracy gradient of the scans performed with an intraoral scanner, on a totally edentulous maxilla, in order to identify the anatomical areas in which accuracy tends to be less favorable. A comparison was also made between two systems that are based on the use of artificial anatomical landmarks, aimed at increasing the efficiency of the stitching algorithm of intraoral scanners.

Besides, with attention to the totally edentulous maxilla, a further study investigated the influence that different palatal morphologies can have on the accuracy of the scans performed with an intraoral scanner in the case of medium, reduced, and greater depth palatine vaults, either in the presence or absence of palatine wrinkles.

The final part of the chapter is focused on removable prosthetic rehabilitation in the case of patients with congenital and/or acquired jaw defects. Some excerpts from the Author's publications on this topic will be shown, aimed at indicating the status of the art on rehabilitations in patients with either upper or lower jaw defects. Furthermore, the effectiveness of digitization obtained from nuclear magnetic resonance was investigated in order to create a prosthesis for these patients.

SUMMARY:

2.1 *ACCURACY OF THREE IMPRESSION MATERIALS ON THE TOTALLY EDENTULOUS MAXILLA: IN VITRO/IN SILICO COMPARATIVE ANALYSIS*

2.2 *ACCURACY OF A CHAIRSIDE INTRAORAL SCANNER COMPARED WITH A LABORATORY SCANNER FOR THE COMPLETELY EDENTULOUS MAXILLA: AN IN VITRO 3-DIMENSIONAL COMPARATIVE ANALYSIS*

2.3 *COMPARISON OF DIFFERENT INTRAORAL SCANNING TECHNIQUES ON THE COMPLETELY EDENTULOUS MAXILLA: AN IN VITRO 3-DIMENSIONAL COMPARATIVE ANALYSIS*

2.4 *AREA ACCURACY GRADIENT AND ARTIFICIAL MARKERS: A THREE-DIMENSIONAL ANALYSIS OF THE ACCURACY OF IOS SCANS ON THE COMPLETELY EDENTULOUS UPPER JAW*

2.5 *ACCURACY OF INTRAORAL SCANNER SYSTEM ON DIFFERENT PALATAL MORPHOLOGIES FOR THE EDENTULOUS POPULATION: A THREE-DIMENSIONAL ANALYSIS*

2.6 *DIGITAL DEVICES IN MAXILLOFACIAL PROSTHESIS*

2.1 ACCURACY OF THREE IMPRESSION MATERIALS ON THE TOTALLY EDENTULOUS MAXILLA: IN VITRO/IN SILICO COMPARATIVE ANALYSIS

Fernando Zarone, Gennaro Ruggiero, Maria Irene Di Mauro, Gianrico Spagnuolo,
Marco Ferrari and Roberto Sorrentino
Materials 2020, 13, 515

1. Introduction

Edentulism, defined as "the absence or complete loss of all-natural dentition (teeth)" [1], is a debilitating and irreversible condition [2], considered as the "final marker of disease burden for oral health" [3].

To date, the oldest and most widespread treatment of total edentulism is the conventional complete denture [4–6], in which the first operative step is represented by a correct impression procedure [7]. The procedure can be accomplished using different techniques: mucostatic [8], mucocompressive, selective pressure [9], functional [10], and neutral zone impression [11]. Different impression materials have been suggested over time, such as polysulfide, polyvinyl siloxane, irreversible hydrocolloids, zinc-oxide eugenol pastes, and polyethers [7,12,13].

In the last years, there has been growing interest in a full-digital concept of complete dentures focusing on the use of optical impressions in the field of removable prosthodontics [14–18]. The protocol for a digitally produced complete denture starts with the digitization of an edentulous arch that can be performed using intraoral or laboratory scanners. The use of an intraoral scanner (IOS) does not require any physical gypsum model or physical impression. Instead, using a laboratory scanner, it is possible to obtain digitization by scanning the physical gypsum model obtained with a conventional impression procedure or by scanning the physical impression itself. In this last case, the file is reversed to obtain a positive reproduction of the digital model [19].

The present study was aimed at comparing the accuracy of scans obtained by digitizing impressions made with three different impression materials: polysulfide, polyether, and polyvinyl siloxane, on a reference typodont of a totally edentulous maxilla.

The null hypothesis stated that there was no difference between the accuracy obtained by scanning each of the three different impression materials and that of the reference scan.

2. Materials and Methods

2.1. Preparation of the Reference Typodont

A real model of a totally edentulous maxilla, previously obtained from a dental patient, was duplicated using a dedicated silicone material (Elite Double; Zhermack SpA). We created a mold inside which polyurethane resin (PRIMA-DIE; Gerhò SPA) was poured with the purpose of fabricating the reference typodont (RT) (Figure 1).

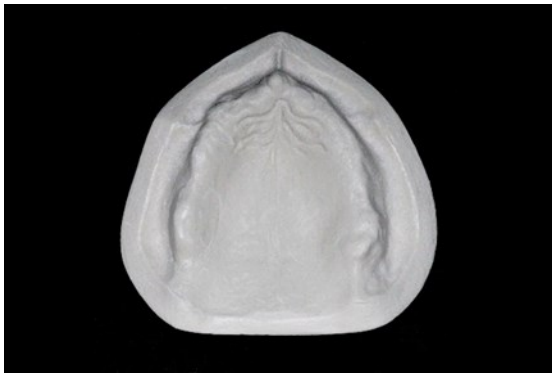

Figure 1. Reference typodont (RT) in polyurethane resin.

A digital reference typodont (dRT) file was obtained and saved in .stl format, scanning the RT with a metrological desktop scanner (Atos Core 80; GOM, Braunschweig, Germany), based on a structured white-light technology, with the following settings: measure accuracy = ± 0.0025 mm, point spacing = 0.03 mm, and working distance = 170 mm.

2.2. Conventional Impression Procedure

Ten impressions were made using each of the three different impression materials (Figure 2): polysulfide (Permlastic Regular body; Kerr, Orange, California, USA), polyether (Impregum Penta medium-bodied; 3M ESPE, Maplewood, Minnesota, USA), and polyvinyl siloxane (Vestige medium; Trayart srl, Padova, Italy), in a standardized and reproducible way. All the impressions were made by the same experienced prosthodontist, during the same morning and in the same room, under similar environmental conditions: temperature of 22 °C, air pressure of 760 ± 5

mmHg, and 45% relative humidity. Five initial impressions were made for each of the three impression materials and then discarded, accomplishing a training session.

(**a**) (**b**) (**c**)

Figure 2. Physical impressions made of: (**a**) polysulfide; (**b**) polyvinyl siloxane; (**c**) polyether.

To get predictable and consistent impression procedures, a custom impression tray was made first by placing a 3.0 mm layer of wax (Tenasyle; Kemdent, Swindon, England) onto the RT, as a spacer between the pre-formed light-curing resin base (ValSax; Capuozzo S.r.l., Naples, Italy) and the RT [20]. The margins of the impression tray were 2 mm short for the bottom of the buccal fornices, according to construction techniques of the custom tray employed for the impression procedure, described in the Passamonti's protocol for the realization of a complete denture [21].

Figure 3. Standardized testing device for impression making.

No handle was made on the impression tray (Figure 3), in that the tray was designed to be secured to a specific tester base using 3 cylinders protruding from the external surface of the tray itself, as reference positioning points. No tissue stops were made because the evenness of impression material thickness was guaranteed by the design and modality of the working of the tester. A duplication silicone (ADDISIL A + B 85; Bartolini Dental Group S.r.l., Terni, Italy) was used to create a mold of the reference tray, inside which a self-curing resin (BI CRYL COLD N A + B; Bartolini Dental Group S.r.l.) was cast to allow the duplication of the reference tray. The

silicone and the resin were then placed in an electronic polymerizer with water at 55 °C and electronically controlled pressure at 5 × 105 Pa for 8 min. Using this method, 30 identical impression trays were fabricated and used after 48 h.

The tester used in this study was a custom-made mechanical precision instrument, made of iron to guarantee precision and consistency of the impression procedures. It had a square support base (side = 17 cm), with 3 holes allowing the fitting of the 3 reference cylinders of the tray, keeping it fixed in a constant and stable position. The metal base supported 4 perpendicular cylinders of 16.5 cm in length and 1.5 cm in diameter, parallel to each other, lubricated with petroleum jelly, thereby allowing an upper, identical metal square plate to slide smoothly onto the base. The upper base had 3 holes through which the typodont could be blocked to its lower surface, on account of 3 passing screws. Four polyvinyl chloride (PVC) tubes of 3.1 cm in length, positioned around the iron cylinders, provided a mechanical stop to leave a 3.0 mm free space between the RT and the tray. A constant, repeatable pressure during impression making of the RT was guaranteed by a weight of 5 kg placed on the upper plate of the tester, aimed at pressing the typodont onto the impression tray containing the impression material (Figure 3).

In this study, the three impression materials were mixed following the instructions provided by the manufacturers. However, it is worth noting that the setting time in the present in vitro test was increased compared to the intra-oral environment, being the impressions made under different temperatures (22 °C) compared to the intra-oral conditions (35–36 °C) [22]. The following timetable was applied for each impression material:

Polysulfide: manual mixing time = 50 s (mixing ratio 1:1); material placement into the tray and impression making = 20 s; removal of the impression tray from the tester = 15 min from the beginning of mixing;

Polyvinyl siloxane: for initial use, a small amount of material was extruded for 5 s and then discarded; the extruded material was deleted, then it was mounted on the mixing tip; auto-mixing (mixing ratio 1:1); material placement into the tray and impression making = 30 s; removal of the impression tray from the tester = 15 min from the beginning of mixing;

Polyether: for initial use, a small amount of material was extruded for 5 s and then discarded; auto-mixing (mixing ratio 5:1, 300 ml of base paste and 60 ml of catalyst paste); material placement into the tray and impression making = 30 s; removal of the impression tray from the tester = 15 min from the beginning of mixing.

All the elastomers were mixed by following the manufacturers' instructions. The polysulfide was mixed manually using a stainless steel spatula on a glass slab; the polyvinyl siloxane was auto-mixed in a dedicated dispenser with two separate equally sized cylinders for the base paste and the

catalyst paste and a mixing tip (Universal manual dispenser; Trayart srl); the polyether was auto-mixed in a motorized mixing device, with two parallel pistons and a mixing tip (Pentamix™ 3 Automatic Mixing Unit; 3M ESPE). After mixing, the polysulfide was applied onto the custom tray with a spatula. Meanwhile, the polyvinyl siloxane and the polyether were applied onto the impression tray directly from the mixing tip. Impressions were removed from typodont by lifting the upper base of the tester from the impression tray. To facilitate this procedure, we created an air gap between the impression material and the typodont by inserting a steel spatula between these two surfaces in the external area beyond the perimeter of the buccal fornices. In this way, the procedure was reproducible without altering the area of the impressions relevant to digital analyses.

2.3. Digitization of the Conventional Impressions

After 30 min, the impressions were removed from the typodont [23], and each of them was eventually scanned using an extraoral laboratory scanner (DScan 3; EGSolutions, Bologna, Italy), employing a structured blue led light. For each experimental group, 10 digital models were obtained using dedicated software (DScan v6.2.2; EGSolutions) after activating the function "Invert Selected Normals" (Figure 4). All the areas needed for the fabrication of a complete maxillary denture was included in the digitization. Three groups of scans were made (n = 10) and respectively named “polysulfide,” “polyvinyl siloxane,” and “polyether.”

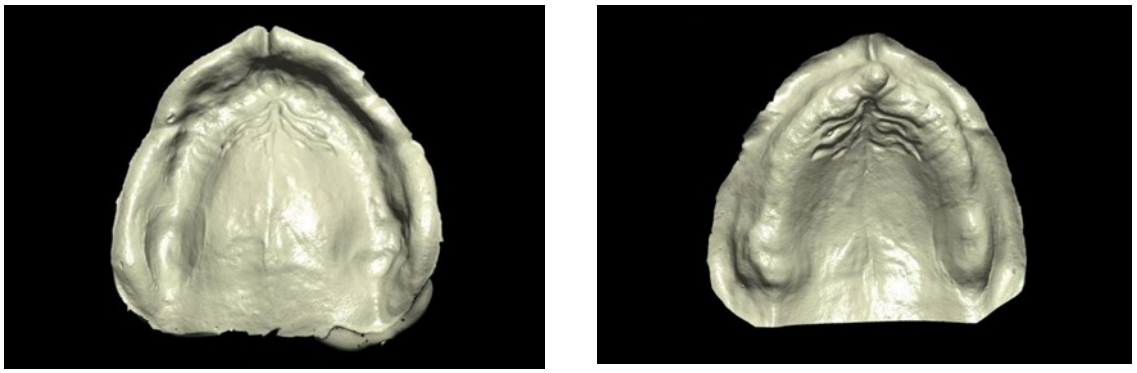

(**a**) (**b**)

Figure 4. (**a**) Scan of a physical impression obtained from the extraoral laboratory scanner; (**b**) Digital model obtained from the inversion of the scan of a physical impression.

2.4. Digital analysis

The .stl files acquired using the extraoral laboratory scanner were imported into a dedicated software (Meshlab v2016.12; ISTI-CNR, Pisa, Italy) using the dRT as a guide for cutting the surplus surfaces of each digital 3D experimental model of the extraoral laboratory scanner. Both the dRT and consequently each digital model was imported into Geomagic Control X (Geomagic Control X v.2018.0.1; 3D SYSTEMS, Morrisville, North Carolina, USA) and then superimposed, choosing the dRT as the software's "reference data" to determine the accuracy for measuring trueness and precision in μm [24].

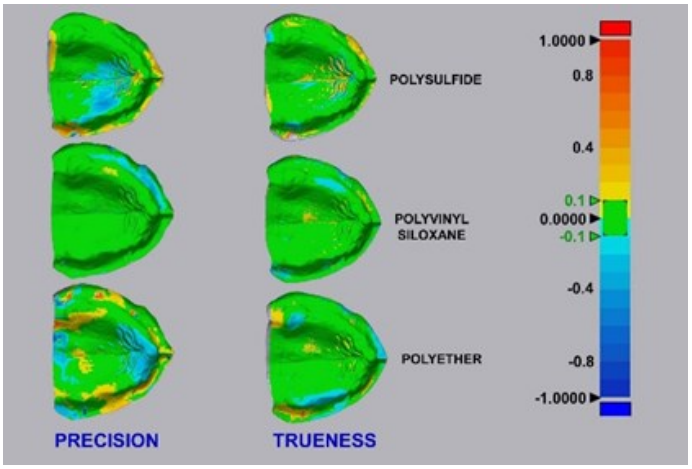

Figure 5. Evaluation of trueness and precision: best superimposition for each group of scans. The green areas indicate a minimum displacement of the digital model compared to the reference data, while red and blue areas indicate an outward and inward displacement between the surfaces, respectively.

An "initial alignment" was done, accompanied by a "best fit alignment," then the "3D comparison" was enabled. The parameters in the "color bar map" were: max/min range = ±1 mm and specific tolerance = ±0.1 mm. Eventually, the standard deviation value (SD) was picked from the "tabular view-3D compare"; where this software-based value (SD) represented the mean of positive and negative deviations resulting from each superimposition between the digital surfaces. For this reason, to determine trueness and precision, the mean between SD values was chosen [25].

A "color map" was generated using this method, for a graphical observation of the displacement between the surfaces of the superimposed digital models. The green areas represent a minimal displacement of ±0.1 mm of the digital model relative to the "reference data," while the red and blue areas show outward and inward displacements of +1 mm and -1 mm, respectively. (Figure 5).

According to ISO-5725, two parameters describe the accuracy of a measurement method: "trueness" and "precision." Trueness refers to the proximity of agreement between the arithmetic mean of a large number of test results and the reference value. Precision describes the proximity of agreement between intra-group data obtained through repetitive measurements [26,27]. In other terms, trueness determines how a measurement relates to the actual value, while precision represents the consistency of repeated measurements.

For each of the 3 experimental groups, the trueness was calculated as the mean (SD) of each model from dRT. The precision was evaluated as the mean (SD) of each 3D surface model from the model that had obtained the best result of trueness in each of the 3 experimental groups, after superimposing on the dRT. Consequently, all the scans of the same group were superimposed on this selected 3D surface model, and the precision of each experimental group was calculated as the mean (SD) resulting from each of these superimpositions [25].

2.5. Statistical Analysis

A dedicated software (IBM SPSS v25; IBM, Armonk, New York, USA) was used to conduct statistical analyses. Both for the analysis of trueness and precision, descriptive statistics (i.e., mean, standard deviation, 95 % confidence interval or CI) and specific tests to determine the overall statistical significance of the differences between the groups ($p = 0.05$).

In particular, the Shapiro–Wilk test was used to check data normality, the Levene test was conducted to evaluate the homogeneity of variances, and the Kruskal-Wallis test was conducted to analyze differences between groups.

3. Results

Concerning trueness, the results are summarized in Table 1 and Figure 6. The mean values were not normally distributed for all the groups of scans, as detected by the Shapiro-Wilk test (p

< 0.05). Levene's test showed that variances were homogeneous (p = 0.272) for the different groups. The Kruskal-Wallis test (p = 0.197) showed no statistically significant differences between the mean values of the three experimental groups. Multiple comparisons were not performed because the overall test did not show significant differences across samples.

Table 1. Descriptive statistics for trueness (µm).

Material scanned	Lower-Upper bound (95% CI)	Mean	Standard Error
polysulfide	121.3–378.5	249.9	56.8531
polyvinyl siloxane	123.1–310.6	216.8	41.4459
polyether	219.9–362.3	291.1	31.4736

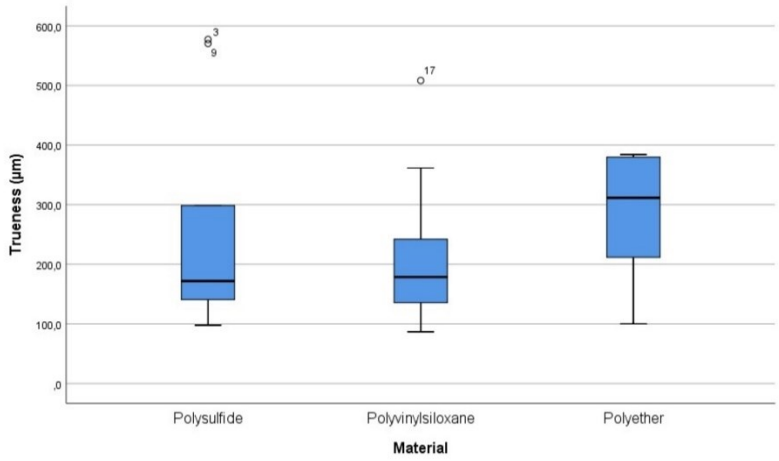

Figure 6. Box plot chart of trueness values. The central rectangle spans the first quartile to the third quartile and whiskers above and below the box show the locations of the minimum and maximum. The segments inside the rectangle shows the median, and unfilled circles represent suspected outliers.

Regarding precision, the results are summarized in Table 2 and Figure 7. The mean values were not normally distributed for all the groups of scans, as detected by the Shapiro-Wilk test (p < 0.05). Levene's test showed that there was no homogeneity of variances (p = 0.033) for the different groups. A log10 transformation of the data was performed to run a one-way ANOVA. This was because the assumptions of normal distribution and homogeneity of variances were violated. After this transformation, the Shapiro-Wilk test detected again a non-normal distribution

($p < 0.05$) while the Levene's test reported homogeneity of the variances ($p = 0.073$). The Kruskal-Wallis test ($p = 0.155$) showed no statistically significant differences between the mean values of the three groups. Multiple comparisons were not performed because the overall test did not show significant differences across samples.

Table 2. Descriptive statistics for precision (µm).

Material scanned	Lower-Upper bound (95% CI)	Mean	Standard Error
polysulfide	108.8–415	261.9	66.4043
polyvinyl siloxane	111.9–306.8	209.4	42.2547
polyether	227.9–338.1	283	23.8969

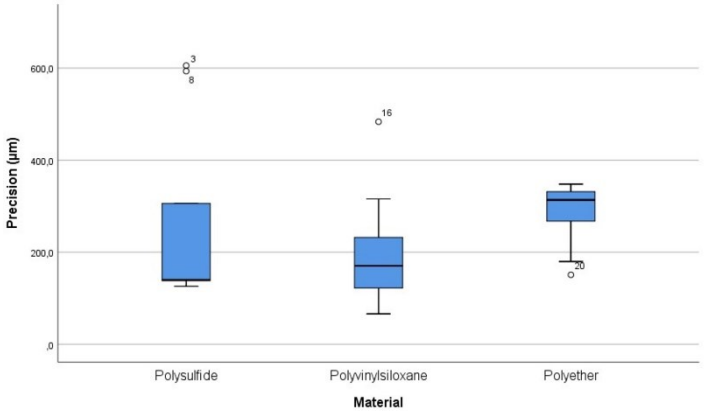

Figure 7. Box plot chart of precision values. The central rectangle spans the first quartile to the third quartile and whiskers above and below the box show the locations of the minimum and maximum. The segments inside the rectangle shows the median, and unfilled circles represent suspected outliers.

The trueness values measured in µm (95% CI) were: polysulfide = 249.9 (121.3–378.5), polyvinyl siloxane = 216.8 (123.1–310.6), polyether = 291.1 (219.9–362.3). The precision values measured in µm (95% CI) were: polysulfide = 261.9 (108.8–415), polyvinyl siloxane = 209.4 (111.9–306.8), polyether = 283 (227.9–338.1).

4. Discussion

Removable complete dentures represent the most frequently used typology of prosthetic treatment of total edentulism [4–6]. One of the most relevant clinical steps in this kind of rehabilitation is the impression making of the edentulous arches [7].

As previously presented in the Introduction, it is possible to make an impression using different techniques: mucostatic [8], mucocompressive, selective pressure [9], functional [10], and neutral zone impressions [11]. In addition, different impression materials can be used, such as polysulfide, polyvinyl siloxane, irreversible hydrocolloids, zinc-oxide eugenol pastes, and polyethers.

Conventionally, study impressions are made using irreversible hydrocolloids and/or impression compounds, using stock trays [7,28]. Conversely, final impressions are made with zinc-oxide eugenol pastes [12] or with elastomers such as polyethers, polyvinyl siloxanes, or polysulfides, to guarantee a good level of precision [7,13]. Some authors [29] described a third step that aimed to make a circumscribed compression of the tissues to improve prosthetic retention, with the addition of a separate layer of zinc-oxide eugenol for the inner seal [19,29].

As reported by Regis et al. [30], a 2-step impression procedure is not mandatory for ensuring clinical success in terms of technical quality, patients' degree of satisfaction, or improvements in oral health-related quality of life and masticatory function [30].

To date, the use of optical impressions in removable prosthodontics derives from a growing interest in a complete digital workflow for the production of complete dentures [14–18]. Although a few anecdotal studies discussed the use of optical impressions on fully edentulous arches [31,32], according to Mangano et al [33], to date the use of IOSs is contraindicated for the fabrication of complete removable dentures. This is due to the absence of reference points and the impossibility of registering soft-tissue dynamics [33].

Compared to the conventional production process for complete dentures, a digital workflow allows different advantages: better prosthetic fit [34–36] and mechanical performance [34]. This is due to a better quality of materials as industrially produced into CAD/CAM blanks, compared to the resin materials pressed into a mold [36] that determine more flaws, porosities, and worse final quality of the base, besides distortions related to materials setting and polymerization shrinkage [34–36]. This process saves money and time [34,37], and provides ease of denture duplication due to the accurate reproducibility of the stored digital data [34].

The protocol for a digitally produced complete denture starts with the digitization of an edentulous arch that can be performed using intraoral or laboratory scanners.

With a laboratory scanner, it is possible to obtain digitization by scanning of the physical gypsum model obtained using a conventional impression procedure or scanning the physical

impression itself. In this last case, the file is reversed to obtain a positive reproduction of the digital model. Both the procedures performed with a laboratory scanner are to be considered “hybrid” as they require a physical impression, while the use of an IOS does not require any physical gypsum model or physical impression [19].

Further in vitro and in vivo studies will be needed to clarify which impression technique, conventional or digital, is the most accurate, in particular, in the treatment of edentulous patients. Significant differences in the accuracy of digitization were found between different IOSs (mean trueness values ranged from 44.1 to 591.8 μm. Mean precision values ranged from 21.6 to 698.0 μm) [38], between IOSs (video IOS = 197 ± 4 μm; still image IOS = 378 ± 11 μm) and laboratory scanners (170 ± 12μm) [39], and between cone-beam computed tomography (CBCT) scanners (without scanner-spray = 1.2 ± 0.3 μm; with scanner-spray = 1.1 ± 0.2 μm.) and laboratory scanners (without scanner-spray = 4.0 ± 0.3 μm; with scanner-spray = 3.0 ± 0.3 μm) [40].

The present study focused on the first step of the production workflow for complete dentures. It was used as model digitization, obtained by a metrological scanner, as a reference to compare the accuracy of different scans of impressions made using three impression materials: polysulfide, polyether, and polyvinyl siloxane on a reference typodont of a totally edentulous maxilla.

Until now, only the study by Nedelcu et al. was performed using in vivo a metrological device, but the obtained reference digitization was limited to the buccal surfaces of maxillary anterior teeth and premolars. This was due to the impossibility to use of such a bulky device to perform deeper intraoral scans or to create impressions of edentulous arches [41]. Furthermore, making impression samples directly in the mouth does not guarantee standardized conditions for impression making for the many variables involved in the environmental conditions of the oral cavity. In particular, temperature, humidity, and resilience of soft tissues.

In the present study, the polyurethane resin was chosen for the reference cast because this material has favorable light diffusion and high mechanical resistance [42].

Polysulfide, polyvinyl siloxane, and polyether are supplied as base and catalyst pastes. Particularly, polysulfides are composed of a base paste containing polysulfide polymer (mercaptan with sulfridyl groups -SH), titanium oxide, zinc, sulfate, copper carbonate or silica and dibutyl phthalate. Meanwhile, the catalyst paste is made up of lead dioxide, hydrated copper oxide or organic peroxide, sulfur, oleic acid, or stearic acid. As for polyvinyl siloxanes, the base paste contains polymethylhydrosiloxane and fillers, while the accelerator incorporates divinyl polymethyl siloxane, other siloxane pre-polymers, platinum salt, and retarder. Regarding polyethers, the base paste is composed of polyether polymer with colloidal silica, glycol ether, or phthalate, while the catalyst paste contains alkyl aromatic sulfonate, filler, and plasticizer [43].

The evaluation of trueness and precision obtained using different digitization's of impressions made in polysulfide, polyether, and polyvinyl siloxane showed that the scans performed directly on the polyvinyl siloxane were more accurate in term of trueness [216.8 (123.1–310.6)] and precision [209.4 (111.9–306.8)] compared to polysulfide [trueness = 249.9 (121.3–378.5); precision = 261.9 (108.8–415)]. Moreover, the polyether showed the worst values of trueness [291.1 (219.9–362.3)] and precision [283 (227.9–338.1)] compared to both the polysulfide and the polyvinyl siloxane. However, it is worth noting that the differences between the means of the experimental groups of scans were not statistically significant. So, it can be inferred that the type of impression material, between the ones tested, did not affect the accuracy of fully edentulous maxilla impressions scanned using a laboratory scanner. This evidence could be explained considering that all three tested materials do not have the physical properties to outperform each other in terms of accuracy on a totally edentulous maxilla.

Polyether is considered favorable for making full-arch impressions in tooth- or implant-supported restorations, and it is a material with a low wetting angle [44]. Compared to polysulfide and polyvinyl siloxane, it shows lower elastic recovery during its removal and high rigidity, together with low flexibility during removal from the oral cavity [7,44–46].

Polysulfide exhibits a low wetting angle, good tear strength, and the best flexibility for removal compared to other tested materials. On the contrary, it has low rigidity and elastic recovery [7,45,46].

Finally, polyvinyl siloxane shows the best elastic recovery, but it has a high wetting angle and low tear strength. Moreover, polyvinyl siloxane is more rigid than polysulfide, but it is less than polyether [7,44–46].

Such physical properties have to be carefully evaluated during clinical procedures, to select the most appropriate impression material according to the presence of anatomical undercuts and mucosal resilience.

To date, the clinically accepted accuracy for impressions to fabricate complete dentures has not been established univocally. However, the maximum compressibility of the supporting soft tissues ranges between 0.5–2.0 mm [47]. Therefore, the accuracy required for complete dentures is lower than that required in fixed prosthodontics, in which marginal fit is inside acceptable clinical parameters below 100 μm [48–50].

The null hypothesis stating that there was no difference between the accuracy obtained by the various scanning of the 3 experimental materials and that of the reference scan was accepted.

The present study had some limitations, mainly due to its mixed in vitro/in silico nature, because this experimental design did not consider relevant factors related to the oral environment. These factors included humidity, temperature, intraoral anatomic limitations, and the

mobility/resilience of soft tissues, affecting the final accuracy of impressions. Further experimental studies involving a larger number of samples should be carried out to shed light on the accuracy of elastomeric impressions on totally edentulous arches.

5. Conclusions

Within the limitations of the present in vitro/in silico comparative study, statistically significant differences were not observed between the accuracy of scans performed on the impressions made of polyvinyl siloxane, polysulfide, and polyether on a fully edentulous maxilla. In this research, the different tested materials did not affect the accuracy of a fully edentulous maxilla impression.

Consequently, all the tested materials are clinically suitable to make precise, accurate, and reliable impressions of the fully edentulous maxilla.

Further, in vitro and in vivo studies, and specifically clinical trials, are needed to validate the results of the present experimentation and identify the most accurate impression material for fully edentulous arches.

References

1. www.encyclopedia.com. Available online: https://www.encyclopedia.com/education/encyclopedias-almanacs-transcripts-and-maps/edentulism (accessed on 3 December 2019).
2. Emami, E.; de Souza, R.F.; Kabawat, M.; Feine, J.S. The impact of edentulism on oral and general health. *Int. J. Dent.* **2013**, *2013*, 498305. doi:10.1155/2013/498305.
3. Cunha-Cruz, J.; Hujoel, P.P.; Nadanovsky, P. Secular trends in socio-economic disparities in edentulism: USA, 1972–2001. *J. Dent. Res*. **2007**, *86*, 131–136.
4. Allen, J. Artificial Dentures. *Am. J. Dent. Sci*. **1860**, *10*, 16–20.
5. Allen, J. Artificial Dentures. *Am. J. Dent. Sci*. **1860**, *10*, 239–242.
6. Lemos, M.M.C.; Zanin, L.; Jorge, M.L.R.; Florio, F.M. Oral health conditions and self-perception among edentulous individuals with different prosthetic status. *Braz. J. Oral Sci*. **2013**, *12*, 5–10.
7. Rameez, M.; Razi, S.S.; Farhan, F.; Kumar, B.; Rashid, H. Clinical implications of elastomeric impression materials used for complete denture construction. *Dent. Med. Res*. **2018**, *6*, 19–23.
8. Page, H.L. Mucostatics—A practical comparison. *TIC* **1947**, *4*, 2–10.
9. Boucher, C.O. Impressions for complete dentures. *J. Am. Dent. Assoc*. **1943**, *30*, 14–25.
10. Boucher, C.O. A critical analysis of mid-century impression techniques for full dentures. *J. Prosthet. Dent.* **1951**, *1*, 472–491.
11. Rashid, H.; Vohra, F.A.; Haidry, T.Z.; Devi, G. Stabilizing mandibular complete dentures using the neutral zone impression technique. *J. Pak. Dent. Assoc*. **2013**, *22*, 154–159.
12. Drago, C.J. A retrospective comparison of two definitive impression techniques and their associated postinsertion adjustments in complete denture prosthodontics. *J. Prosthodont*. **2003**, *12*, 192–197.
13. McCord, J.F.; Grant, A.A. Impression making. *Br. Dent. J*. **2000**, *188*, 484–492.
14. Lee, J.H. Improved digital impressions of edentulous areas. *J. Prosthet. Dent.* **2017**, *117*, 448–449.
15. Fang, J.H.; An, X.; Jeong, S.M.; Choi, B.H. Digital intraoral scanning technique for edentulous jaws. *J. Prosthet. Dent.* **2018**, *119*, 733–735.

16. Goodacre, B.J.; Goodacre, C.J.; Baba, N.Z. Using Intraoral Scanning to Capture Complete Denture Impressions, Tooth Positions, and Centric Relation Records. *Int. J. Prosthodont*. **2018**, *31*, 377–381.

17. Fang, Y.; Fang, J.H.; Jeong, S.M.; Choi, B.H. A Technique for Digital Impression and Bite Registration for a Single Edentulous Arch. *J. Prosthodont*. **2019**, *28*, 519–523.

18. Fang, J.H.; An, X.; Jeong, SM.; Choi, BH. Development of complete dentures based on digital intraoral impressions-Case report. *J. Prosthodont. Res*. **2018**, *62*, 116–120.

19. Chebib, N.; Kalberer, N.; Srinivasan, M.; Maniewicz, S.; Perneger, T.; Müller, F. Edentulous jaw impression techniques: An in vivo comparison of trueness. *J. Prosthet. Dent.* **2019**, *121*, 623–630.

20. Jain, A.R.; Dhanraj, M. A clinical review of spacer design for conventional complete denture. *Biol. Med.* **2016**, *8*, 5.

21. Passamonti, G. Relationship between the two arches and its effect in the diagnosis and treatment of complete denture prosthesis. *Quintessence Int. Dent. Dig*. **1979**, *10*, 37–51.

22. Moore, R.J.; Watts, J.T.; Hood, J.A.; Burritt, D.J. Intra-oral temperature variation over 24 hours. *Eur. J. Orthod*. **1999**, *21*, 249–261.

23. Gonçalves, F.S.; Popoff, D.A.; Castro, C.D.; Silva, G.C.; Magalhães, C.S.; Moreira, A.N. Dimensional stability of elastomeric impression materials: A critical review of the literature. *Eur. J. Prosthodont. Restor. Dent*. **2011**, *19*, 163–166.

24. Mandelli. F.; Gherlone, E.; Gastaldi, G.; Ferrari, M. Evaluation of the accuracy of extraoral laboratory scanners with a single-tooth abutment model: A 3D analysis. *J. Prosth. Res*. **2017**, *61*, 363–370.

25. Imburgia, M.; Logozzo, S.; Hauschild, U.; Veronesi, G.; Mangano, C.; Mangano, F.G. Accuracy of four intraoral scanners in oral implantology: A comparative in vitro study. *BMC Oral Health* **2017**, *17*, 92.

26. International Organization for Standardization. ISO 5725-1;1994. Accuracy (trueness and precision) of measurement methods and results Part 1: General principles and definitions. *Stat. Methods Qual. Control* **1994**, *2*, 9–29.

27. Sim, J.Y.; Jang, Y.; Kim, W.C.; Kim, H.Y.; Lee, D.H.; Kim, J.H. Comparing the accuracy (trueness and precision) of models of fixed dental prostheses fabricated by digital and conventional workflows. *J. Prosthodont. Res.* **2019**, *63*, 25–30.

28. Marino, G.; Canton, A.; Marino, A. *Moderno Trattato di Protesi Mobile Completa*, 1st ed.; Edizioni Martina: Bologna, Italy, 2014; pp. 34–38.

29. Utz, K.H. Abformung zahnloser Kiefer. In *Totalprothesen*, 4th ed.; Koeck, B., Ed.; Elsevier: Munich, Germany, 2005; pp. 57–94.

30. Regis, R.R.; Alves, C.C.; Rocha, S.S.; Negreiros, W.A.; Freitas-Pontes, K.M. The importance of a two-step impression procedure for complete denture fabrication: A systematic review of the literature. *J. Oral Rehabil.* **2016**, *43*, 771–777.

31. Lo Russo, L.; Salamini, A. Removable complete digital dentures: A workflow that integrates open technologies. *J. Prosthet. Dent.* **2018**, *119*, 727–732.

32. Lo Russo, L.; Salamini, A. Single-arch digital removable complete denture: A workflow that starts from the intraoral scan. *J. Prosthet. Dent*. **2018**, *120*, 20–24.

33. Mangano, F.; Gandolfi, A.; Luongo, G.; Logozzo, S. Intraoral scanners in dentistry: A review of the current literature. *BMC Oral Health* **2017**, *17*, 149.

34. Bilgin, M.S.; Baytaroğlu, E.N.; Erdem, A.; Dilber, E. A review of computer-aided design/computer-aided manufacture techniques for removable denture fabrication. *Eur. J. Dent*. **2016**, *10*, 286–291.

35. AlHelal, A.; AlRumaih, H.S.; Kattadiyil, M.T.; Baba, N.Z.; Goodacre, C.J. Comparison of retention between maxillary milled and conventional denture bases: A clinical study. *J. Prosthet. Dent.* **2017**, *117*, 233–238.

36. McLaughlin, J.B.; Ramos, V., Jr.; Dickinson, D.P. Comparison of Fit of Dentures Fabricated by Traditional Techniques Versus CAD/CAM Technology. *J. Prosthodont.* **2019**, *28*, 428–435.

37. Bidra, A.S.; Taylor, T.D.; Agar, J.R. Computer-aided technology for fabricating complete dentures: Systematic review of historical background, current status, and future perspectives. *J. Prosthet. Dent*. **2013**, *109*, 361–366.

38. Patzelt, S.B.; Vonau, S.; Stampf, S.; Att, W. Assessing the feasibility and accuracy of digitizing edentulous jaws. *J. Am. Dent. Assoc.* **2013**, *144*, 914–920.

39. Jeong, I.D.; Lee, J.J.; Jeon, J.H.; Kim, J.H.; Kim, H.Y.; Kim, W.C. Accuracy of complete-arch model using an intraoral video scanner: An in vitro study. *J. Prosthet. Dent.* **2016**, *115*, 755–759.

40. Peng, L.; Chen, L.; Harris, B.T.; Bhandari, B.; Morton, D.; Lin, W.S. Accuracy and reproducibility of virtual edentulous casts created by laboratory impression scan protocols. *J. Prosthet. Dent*. **2018**, *120*, 389–395.

41. Nedelcu, R.; Olsson, P.; Nyström, I.; Rydén, J.; Thor, A. Accuracy and precision of 3 intraoral scanners and accuracy of conventional impressions: A novel in vivo analysis method. *J. Dent.* **2018**, *69*, 110–118.

42. Patzelt, S.B.; Emmanouilidi, A.; Stampf, S.; Strub, J.R.; Att, W. Accuracy of full-arch scans using intraoral scanners. *Clin. Oral Investig.* **2014**, *18*, 1687–1694.

43. Spoto, G. *Materiali e Tecnologie Odontostomatologiche*, 2nd ed.; Ariesdue: Milan, Italy, 2013; pp. 169–174.

44. Craig, R.G.; Robert, G. *Restorative Dental Materials*, 11th ed.; Elsevier: Amsterdam, The Netherlands, 2002; p. 12.

45. Rubel, B.S. Impression materials: A comparative review of impression materials most commonly used in restorative dentistry. *Dent. Clin. North Am*. **2007**, *51*, 629–642.

46. Giordano, R. Impression materials: Basic properties. *Gen. Dent.* **2000**, *48*, 510–516.

47. Marino, G.; Canton, A. *La Protesi Parziale Rimovibile Dalla Teoria Alla Pratica*, 1st ed.; Edizioni Martina: Bologna, Italy, 2002; pp. 6–7.

48. Reich, S.; Gozdowski, S.; Trentzsch, L.; Frankenberger, R.; Lohbauer, U. Marginal fit of heatpressed vs. CAD/CAM processed all-ceramic onlays using a milling unit prototype. *Oper. Dent.* **2008**, *33*, 644–650.

49. Ushiwata, O.; de Moraes, J.V. Method for marginal measurements of restorations: Accessory device for toolmakers microscope. *J. Prosthet. Dent.* **2000**, *83*, 362–366.

50. Heboyan, A.G. Marginal and internal fit of fixed prosthodontic constructions: A literature review. *Int. J. Dent. Res. Rev.* **2019**, *2*, 19.

2.2 ACCURACY OF A CHAIRSIDE INTRAORAL SCANNER COMPARED WITH A LABORATORY SCANNER FOR THE COMPLETELY EDENTULOUS MAXILLA: AN IN VITRO 3-DIMENSIONAL COMPARATIVE ANALYSIS

Zarone Fernando, Ruggiero Gennaro, Ferrari Marco, Mangano Francesco, Joda Tim, Sorrentino Roberto

J Prosthet Dent. 2020;124:761.e1-761.e7

Introduction

Interest in fabricating completely digital complete dentures has focused on the use of intraoral scanners (IOSs), as these may offer faster treatment, better prosthesis fit, and ease of denture duplication.[1] Moreover, the fabrication of completely digital dentures based on computer-aided design and computer-aided manufacturing (CAD-CAM) technology might offer time and cost savings,[1,2] better mechanical performance,[1] optimum prosthetic fit,[1,3,4] and ease of denture duplication and reproduction.[1] Currently laboratory costs are still higher than conventional denture processing by pressing heat-polymerizing resin,[1,2,5] as the resin disks are expensive.

The protocol for a digital complete denture starts by digitizing an edentulous arch; this can be accomplished in different ways.[6-8] A laboratory scanner can be used to obtain a file from a conventional stone cast. Alternatively, the physical impression can be scanned by a laboratory scanner, and then the file reversed to make a positive digital cast.[6-8] A third option is making a digital scan of the edentulous arch with an IOS.[6-12]

Studies on digital procedures for completely edentulous arches are still scarce, in particular with regard to scanning methods, clinical usage, and digitization accuracy. The accuracy of a measurement method is described by trueness and precision.[13] Trueness refers to

the closeness of agreement among the mean of a large number of test results and the reference value; precision describes the closeness of agreement among intragroup data obtained by repetitive measurements.[13,14] Differences in accuracy have been reported among different IOSs,[15] between IOSs and laboratory scanners,[16] and between cone beam computed tomography (CBCT) and laboratory scans.[17]

Conventional elastomeric impression making and stone cast pouring lead to inaccuracy of the definitive cast[18,19] because of the expansion, shrinkage, and distortion of impression materials[20-24] and/or stone casts.[25,26] Additionally, detachment of the impression material from the tray surface during impression removal,[23] transfer to the laboratory,[21] changes in temperature,[21,24] and the influence of disinfection agents[27-30] may also lead to errors. Conversely, the technology of the IOS, the scanning procedure, and the anatomy of the tissues can affect accuracy.[15,31] When a flat and smooth edentulous ridge and palatal vault are scanned, the stitching processing of images or videos can introduce errors because of the lack of anatomic landmarks.[15,31] Accurate border molding and providing a posterior palatal seal are not currently possible when using an IOS because a method of soft tissue displacement is lacking.[7,8,10,12]

The purpose of the present in vitro investigation was to compare the trueness and precision of different intraoral and extraoral scanning approaches on a reference typodont of a completely edentulous maxilla. The null hypothesis was that no difference would be found in trueness and precision among the protocols.

Material and methods

A reference typodont (RT) (Fig. 1) was fabricated by pouring polyurethane resin (PRIMA-DIE; Gerhò S.P.A) into a mold of an edentulous maxilla obtained from a cast used for a clinical purpose and duplicated with a silicone material (Elite Double 8; Zhermack SpA). Polyurethane resin was used because of its high mechanical resistance[32] and optimal light diffusion.[33] The RT was then scanned with a metrological scanner (Atos Core 80; GOM GmbH) based on a structured white-light technology with a working distance=170 mm, point spacing=0.03 mm, and measure accuracy=±2.5 μm to obtain a digital reference typodont (dRT) in standard tessellation language (STL) format.

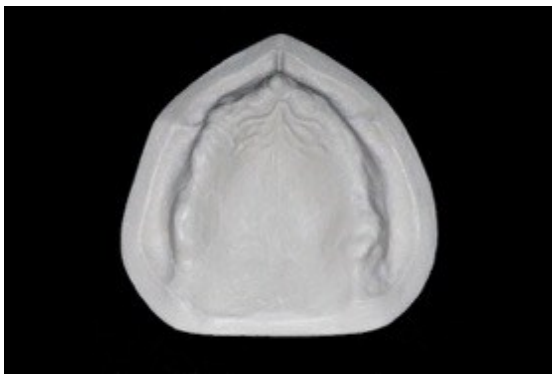

Figure 1. Reference typodont in polyurethane resin.

The RT was scanned by using an IOS (TRIOS 3 Pod; 3Shape A/S) with an accuracy of 6.9 ±0.9 μm. After the calibration procedure of the IOS, 10 initial scans were made as a test and then discarded. Subsequently, 10 digital IOS casts (dIOC) (Fig. 2) were obtained by scanning the RT along the ridge of the arch, starting from the right maxillary tuberosity and ending at the left one and then continuing on the buccal side and finally on the palatal vault with a clockwise movement (Fig. 3). One prosthodontist (G.R.) performed all the scans sequentially with an interval of 10 minutes to rest and allow the IOS to cool.[34,35] The numbers of images per scan varied between 743 and 1126, and the scanning time was between 1 and 2 minutes.

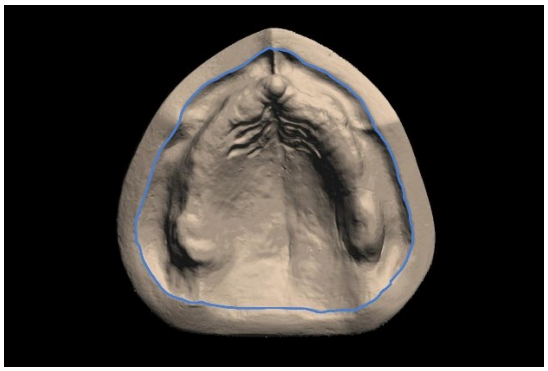

Figure 2. Scan of reference typodont with intraoral scanner. *Blue line* represents border line of specimens for superimposition.

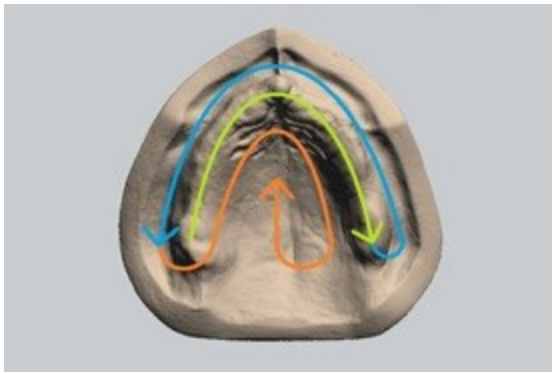

Figure 3. Scanning strategy with intraoral scanner. *Green arrow* indicates top ridge scanning.

Blue arrow indicates scanning strategy of buccal ridge. *Orange arrow* indicates scanning strategy of palatal vault.

Ten conventional polysulfide (Permlastic, regular body; Kerr Corp) impressions of the RT were made in a standardized and reproducible way with a dedicated tester. The solid typodont in polyurethane resin was hydrophobic and had undercuts at the edentulous crests; for these reasons, polysulfide was chosen, as it is hydrophobic, with reduced rigidity and higher tear strength and flexibility during removal than polyether, polyvinyl siloxane, or condensation silicones.[6,36-38] A custom impression tray was made placing a 3-mm layer of wax (Tenasyle; Associated Dental Products Ltd) onto the RT as a spacer between the preformed light-polymerizing resin base (ValSax; Capuozzo S.r.l.) and the RT. The border area of the impression tray was 2 mm short of the buccal vestibule.[39] The tray was border molded with modeling plastic impression compound (ISO Functional Sticks; GC EUROPE A.G.). No handle was designed on the tray because the tray was secured to the tester base with 3 cylinders protruding from the external surface of the tray. The impression trays were replicated with a silicone material (ADDISIL A+B 85; Bartolini Dental Group S.r.l.) poured with an autopolymerizing resin (BI CRYL COLD A+B; Bartolini Dental Group S.r.l.).

The tester was a custom-made, steel mechanical precision device with a square support base. Three holes in the base corresponded to the 3 reference cylinders of the tray. The base supported 4 perpendicular cylinders, allowing the upper plate to slide smoothly onto the base. The upper base had 3 holes to block the typodont to its lower surface with 3 passing screws. The upper plate was loaded (49 N) to lock the typodont to the tray containing the polysulfide. This force was higher than that used clinically (approximately 10 N)[40] but did not compress the impression material because 4 polyvinyl chloride tubes were used as a mechanical stop to provide a 3-mm space. Ten polysulfide impressions were made: manual mixing time=50 seconds (mixing ratio 1:1); placing material into the tray and impression making=60 seconds; removal of the tray from the tester=15 minutes from the beginning of mixing. Since the manufacturer advises pouring an impression between 30 minutes to 8 hours after impression making and polysulfide-based materials are dimensionally stable for up to 12 hours,[41] each impression was scanned with a laboratory extraoral scanner (DScan 3; EGS S.R.L.) using a structured blue light-emitting diode (LED) after 2 hours. Ten digital casts (dREC) were obtained by activating the function “Invert Selected Normals” of a software program (DentalCad 6.2; EGS S.R.L.) (Fig. 4, A,B).

A 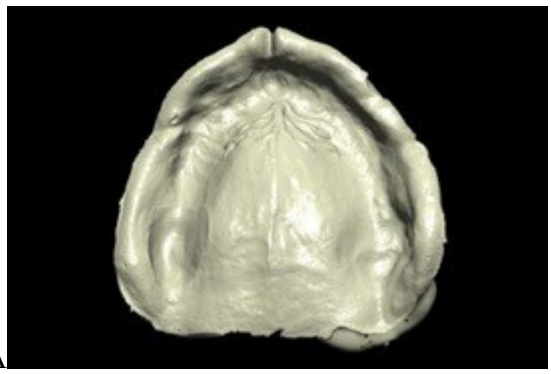 B 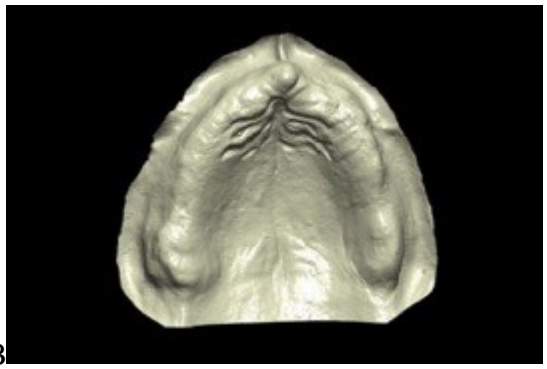

C 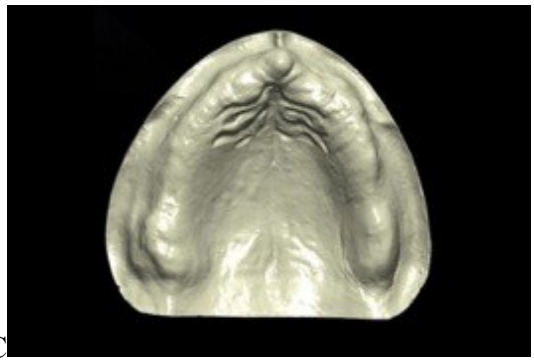

Figure 4. Scans tested. A, Scan of physical impression in polysulfide with laboratory scanner. B, Digital cast (dREC) obtained from inversion of scan of polysulfide impression. C, Scan of stone cast with laboratory scanner (dEOC).

A Type IV stone (Elite Stone; Zhermack SpA) was mixed according to the manufacturer's instructions (150 g powder, 37.5 mL water, 60-second manual mix, and 30-second vacuum mix, poured into the impressions, and removed after 45 minutes). They were immediately scanned with the laboratory extraoral scanner to obtain 10 digital casts (dEOC) (Fig. 4C). These procedures were performed in the same room under similar environmental conditions (temperature 24 °C, pressure 760 ±5 mmHg, and 50% relative humidity). The same experienced and calibrated operator (R.S.) made and poured the impressions. The 3 groups of STL files (n=10) were imported into an inspection software program (Geomagic Control X; 3D SYSTEMS) to calculate trueness and precision in μm.

All the STL files were imported into a dedicated software program (Meshlab v2016.12; ISTI-CNR) by using the dRT as a guide to cut the surplus surfaces of each digital experimental cast. The border line of specimens for superimposition was delineated at the boxing line of the native cast from which RT was obtained (Fig. 2). The dRT and every digital cast were imported into Geomagic Control X to be superimposed (Fig. 5), indicating dRT as "reference data" in the software program.[42]

The 2 digital casts were superimposed in the software program by activating the function "initial alignment" and then the function "best fit alignment," which aligned the 2 digital casts with a minimal distance between the superimposed surfaces.[43] Then the "3D compare" function was activated, and the value of standard deviation (SD) was chosen from the "tabular view-3D compare." The SD value calculated by the software indicated a mean between the positive and negative deviations resulting from each superimposition of the digital surfaces, and the mean of the SD values was chosen to evaluate the trueness and precision.[6,34] With this procedure, a color map was created to visualize the displacement between the superimposed digital casts (Fig. 5). For each experimental group, the trueness was calculated as the mean of the SD values resulting from the superimposition of each cast and the dRT. The precision was evaluated as the mean of the SD values recorded after the superimposition between each cast of an experimental group and the cast that recorded the best result of trueness in the same group. Therefore, all the scans of the same group were superimposed onto this selected cast, whose trueness corresponded to the actual reference value for precision.[6,34]

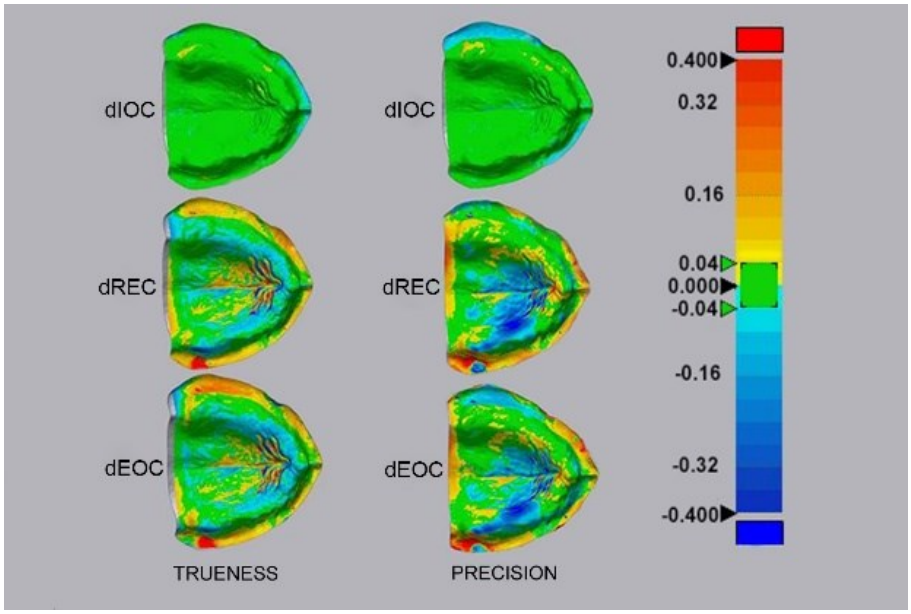

Figure 5. Evaluation of trueness and precision: Best superimposition for each group of scans. *Green areas* indicate minimum displacements of ±0.04 mm of digital cast compared with reference data. *Red areas* indicate outward displacement of +0.4 mm. *Blue areas* indicate inward displacement of -0.4 mm.

Statistical analysis was performed with a statistical software program (IBM SPSS Statistics, v25; IBM Corp). Both for the evaluation of trueness and precision, descriptive statistics (mean, standard error, 95% confidence intervals) and confirmatory factor analysis tests

were determined. The sample size was determined to be appropriate for factor analysis by using the Kaiser-Meyer-Olkin (KMO) measure of sampling adequacy and the Bartlett test of sphericity. Thus, the KMO value should be higher than .500 and the chi-square value of the Bartlett test must be significant at the .05 level.[44] The Shapiro-Wilk test was used to check data normality, the Levene test was run to evaluate variance homogeneity, and the 1-way ANOVA followed by the Bonferroni test or the Kruskal-Wallis and the Dunn tests were run to evaluate the statistical significance of the differences among the groups (α=.05).

Results

The trueness and precision of the KMO statistic were respectively .572 and .650, values higher than the recommended .500, and the Bartlett test was statistically significant both for trueness (*P*=.009) and precision (*P*=.007). The results for trueness are summarized in Table 1; mean values were not normally distributed for all groups of scans, as detected by the Shapiro-Wilk test (*P*<.05). The Levene test showed no homogeneity of the variances (*P*=.002) for the different groups. A $\log_{10}$ transformation of the data was performed because the assumptions on the normal distribution and the homogeneity of the variances were violated to evaluate differences with a 1-way ANOVA. After this transformation, the Shapiro-Wilk test detected a normal distribution (*P*>.05), and the Levene test reported homogeneity of the variances (*P*=.079). Furthermore, the Bonferroni test detected statistically significant differences between the means values of dIOC and dREC (*P*<.001) and between dIOC and dEOC (*P*<.001).

Table 1. Mean with 95% CI for trueness measures in μm by scanning methods. dEOC, digital extraoral scanner cast; dIOC, digital intraoral scanner cast; dREC, digital reversed cast

Type of cast	Mean	Lower-Upper bound (95% CI)	Standard Error
dIOC	48.720	37.876-59.564	4.793
dREC	249.960	121.349-378.571	56.853
dEOC	308.820	186.641-430.999	54.009

The results for precision with the actual reference values are summarized in Table 2; mean values were not normally distributed for all groups of scans, as detected by the Shapiro-Wilk test (*P*<.05). The Levene test showed no homogeneity of the variances (*P*=.002) for the

different groups. A $\log_{10}$ transformation of the data was performed because the assumptions on the normal distribution and the homogeneity of the variances were violated to evaluate differences with a 1-way ANOVA. After this transformation, the Shapiro-Wilk test did not detect a normal distribution (P<.05), while the Levene test reported homogeneity of the variances (P=.083). The Kruskal-Wallis (P<.001) and the Dunn tests were performed with the Bonferroni correction, and statistically significant differences were detected between the means of dIOC and dREC (P=.003) and between dIOC and dEOC (P=.001). P values of post hoc comparisons are reported in Table 3.

Table 2. Mean with 95% CI and actual reference values for precision measures in μm by scanning methods. dEOC, digital extraoral scanner cast; dIOC, digital intraoral scanner cast; dREC, digital reversed cast

Type of cast	Mean	Lower-Upper bound (95% CI)	Standard Error	Actual reference value
dIOC	46.767	29.780-63.754	7.366	32.4
dREC	271.250	94.606-447.894	74.702	97.6
dEOC	341.438	175.500-507.375	70.175	136.9

Table 3. Post hoc comparisons among scanning methods. dEOC, digital extraoral scanner cast; dIOC, digital intraoral scanner cast; dREC, digital reversed cast

	Type of scan		*P*
Log_{10} TRUENESS	dIOC	dREC	<.001*
		dEOC	<.001*
	dREC	dEOC	.696
Log_{10} PRECISION	dIOC	dREC	.003*
		dEOC	.001*
	dREC	dEOC	1.00

*Statistically significant differences (*P*<.05).

The trueness and precision were better with the IOS than with the laboratory scanner. No significant differences were detected between scanning the polysulfide impressions or the stone casts. From the analysis of the color maps (Fig. 5), dREC and dEOC exhibited more displacement than dIOC. Particularly, outward displacements were detected at the buccal vestibule up to 400 µm, and inward displacements were observed at the palatal vault and on the top of the edentulous crest up to 320 µm.

Discussion

The null hypothesis that no difference would be found in the trueness and precision among the various scanning typologies tested was rejected because statistically significant differences were detected between the means of dIOC and dREC (trueness: *P*<.001; precision: *P*=.003) and between dIOC and dEOC (trueness: *P*<.001; precision *P*=.001). The evaluation of trueness and precision obtained with different digitization techniques showed that scanning the typodont directly with an IOS (dIOC) was more accurate in terms of trueness and precision, with statistically significant differences compared with the reverse scans of the physical impression (dREC) and with the scans of the stone casts (dEOC), both with a laboratory scanner. These results could be explained by the absence of material distortions when direct scanning with an IOS, particularly the negative effects of both polysulfide[25,26] and stone[20-24] deformation on the final accuracy.

Although significant differences were detected, because of the experimental and comparative nature of the present investigation, the clinical impact of these differences may be small. The findings suggest no difference for trueness and precision in scans performed with a laboratory scanner among the polysulfide impressions and the corresponding stone casts, despite the mean of the polysulfide impressions showing values of trueness and precision better than the stone casts. Moreover, the tested IOS has better trueness and precision than conventional impression making for recording the test cast, notwithstanding the limitations of a solid object. However, using an IOS in the oral cavity causes passive and excessive displacements of soft tissues, making the definition of the denture borders inaccurate.[7,8,10,12]

Limitations of the present investigation included its in vitro design with a solid polyurethane typodont. Factors, in particular, the temperature, humidity, optical features, resilience, and mobility of soft tissues, related to the intraoral anatomic limitations and to the oral environment were not taken into account. Moreover, the experimental impressions were made at room temperature, making them more accurate than clinical impressions because of the absence of the thermal contraction of the impression materials from the intraoral to room temperature.[45] Further experimental studies with a larger number of specimens should be made to confirm the outcomes of the present investigation.

Conclusions

Based on the findings of this in vitro study, the following conclusions were drawn:

1. Direct scanning of a solid typodont of a completely edentulous maxilla with an IOS produced better trueness and precision than indirect digitization of both polysulfide impressions and stone casts with an extraoral laboratory scanner.
2. With the extraoral laboratory scanner, no significant differences in trueness and precision were detected between the scans of the polysulfide impressions and of the corresponding stone casts on the reference typodont.

References

1. Bilgin MS, Baytaroğlu EN, Erdem A, Dilber E. A review of computer-aided design/computer-aided manufacture techniques for removable denture fabrication. Eur J Dent 2016;10:286-91.
2. Bidra AS, Taylor TD, Agar JR. Computer-aided technology for fabricating complete dentures: Systematic review of historical background, current status, and future perspectives. J Prosthet Dent 2013;109:361-6.
3. AlHelal A, AlRumaih HS, Kattadiyil MT, Baba NZ, Goodacre CJ. Comparison of retention between maxillary milled and conventional denture bases: A clinical study. J Prosthet Dent 2017;117:233-8.
4. McLaughlin JB, Ramos V Jr, Dickinson DP. Comparison of fit of dentures fabricated by traditional techniques versus CAD/CAM technology. J Prosthodont 2019;28:428-35.
5. Bonnet G, Batisse C, Bessadet M, Nicolas E, Veyrune JL. A new digital denture procedure: a first practitioners appraisal. BMC Oral Health 2017;17:155.
6. Zarone F, Ruggiero G, Di Mauro MI, Spagnuolo G, Ferrari M, Sorrentino R. Accuracy of three impression materials on the totally edentulous maxilla: in vitro/in silico comparative analysis. Materials (Basel) 2020;13:515.
7. Lo Russo L, Caradonna G, Troiano G, Salamini A, Guida L, Ciavarella D. Three-dimensional differences between intraoral scans and conventional impressions of edentulous jaws: A clinical study. J Prosthet Dent 2020;123:264-8.
8. Lo Russo L, Salamini A. Single-arch digital removable complete denture: A workflow that starts from the intraoral scan. J Prosthet Dent 2018;120:20-4.
9. Lo Russo L, Salamini A. Removable complete digital dentures: A workflow that integrates open technologies. J Prosthet Dent 2018;119:727-32.
10. Goodacre CJ, Garbacea A, Naylor WP, Daher T, Marchack CB, Lowry J. CAD/CAM fabricated complete dentures: Concepts and clinical methods of obtaining required morphological data. J Prosthet Dent 2012;107:34-46.
11. Chebib N, Kalberer N, Srinivasan M, Maniewicz S, Perneger T, Müller F. Edentulous jaw impression techniques: An in vivo comparison of trueness. J Prosthet Dent 2019;121:623-60.
12. Unkovskiy A, Wahl E, Zander AT, Huettig F, Spintzyk S. Intraoral scanning to fabricate complete dentures with functional borders: a proof-of-concept case report. BMC Oral Health 2019;19:46.
13. International Organization for Standardization. ISO 5725-1. Accuracy (trueness and precision) of measurement methods and results. Part 1: General principles and definitions. Berlin: International Organization for Standardization; 1994. Available at: http://www.iso.org/iso/home.html.

14. Sim JY, Jang Y, Kim WC, Kim HY, Lee DH, Kim JH. Comparing the accuracy (trueness and precision) of models of fixed dental prostheses fabricated by digital and conventional workflows. J Prosthodont Res 2019;63:25-30.
15. Patzelt SB, Vonau S, Stampf S, Att W. Assessing the feasibility and accuracy of digitizing edentulous jaws. J Am Dent Assoc 2013;144:914-20.
16. Jeong ID, Lee JJ, Jeon JH, Kim JH, Kim HY, Kim WC. Accuracy of complete-arch model using an intraoral video scanner: An in vitro study. J Prosthet Dent 2016;115:755-9.
17. Peng L, Chen L, Harris BT, Bhandari B, Morton D, Lin WS. Accuracy and reproducibility of virtual edentulous casts created by laboratory impression scan protocols. J Prosthet Dent 2018;120:389-95.
18. Sorrentino R, Gherlone EF, Calesini G, Zarone F. Effect of implant angulation, connection length, and impression material on the dimensional accuracy of implant impressions: an in vitro comparative study. Clin Implant Dent Relat Res 2010;12:63-76.
19. Calesini G, Zarone F, Sorrentino R, Micarelli C, Fabianelli A, Papacchini F, et al. Effect of 2 impression techniques on the dimensional accuracy of working implant prosthesis models: an in vitro study. J Craniofac Surg 2014;25:822-7.
20. Eames WB, Wallace SW, Suway NB, Rogers LB. Accuracy and dimensional stability of elastomeric impression materials. J Prosthet Dent 1979;42:159-62.
21. Gonçalves FS, Popoff DA, Castro CD, Silva GC, Magalhães CS, Moreira AN. Dimensional stability of elastomeric impression materials: a critical review of the literature. Eur J Prosthodont Restor Dent 2011;19:163-6.
22. Valderhaug J, Fløystrand F. Dimensional stability of elastomeric impression materials in custom-made and stock trays. J Prosthet Dent 1984;52:514-7.
23. Chai J, Takahashi Y, Lautenschlager EP. Clinically relevant mechanical properties of elastomeric impression materials. Int J Prosthodont 1998;11:219-23.
24. Re D, De Angelis F, Augusti G, Augusti D, Caputi S, D'Amario M, et al. Mechanical properties of elastomeric impression materials: an in vitro comparison. Int J Dent 2015;2015:428286.
25. Heshmati RH, Nagy WW, Wirth CG, Dhuru VB. Delayed linear expansion of improved dental stone. J Prosthet Dent 2002;88:26-31.
26. Gujjarlapudi MC, Reddy SV, Madineni PK, Ealla KK, Nunna VN, Manne SD. Comparative evaluation of few physical properties of epoxy resin, resin-modified gypsum and conventional type IV gypsum die materials: an in vitro study. J Contemp Dent Pract 2012;13:48-54.
27. Oda Y, Matsumoto T, Sumii T. Evaluation of dimensional stability of elastomeric impression materials during disinfection. Bull Tokyo Dent Coll 1995;36:1-7.

28. Kamble SS, Khandeparker RV, Somasundaram P, Raghav S, Babaji RP, Varghese TJ. Comparative evaluation of dimensional accuracy of elastomeric impression materials when treated with autoclave, microwave, and chemical disinfection. J Int Oral Health 2015;7:22-4.
29. Thouati A, Deveaux E, Iost A, Behin P. Dimensional stability of seven elastomeric impression materials immersed in disinfectants. J Prosthet Dent 1996;76:8-14.
30. Thota KK, Jasthi S, Ravuri R, Tella S. A comparative evaluation of the dimensional stability of three different elastomeric impression materials after autoclaving - an invitro study. J Clin Diagn Res 2014;8:48-50.
31. Andriessen FS, Rijkens DR, Van der Meer WJ, Wismeijer DW. Applicability and accuracy of an intraoral scanner for scanning multiple implants in edentulous mandibles: a pilot study. J Prosthet Dent 2014;111:186-94.
32. Kim JH, Kim KB, Kim WC, Kim JH, Kim HY. Accuracy and precision of polyurethane dental arch models fabricated using a three-dimensional subtractive rapid prototyping method with an intraoral scanning technique. Korean J Orthod 2014;44:69-76.
33. Nedelcu R, Olsson P, Nyström I, Rydén J, Thor A. Accuracy and precision of 3 intraoral scanners and accuracy of conventional impressions: A novel in vivo analysis method. J Dent 2018;69:110-8.
34. Imburgia M, Logozzo S, Hauschild U, Veronesi G, Mangano C, Mangano FG. Accuracy of four intraoral scanners in oral implantology: a comparative in vitro study. BMC Oral Health 2017;17:92.
35. Mangano FG, Veronesi G, Hauschild U, Mijiritsky E, Mangano C. Trueness and precision of four intraoral scanners in oral implantology: a comparative in vitro study. PLoS One 2016;11:e0163107.
36. Rameez M, Razi SS, Farhan F, Kumar B, Rashid H. Clinical implications of elastomeric impression materials used for complete denture construction. Dent Med Res 2018;6:19-23.
37. Rubel BS. Impression materials: A comparative review of impression materials most commonly used in restorative dentistry. Dent Clin North Am 2007;51:629-42.
38. Giordano R. Impression materials: Basic properties. Gen Dent 2000;48:51-6.
39. Passamonti G. Relationship between the two arches and its effect in the diagnosis and treatment of complete denture prosthesis. Quintessence Int Dent Dig 1979;10:37-51.
40. Chopra S, Gupta NK, Tandan A, Dwivedi R, Gupta S, Agarwal G. Comparative evaluation of pressure generated on a simulated maxillary oral analog by impression materials in custom trays of different spacer designs: An in vitro study. Contemp Clin Dent 2016;7:55-60.
41. Gonçalves FS, de Freitas Oliveira W, Soares LA, Cario HL, da Mota AS, Popoff DAV, et al. Impression materials and storage time influence on cast models accuracy. Int J Exp Dent Sci

2013;2:18.
42. Mandelli F, Gherlone E, Gastaldi G, Ferrari M. Evaluation of the accuracy of extraoral laboratory scanners with a single-tooth abutment model: A 3D analysis. J Prosthodont Res 2017;61:363-70.
43. Marani R, Reno V, Nitti M, D'Orazio T, Stella E. A modified iterative closest point algorithm for 3D point cloud registration. Comput Aided Civil Infrastruct Eng 2016;31:515-34
44. Harper D, Kim JO, Mueller CW. Introduction to factor analysis: what it is and how to do it. Contemp Sociol 1980;9:562.
45. Kim KM, Lee JS, Kim KN, Shin SW. Dimensional changes of dental impression materials by thermal changes. J Biomed Mater Res 2001;58:217-20.

2.3 COMPARISON OF DIFFERENT INTRAORAL SCANNING TECHNIQUES ON THE COMPLETELY EDENTULOUS MAXILLA: AN IN VITRO 3-DIMENSIONAL COMPARATIVE ANALYSIS

Zarone Fernando, Ruggiero Gennaro, Ferrari Marco, Mangano Francesco, Joda Tim, Sorrentino Roberto

J Prosthet Dent. 2020;124:762.e1-762.e8.

Introduction

Digital technology and intraoral scanners (IOSs) have become popular in dental practice and have advantages over conventional impression techniques, including reduced laboratory and chair-time[1-14] and implementation of a completely digital production workflow.[1,14] However, disadvantages include the learning curve,[15] the limited accuracy for completely edentulous arches[16] and complete-arch implant-supported prostheses,[17] and the cost of the IOS.[14] Nevertheless, cost savings can be expected on materials, shipping, and dental laboratory bills, and the procedure should be more efficient with fewer remakes.[2,18]

IOS systems have been reported to have variable levels of overall accuracy in digital datasets,[19,20] with in vitro and in vivo investigations reporting differences from confounders such as the IOS system, scanning technique, light source, imaging type, necessity of coating or powdering, tooth morphology, tissue mobility, and span length.[14,16,21,22] Significant differences have been reported among dentate, partially, or completely edentulous scans.[14,23] The accuracy of optical scans has been reported to be clinically satisfactory for single crowns and in fixed dental prostheses up to 5 units[8,24]; however, the accuracy of digitizing complete dental arches depends on the technology of the IOS, and clinically acceptable results have been reported to be reliable only for scans of less than half the arch.[25,26]

The scanning of partially and completely edentulous arches still represents a clinical challenge, particularly because of the lack of clear landmarks in edentulous areas with the absence of anatomic reference points,[14,16,22,25] the anatomic limitations to the IOS access in the posterior regions,[14] the impossibility of recording the tissues under selective pressure,[27,28] and the inability to record the soft tissue dynamics (activated borders of denture bearing areas).[14,28] The trueness for complete dentition scanning has been reported to be between approximately 17 μm and 378 μm, and the precision between 55 μm and 116 μm.[25] For edentulous arches, the trueness ranged between 44.1 μm and 591 μm while the precision was up to 698 μm.[22] In general, all scanners can be considered accurate for scanning a complete dentition, particularly for single prepared teeth, while for edentulous arches, scanner accuracy remains questionable because of high variability.[22,25]

Traceable structures and rough surfaces provide much optical information to improve the stitching process of images and videos with dedicated software programs, thereby enhancing the scanning accuracy.[16,29] Conversely, the scanning of flat or smooth surfaces, as for anterior teeth or level edentulous ridges, can lead to software errors in the digitization.[16,21,29] Moreover, the palatal vault may negatively affect the accuracy of scans,[16,29] and the placement of artificial landmarks in edentulous areas could enhance scan accuracy.[22] Whether the surface topography of palatal rugae, representing potential traceable structures on the completely edentulous maxilla, affects the accuracy of scanning is unclear.

The fully digital workflow has become popular in removable prosthodontics because of the improvement in optical scanners and the development of dedicated functions in the related software programs.[30-34] Different scanning techniques have been compared for dentate arches[35-39] and for completely edentulous arches.[30,31] These have been described in clinical reports[32-34] and in experimental studies,[16,40,41] but comparative data are lacking.

The purpose of the present in vitro study was to compare the accuracy of 3 different scanning techniques with one IOS (TRIOS 3 Pod; 3Shape A/S) on 2 similar reference typodonts representing the completely edentulous maxilla, characterized by the presence or absence of palatal rugae. The null hypothesis was that no significant differences would be found among the different scanning strategies performed with IOS on 2 reference typodonts.

Material and methods

Two reference typodonts (Fig. 1) were manufactured by pouring polyurethane resin (PRIMA-DIE; Gerhò S.P.A.) into a mold of a standard edentulous maxilla with well-defined palatal rugae obtained from a patient's cast previously used for a clinical procedure and duplicated with a silicone material (Elite Double 8; Zhermack SpA). Subsequently, one of these typodonts was

modified by removing the palatal rugae and smoothing the surface of the edentulous ridge with rotary instruments (AcryPoint; Shofu INC) and polishing paste (Universal Polishing Paste; Ivoclar Vivadent AG). In this way, compared with the "wrinkled typodont" (WT), the "smooth typodont" (ST) exhibited less defined anatomic landmarks because of the absence of palatal rugae and the edentulous ridges were smooth. Both typodonts had a matt finish, and, because polyurethane acts as an optimal light diffuser[42] for IOS procedures,[19] no surface treatments that might have influenced the scanning were made. WT and ST were scanned by using a metrological scanning machine (Atos Core 80; GOM) based on a structured white-light technology with the following settings: working distance=170 mm, point spacing=0.03 mm, and measure accuracy=±0.0025 mm. Subsequently, 2 digital reference scans were made in standard tessellation language (STL) format: "dWT" for WT and "dST" for ST.

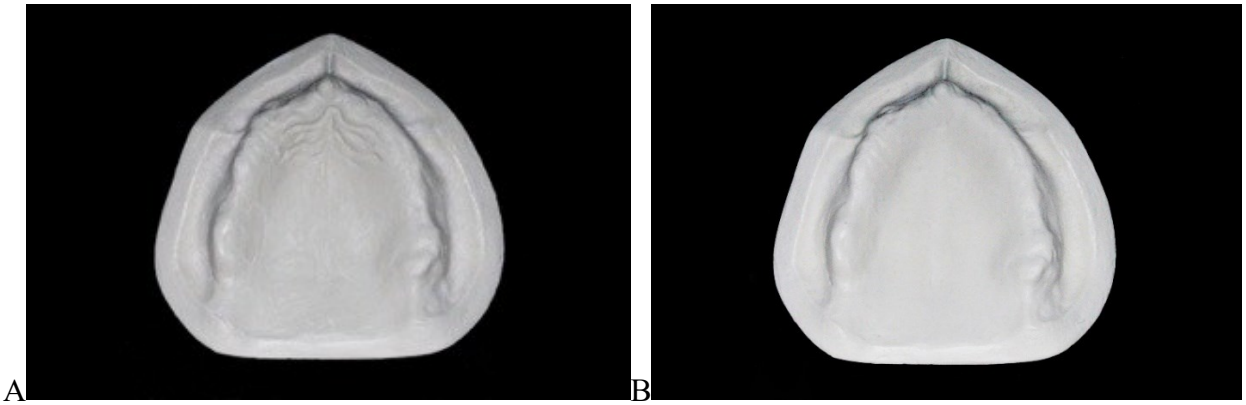

Figure 1. Reference typodonts. A, Wrinkled typodont (WT) with palatal rugae. B, Smooth typodont (ST) without rugae.

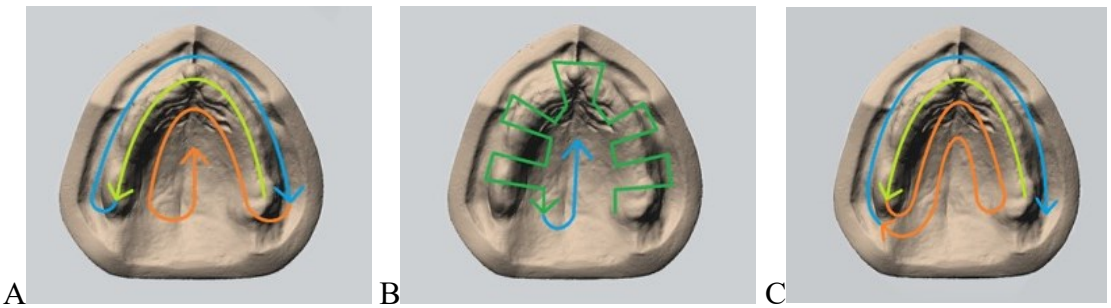

Figure 2. Scanning techniques. A, Buccopalatal (BP). B, S-shaped (SS). C, Palatobuccal (PB).

The 2 reference typodonts were then scanned by using an IOS system (TRIOS 3 Pod; 3Shape A/S) according to 3 scanning techniques to obtain 10 experimental scans per group. The number of scans per group was determined based on convenience criteria validated by previous investigations.[27,36,43-45] The 3 scanning techniques were the following: in the buccopalatal technique (BP), the ridge top side of the edentulous arch was first scanned starting from the left maxillary tuberosity, proceeding longitudinally along the ridge, ending at the right tuberosity, and then continuing on the buccal side and finally on the palatal vault; the latter was first

scanned with a counterclockwise movement along the palatal vault and finally with a longitudinal movement in the postero-anterior direction to close the gap along the midline of the palate (Fig. 2A); in the S-shaped technique (SS), the scanning started from the palatal side of the left maxillary tuberosity by moving the scanner tip with alternate palatobuccal and buccopalatal S-shaped movements along the ridge, from one side to the other; finally, the area along the palatal midline was recorded in the posterior-anterior direction (Fig. 2B); in the palatobuccal technique (PB), the scanning proceeded longitudinally along the ridge top side of the complete arch, starting from the left maxillary tuberosity and ending at the right one, and then continuing on the palatal side and finally on the buccal side. The palatal side was scanned with a circular movement in a clockwise direction along the palatal vault up to the left maxillary tuberosity and finally with a counterclockwise movement up to the contralateral tuberosity (Fig. 2C).

One prosthodontist (G.R.) performed all the scans during the same day and in the same room under similar light and environmental conditions: temperature of 22 °C, air pressure of 760 ±5 mmHg, and 45% relative humidity. The number of images per scan varied between 408 and 1126, and the scanning time was between 1 and 2 minutes. To reduce the effect of operator fatigue and to prevent related bias, the scanning sequence was randomized by using a random sequence generator (Random Number Generator Pro v.1.72; Segobit Software), and an interval of 10 minutes was allowed so that the operator could rest and the device could properly cool.[1,46] All STL files acquired with the IOS were imported into a dedicated software program (Meshlab v2016.12; ISTI-CNR) by using dWT and dST as guides to cut the surplus surfaces of each experimental scan.

Both the reference and experimental scans were imported into an inspection software program (Geomagic Control X; 3D SYSTEMS) (Fig. 3), and the accuracy of each one was evaluated by calculating trueness and precision in μm.[47] The scans made on WT were superimposed on dWT, while those made on ST were superimposed on dST. An “initial alignment” was performed by the software program, followed by a “best fit alignment,” and then the “3D compare” function was activated. The parameters in the “color bar option” were max range=0.4 mm, min range=0.4 mm, and use of specific tolerance=±0.04 mm. The value of standard deviation (SD) was chosen from the “tabular view-3D compare.” This value (SD), calculated by the software, indicates a mean between the positive and negative deviations resulting from each superimposition of the digital scans. For this reason, the mean among SD values was chosen to evaluate the trueness and precision.[1,48] With this procedure, a “color map” was created for visual analysis of the displacements between the superimposed digital surfaces (Fig. 3).

A 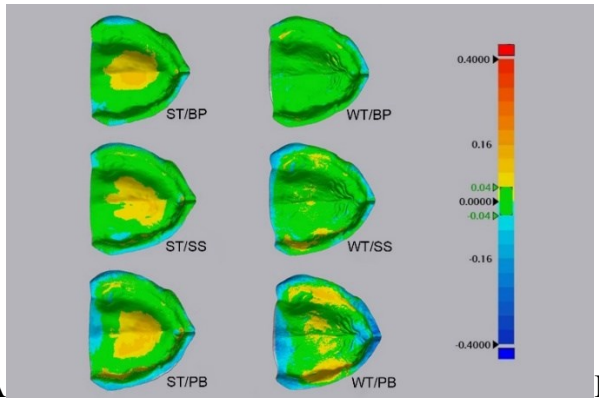

B 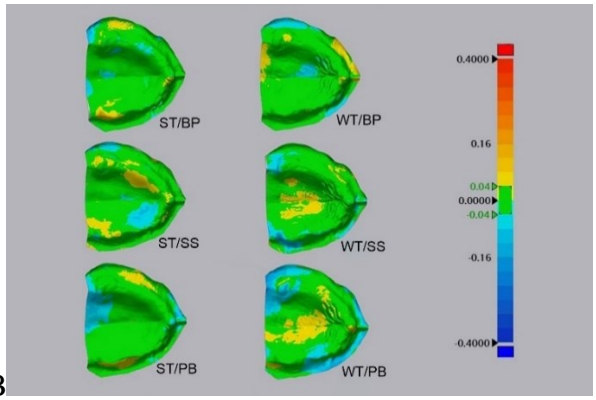

Figure 3. Best superimposition for each group of scans: *Green* areas indicate minimum displacements of ±0.04 mm of digital cast compared with reference data. *Red* areas indicate outward displacement of +0.4 mm and *blue* areas inward displacements of -0.4 mm. A, Evaluation of trueness. B, Evaluation of precision.

The accuracy of a measurement method is described by "trueness" and "precision." Trueness refers to the closeness of agreement among the mean of a large number of test results and the reference value; precision describes the closeness of agreement among intragroup data obtained by repeated measurements.[49,50] For each experimental group, the trueness was calculated as the mean of the SD values resulting from the superimposition between each typodont and the corresponding digital reference model (dWT or dST). Differently, the precision was evaluated as the mean of SD values for each typodont and the 3D surface model that had obtained the best result of trueness after superimposition on the corresponding digital reference model in each experimental group. All the scans of the same group were superimposed on this selected 3D surface model, and the precision of each group was obtained as the mean of SD values detected by each of these superimpositions.[1,48]

Statistical analyses were performed with a statistical software program (IBM SPSS Statistics, v25; IBM Corp). To evaluate both trueness and precision, descriptive statistics (mean, standard error, median, interquartile range, 95% confidence interval - CI95) were determined. The Shapiro-Wilk test was used to evaluate data normality, the Levene test to evaluate the homogeneity of variances, and the 2-factor ANOVA on the ranks of the data to identify a potential interaction among typodont types and scanning techniques. The Kruskal-Wallis and the Dunn tests with the Bonferroni correction were used to analyze differences among groups (α=.05). In order to consider only clinically relevant comparisons, all the possible pairwise comparisons among the 6 experimental groups were not performed; consequently, whether differences existed between typodonts within a scanning technique and among scanning techniques within a typodont was evaluated.

Results

The results of the analysis of trueness are summarized in Table 1 and shown in Figure 4A. Mean values were not normally distributed for all the groups, as detected by the Shapiro-Wilk test (P<.05). The Levene test showed homogeneity of variances (P=.235) for different groups. The 2-factor ANOVA (Table 2) detected statistically significant differences between the typodonts (WT versus ST) (P=.002), among the scanning techniques (P<.001), and within their mutual interaction (P=.018). Subsequently, the Kruskal-Wallis (P<.001) and the Dunn tests were run to detect any difference among the scanning techniques, and a significant difference was recorded between BP and PB (P<.001). The Kruskal-Wallis (P<.001) and the Dunn tests were run again to evaluate whether there were any statistically significant differences between typodonts within a scanning technique and among scanning techniques within a typodont, and a significant difference was detected between WT and BP versus WT and PB (P<.001).

Table 1. Results (μm) for trueness: mean, lower-upper bound (95% confidence intervals), standard error, median, and interquartile range

Groups	Mean	Lower-Upper bound	Standard Error	Median	Interquartile range
WT/BP	48.7	37.8-59.5	4.7	43.4	14.8
WT/SS	65.9	54.9-77.4	5.1	64.6	16.8
WT/PB	109.7	96.1-123.4	6	106.1	33.4
ST/BP	48.1	42.4-53.7	2.4	48.9	13.7
ST/SS	56.4	43.9-68.9	5.5	53.3	27.3
ST/PB	61.1	53.3-69	3.4	59.6	14.1
BP	48.4	42.9-53.9	2.6	45.3	13.3
SS	61.1	53.1-69.1	3.8	62.9	19.0
PB	85.4	71.8-99.1	6.5	80.3	46.7
ST	55.2	50.2-60.2	2.4	53.4	17.8
WT	74.8	63.2-86.3	5.6	67.2	57.8

Table 2. 2-factor ANOVA results for trueness analysis

Source	SS	Df	MS	F	*P*
Corrected Model	9685.65	5	1937.13	12.59	<.001*
Intercept	55815	1	55815	362.76	<.001*
Typodont	1601.66	1	1601.66	10.41	.002*
Technique	6760.07	2	3380.03	21.96	<.001*
Typodont×Technique	1323.90	2	661.95	4.30	.018*
Error	8308.35	54	153.85		
Total	73809	60			
Corrected Total	17994	59			

ANOVA, analysis of variance; SS, sum of squares; df, degree of freedom (n-1); MS, mean squares. *Significant at *P*<.05.

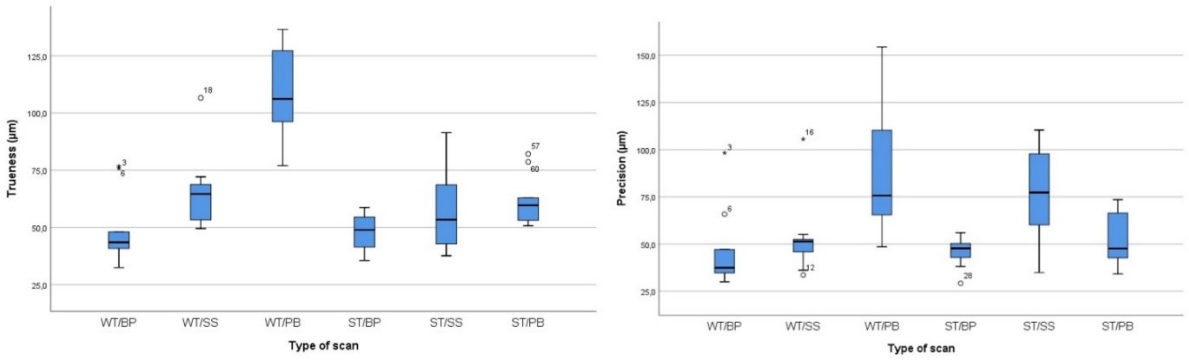

A B

Figure 4. Box plot charts. Whiskers: minimum and maximum; Box spans: first quartile to third quartile. Median: segments inside box. Suspected outliers: unfilled circles. A, Trueness. B, Precision.

The results of the analysis of precision are shown in Table 3 and Figure 4B. The mean values were not normally distributed for all the groups of scans, as detected by the Shapiro-Wilk test (*P*<.05). The Levene test determined that the variances were not homogenic (*P*=.004) for the different groups. The 2-factor ANOVA (Table 4) detected statistically significant differences among the scanning techniques (*P*=.005) and within the mutual interaction of the study variables (*P*=.009). The Kruskal-Wallis (*P*=.011) and the Dunn tests were run to identify whether there were any statistically significant differences among the scanning techniques, and a significant difference was recorded between BP and PB (*P*=.032). These tests were repeated (*P*=.005) to evaluate whether there were any statistically significant differences between typodonts within a scanning technique and among scanning techniques within a typodont, and a significant

difference was detected between the means of WT and BP versus WT and PB (*P*=.012) (Table 5).

Table 3. Results (μm) for precision: mean, lower-upper bound (95% confidence intervals), standard error, median and interquartile range

Groups	Mean	Lower-Upper bound	Standard Error	Median	Interquartile range
WT/BP	46.7	29.7-63.7	7.3	37.4	22.6
WT/SS	53.6	37.6-69.7	6.9	51.4	12.8
WT/PB	90	59.1-120.9	13.4	75.7	73.1
ST/BP	46	39.7-52.3	2.7	47.7	11.1
ST/SS	76	55.5-96.6	8.9	77.3	48.1
ST/PB	52.9	41.9-63.8	4.7	47.6	26.5
BP	46.4	38.3-54.4	3.8	45	15.6
SS	64.8	51.9-77.7	6.1	53.8	45.5
PB	71.5	54-88.8	8.2	65.9	31.7
ST	58.3	49-66.9	4.1	50.3	24.1
WT	63.5	50-76.9	6.5	51.4	38.3

Table 4. 2-factor ANOVA results for precision analysis

Source	SS	df	MS	F	*P*
Corrected Model	4180.83	5	836.16	4.49	.002*
Intercept	40837.50	1	40837.50	219.34	<.001*
Typodont	0.01	1	0.01	0	.992
Technique	2252.11	2	1126.05	6.04	.005*
Typodont×Technique	1928.70	2	964.35	5.18	.009*
Error	8936.66	48	186.18		
Total	53955	54			
Corrected Total	13117.50	53			

ANOVA, analysis of variance; SS, sum of squares; df, degree of freedom (n-1); MS, mean squares. *Significant at *P*<.05.

Table 5. *P* values of post hoc comparisons

	TRUENESS	PRECISION
WT/BP-WT/SS	.268	1
WT/BP-WT/PB	<.001*	.012*
WT/SS-WT/PB	.225	.431
ST/BP-ST/SS	1	.399
ST/BP-ST/PB	.951	1
ST/SS-ST/PB	1	1
WT/BP-ST/BP	1	1
WT/SS-ST/SS	1	1
WT/PB-ST/PB	.071	.415
BP-SS	.054	.1
BP-PB	<.001*	.032*
SS-PB	.058	1

*=Statistically significant differences (*P*<.05).

From the analysis of trueness from the color bar maps with the best superimposition for each group of scans, outward displacements of up to 200 μm were detected at the level of the palatal vault and rugae, regardless of the scanning technique and mostly in ST. Differently, greater inward displacements of up to 320 μm were noticed at the buccal vestibule, particularly for the PB scanning technique (Fig. 3A). For precision, outward displacements of up to 120 μm were detected on the lateral sides of the alveolar ridges in ST and at the level of the palatal vault in WT. Differently, greater inward displacements of up to 200 μm were noticed at the level of both the buccal and posterior peripheral borders, regardless of the performed scanning technique; uniquely, significant inward displacements of up to 200 μm were also noticed in the anterior left area of ST and SS (Fig. 3B).

Discussion

The present in vitro study compared the accuracy of 3 different scanning techniques with one IOS (TRIOS 3 Pod; 3Shape A/S). According to the obtained results, the null hypothesis was rejected, since statistically significant differences were found.

The significant difference detected between the trueness of WT and ST (*P*=.002) showed that the scans made on the typodont with more defined anatomic landmarks (WT) had worse trueness than those on the typodont with less defined anatomic reference points (ST). This result might seem to conflict with those of previous studies, which reported the importance of reference

points to improve the accuracy of IOS in edentulous arches.[14-17,22,26,29-31] Furthermore, in the visual analysis of the color maps for trueness, outward displacements of up to 200 μm were detected at the level of the palatal rugae (Fig. 3A). However, these results do not imply that the presence of palatal rugae would lead to less accurate clinical scans of the edentulous maxilla because the software used for the digital analysis of the superimposed scans calculated the SD value of the global displacement between the whole superimposed surfaces. For this reason, the calculated mean value was influenced by the area of the palatal rugae.

A further statistically significant difference was recorded between BP and PB for both precision (P=.032) and for trueness (P<.001). The post hoc tests also recorded a significant difference between WT and BP versus WT and PB, for both trueness (P<.001) and precision (P=.012). This result showed that the difference between BP and PB was present only on WT and could be explained by considering that in PB the palatal area was scanned before the buccal vestibule. Since the presence of palatal rugae negatively affected the stitching process of the IOS, starting from the palatal side could result in higher surface displacements (Fig. 5), determining the accumulation of matching errors during the following scanning of the buccal vestibule and ultimately altering the global accuracy of the scan.

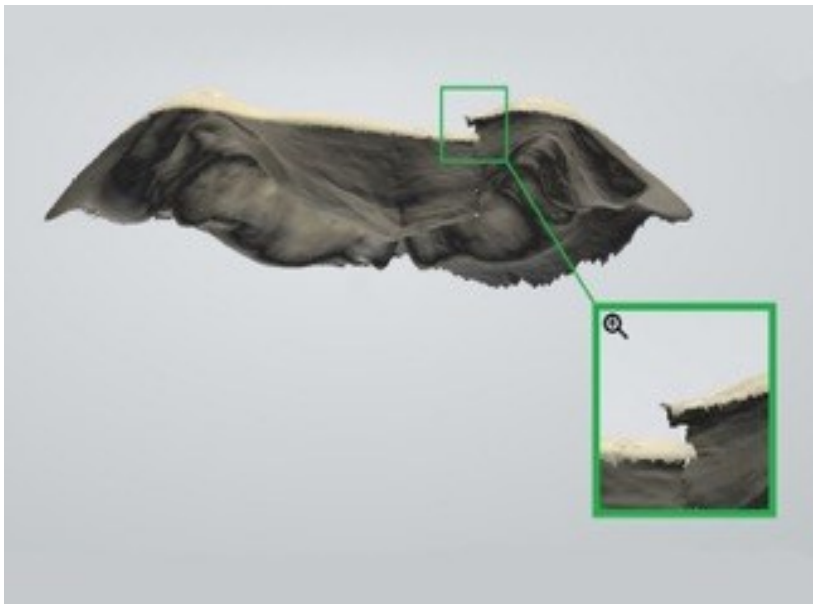

Figure 5. Displacement of palatal digital surface resulting from incorrect stitching process.

Although significant differences were found among the tested scanning techniques, because of the experimental and comparative nature of the present investigation, the clinical impact of such differences cannot be answered unequivocally. However, using the BP scanning technique in the completely edentulous maxilla is recommended.

Limitations of the present investigation included its in vitro design, scanning polyurethane typodonts. Clinically relevant factors related to the oral environment, particularly temperature, humidity, optical features, resilience, the mobility of soft tissues, and intraoral anatomic limitations, were not modelled. Further studies, including clinical trials, involving a larger sample size should be made to support the outcomes of the present investigation.

Conclusions

Based on the findings of the present in vitro comparative study, the following conclusions were drawn:

1. Scans performed on the typodont with less defined anatomic landmarks had better trueness than scans made on the typodont with more defined anatomic landmarks.
2. In the ST scenario, no differences were noticed among the 3 scanning approaches.
3. In the WT scenario, the BP scanning technique showed higher accuracy than the PB with the tested IOS, while SS did not show any significant difference.
4. The scanning strategy had a significant influence on the accuracy of scans of the completely edentulous maxilla.

References

1. Imburgia M, Logozzo S, Hauschild U, Veronesi G, Mangano C, Mangano FG. Accuracy of four intraoral scanners in oral implantology: a comparative in vitro study. BMC Oral Health 2017;17:92.

2. Bilgin MS, Baytaroğlu EN, Erdem A, Dilber E. A review of computer-aided design/computer-aided manufacture techniques for removable denture fabrication. Eur J Dent 2016;10:286-91.

3. Goracci C, Franchi L, Vichi A, Ferrari M. Accuracy, reliability, and efficiency of intraoral scanners for full-arch impressions: a systematic review of the clinical evidence. Eur J Orthod 2016;38:422-8.

4. Yuzbasioglu E, Kurt H, Turunc R, Bilir H. Comparison of digital and conventional impression techniques: evaluation of patients' perception, treatment comfort, effectiveness and clinical outcomes. BMC Oral Health 2014;14:10.

5. Burhardt L, Livas C, Kerdijk W, van der Meer WJ, Ren Y. Treatment comfort, time perception, and preference for conventional and digital impression techniques: A comparative study in young patients. Am J Orthod Dentofac Orthop 2016;150:261-7.

6. Grünheid T, McCarthy SD, Larson BE. Clinical use of a direct chairside oral scanner: an assessment of accuracy, time, and patient acceptance. Am J Orthod Dentofac Orthop 2014;146:673-82.

7. Schepke U, Meijer HJ, Kerdijk W, Cune MS. Digital versus analog complete arch impressions for single-unit premolar implant crowns: Operating time and patient preference. J Prosthet Dent 2015;114:403-6.

8. Sakornwimon N, Leevailoj C. Clinical marginal fit of zirconia crowns and patients' preferences for impression techniques using intraoral digital scanner versus polyvinyl siloxane material. J Prosthet Dent 2017;118:386-91.

9. Lee SJ, Gallucci GO. Digital vs. conventional implant impressions: efficiency outcomes. Clin Oral Implants Res 2013;24:111-5.

10. Joda T, Bragger U. Time-efficiency analysis comparing digital and conventional workflows for implant crowns: a prospective clinical crossover trial. Int J Oral Maxillofac Implants 2015;30:1047-53.

11. Joda T, Bragger U. Digital vs. conventional implant prosthetic workflows: a cost/time analysis. Clin Oral Implants Res 2015;26:1430-5.

12. Patzelt SB, Lamprinos C, Stampf S, Att W. The time efficiency of intraoral scanners: an in vitro comparative study. J Am Dent Assoc 2014;145:542-51.

13. Joda T, Lenherr P, Dedem P, Kovaltschuk I, Bragger U, Zitzmann NU. Time efficiency, difficulty, and operator's preference comparing digital and conventional implant impressions: a randomized controlled trial. Clin Oral Implants Res 2017;28:1318-23.
14. Mangano F, Gandolfi A, Luongo G, Logozzo S. Intraoral scanners in dentistry: a review of the current literature. BMC Oral Health 2017;17:149.
15. Al Hamad KQ. Learning curve of intraoral scanning by prosthodontic residents. J Prosthet Dent 2020;123:277-83.
16. Patzelt SB, Vonau S, Stampf S, Att W. Assessing the feasibility and accuracy of digitizing edentulous jaws. J Am Dent Assoc 2013;144:914-20.
17. Andriessen FS, Rijkens DR, Van der Meer WJ, Wismeijer DW. Applicability and accuracy of an intraoral scanner for scanning multiple implants in edentulous mandibles: a pilot study. J Prosthet Dent 2014;111:186-94.
18. Bidra AS, Taylor TD, Agar JR. Computer-aided technology for fabricating complete dentures: Systematic review of historical background, current status, and future perspectives. J Prosthet Dent 2013;109:361-6.
19. Patzelt SB, Emmanouilidi A, Stampf S, Strub JR, Att W. Accuracy of full-arch scans using intraoral scanners. Clin Oral Investig 2014;18:1687-94.
20. Nedelcu R, Olsson P, Nyström I, Thor A. Finish line distinctness and accuracy in 7 intraoral scanners versus conventional impression: an in vitro descriptive comparison. BMC Oral Health 2018;18:27.
21. Abduo J, Elseyoufi M. Accuracy of Intraoral Scanners: A Systematic Review of Influencing Factors. Eur J Prosthodont Restor Dent 2018;26:101-21.
22. Kim JE, Amelya A, Shin Y, Shim JS. Accuracy of intraoral digital impressions using an artificial landmark. J Prosthet Dent 2017;117:755-61.
23. Lo Russo L, Salamini A. Removable complete digital dentures: A workflow that integrates open technologies. J Prosthet Dent 2018;119:727-32.
24. Chochlidakis KM, Papaspyridakos P, Geminiani A, Chen CJ, Feng IJ, Ercoli C. Digital versus conventional impressions for fixed prosthodontics: A systematic review and meta-analysis. J Prosthet Dent 2016;116:184-90.
25. Bohner L, Gamba DD, Hanisch M, Marcio BS, Tortamano Neto P, Laganá DC, et al. Accuracy of digital technologies for the scanning of facial, skeletal, and intraoral tissues: A systematic review. J Prosthet Dent 2019;121:246-51.
26. Flügge TV, Att W, Metzger MC, Nelson K. Precision of dental implant digitization using intraoral scanners. Int J Prosthodont 2016;29:277-83.

27. Lo Russo L, Caradonna G, Troiano G, Salamini A, Guida L, Ciavarella D. Three-dimensional differences between intraoral scans and conventional impressions of edentulous jaws: A clinical study. J Prosthet Dent 2020;123:264-8.
28. Lo Russo L, Salamini A. Single-arch digital removable complete denture: A workflow that starts from the intraoral scan. J Prosthet Dent 2018;120:20-4.
29. Gan N, Xiong Y, Jiao T. Accuracy of intraoral digital impressions for whole upper jaws, including full dentitions and palatal soft tissues. PLoS One 2016;11:e0158800.
30. Lee JH. Improved digital impressions of edentulous areas. J Prosthet Dent 2017;117:448-9.
31. Fang JH, An X, Jeong SM, Choi BH. Digital intraoral scanning technique for edentulous jaws. J Prosthet Dent 2018;119:733-5.
32. Goodacre BJ, Goodacre CJ, Baba NZ. Using intraoral scanning to capture complete denture impressions, tooth positions, and centric relation records. Int J Prosthodont 2018;31:377-81.
33. Fang Y, Fang JH, Jeong SM, Choi BH. A Technique for digital impression and bite registration for a single edentulous arch. J Prosthodont 2019;28:519-23.
34. Fang JH, An X, Jeong SM, Choi BH. Development of complete dentures based on digital intraoral impressions-Case report. J Prosthodont Res 2018;62:116-20.
35. Müller P, Ender A, Joda T, Katsoulis J. Impact of digital intraoral scan strategies on the impression accuracy using the TRIOS Pod scanner. Quintessence Int 2016;47:343-9.
36. Medina-Sotomayor P, Pascual-Moscardó A, Camps I. Accuracy of four digital scanners according to scanning strategy in complete-arch impressions. PLoS One 2018;13:e0202916.
37. Latham J, Ludlow M, Mennito A, Kelly A, Evans Z, Renne W. Effect of scan pattern on complete-arch scans with 4 digital scanners. J Prosthet Dent 2020;123:85-95.
38. Park GH, Son K, Lee KB. Feasibility of using an intraoral scanner for a complete-arch digital scan. J Prosthet Dent 2019;121:803-10.
39. Mandelli F, Gherlone E, Keeling A, Gastaldi G, Ferrari M. Full arch intraoral scanning: comparison of two different strategies and their accuracy outcomes. J Osseointegr 2018;10:65-74.
40. Chebib N, Kalberer N, Srinivasan M, Maniewicz S, Perneger T, Müller F. Edentulous jaw impression techniques: An in vivo comparison of trueness. J Prosthet Dent 2019;121:623-60.
41. D'Arienzo LF, D'Arienzo A, Borracchini A. Comparison of the suitability of intra-oral scanning with conventional impression of edentulous maxilla in vivo. A preliminary study. J Osseointegr 2018;10:115-20.
42. Nedelcu R, Olsson P, Nyström I, Rydén J, Thor A. Accuracy and precision of 3 intraoral scanners and accuracy of conventional impressions: A novel in vivo analysis method. J Dent 2018;69:110-8.

43. Treesh JC, Liacouras PC, Taft RM, Brooks DI, Raiciulescu S, Ellert DO, et al. Complete-arch accuracy of intraoral scanners. J Prosthet Dent 2018;120:382-8.
44. Ender A, Zimmermann M, Mehl A. Accuracy of complete- and partial-arch impressions of actual intraoral scanning systems in vitro. Int J Comput Dent 2019;22:11-9.
45. Mangano FG, Hauschild U, Veronesi G, Imburgia M, Mangano C, Admakin O. Trueness and precision of 5 intraoral scanners in the impressions of single and multiple implants: a comparative in vitro study. BMC Oral Health 2019;19:101.
46. Mangano FG, Veronesi G, Hauschild U, Mijiritsky E, Mangano C. Trueness and precision of four intraoral scanners in oral implantology: a comparative in vitro study. PLoS One 2016;11:e0163107.
47. Mandelli F, Gherlone E, Gastaldi G, Ferrari M. Evaluation of the accuracy of extraoral laboratory scanners with a single-tooth abutment model: A 3D analysis. J Prosthodont Res 2017;61:363-70.
48. Zarone F, Ruggiero G, Di Mauro MI, Spagnuolo G, Ferrari M, Sorrentino R. Accuracy of three impression materials on the totally edentulous maxilla: in vitro/in silico comparative analysis. Materials (Basel) 2020;13:515.
49. International Organization for Standardization. ISO 5725-1. Accuracy (trueness and precision) of measurement methods and results. Part 1: General principles and definitions. Berlin: International Organization for Standardization; 1994. Available at: http://www.iso.org/iso/home.html.
50. Sim JY, Jang Y, Kim WC, Kim HY, Lee DH, Kim JH. Comparing the accuracy (trueness and precision) of models of fixed dental prostheses fabricated by digital and conventional

2.4 AREA ACCURACY GRADIENT AND ARTIFICIAL MARKERS: A THREE-DIMENSIONAL ANALYSIS OF THE ACCURACY OF IOS SCANS ON THE COMPLETELY EDENTULOUS UPPER JAW

Sorrentino Roberto, Ruggiero Gennaro, Leone Renato, Ferrari Marco, Zarone. Fernando
Journal of Osseointegration, 13(4 Supplement), S257-S264

1. Introduction

Intraoral scanning systems (IOSs) are increasing in popularity due to several benefits over conventional impression procedures. Patient stress and discomfort are reduced (1,2), clinical procedures are simplified, time is saved (3,4), patient and dental technician communication is improved (5,6), and the gypsum cast is no longer used (1,7).

Among the different investigations available in the literature, some compared several IOSs commercially available (8-10), others compared conventional impression procedures with IOS on natural teeth (11,12) or on the completely edentulous upper jaw (13), resulting in better trueness and precision in case of IOS scans. Besides, the best scanning strategies were investigated both on natural tooth abutment (14), implant-abutment (15), and full edentulous maxilla (16,17).

To date, it is not possible to provide a range of values about the accuracy of scans made with IOS on a completely edentulous maxilla because of the various scanning protocols followed in the literature. Indeed, different IOS were tested and the scans were made by several operators not in the same environmental conditions or on comparable reference casts, and various parameters were analyzed such as the root mean square, standard deviation, or mean absolute distance of the superimposed surfaces (16,18,19).

The accuracy of scans made on the edentulous mucosa could be affected by the length and distribution of the edentulous area (20,21), as well as the operator's expertise (22,23), the size of the IOS tip (19,22,24,25), or the features of the soft tissue, such as their mobility, dimension, and

flexibility (23,26-28). About these last factors, it is worth noticing that if the ridges are firm and surrounded with adherent mucosa, then IOS accuracy will be comparable to a conventional impression (18). Therefore, the available IOS systems cannot be acceptable alternatives to conventional procedures in recording tissue movement, which is a critical step for denture manufacturing (18). They can only be used for preliminary or mucostatic impressions (18).
In literature, it is reported that the accuracy of IOS on edentulous areas might be improved by placing artificial markers, in order to facilitate the algorithm of stitching (29), that matches the images captured by the sensor.
Several authors proposed different scanning strategies using artificial markers in edentulous areas, to improve the accuracy of IOS scans (30,31). In particular, in their case report, Fang et al. showed a protocol based on placing resin composite markers, with semispherical shape, directly on the palate that could be considered as one of the more difficult areas to be scanned, due to the absence of natural markers and the morphology of the vault (30). With the same purpose, Lee drew strips made of zinc oxide-eugenol cement on the palate (31). Nevertheless, no experimental data or findings were reported about the effectiveness of these 2 approaches.
Furthermore, several authors placed fiducial markers on the hard palate to enhance the superimposition between the intraoral scans made on the edentulous maxilla, either with the interim prosthesis (32) or the occlusion rim (33), and the scans without these aids. This process is useful to articulate these scans in order to transfer the patient's information from the interim prosthesis or the occlusion rim (32,33).
Although artificial markers could improve the scanning accuracy on an edentulous area (29), there is no evidence about the best protocol to follow and the typology of artificial markers that should be placed on a totally edentulous maxilla.
Also, the accuracy gradient of the area of a completely edentulous maxilla has not been established yet.
The present study aimed to assess the area accuracy gradient of the IOS scans on a completely edentulous maxilla and the accuracy of scans made on a reference cast with different artificial markers systems.
The first null hypothesis is that there is no difference in the accuracy gradient map among the various anatomic areas of completely edentulous maxilla scans made with an IOS.
The second null hypothesis is that no difference might be found between the accuracy of scans made with different reference markers systems.

2. Materials and methods

2.1 Reference cast

A reference cast (RC) (Fig. 1) was manufactured pouring polyurethane resin (PRIMA-DIE; Gerhò S.P.A) inside a mold of a standard edentulous maxilla, obtained from a real model previously used for a clinical purpose and duplicated through a dedicated silicone material (Elite Double; Zhermack SpA).

The RC was then scanned using an industrial metrological scanning machine (Atos Core 80; GOM), based on a structured white-light technology with the following settings: working distance = 170 mm, point spacing = 0.03 mm, measure accuracy = ±0.0025 mm. Subsequently, a digital reference cast (dRC) file was obtained and saved in Standard Tessellation Language (STL) format.

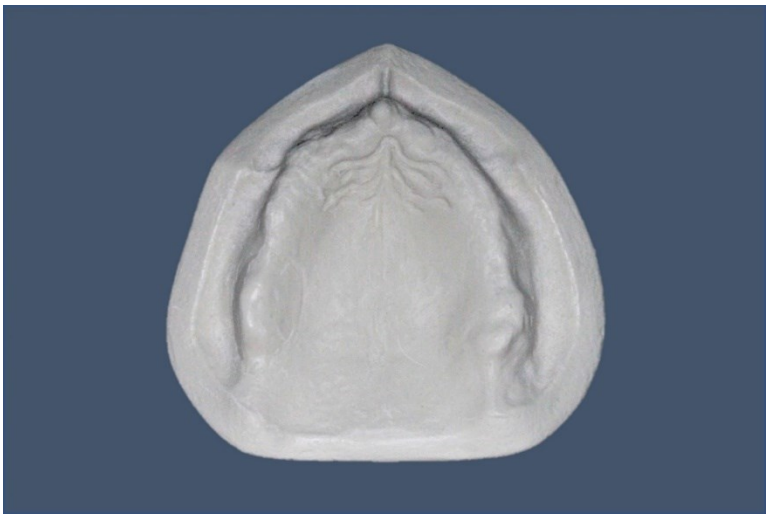

Fig. 1. Reference cast of a completely edentulous maxilla, made of polyurethane resin.

2.2 IOS scanning protocol for sample making and area accuracy gradient

The first part of the study was performed scanning the RC (Fig. 1) with an IOS (Trios 3 Pod; 3Shape, software v1.4.7.5). After the standard calibration procedure of the IOS, ten initial scans were made and then discarded, accomplishing a training session. Subsequently, ten scans were performed following a dedicated scanning strategy suggested in the literature (16). The scanning started from the left maxillary tuberosity, proceeding longitudinally along the ridge top side of the arch and ending at the right one, then continuing on the buccal side and finally on the palatal vault. The latter was first scanned with a clockwise movement along with the palatine vault and finally with a longitudinal movement in the posteroanterior direction to close the gap along with the midline of the palate (16).

Anatomic areas needed for the fabrication of a complete maxillary denture were included in the scans. All scans were performed by one experienced prosthodontist (G.R.), during the same day and in the same room, under similar light and environmental conditions: temperature of 22 °C, air pressure of 760 ±5 mmHg, and 45% relative humidity. The scanning sequence was randomized using a random sequence generator (Random Number Generator Pro v.1.72, Segobit Software) to reduce the effects of operator fatigue and prevent related bias, as well as with an 8-minute interval to allow the operator to rest and the device to cool properly.

All STL files acquired with the IOS were imported into dedicated software (Meshlab v2016.12; ISTI-CNR) using the dRC as a guide to cut the surplus surfaces of each three-dimensional experimental scan. Both the reference and experimental scans (n = 10) were imported into Geomagic Control X (3D SYSTEMS, software v2018.0.1). The dRC was input as "reference data" in the software (34).

An "initial alignment" was performed by the software, followed by a "best fit alignment". After aligning the 2 digital surfaces, the "3D compare" function was activated. The parameters in the "color bar option" were max range = 0.6 mm, min range= 0.6 mm, use of specific tolerance = ±0.06 mm. With this procedure, a "color map" was created for visual analysis of the displacements between the surfaces of the superimposed scans, in order to display the area accuracy gradient (Fig. 2). The green areas indicated a minimum displacement of ±0.06 mm of the digital model compared to the "reference data"; the red and blue areas indicated outward and inward displacements respectively of + 0.6 mm and - 0.6 mm (Fig. 2).

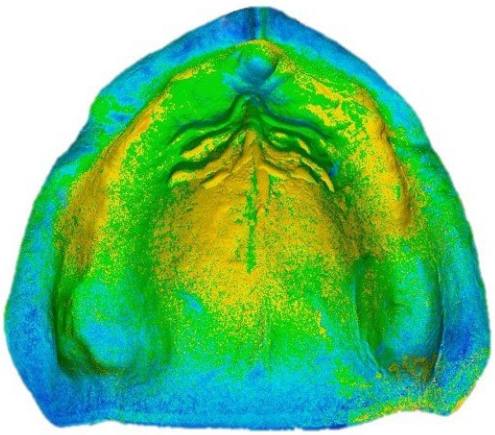

Fig. 2. Accuracy gradient of the areas on completely edentulous maxillary scans, made with IOS. Palate, flattened ridges area, posterior aspect of the papilla, and tubers are the less accurate areas.

2.3 Artificial markers systems

After the first part of the study, the authors discussed the scanning systems involving artificial markers and concluded that the protocols to be followed must have had specific characteristics. First of all, their position on the edentulous maxilla had to follow a criterion based on the areas' accuracy gradient. So, the markers were placed on the less accurate areas: the palate, ridges' flattened areas, posterior aspect of the papilla, and tubers. Furthermore, the process of markers placing had to be quick, easy, reproducible, and with materials or devices easily available in a dental office. In order to satisfy these requirements, the authors designed two approaches. In the first one, embossed markers made of light-cured flowable composite resin (Color A2, Clearfil Majesty Flow, Kuraray Noritake) (Fig. 3A) were used, with semispherical morphology and a 2-mm diameter. In the second system, flat markers of the same size were drawn using a dermographic pen (ID&CO S.r.l.) (Fig. 3B).

A B

Fig. 3. Artificial markers on the reference cast. A, Embossed resin composite markers; B, Flat markers made with dermographic pen.

After applying these markers, the above described IOS scanning protocol for sample making was followed. In the Meshlab software, the embossed markers were cut from each experimental scan, so they were not considered during the 3D analyses. Eventually, three experimental groups were obtained: the control group called "no markers" made of scans without markers, the "embossed markers" group for the resin composite markers, and the "flat markers" for the group with markers made using a dermographic pen. The choice of the sample size (n = 10) was supported not only by previous studies (35-38) but also by factor analysis conducted with the Kaiser-Meyer-Olkin (KMO) measure of sampling adequacy and the Bartlett test of sphericity (39).

The accuracy of each experimental scan was evaluated calculating trueness and precision, measured in μm. According to ISO-5725 (40), the accuracy of a measurement method is described by 2 parameters: trueness and precision. "Trueness" refers to the closeness of agreement between the arithmetic mean of many test results and the reference value. “Precision” describes the closeness of agreement between intragroup data obtained by repetitive measurements (40,41). In other terms, trueness defines how a measurement matches the actual value while precision describes the consistency of repeated measurements.

In the software for metrological analysis (Geomagic Control X), the value of standard deviation (SD) was chosen from the "tabular view-3D compare”. This value (SD), calculated by the software, indicates a mean between positive and negative deviations resulting from each superimposition of the digital surfaces. For this reason, the mean between SD values was chosen to evaluate the trueness and precision (5,42) (Fig. 4). The trueness was calculated as the mean SD of each experimental scan from the dRC. Differently, the precision was evaluated as the mean SD of each experimental scan from the one that had obtained the best result about trueness, after the superimposition on the dRC in each of the 3 test groups. In this way, all the intraoral scans of the same group were superimposed on this selected surface model and the precision of each experimental group was obtained as the mean SD detected by each of these superimpositions (5,42).

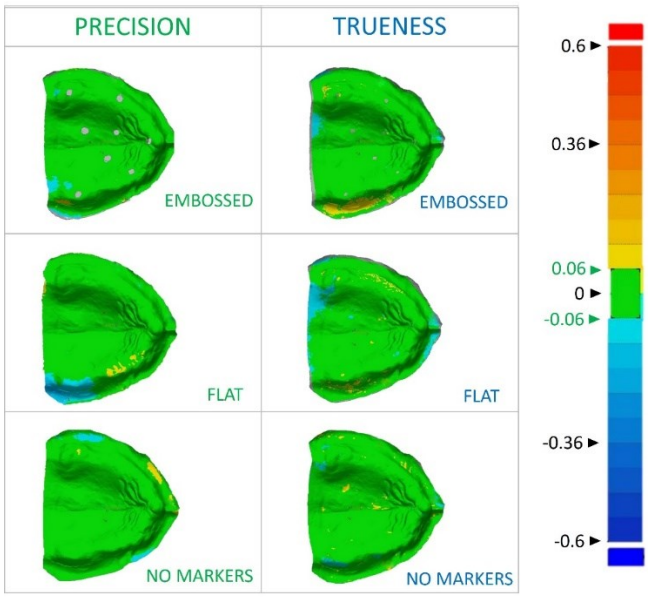

Fig. 4. Analyses of trueness and precision: Best superimposition for each experimental scan group. Green areas indicate minimum displacement of the experimental scan compared to the reference one. Blue and red areas show respectively an inward and outward displacement between the surfaces.

2.4 Statistical analysis

Statistical analyses were performed with dedicated software (IBM SPSS v25; IBM). Descriptive statistics (i.e., mean, standard error, median, interquartile range, 95% confidence interval - c.i. 95%) were run for both trueness and precision measurements. Besides, the Shapiro-Wilk test was used to check data normality, the Levene test was run to evaluate the homogeneity of the variances, while the Welch robust test of equality of means, the Games-Howell, and The Kruskal-Wallis test were conducted to analyze differences among groups ($p = .05$).

3. Results

Both for trueness and precision, the KMO statistics reported $p = .5$, matching with the recommended 0.5 value, and the Bartlett test was statistically significant for trueness ($p = .702$) and precision ($p = .914$).

Figure 2 shows the area accuracy gradient, indicating the areas that exceed the range of specific tolerance of ±60 µm with inward (blue) displacements on the posterior portion of the papilla and the tubers, or outward (orange) displacements on the palate and the flattened areas of the edentulous ridges (Fig. 2). The buccal vestibule and the area posteriorly to the prosthetic seal

were not considered because they are virtual cavities and surfaces which can mobilize during the making of the optical impression due to their attached muscles.
The descriptive statistics for trueness (c.i. 95%) with upper-lower bounds, means, and standard errors are summarized in Table 1 and shown in Figure 5.

Table 1. Descriptive statistics for trueness (µm)

Experimental Group	Lower-Upper bound (95% c.i.)	Mean	Standard Error
No Markers	39.2 - 58.3	48.8	4.21
Embossed Markers	37.5 - 40.8	39.2	0.74
Flat Markers	47.7 - 73.4	60.5	5.68

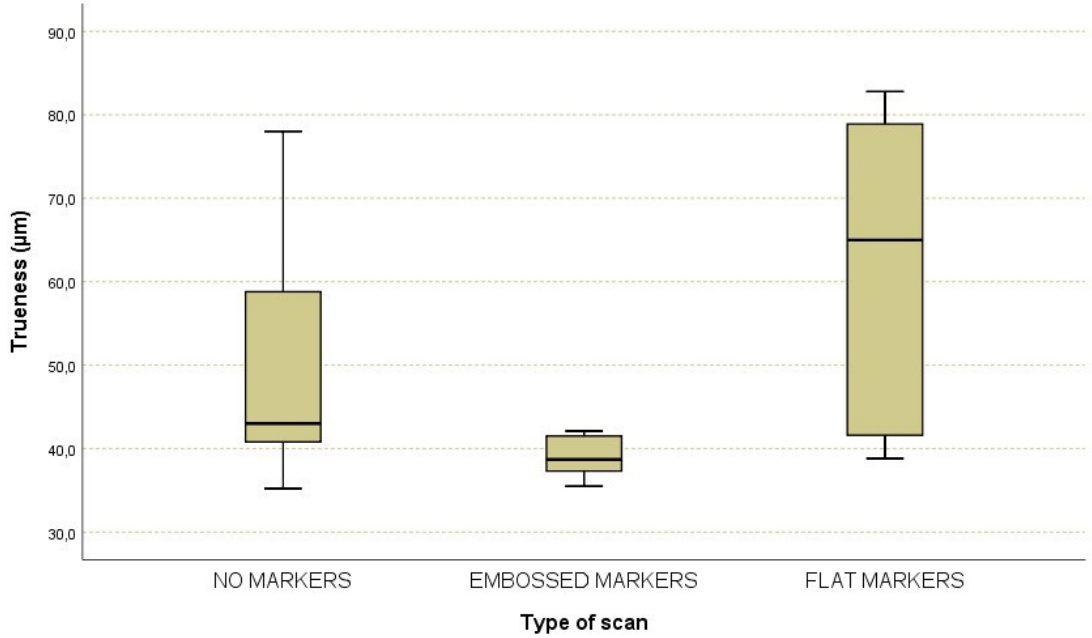

Fig. 5. Box plot chart of trueness descriptive statistics. Whiskers above and below boxes show minimum and maximum, while box spans exhibit the first quartile to the third quartile. The median is displayed by segments inside the box. Possible outliers are unfilled circles.

The mean values were normally distributed for each experimental group, as detected by the Shapiro-Wilk test ($p>.05$). The Levene test did not show homogeneity of the variances ($p<.001$) for the experimental groups. Welch robust test of equality of means reported a significative value ($p = .004$) and statistically significant differences were detected with the Games-Howell post hoc test between embossed markers and flat markers ($p = .011$). No significant differences were found between the control group and embossed markers ($p = .113$) and between the control group and flat markers ($p = .249$) (Table 2).

As regards the analysis of precision, the descriptive statistics (c.i. 95%) with upper-lower bounds, means, and standard errors are shown in Table 3 and displayed in Figure 6.

The mean values were not normally distributed for all the groups, as reported by the Shapiro-Wilk test ($p<.05$). The Levene test showed no homogeneity of the variances ($p = .002$) for the experimental groups. A log10 transformation of the data was performed because the assumptions on the normal distribution and the homogeneity of the variances were violated to run a One-Way ANOVA. After this transformation, again the Shapiro-Wilk test detected no normal distribution ($p<.05$), but the Levene test reported homogeneity of the variances ($p = .118$). Therefore, the Kruskal-Wallis ($p = .002$) and the Dunn tests were run to evaluate if there were any statistically significant differences between the mean values of the 3 groups, and the significance values were calculated according to the Bonferroni correction. Statistically significant differences were found between flat markers with both the control group ($p = .005$) and embossed markers ($p = .008$) (Table 2).

About the analysis of trueness and precision, the color bar map of the best superimposition for each group of scans did not show outward and inward displacements greater than 360 µm (Fig. 4).

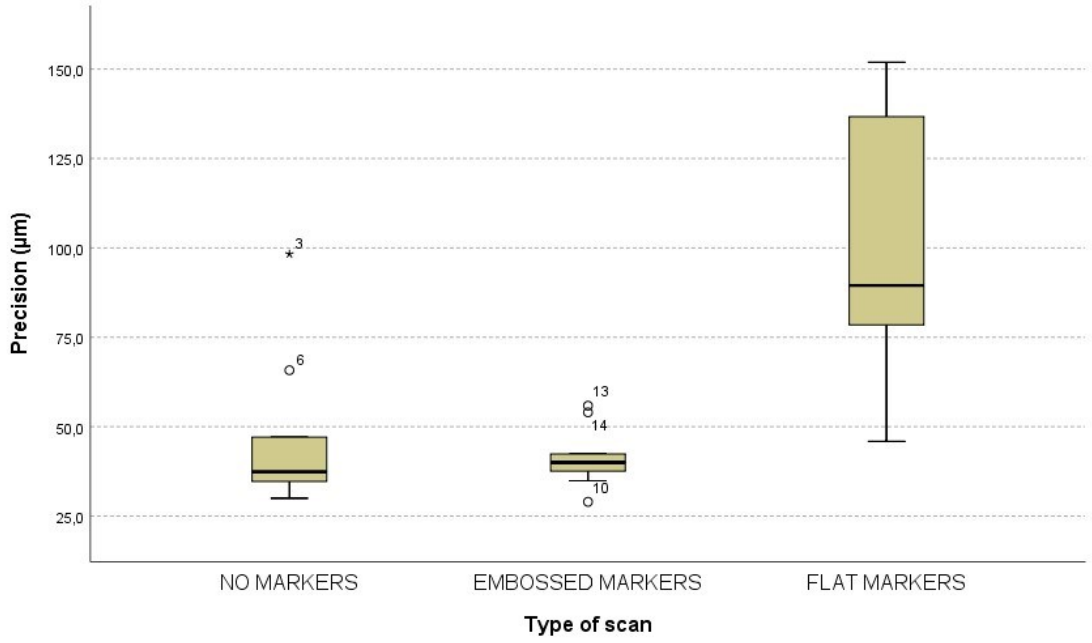

Fig. 6. Box plot chart of precision descriptive statistics. Whiskers above and below boxes show minimum and maximum, while box spans exhibit the first quartile to the third quartile. The median is displayed by segments inside the box. Possible outliers are unfilled circles.

Table 2. *P* values of post hoc comparisons

Experimental Group	Trueness	Precision
No Markers – Embossed Markers	.113	1
No Markers – Flat Markers	.249	.005*
Embossed Markers – Flat Markers	.011*	.008*

*=Statistically significant differences (p<.05).

Table 3. Descriptive statistics for precision (μm)

Experimental Group	Lower-Upper bound (95% c.i.)	Mean	Standard Error
No Markers	29.7 - 63.7	46.7	7.36
Embossed Markers	34.7 - 48	41.4	2.87
Flat Markers	69.3 - 130.3	99.8	13.22

4. Discussion

The present study was aimed to assess the accuracy gradient for the areas of scans made with IOS on a completely edentulous maxilla, and the accuracy of scans made using two different systems involving artificial markers. According to the color bar map (Fig. 2), the first null hypothesis stating that there is no difference among the several anatomic areas of a totally edentulous maxilla scan was rejected.

Also, the second null hypothesis was rejected because some statistically significant differences were found among the trueness and precision of scans made with the two tested systems involving artificial markers and the control group.

The three-dimensional analysis of the superimposed scans (Fig. 2) revealed that the accuracy is worse in the flattened areas of the ridges, the maxillary tuberosities, the posterior aspect of the papilla, and the palate. The reason might be that the typical smooth surface without anatomical landmarks of the tubers and ridges' flat areas makes the stitching process very difficult (20,21,29). Regarding the palate and the posterior aspect of the papilla, the stitching algorithm is hampered by the palatine vault that hinders the IOS movements due to the cumbersome size of the tip (19,22,23,27).

However, it is important to underline that the areas of the buccal vestibule and the soft palate were not considered in this three-dimensional analysis, because, as reported in the literature, they

could be mobilized by the attached musculature, providing unrealistic virtual surfaces during the scanning process (18,23,26-28).

Post hoc comparisons between the 3 experimental groups (no markers, embossed markers, and flat markers) revealed statistically significant differences for the precision between flat markers and the control group ($p = .005$) and both for trueness and precision between flat markers and embossed ones (trueness: $p = .011$; precision: $p = .008$). These data show that the use of flat markers not only does not improve the accuracy but also worsens the precision. The reason might be that the ink the markers are made of, could be able to reflect the IOS light beam in an altered way towards its sensor. Furthermore, according to the literature (16,29), the areas with variations in the surface geometry can enhance the stitching process. Therefore, it should be considered as efficient markers only those which determine variations in the surface and not in the color of an area. At the same time, no statistically significant differences were found between scans made with embossed markers and the control group, despite both the trueness and precision of the embossed markers scans were better (trueness means: embossed markers = 39.2 μm, no markers = 48.8 μm; precision means: embossed markers = 41.4 μm, no markers = 46.7 μm).

Besides, the values of the lower-upper bounds (c.i. 95%) of the 3 experimental groups oscillate between 37.5-73.4 μm for the trueness and 29.7-130.3 μm for the precision. These values are comparable to those reported in other studies with similar research designs (16,19), and above all, they are clinically acceptable as they do not exceed the threshold of 500 μm, considered as the tolerated error for the fabrication of a removable denture (18).

According to the present results, the tested IOS (TRIOS 3) has been confirmed to be suitable for detecting residual ridges and palate, as reported by Rasaie et al (18).

The present investigation had some limitations, primarily due to its in vitro / in silico nature. Specifically, the experimental samples were scanned with the IOS on an edentulous maxillary cast, therefore, clinically relevant factors such as humidity, temperature, optical aspects, resilience and mobility of soft tissues, and intraoral anatomic limitations were not factored. To corroborate the findings of this study, further research should be done, including a larger sample size and clinical trials.

5. Conclusions

Based on the findings of the present in silico analysis, the following conclusions can be drawn with the tested IOS, on a completely edentulous maxillary cast:

1. the most inaccurate scans areas were the tuberosities, palate, posterior portion of the papilla, and flattened areas of the ridges;
2. both trueness and precision of scans made using embossed markers were better than those made with flat markers;
3. the precision of scans made with flat markers was worse than those without markers, but no difference was detected for the trueness;
4. no differences in trueness and precision occurred between scans made with embossed markers and without markers;
5. the accuracies of the tested scans were clinically acceptable to manufacture a removable denture;

Further in vitro and in vivo studies, and randomized controlled trials, are needed to support the outcomes of the present paper.

References

1. Zimmermann M, Mehl A, Mörmann WH, Reich S. Intraoral scanning systems - a current overview. Int J Comput Dent 2015;18(2):101-29.

2. Ahlholm P, Sipilä K, Vallittu P, Jakonen M, Kotiranta U. Digital Versus Conventional Impressions in Fixed Prosthodontics: A Review. J Prosthodont 2018;27(1):35-41.

3. Joda T, Lenherr P, Dedem P, Kovaltschuk I, Bragger U, Zitzmann NU. Time efficiency, difficulty, and operator's preference comparing digital and conventional implant impressions: a randomized controlled trial. Clin Oral Implants Res 2017;28(10):1318-23.

4. Goracci C, Franchi L, Vichi A, Ferrari M. Accuracy, reliability, and efficiency of intraoral scanners for full-arch impressions: a systematic review of the clinical evidence. Eur J Orthod 2016;38(4):422-8.

5. Imburgia M, Logozzo S, Hauschild U, Veronesi G, Mangano C, Mangano FG. Accuracy of four intraoral scanners in oral implantology: a comparative in vitro study. BMC Oral Health 2017;17(1):92.

6. Lawson NC, Burgess JO. Clinicians reaping benefits of new concepts in impressioning. Compend Contin Educ Dent 2015;36(2):152-3.

7. Marti AM, Harris BT, Metz MJ, Morton D, Scarfe WC, Metz CJ, Lin WS. Comparison of digital scanning and polyvinyl siloxane impression techniques by dental students: instructional efficiency and attitudes towards technology. Eur J Dent Educ 2017;21(3):200-5.

8. Amornvit P, Rokaya D, Sanohkan S. Comparison of Accuracy of Current Ten Intraoral Scanners. Biomed Res Int 2021;2021:2673040.

9. Nedelcu R, Olsson P, Nyström I, Thor A. Finish line distinctness and accuracy in 7 intraoral scanners versus conventional impression: an in vitro descriptive comparison. BMC Oral Health 2018;18(1):27.

10. Nulty AB. A Comparison of Full Arch Trueness and Precision of Nine Intra-Oral Digital Scanners and Four Lab Digital Scanners. Dent J (Basel). 2021;9(7):75.

11. Koulivand S, Ghodsi S, Siadat H, Alikhasi M. A clinical comparison of digital and conventional impression techniques regarding finish line locations and impression time. J Esthet Restor Dent 2020;32(2):236-43.

12. Sakornwimon N, Leevailoj C. Clinical marginal fit of zirconia crowns and patients' preferences for impression techniques using intraoral digital scanner versus polyvinyl siloxane material. J Prosthet Dent 2017;118(3):386-91.

13. Zarone F, Ruggiero G, Ferrari M, Mangano F, Joda T, Sorrentino R. Accuracy of a chairside intraoral scanner compared with a laboratory scanner for the completely edentulous maxilla: An in vitro 3-dimensional comparative analysis. J Prosthet Dent 2020;124(6):761.e1-761.e7.

14. Chochlidakis KM, Papaspyridakos P, Geminiani A, Chen CJ, Feng IJ, Ercoli C. Digital versus conventional impressions for fixed prosthodontics: A systematic review and meta-analysis. J Prosthet Dent 2016;116(2):184-190.e12.

15. Flügge TV, Att W, Metzger MC, Nelson K. Precision of Dental Implant Digitization Using Intraoral Scanners. Int J Prosthodont 2016;29(3):277-83.

16. Zarone F, Ruggiero G, Ferrari M, Mangano F, Joda T, Sorrentino R. Comparison of different intraoral scanning techniques on the completely edentulous maxilla: An in vitro 3-dimensional comparative analysis. J Prosthet Dent 2020;124:768.

17. Zhongpeng Y, Tianmin X, Ruoping J. Deviations in palatal region between indirect and direct digital models: an in vivo study. BMC Oral Health 2019;19:66.

18. Rasaie V, Abduo J, Hashemi S. Accuracy of Intraoral Scanners for Recording the Denture Bearing Areas: A Systematic Review. J Prosthodont 2021;30:520-39.

19. Patzelt SB, Vonau S, Stampf S, Att W. Assessing the feasibility and accuracy of digitizing edentulous jaws. J Am Dent Assoc 2013;144:914-20.

20. Lee JH, Yun JH, Han JS, Yeo IL, Yoon HI. Repeatability of Intraoral Scanners for Complete Arch Scan of Partially Edentulous Dentitions: An In Vitro Study. J Clin Med 2019;8(8):1187.

21. Tasaka A, Uekubo Y, Mitsui T, Kasahara T, Takanashi T, Homma S, Matsunaga S, Abe S, Yoshinari M, Yajima Y, Sakurai K, Yamashita S. Applying intraoral scanner to residual ridge in edentulous regions: in vitro evaluation of inter-operator validity to confirm trueness. BMC Oral Health. 2019;19(1):264.

22. Schimmel M, Akino N, Srinivasan M, Wittneben JG, Yilmaz B, Abou-Ayash S. Accuracy of intraoral scanning in completely and partially edentulous maxillary and mandibular jaws: an in vitro analysis. Clin Oral Investig 2021;25(4):1839-47.

23. Deferm JT, Schreurs R, Baan F, Bruggink R, Merkx MAW, Xi T, Bergé SJ, Maal TJJ. Validation of 3D documentation of palatal soft tissue shape, color, and irregularity with intraoral scanning. Clin Oral Investig 2018;22:1303-9.

24. Mennito AS, Evans ZP, Nash J, Bocklet C, Kelly AL, Bacro T, Cayouette M, Ludlow M, Renne WG. Evaluation of the trueness and precision of complete arch digital impressions on a human maxilla using seven different intraoral digital impression systems and a laboratory scanner. J Esthet Restor Dent 2019;31(4):369-77.

25. Osnes CA, Wu JH, Venezia P, Ferrari M, Keeling AJ. Full arch precision of six intraoral scanners in vitro. J Prosthodont Res 2020;64(1):6-11.

26. Hack G, Liberman L, Vach K, Tchorz JP, Kohal RJ, Patzelt SBM. Computerized optical impression making of edentulous jaws - An in vivo feasibility study. J Prosthodont Res 2020;64(4):444-53.

27. Gan N, Xiong Y, Jiao T: Accuracy of intraoral digital impressions for whole upper jaws, including full dentitions and palatal soft tissues. PLoS One 2016;11:e0158800.

28. Chebib N, Kalberer N, Srinivasan M, Maniewicz S, Perneger T, Müller F. Edentulous jaw impression techniques: An in vivo comparison of trueness. J Prosthet Dent 2019;121(4):623-30.

29. Kim JE, Amelya A, Shin Y, Shim JS. Accuracy of intraoral digital impressions using an artificial landmark. J Prosthet Dent 2017;117:755-61.

30. Fang JH, An X, Jeong SM, Choi BH. Digital intraoral scanning technique for edentulous jaws. J Prosthet Dent 2018;119:733-5.

31. Lee JH. Improved digital impressions of edentulous areas. J Prosthet Dent 2017;117:448-9.

32. Papaspyridakos P, Chen YW, Gonzalez-Gusmao I, Att W. Complete digital workflow in prosthesis prototype fabrication for complete-arch implant rehabilitation: A technique. J Prosthet Dent 2019;122(3):189-92.

33. Negreiros WM, Hamilton A, Gallucci GO. A completely digital workflow for the transition from a failed dentition to interim complete-arch fixed implant-supported prostheses: A clinical report. J Prosthet Dent 2020:S0022-3913(20)30698-3.

34. Mandelli F, Gherlone E, Gastaldi G, Ferrari M. Evaluation of the accuracy of extraoral laboratory scanners with a single-tooth abutment model: a 3D analysis. J Prosthodont Res 2017;61:363-70.

35. Medina-Sotomayor P, Pascual-Moscardó A, Camps I. Accuracy of four digital scanners according to scanning strategy in complete-arch impressions. PLoS One 2018;13:e0202916.

36. Ender A, Zimmermann M, Mehl A. Accuracy of complete- and partial-arch impressions of actual intraoral scanning systems in vitro. Int J Comput Dent 2019;22(1):11-19.

37. Treesh JC, Liacouras PC, Taft RM, Brooks DI, Raiciulescu S, Ellert DO, Grant GT, Ye L. Complete-arch accuracy of intraoral scanners. J Prosthet Dent 2018;120(3):382-8.

38. Mangano FG, Hauschild U, Veronesi G, Imburgia M, Mangano C, Admakin O. Trueness and precision of 5 intraoral scanners in the impressions of single and multiple implants: a comparative in vitro study. BMC Oral Health 2019;19:101.

39. Harper D, Kim JO, Mueller CW. Introduction to factor analysis: what it is and how to do it. Contemp Sociol 1980;9:562.

40. International Organization for Standardization. ISO 5725-1. Accuracy (trueness and precision) of measurement methods and results. Part 1: general principles and definitions. Berlin: International Organization for Standardization; 1994.

41. Sim JY, Jang Y, Kim WC, Kim HY, Lee DH, Kim JH. Comparing the accuracy (trueness and precision) of models of fixed dental prostheses fabricated by digital and conventional workflows. J Prosthodont Res 2019;63:25-30.

42. Zarone F, Ruggiero G, Di Mauro MI, Spagnuolo G, Ferrari M, Sorrentino R. Accuracy of Three Impression Materials on the Totally Edentulous Maxilla: In Vitro/In Silico Comparative Analysis. Materials (Basel) 2020;13(3):515. doi:10.3390/ma13030515.

2.5 ACCURACY OF INTRAORAL SCANNER SYSTEM ON DIFFERENT PALATAL MORPHOLOGIES FOR THE EDENTULOUS POPULATION: A THREE-DIMENSIONAL ANALYSIS

Ruggiero Gennaro, Sorrentino Roberto, Leone Renato, Joda Tim, Zarone Fernando

Article in press

INTRODUCTION

Digital technologies are increasingly used in clinical dentistry and among these, the intraoral scanner (IOS) brings significant advantages compared to traditional procedures for making impressions. In particular, thanks to IOS there is a simplification of clinical procedures, with a reduction in operating times and the prosthesis' fabrication [1-2], better communication with patients and dental technicians [3-4], absence of gypsum casts [5-6], and less stress and discomfort for the patients [5, 7].

However, to date, it is challenging to detect accurate intraoral scans in the case of a completely edentulous maxilla, due to the absence of natural landmarks, such as teeth, which facilitate the IOS stitching algorithm [8]. In this regard, it has been reported in the literature that scanning accuracy in an edentulous area can be improved by placing artificial landmarks [8-9]. Several authors have tried to use artificial landmarks positioned intraorally on the upper jaw. Among them, Fang et al. suggested placing semispherical resin composite markers, directly on the palate, as it is one of the most difficult areas to be detected, because of the morphology of the vault and the absence of natural markers [10-11]. Differently, Lee drew strips made of zinc oxide-eugenol on the palatal mucosa [12]. Nevertheless, no experimental data or findings were reported about the effectiveness of these 2 approaches. We also tried to figure out what shape and material these markers should be and where to place them on the upper jaw [11]. Besides,

some regions have a low accuracy gradient, among these, there are tuberosities, the posterior portion of the papilla, the flattened areas of the ridges, and above all the palate [11].
Several studies have evaluated the accuracy of IOS scans in the palatal area. Deferm et al. [13] showed that the width of the palatal vault may negatively affect the accuracy of the scans, while the depth of the vault may have no influence [13]. Similar trueness results were reported by Gan et al. [14] at the palatal level [14].
In contrast, Zhongpeng et al. [15] investigated the scan sequences and found that the trueness in the palatal region is affected by the scanning strategy and that the palate should be scanned starting from the palatal aspect of the molars [15].
Furthermore, in the study made by Mennito et al, no significant differences in palatal accuracy were found between several IOSs tested [16]. It is worth noticing that, in these studies on the palate, the teeth were present in the arch, and this could have affected the accuracy of the scans in the palatal region, as the teeth can be considered anatomical landmarks.
To date, only the study by Osman et al. evaluated the palate in the case of complete edentulism and reported that no significant difference was found for different depths of the palatal vault [17].
However, an important role could be played by the palatal wrinkles (also named “palatal rugae”), which, when present, could represent valid anatomical landmarks in the palatal region, able of increasing accuracy [18]. Suffice it to consider that due to their morphological characterizations, they are usually used in orthodontics to evaluate dental changes through three-dimensional superimpositions [19-21].
Given these premises, it is fair to hypothesize that different palatal depths could influence the accuracy of scans on the edentulous maxilla. Furthermore, the presence of anatomical landmarks such as the palatine rugae can be an element able of increasing the accuracy of the scans.
To date, in the literature, there is a lack of data regarding the accuracy of different palatal morphologies and their influence on scans. Furthermore, it is not clear whether the palatal rugae, as anatomical landmarks, could be a positive factor for the accuracy of scans on completely edentulous upper jaws.
Given the increase in life expectancy of the world population and the growing demand for prostheses in the edentulous [22], it is important to know each factor, including palatal morphologies, that could affect the accuracy of IOS scans.
The first aim of the present study is to evaluate whether different depths of the palate can influence the accuracy of the scans. The second is to evaluate whether the accuracy could be enhanced by the presence of palatal rugae.

The null hypothesis is that there are no significant differences among the different experimental groups of scans performed in the case of different palatal morphologies.

MATERIALS AND METHODS

A reference typodont was manufactured by pouring polyurethane resin (PRIMA-DIE; Gerhò S.P.A.) inside a mold of a standard edentulous maxilla showing well-defined palatal rugae, obtained from a real model previously used for a clinical purpose and duplicated through a dedicated silicone material (Elite Double; Zhermack SpA). The present typodont was scanned using an industrial metrological scanning machine (Atos Core 80; GOM), based on a structured white light technology with the following settings: working distance = 170 mm, point spacing = 0.03 mm, measure accuracy = ±0.0025 mm. The model scan (MS) was edited with CAD software (Exocad Galway 3.0, exocad GmbH; Darmstadt, Germany) in order to obtain 6 different typodonts, with flat, medium, and deep palates with and without palatal rugae (Fig. 1).

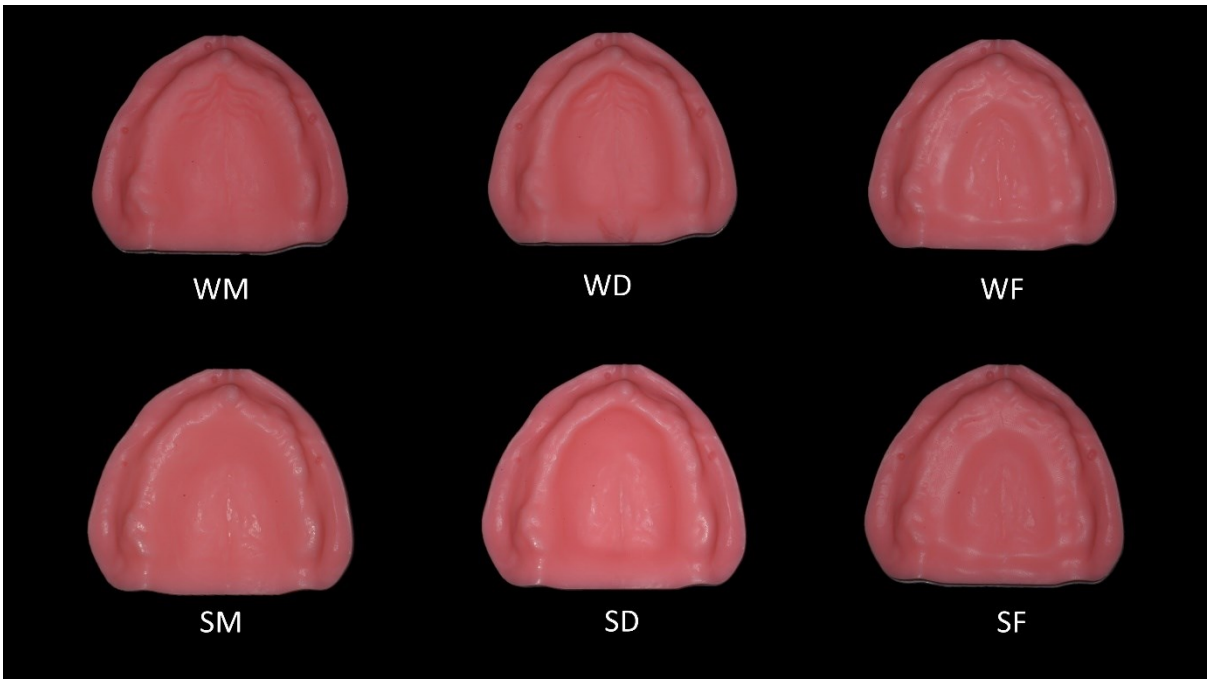

Figure 1. Reference typodonts for each tested depth, with or without palatal wrinkles. WM: wrinkled medium; WD, wrinkled deep; WF, wrinkled flat; SM, smooth medium; SD, smooth deep; SF, smooth flat.

The 6 reference digital models were named as follows: dSM, dSD, and dSF for the smooth models respectively for medium, deep, and flat palate; while for the models with wrinkles they were called dWM, dWD, and dWF, respectively for medium, deep and flat palate. The models with the medium palate (dWM and dSM) maintained the original palatal depth of MS, while

dSD and dWD had a 5 mm deepening of the palate. Conversely, a 5mm elevation was made for dSF and dWF in order to create a flatter palate.

After the CAD design, the 6 typodonts were printed with a three-dimensional printing machine (Anycubic Photon S, Shenzhen, China) with a dedicated resin (Anycubic 3D Printing UV Sensitive Resin, Shenzhen, China) in order to obtain the corresponding physical reference models (SM, SD, SF, WM, WD, and WF).

The six reference models were then scanned using one IOS system (Trios 4, software v21.4, 3Shape, Copenhagen, Denmark), according to a validated scanning technique [18] to obtain 10 scans for each experimental group.

As regards the scanning technique, the ridge top side of the edentulous arch was first scanned, starting from the left maxillary tuberosity, proceeding longitudinally along the ridge and ending at the right tuberosity, then continuing on the buccal side and finally on the palatal vault; the latter was first scanned with a counterclockwise movement along the palatal vault and finally with a longitudinal movement in the postero-anterior direction to close the gap along the midline of the palate. The palatal side was scanned with a circular movement in a clockwise direction along the palatal vault until the left maxillary tuberosity and finally with a counterclockwise movement until the contralateral tuberosity [18].

Anatomic areas needed for the fabrication of a complete maxillary denture were included in the scans. All scans were performed by the same experienced prosthodontist (R.L.), on the same day and in the same room, under similar light and environmental conditions: temperature of 22 °C, air pressure of 760 ± 5 mmHg, and 45% relative humidity. The scans were made sequentially, with an interval of 10 minutes, in order to allow the operator to rest and to enable a proper cooling of the device [3, 23]. The number of shots per scan varied between 537 and 1109 and the time for a full-arch scan was comprised of between 1 and 2 minutes.

All STL-files acquired with the IOS were imported into dedicated software (Meshlab v2016.12; ISTI-CNR) using the digital reference model as guides to cut the surplus surfaces of each three-dimensional digital experimental model. Both the reference scans and, subsequently, the 6 groups of .stl files were imported into Geomagic Control X (3D SYSTEMS, software v2018.0.1) (Figs. 2, 3) and the accuracy of each one was evaluated by calculating trueness and precision, measured in μm.

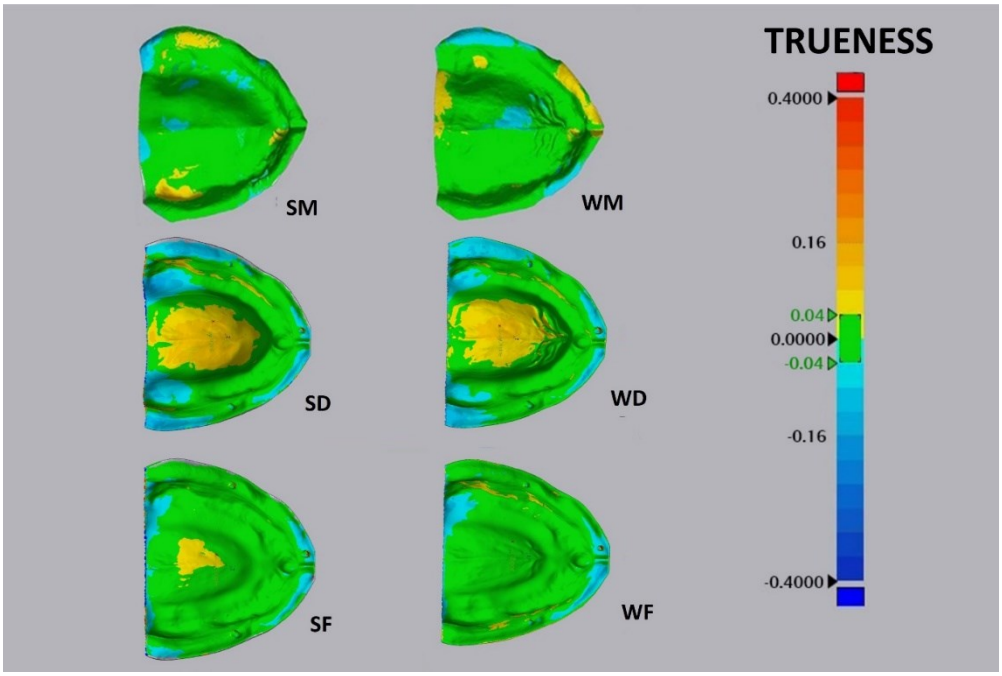

Figure 2. Color bar map for trueness. The best superimpositions for each experimental group. The red areas indicate outward displacements while the blue areas represent inward displacements

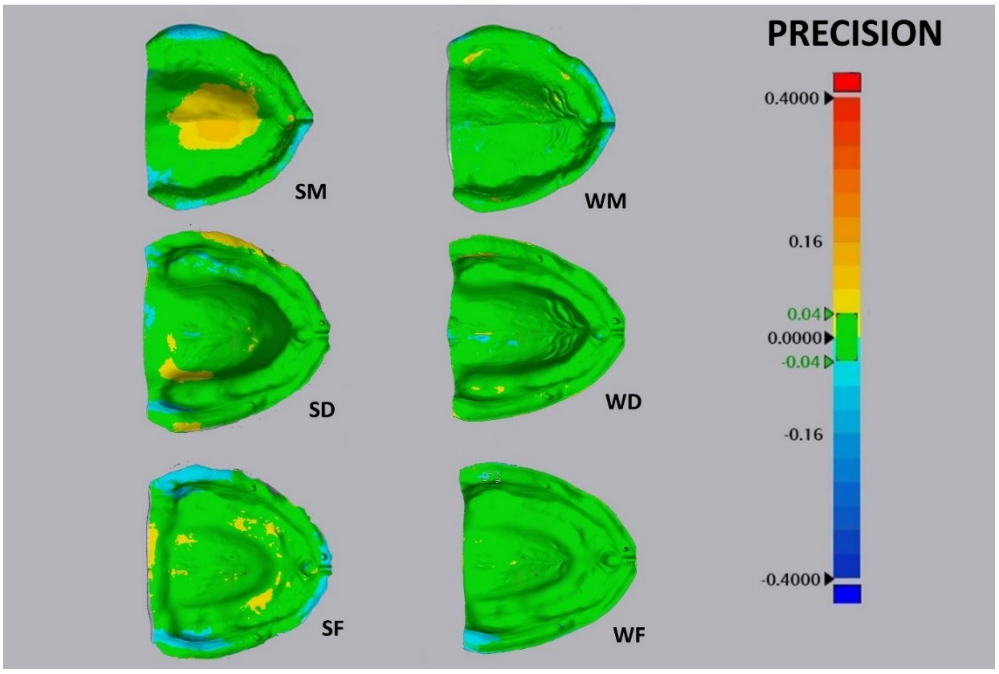

Figure 3. Color bar map for precision. The best superimpositions for each experimental group. The red areas indicate outward displacements while the blue areas represent inward displacements

The sample size (n = 10) was supported by previous studies [24-26] and factor analysis run with the Kaiser-Meyer-Olkin measure of sampling adequacy (KMO) and the Bartlett test of sphericity [27].

The reference typodont scans were input as "reference data" in the software [28]. The scans made on each physical typodont were superimposed on the corresponding digital reference model (e.g., scans made on SM were superimposed on dSM).

An "initial alignment" was performed by the software, followed by a "best fit alignment". After aligning the 2 digital models, the "3D compare" function was activated. The parameters in the "color bar option" were: max range = 0.4 mm, min range= 0.4 mm, and use of specific tolerance = ±0.04 mm. Finally, the value of standard deviation (SD) was chosen from the "tabular view-3D compare". This value (SD), calculated by the software, indicates a mean between positive and negative deviations resulting from each superimposition of the digital surfaces. For this reason, the mean between SD values was chosen to evaluate the trueness and precision [3, 29-30]. With this procedure, a "color map" was created for visual analysis of the displacements between the surfaces of the superimposed digital models. The green areas indicated a minimum displacement of ±0.04 mm of the digital model compared to the "reference data"; the red and blue areas indicated outward and inward displacements respectively of +0.4 mm and -0.4mm (Figs. 2, 3).

According to ISO-5725, the accuracy of a measurement method is described by 2 parameters: "trueness" and "precision". "Trueness" refers to the closeness of agreement between the arithmetic mean of a large number of test results and the reference value; "precision" describes the closeness of agreement between intragroup data obtained by repetitive measurements [31-32]. In other terms, trueness defines how a measurement matches the actual value while precision describes the consistency of repeated measurements.

For each of the 6 experimental groups, the trueness was calculated as the mean (SD) of each model from the corresponding digital reference model. Differently, the precision was evaluated as the mean (SD) of each model from the 3D surface model that had obtained the best result of trueness after the superimposition on the corresponding digital reference model in each of the 6 test groups. Consequently, all the IOS scans of the same group were superimposed on this selected 3D surface model, and the precision of each experimental group was obtained as the mean (SD) detected by each of these superimpositions [3, 29-30].

Statistical analyses were performed with dedicated software (IBM SPSS v25; IBM). To evaluate both trueness and precision, descriptive statistics (i.e. mean, standard error, 95% confidence interval - CI95) and additional calculations to evaluate the overall statistical significance of the differences between the groups (p = .05) were performed. Particularly, the Kolmogorov-Smirnov and Shapiro-Wilk's tests were used to check data normality, the Levene's test was run to evaluate

the homogeneity of variances, and the Kruskal-Wallis and Dunn's test with the Bonferroni's correction were carried out to analyze between-groups differences.
Each possible pairwise comparison between the 6 experimental groups was not conducted in order to evaluate only clinically relevant comparisons. Therefore, it was determined whether differences existed between palatal morphologies with or without rugae, and between the presence or absence of rugae within the different palatal depths.

RESULTS

Both for trueness and precision, the KMO statistics reported $p = .5$, matching with the recommended 0.5 value, and the Bartlett test was statistically significant for trueness ($p = .612$) and precision ($p = .743$).
The results of the descriptive statistics of "trueness" are summarized in Table 1 and displayed in Figure 4. Mean values were not normally distributed for all the groups of scans as reported by the Kolmogorov-Smirnov and Shapiro-Wilk tests ($p < .05$). The Levene test did not show homogeneity of the variances ($p = .017$). A $\log_{10}$ transformation of the data was performed because the assumptions on the normal distribution and the homogeneity of the variances were violated in order to run a One-Way ANOVA. After this transformation, the mean values were not normally distributed for all the groups, as reported by the Kolmogorov-Smirnov and Shapiro-Wilk tests ($p < .05$), and the Levene test did not show homogeneity of the variances ($p < .001$). The Kruskal-Wallis and Dunn tests were performed to evaluate if there were any statistically significant differences between the mean values of the 6 groups of scans. These tests indicated to rejection of the null hypothesis ($p < .001$). After the Bonferroni correction, statistically significant differences were found between SM vs SD ($p < .001$), SM vs SF ($p < .001$), and WF vs SF ($p = .003$). The p-values of post-hoc comparisons are reported in Table 2.

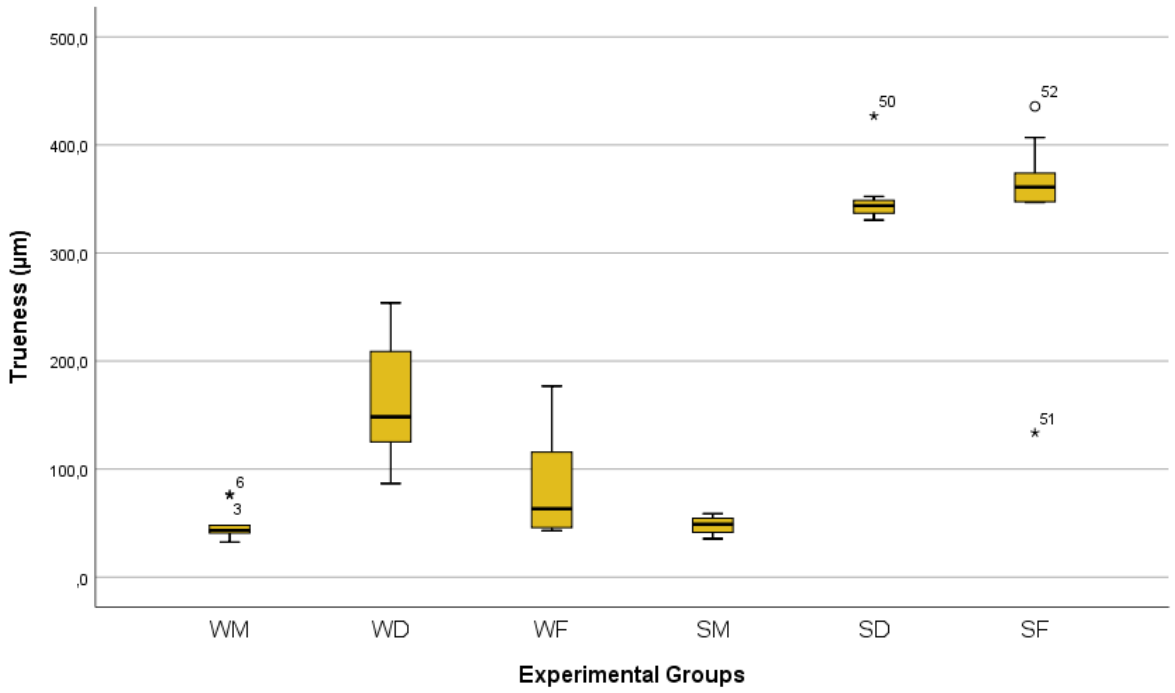

Figure 4. Box plots for trueness. Box spans display the first quartile to the third quartile, while whiskers above and below boxes indicate minimum and maximum. Segments inside the box represent the median. Unfilled circles are possible outliers.

Table 1. Descriptive statistics for trueness (µm) with 95%-confidence intervals (CI95)

Experimental Group	Upper-Lower bound (95% CI)	Mean	Standard Error
WM	37.8-59.5	48.7	4.7
WD	120-203.4	161.7	18.43
WF	49.6-122.2	85.9	16.05
SM	42.4-53.7	48.1	2.47
SD	329.8-369.9	349.9	8.84
SF	291.3-406.8	349.1	25.53

Table 2. *P*-values of post hoc comparisons

Experimental Group	Trueness	Precision
WM vs WD	1.0	1.0
WM vs WF	1.0	1.0
WD vs WF	1.0	1.0
SM vs SD	<.001*	.193
SM vs SF	<.001*	1.0
SD vs SF	1.0	1.0
WM vs SM	1.0	1.0
WF vs SF	.003*	1.0
WD vs SD	1.0	.015*

*=Statistically significant differences ($P < .05$).

The results of the precision descriptive statistics are shown in Table 3 and depicted in Figure 5. Mean values were not normally distributed for all the groups of scans, as detected by the Kolmogorov-Smirnov and Shapiro-Wilk tests ($p < .05$). The Levene test evidenced no homogeneity of variances ($p < .001$) for the different groups. A $\log_{10}$ transformation of the data was performed as to the trueness evaluation. After this transformation, the Shapiro-Wilk test detected again a non-normal distribution ($p < .05$) while the Levene test reported no homogeneity of variances ($p = .001$). The Kruskal-Wallis and Dunn tests indicated to rejection the null hypothesis ($p < .001$). According to Bonferroni correction, statistically significant differences were detected between the means of WD vs SD ($p = .015$). The p-values of post-hoc comparisons are reported in Table 2.

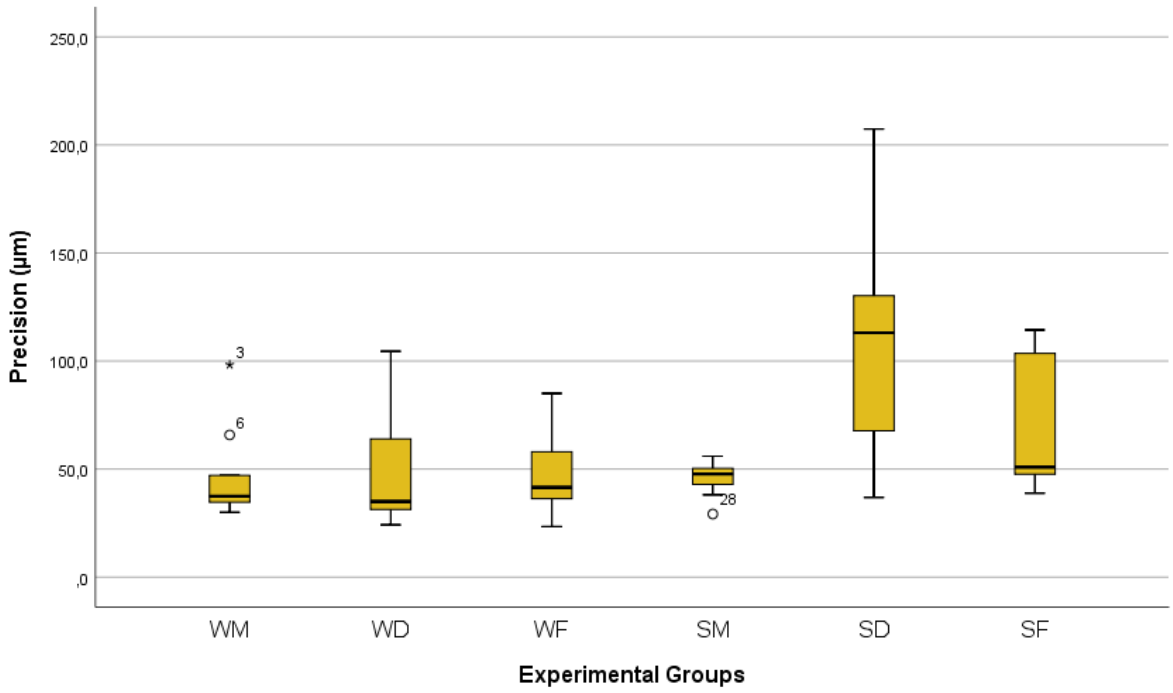

Figure 5. Box plots for precision. Box spans display the first quartile to the third quartile, while whiskers above and below boxes indicate minimum and maximum. Segments inside the box represent the median. Unfilled circles are possible outliers.

Table 3. Descriptive statistics for precision (µm) with 95%-confidence intervals (CI95)

Experimental Group	Upper-Lower bound (95% CI)	Mean	Standard Error
WM	29.7-63.7	46.7	7.36
WD	26-67.7	46.9	9.03
WF	33.3-64.5	48.9	6.78
SM	39.7-52.3	46	2.74
SD	65.7-146	105.9	17.4
SF	47.5-97.7	72.6	10.8

Figures 2-3 show the color bar maps of the best superimposition for each experimental group. The areas exceeding the range of specific tolerance of ±40 µm are represented with inward (blue)

and outward (orange-yellow) displacements. Regarding the trueness of color bar maps in the case of deeper palatal morphologies, it is possible to observe outward displacement (orange) at the bottom of the palatal vault and inward displacement (blue) at the maxillary tubers. No significant results appeared from the precision evaluation of the color bar maps.

Both for trueness and precision, outward and inward displacements greater than 400 μm were not detected (Figs. 2, 3).

The regions posterior to the prosthetic seal and the buccal vestibule were not taken into consideration, because, due to their attached muscles, they are virtual spaces and surfaces that can move during the impression-making with IOS.

DISCUSSION

The present study aimed to compare the trueness and precision of scans performed with an IOS (TRIOS 4, 3Shape) in the case of different palatal depths with or without natural landmarks, such as the palatal rugae.

The null hypothesis stated that there were no significant differences among the experimental groups of scans performed in different palatal morphologies. According to the results of the present study, it was partially rejected.

Although the best trueness and precision were found in the case of medium palatal depth (Tables 1, 3), significant differences were detected only for the trueness between SM vs SD and SM vs SF (Table 2). This means that palatal depth is a relevant factor for trueness in the absence of palatal rugae, while it is not relevant in their presence. The reason why a mid-depth palate is better may be that on a shallow palate, there is an almost smooth surface with no natural landmarks. Additionally, a very deep vault can cause worse trueness than a medium one, and to prove it, Figure 2 shows that for deeper palates, a considerable inaccuracy was found at the bottom of the palatal vault (Figure 2). Furthermore, the presence of a lower accuracy gradient in the palate region is in agreement with another study of ours [11]. For palates with rugae, however, there were no differences in the case of different depths of the palatal vault and this is in agreement with what was reported in recent studies that tested palates with palatal wrinkles [13, 17].

Regarding the influence that palatal rugae may have on accuracy, the results are still controversial. For deep palatal morphologies, the presence of palatal rugae improved the precision of the scans made, but no difference was found in the trueness. Conversely, the trueness of flat palates in the presence of rugae was better than without them. No difference in precision was reported. Furthermore, no difference occurred with or without rugae for medium depth.

Unfortunately, there are no sufficient data in the literature with which to compare our results, but as reported in our previous study, the presence of palatal rugae may increase the accuracy of scans performed on a totally edentulous maxilla as it facilitates the stitching algorithm, although the global

medium value is worse [8-9, 11, 18]. In particular, it should be considered that the software used for the three-dimensional analysis of the overlapped surfaces (Geomagic Control X) calculated the SD value of the global displacement between the entire superimposed surfaces. This means that the palatal rugae area, where accuracy is often worse, has an impact on the calculated global mean value (SD or RMS), but it does not mean that it is detrimental to the stitching process and consequently to the accuracy.
Finally, the mean values of both trueness and precision were clinically acceptable for the fabrication of a removable denture [29, 33], for each experimental group, as it ranged between 46 to 349.9 μm.
The limitations of the present study are related to its in vitro / in silico nature, in which scans were made on 6 resin typodonts. Some clinically relevant factors related to the oral environment have not been reproduced, such as intraoral temperature and humidity, optical characteristics, soft tissue mobility and resilience, and intraoral anatomical encumbrance. More in vitro and in vivo investigations, involving a larger sample size, are needed to confirm the findings of the present study.

CONCLUSIONS

According to the results of the present in silico study, with the tested IOS, the following conclusions may be drawn:

1. the best accuracy was found for medium palatal depth;
2. in the case of the deepest palates, the presence of rugae improves the precision of the scans;
3. the trueness of flat morphologies with rugae was better than without them;
4. a substantial inaccuracy was found at the bottom of the palatal vault and on the maxillary tubers, in the case of deeper palatal depth;
5. the mean values of both trueness and precision were clinically acceptable for the fabrication of a removable denture.

Further in vivo and in vitro investigations might be necessary to validate the findings of the present study.

REFERENCES

1. Joda T, Lenherr P, Dedem P, Kovaltschuk I, Bragger U, Zitzmann NU. Time efficiency, difficulty, and operator's preference comparing digital and conventional implant impressions: a randomized controlled trial. Clin Oral Implants Res 2017;28(10):1318-23.
2. Goracci C, Franchi L, Vichi A, Ferrari M. Accuracy, reliability, and efficiency of intraoral scanners for full-arch impressions: a systematic review of the clinical evidence. Eur J Orthod 2016;38(4):422-8.
3. Imburgia M, Logozzo S, Hauschild U, Veronesi G, Mangano C, Mangano FG. Accuracy of four intraoral scanners in oral implantology: a comparative in vitro study. BMC Oral Health 2017;17(1):92.
4. Lawson NC, Burgess JO. Clinicians reaping benefits of new concepts in impressioning. Compend Contin Educ Dent 2015;36(2):152-3.
5. Zimmermann M, Mehl A, Mörmann WH, Reich S. Intraoral scanning systems - a current overview. Int J Comput Dent 2015;18(2):101-29.
6. Marti AM, Harris BT, Metz MJ, Morton D, Scarfe WC, Metz CJ, Lin WS. Comparison of digital scanning and polyvinyl siloxane impression techniques by dental students: instructional efficiency and attitudes towards technology. Eur J Dent Educ 2017;21(3):200-5.
7. Ahlholm P, Sipilä K, Vallittu P, Jakonen M, Kotiranta U. Digital Versus Conventional Impressions in Fixed Prosthodontics: A Review. J Prosthodont 2018;27(1):35-41.
8. Kim JE, Amelya A, Shin Y, Shim JS. Accuracy of intraoral digital impressions using an artificial landmark. J Prosthet Dent 2017;117:755-61.
9. Rutkūnas V, Gedrimienė A, Al-Haj Husain N, Pletkus J, Barauskis D, Jegelevičius D, Özcan M. Effect of additional reference objects on accuracy of five intraoral scanners in partially and completely edentulous jaws: An in vitro study. J Prosthet Dent. 2021:S0022-3913(21)00560-6.
10. Fang JH, An X, Jeong SM, Choi BH. Digital intraoral scanning technique for edentulous jaws. J Prosthet Dent 2018;119:733-5.
11. Sorrentino R, Ruggiero G, Leone R, Ferrari M, Zarone F. Area accuracy gradient and artificial markers: a three-dimensional analysis of the accuracy of IOS scans on the completely edentulous upper jaw. J Osseointegr 2021;13(4):S257-S264.
12. Lee JH. Improved digital impressions of edentulous areas. J Prosthet Dent 2017;117:448-9.

13. Deferm JT, Schreurs R, Baan F, Bruggink R, Merkx MAW, Xi T, Bergé SJ, Maal TJJ. Validation of 3D documentation of palatal soft tissue shape, color, and irregularity with intraoral scanning. Clin Oral Investig 2018;22:1303-9.

14. Gan N, Xiong Y, Jiao T. Accuracy of intraoral digital impressions for whole upper jaws, including full dentitions and palatal soft tissues. PLoS One 2016;11:e0158800.

15. Zhongpeng Y, Tianmin X, Ruoping J. Deviations in palatal region between indirect and direct digital models: an in vivo study. BMC Oral Health 2019;19:66.

16. Mennito AS, Evans ZP, Nash J, Bocklet C, Lauer Kelly A, Bacro T, Cayouette M, Ludlow M, Renne WG. Evaluation of the trueness and precision of complete arch digital impressions on a human maxilla using seven different intraoral digital impression systems and a laboratory scanner. J Esthet Restor Dent 2019;31:369-77.

17. Osman R, Nawal A. Does the palatal vault form have an influence on the scan time and accuracy of intraoral scans of completely edentulous arches? An in-vitro study. J Adv Prosthodont 2022;14:294-30446.

18. Zarone F, Ruggiero G, Ferrari M, Mangano F, Joda T, Sorrentino R. Comparison of different intraoral scanning techniques on the completely edentulous maxilla: An in vitro 3-dimensional comparative analysis. J Prosthet Dent. 2020;124(6):762.e1-762.e8.

19. Chen G, Chen S, Zhang XY, et al. Stable region for maxillary dental cast superimposition in adults, studied with the aid of stable miniscrews. Orthod Craniofac Res. 2011;14(2):70–9.

20. Choi DS, Jeong YM, Jang I, et al. Accuracy and reliability of palatal superimposition of three-dimensional digital models. Angle Orthod 2010;80(4):497–503.

21. Choi JI, Cha BK, Jostbrinkmann PG, et al. Validity of palatal superimposition of 3-dimensional digital models in cases treated with rapid maxillary expansion and maxillary protraction headgear. Korean J Orthod 2012;42(5):235–41.

22. Global Health Metrics. Global, regional, and national incidence, prevalence, and years lived with disability for 354 diseases and injuries for 195 countries and territories, 1990-2017: a systematic analysis for the global burden of disease study 2017. Lancet 2018;392:1789-1858.

23. Mangano FG, Veronesi G, Hauschild U, Mijiritsky E, Mangano C. Trueness and precision of four intraoral scanners in oral implantology: a comparative in vitro study. PLoS One 2016;11:e0163107.

24. Medina-Sotomayor P, Pascual-Moscardó A, Camps I. Accuracy of four digital scanners according to scanning strategy in complete-arch impressions. PLoS One 2018;13:e0202916.

25. Ender A, Zimmermann M, Mehl A. Accuracy of complete- and partial-arch impressions of actual intraoral scanning systems in vitro. Int J Comput Dent 2019;22(1):11-19.

26. Treesh JC, Liacouras PC, Taft RM, Brooks DI, Raiciulescu S, Ellert DO, Grant GT, Ye L. Complete-arch accuracy of intraoral scanners. J Prosthet Dent 2018;120(3):382-8.

27. Harper D, Kim JO, Mueller CW. Introduction to factor analysis: what it is and how to do it. Contemp Sociol 1980;9:562.

28. Mandelli F, Gherlone E, Gastaldi G, Ferrari M. Evaluation of the accuracy of extraoral laboratory scanners with a single-tooth abutment model: A 3D analysis. J Prosth Res 2017;61:363-70.

29. Zarone F, Ruggiero G, Di Mauro MI, Spagnuolo G, Ferrari M, Sorrentino R. Accuracy of Three Impression Materials on the Totally Edentulous Maxilla: In Vitro/In Silico Comparative Analysis. Materials (Basel) 2020;13(3):515.

30. Zarone F, Ruggiero G, Ferrari M, Mangano F, Joda T, Sorrentino R. Accuracy of a chairside intraoral scanner compared with a laboratory scanner for the completely edentulous maxilla: An in vitro 3-dimensional comparative analysis. J Prosthet Dent 2020;124(6):761.e1-761.e7.

31. International Organization for Standardization. ISO 5725-1. Accuracy (trueness and precision) of measurement methods and results. Part 1: general principles and definitions. Berlin: International Organization for Standardization; 1994. Available at: http://www.iso.org/iso/home.html.

32. Sim JY, Jang Y, Kim WC, Kim HY, Lee DH, Kim JH. Comparing the accuracy (trueness and precision) of models of fixed dental prostheses fabricated by digital and conventional workflows. J Prosthodont Res 2019;63:25-30.

33. Marino G, Canton A. La Protesi Parziale Rimovibile Dalla Teoria Alla Pratica, 1st ed.; Edizioni Martina: Bologna, Italy, 2002; pp. 6-7.

2.6 DIGITAL DEVICES IN MAXILLOFACIAL PROSTHESIS

Alterations in surgical interventions to improve the prosthetic prognosis in patients with mandibular defects: a review of the literature

Ruggiero Gennaro, Bocca Norma, Carossa Massimo, Gassino Gianfranco

J Osseointegr 2020;12(2):736-743.

It is undisputed that digital technologies have become popular in all fields of dentistry. These technologies can improve the prosthetic prognosis, through the production of a more accurate and highly biocompatible prosthesis and with innovative surgical procedures that enhance the biological and mechanical conditions of the tissues on which the prosthesis interfaces.

More specifically, between these technologies, computer-aided design (CAD) systems, computer tomography (CT), reverse engineering, rapid prototyping, and the milling process, allow following a digital workflow that represents a valid alternative to the conventional procedure to make a maxillofacial prosthesis [1]. Through CAD systems it is possible to design both the denture and the framework on which the denture will be placed. Polyetherketoneketone (PEKK) and zirconia are biocompatible materials that can be used as a framework for dental prostheses on implants inserted in fibula grafts [2-3].

To date, unfortunately, scanning a mandibular defect with an intraoral scanner is not a procedure that allows obtaining an accurate reproduction of the jaw. This is due to soft tissue mobility. For this reason, it is recommended to use the conventional procedure of making the impression with elastomeric materials, to develop the gypsum model that can be scanned with a laboratory scanner. Alternatively, it is possible to scan the elastomeric impression directly with a laboratory scanner and then reverse the scan of the impression to obtain a digital reproduction of the mandible. In this second choice, there is not the inaccuracy caused by the dimensional changes that occur during the setting of the gypsum [4].

Moreover, thanks to digital planning technologies, it is possible to prepare the shape of the new mandible from the fibula graft and place the implants on it before that the graft is placed. The surgical approach that allows this requires 2 main phases. In the first phase, the implants are

inserted into the fibula and covered with a split-thickness skin graft to create a gingival-like tissue. In the second phase, the fibula is harvested, osteotomized, and fixed with the denture on the pre-inserted implants. Therefore, guided by the occlusion, the fibula is placed in its final position [5].

References

1. Singare S, Shenggui C, Sheng L. The use of 3D printing technology in human defect reconstruction-a review of cases study. Med Res Innov 2017;1:1-4.
2. Zarone F, Di Mauro MI, Ausiello P, et al. Current status on lithium disilicate and zirconia: a narrative review. BMC Oral Health 2019;19:134. https://doi.org/10.1186/s12903-019-0838-x
3. Oh KC, Park JH, Lee JH, Moon HS. Treatment of a mandibular discontinuity defect by using a fibula free flap and an implant-supported fixed complete denture fabricated with a pekk framework: a clinical report. J Prosthet Dent 2018;119:1021-4.
4. Zarone F, Ruggiero G, Di Mauro MI, et al. Accuracy of three impression materials on the totally edentulous maxilla: in vitro/in silico comparative analysis. Materials 2020;13:515. https://doi.org/10.3390/ma13030515
5. Freudlsperger C, Bodem JP, Engel E, Hoffmann J. Mandibular reconstruction with a prefabricated free vascularized fibula and implant-supported prosthesis based on fully three-dimensional virtual planning. J Craniofac Surg 2014;25:980-2.

Surgical procedures performed to improve the prosthetic prognosis in case of maxillary defects: a review of the literature

Ruggiero Gennaro, Bocca Norma, Magrini Gabriele, D'addona Antontio, Carossa Massimo, Gassino Gianfranco.

J Osseointegr 2019;11:519-524

In the last years, Computer Aided Design/Computer Aided Manufacturing (CAD-CAM) systems and, more generally, digital technologies have become widespread in every field of Dentistry. Recently, significant progress has been made with the use of implants and with digital technology to design surgical guides, patient-specific sub-periosteal implant, superstructures and craniofacial implants [1-3].

A study of Mertens et al. demonstrated that cross-arch CAD/CAM milled superstructures supported by implants and placed in both residual alveolar ridges and contralateral zygomatic bone could enhance obturator stability and improve functional outcomes [2, 4].

Furthermore, the CAD/CAM superstructures improved retention, without any mechanical or biological complications [2].

In the scientific literature there are several case reports and innovative digital workflows for the construction of an obturator prosthesis. The conventional procedures for the realization of these prostheses, however, are not totally supplanted by new digital technologies, in fact to date there is no protocol that does not require at least an "analogic" step compared to a workflow that therefore can not be defined totally digital, but "hybrid", because of the intercalation of at least one analogic step in a digital workflow.

In some works [5-8] the Authors started from the digitization of the upper jaw; the digitization could be obtained with cone beam computed tomography (CBCT) systems [6-9] sometimes associated with the datasets of a magnetic resonance imaging [8] or of an intraoral scanner (IOS) or a laboratory scanner [5, 7].

Other authors [5] first scanned the upper jaw with an IOS and then they designed and printed (with three-dimensional printer) a metal frame as a support to detect a functional impression of the defect.

George Michelinakis [6] scanned the maxilla using a CBCT system, and printed a three-dimensional model, useful to fabricate a custom acrylic tray for the final impression of the remaining maxilla and the maxillary defect.

References

1. N. Vosselman, B. J. Merema, K. P. Schepman, G. M. Raghoebar: Patient-specific subperiosteal zygoma implant for prosthetic rehabilitation of large maxillary defects after oncological resection. Int. J. Oral Maxillofac. Surg. 2019;48:115–117.
2. Mertens C, de San Jose Gonzalez J, Freudlsperger C, et al. Implant-prosthetic rehabilitation of hemimaxillectomy defects with CAD/CAM suprastructures, Journal of Cranio-Maxillo-Facial Surgery. 2016;44:1812-8.
3. Ariani N, Visser A, van Oort RP, et al. Current state of craniofacial prosthetic rehabilitation. Int J Prosthodont. 2013;26:57-67.
4. Schmidt BL, Pogrel MA, Young CW, Sharma A. Reconstruction of extensive maxillary defects using zygomaticus implants. J Oral Maxillofac Surg. 2004;62:82-9.
5. Park JH, Lee KS, Lee JY, Shin SW. Fabricating a Maxillary Obturator Using an Intraoral Digital Impression: A Case History Report. Int J Prosthodont. 2017;30:266-268.
6. Michelinakis G. The use of cone beam computed tomography and three dimensional printing technology in the restoration of a maxillectomy patient using a dental implant retained obturator. J Indian Prosthodont Soc. 2017;17:406-411.
7. Ye H, Ma Q, Hou Y, et al. Generation and evaluation of 3D digital casts of maxillary defects based on multisource data registration: A pilot clinical study. J Prosthet Dent. 2017;118:790-795.
8. Kortes J, Dehnad H, Kotte ANT, et al. A novel digital workflow to manufacture personalized three-dimensional-printed hollow surgical obturators after maxillectomy. Int J Oral Maxillofac Surg. 2018;47:1214-1218.
9. Tasopoulos T, Kouveliotis G, Polyzois G, Karathanasi V. Fabrication of a 3D Printing Definitive Obturator Prosthesis: a Clinical Report. Acta Stomatol Croat. 2017;51:53-58.

Magnetic Resonance Imaging and digitization of the maxilla

Ruggiero Gennaro, Roberto Sorrentino, Fernando Zarone

In press

As reported in the literature, it is possible to digitize the upper jaw in order to obtain a full digital model of the maxilla, useful for the realization of obturator prostheses. The digitization could be obtained with cone beam computed tomography (CBCT) systems [1-4] sometimes associated with the datasets of magnetic resonance imaging [3] or of an intraoral scanner (IOS), or a laboratory scanner [2, 5].

No data are reported about the ability of Magnetic Resonance Imaging systems (MRI) in digitizing, alone, the maxilla, as reported for CBCT by George Michelinakis [1].

It would have been useful to obtain feasible digitization by means of MRI, as these systems are not as invasive as CBCT. Moreover, the MRI is frequently prescribed by a maxillofacial surgeon or oncologist, for follow-up control.

Nevertheless, MRI is capable of detecting tissues with plenty of water due to the resonance technologies on which it is based. So it is not indicated in the reproduction of bone tissue.

In Figure 1, it could be possible to see the protocol of isolation of the area surrounding the maxillary defect (Fig. 1A-1E) in order to compare the MRI digitization with the one obtained by scanning the gypsum cast with a laboratory scanner (Fig. 1F).

Finally, it appears clear that today it is not possible to obtain an MRI digitization that is capable of reproducing the volumes necessary to make a prosthetic obturator. This technology (MRI), as shown in the figures, creates such an inaccurate reproduction of the jaw that it cannot even be superimposed on an intraoral scan made with an intraoral scanner.

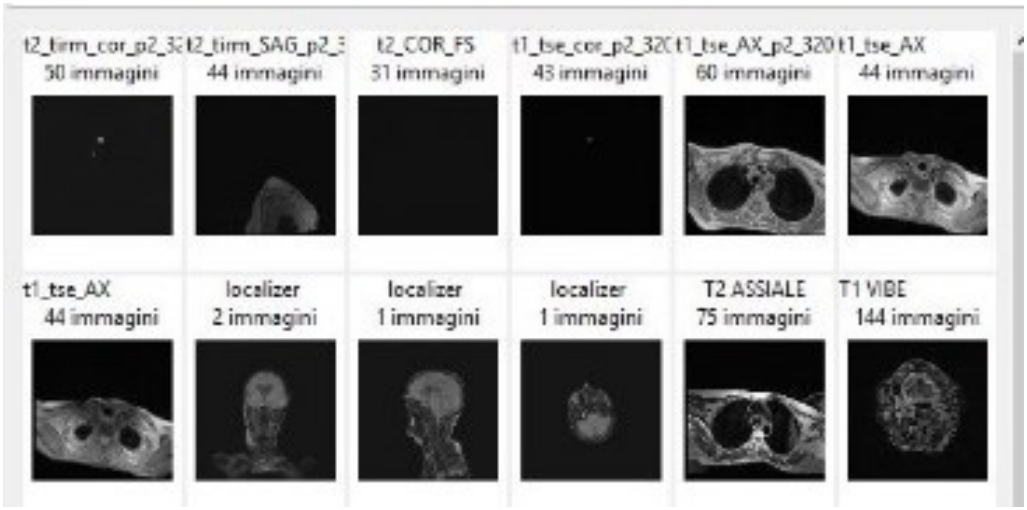
t2_tirm_cor_p2_3
50 immagini
t2_tirm_SAG_p2_3
44 immagini
t2_COR_FS
31 immagini
t1_tse_cor_p2_320
43 immagini
t1_tse_AX_p2_320
60 immagini
t1_tse_AX
44 immagini
t1_tse_AX
44 immagini
localizer
2 immagini
localizer
1 immagini
localizer
1 immagini
T2 ASSIALE
75 immagini
T1 VIBE
144 immagini

A

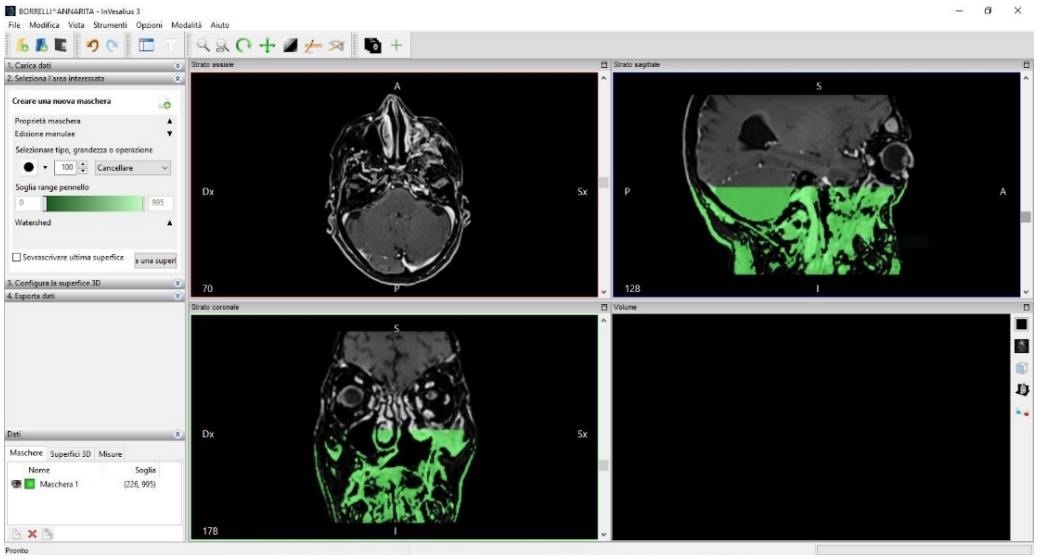
BORRELLI^ANNARITA - InVesalius 3
File Modifica Vista Strumenti Opzioni Modalità Aiuto
1. Carica dati
2. Seleziona l'area interessata
Creare una nuova maschera
Proprietà maschera
Edizione manuale
Selezionare tipo, grandezza o operazione
Cancellare
Soglia range pennello
Watershed
Sovrascrivere ultima superficie
3. Configura la superficie 3D
4. Esporta dati
Dati
Maschere
Superfici 3D
Misure
Nome
Soglia
Maschera 1
(226, 995)
Strato assiale
Strato sagittale
Strato coronale
Volume
Dx
Sx
70
128
178
Pronto

B

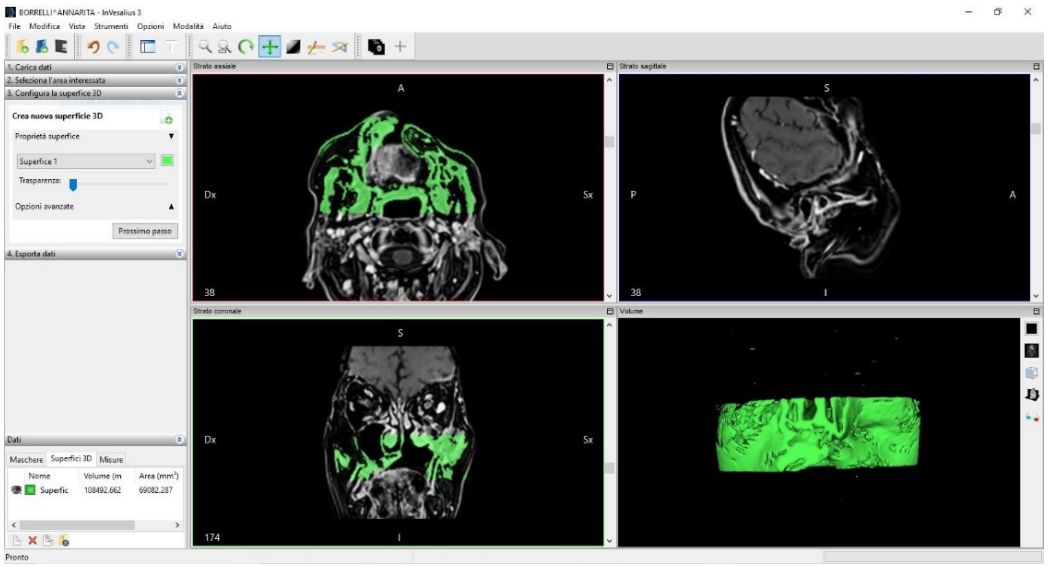
BORRELLI^ANNARITA - InVesalius 3
File Modifica Vista Strumenti Opzioni Modalità Aiuto
1. Carica dati
2. Seleziona l'area interessata
3. Configura la superficie 3D
Crea nuova superficie 3D
Proprietà superficie
Superficie 1
Trasparenza:
Opzioni avanzate
Prossimo passo
4. Esporta dati
Dati
Maschere
Superfici 3D
Misure
Nome
Volume (m
Area (mm²)
Superfic
108492.662
69082.287
Strato assiale
Strato sagittale
Strato coronale
Volume
Dx
Sx
38
38
174
Pronto

C

D 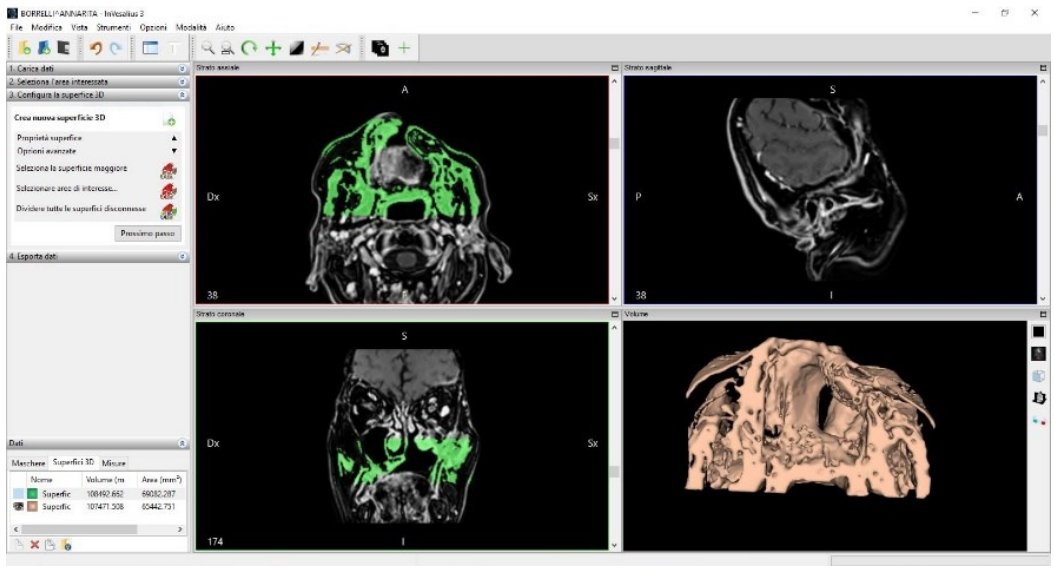

E 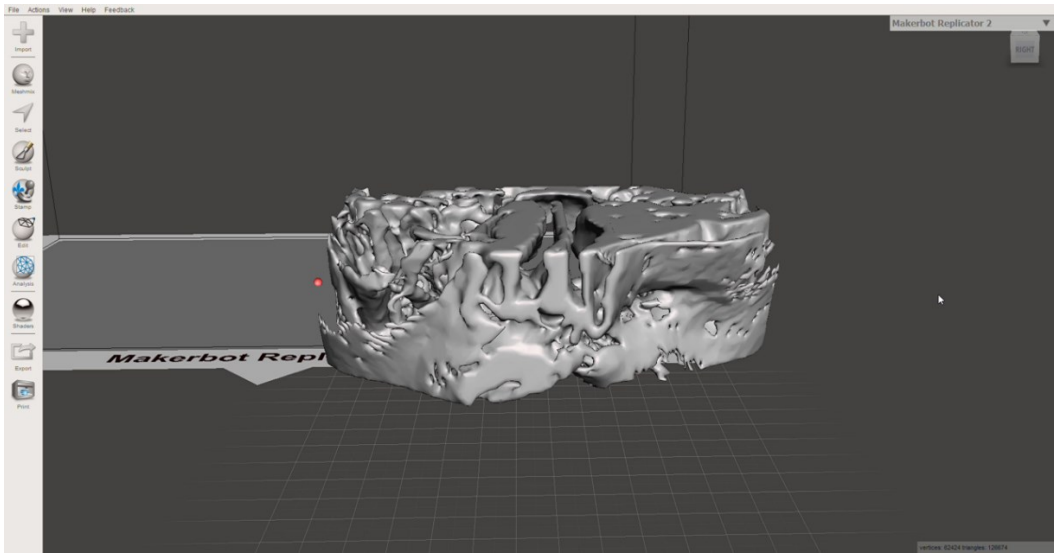

F 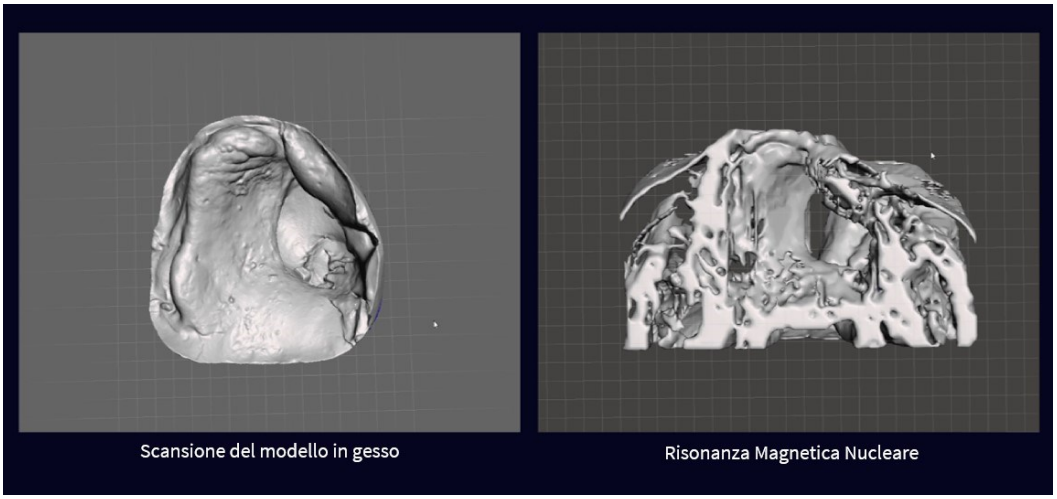

Figure 1. A, The MRI is imported in a dedicated software for visualization; B-D, In the same software, the area surrounding the maxillary defect was isolated (green area); E, the isolated area as it appears in the software Meshmixer; F, Occlusal view that compares the scan of a laboratory scanner on a conventional gypsum cast (left) and the digitization made with MRI.

References

1. Michelinakis G. The use of cone beam computed tomography and three dimensional printing technology in the restoration of a maxillectomy patient using a dental implant retained obturator. J Indian Prosthodont Soc. 2017;17:406-411.
2. Ye H, Ma Q, Hou Y, et al. Generation and evaluation of 3D digital casts of maxillary defects based on multisource data registration: A pilot clinical study. J Prosthet Dent. 2017;118:790-795.
3. Kortes J, Dehnad H, Kotte ANT, et al. A novel digital workflow to manufacture personalized three-dimensional-printed hollow surgical obturators after maxillectomy. Int J Oral Maxillofac Surg. 2018;47:1214-1218.
4. Tasopoulos T, Kouveliotis G, Polyzois G, Karathanasi V. Fabrication of a 3D Printing Definitive Obturator Prosthesis: a Clinical Report. Acta Stomatol Croat. 2017;51:53-58.
5. Park JH, Lee KS, Lee JY, Shin SW. Fabricating a Maxillary Obturator Using an Intraoral Digital Impression: A Case History Report. Int J Prosthodont. 2017;30:266-268.

3. DIGITAL DEVICES IN FIXED PROSTHODONTICS

To date, intraoral scanners (IOSs) are also used to record the morphology of tooth abutments for the rehabilitation of fixed prostheses on natural teeth. Generally, the whole arch is scanned first and then returned to the abutment, after having erased the recorded surface of its margin, in order to place the retractor cord and then resume scanning immediately after removing the cord.

This procedure is intended to provide the clinician with a more accurate reproduction of the finish line/area of the prepared abutments. Indeed, an accurate reproduction of the marginal anatomy of the abutment is critical for clinical success. Generally, when the margins are placed deeply subgingival, it could be difficult for IOS to be able to detect them. This is because the light emitted by IOS does not have the “vis a fronte” of traditional impression materials, which are capable of apically and laterally displacing the soft tissues from the abutments. To shed light on this aspect, in the chapter there is a study made with IOS on two different geometries of marginal preparation: vertical edgeless and horizontal with a 0.8 mm chamfer. These geometries present finish lines/areas placed both at 1 and 2 mm below the free gingival margin.

Furthermore, given the importance of dislocating soft tissue from the finish line/area, this chapter present a literature review about the use of laser systems for gingival retraction. Clarifications on their efficacy, indications, advantages and disadvantages, settings, and comparisons with other retraction procedures or laser technologies are provided.

SUMMARY:

3.1 INTRAORAL SCANNERS ON VERTICAL AND HORIZONTAL DEEP SUBGINGIVAL MARGINS: THREE-DIMENSIONAL ANALYSIS AND ACCURACY

Fernando Zarone, Gennaro Ruggiero and Roberto Sorrentino
Article in press

Introduction

In the last decades, the widespread diffusion of digital technologies in Dentistry, along with the introduction of more and more performing and appealing restorative materials, has led to a profound change in prosthetic paradigms. In particular, intraoral scanners (IOSs) are increasingly gaining ground in daily practice, both in prosthetic treatments and in the production of orthodontic aligners [1], thanks to a series of undeniable advantages: scans are by far preferred to the conventional impressions by patients, reducing stress and discomfort [2,3], offer a simplification and noticeable speed-up of clinical procedures [4-7], are not affected by the dimensional changes of impression materials and gypsum [2,8] open the door to the full digital workflow in the restorative plan [9], ease the communication within the operative team, with the lab and with the patient [7,10] and, last but not least, eliminate the need of casts storage and disposal [11].

In prosthodontics, today, the latest IOSs provide clinically acceptable accuracy in the production of both tooth- and implant-supported restorations [12,13] for both horizontal [14] and vertical [15] tooth preparation designs, independently of the abutment geometry [16]. Nevertheless, a critical issue is the difficulty in detecting the anatomical information when the finish line of the tooth abutment is deeply positioned into the gingival sulcus [1].

As defined in the Glossary of Prosthodontics Terms, the “finish line” or “margin" of the abutment is "the junction of prepared and unprepared tooth structure with the margin of a restorative material” [17]. An adequate record of the marginal anatomy both in the conventional impression and in the digital scanning procedure is of primary importance, in order to achieve an

acceptable marginal fit of the restoration [18], providing the dental laboratory with precious information about the tooth contour [19].

With the use of IOSs, an in vitro study demonstrated that the supragingival finish design is better detected than when it is iuxtagingivally located [20]; moreover, the final result is noticeably affected by clinical factors "obscuring" the apical portion of the preparation, like the proximity of teeth or the marginal gingiva [21].

Conversely, the conventional impression materials can penetrate someway more deeply into the gingival sulcus, so reproducing the apical details thanks to their rheological properties [22], especially when the 2 materials/2 times impression technique is employed, based on the utilization of a medium- or heavy-body material that “pushes” the light-body paste into the gingival sulcus [23], generating a hydraulic force that displaces the gingival margin during the materials setting [24]. In this way, the conventional impression can be a viable solution to record both the subgingival finish line and an apical portion of tooth anatomy beyond it.

Several *in vitro* [25] and *in vivo* [26,27] studies are present in the literature about IOSs, comparing the digital scan with the conventional impression-making procedure, on natural teeth [26,27] and on a fully edentulous maxilla [25], in any case reporting better results in terms of trueness and precision for IOSs. Furthermore, studies were made also to compare, among them, different IOSs devices available on the market [28-30]. Another hot topic is focused on the best scanning strategies for implant abutments [31], natural tooth abutments [32], and full edentulous maxilla [33,34].

To date, there is no sound scientific evidence about the levels of accuracy of IOSs on tooth abutments in the presence of either horizontal or vertical preparations, located at different depths below the free gingival margin. Moreover, there are no sufficient data about the efficiency of IOS to detect the tooth anatomic surface beyond the finish line/area. Some *in vitro* [20] and *in vivo* [35,36] studies have reported that the deeper a crown margin is positioned, the more difficult is to detect the finish line and the surface beyond it [20,35,36]. Besides, scanning systems based on ultrasound technologies have been proposed to solve this difficulty and take impressions of subgingival margins [37].

The present research has two finalities. The first aim is to assess the accuracies of 2 IOSs (i700, Medit, Seoul, Korea; TRIOS 4, 3Shape, Copenhagen, Denmark) on models of tooth abutments prepared with either vertical or horizontal designs, at different depths of the finish line (1 or 2 mm under the free gingival margin). The second aim is to evaluate if it is possible to detect a portion of the "non-prepared" area of the tooth beyond the finish margin in the presence of these different levels and designs of preparation.

The first null hypothesis is that there is no difference within the accuracies of scans made on tooth abutments with horizontal and vertical geometries at 1 and 2 mm below the gingival margin.
The second null hypothesis is that there is no association between the tested IOSs and the possibility to detect the surface beyond the finish lines/areas of the tested tooth abutments.

Materials and methods

One reference maxillary typodont (ANA-4 V CER, Frasaco GmbH, Tettnang, Germany) (Fig. 1a) of a standard permanent dentition was used. Its artificial teeth were in ivorine and could be removed from or fixed to the typodont thanks to a screw-based system.

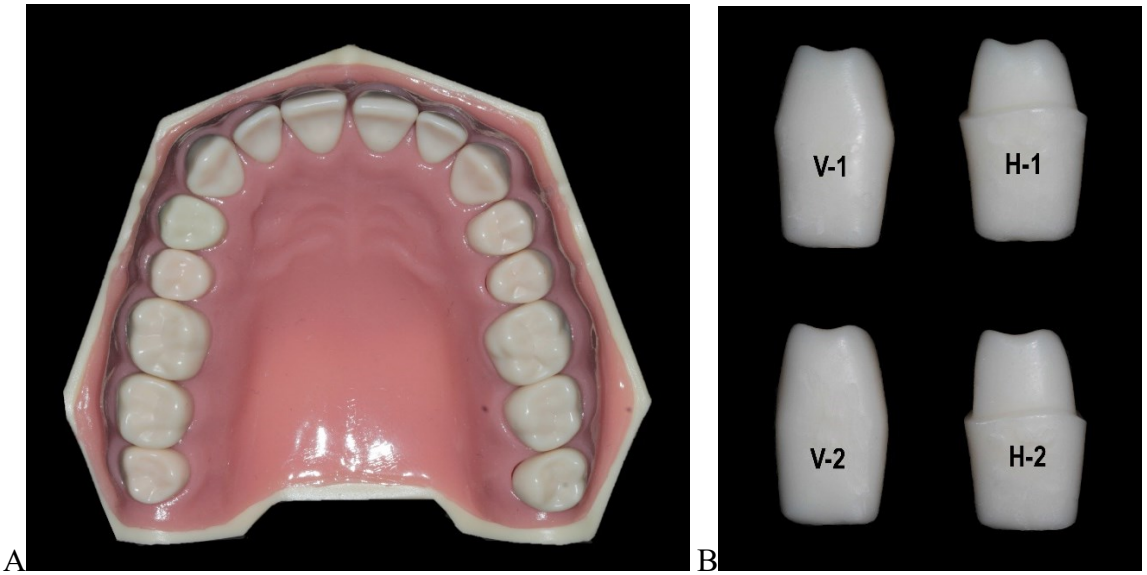

Fig. 1. A, Reference typodont. B, printed abutments: H-1, Horizontal -1 mm; H-2, Horizontal -2 mm; V-1, Vertical -1 mm; V-2, Vertical -2 mm.

After scanning the typodont with a laboratory scanner (DScan 3; EGSolutions, Bologna, Italy), 4 removable and screwable abutments were designed for the reference typodont, using the DentalCAD 3.0 Galway software (Exocad GmbH, Darmstadt, Germany) (Fig. 1b). These abutments were designed with 2 different preparation geometries: one horizontal with 0.8 mm chamfer and one vertical with an edgeless design. Both preparations were drawn at 1 and 2 mm below the free gingival margin. In this way, 4 digital reference abutments were obtained: horizontal -1 mm (H-1), horizontal -2 mm (H-2), vertical -1 mm (V-1), and vertical -2 mm (V-2). As regards the total occlusal convergence (TOC), a 5° angle of each opposing axial surface was used, resulting in an overall TOC of 10°, since such abutment preparation angle showed the best

value for reproducibility in a previous study [38]. In the horizontal design, the bottom of the gingival sulcus was 0.5 mm wide, and such distance was uniform along the whole intrasulcular portion of the test abutments; differently, in the vertical geometry, the distance between the axial surface and the col of the papilla was 1.2 mm and progressively decreased along the intrasulcular space in the apical direction, until the bottom of the sulcus and the root surface of the test abutments were in contact. In order to keep the aforementioned measurements constant while going from 1 to 2 mm subgingival, the abutments were sunk vertically in the apical direction, then adding that missing volume at the occlusal level in the -2 mm preparations, in order to extend the occlusal surface of 1 mm and reduce any possible modification of the occlusal area to be scanned with the IOSs.

The presumed occlusal surface variation (ΔS) of the abutments, when the preparation margins were sunk from 1 to 2 mm subgingivally at a constant axial surface angulation of 5°, was calculated with the following equation:

$$\Delta S = 1 - \frac{P tan\alpha}{R_1}$$

P is the measure of the abutment deepening (1 mm) while α is the 5° axial angulation of the abutment. R_1 is the radius of the occlusal surface of the abutment with the margin at 1 mm below the gingiva. A schematic representation of ΔS is displayed in Figure 2.

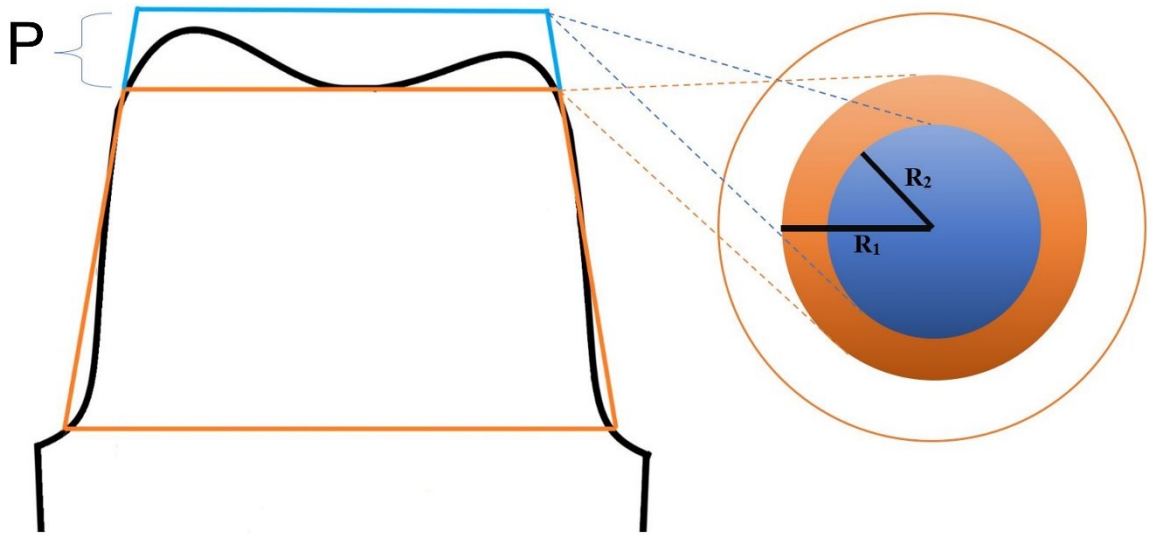

Fig. 2. Scheme for the calculation of the presumed occlusal surface variation (ΔS) with 1 mm deepening of the abutment and 5° axial angulation. P is the measure of the abutment deepening (1 mm). R_1 is the radius of the occlusal surface of the abutment with margin at 1 mm below the gingiva and R_2 at 2 mm.

The designed reference abutments were fabricated with a 3D printer (Anycubic Photon S, Anycubic 3D Printing, Shenzhen, China) using Anycubic UV Resin (Anycubic 3D Printing, Shenzhen, China) with a printing wavelength of 405 nm, making an apical hole in order to screw each abutment to the reference typodont.

To obtain the experimental scans, the reference typodont was scanned using 2 IOSs, TRIOS 4 (software v21.4, 3Shape, Copenhagen, Denmark) and Medit i700 (software Medit Link v2.5, Medit, Seoul, Korea). The IOSs were calibrated, then 10 nonexperimental scans were made as a test and to warm up these devices. The scanning strategy recommended by the manufacturers was performed. The scan started from the occlusal surface of the right third molar continuing longitudinally up to the contralateral one, then moving buccally and finally palatally. At the end of this scanning flow, it was zoomed in on the abutment to assess if there were any gaps, in the positive case the scan was resumed from the surfaces adjacent to the gaps, in order to fill them (Fig. 3). In the TRIOS 4 scans, the high-resolution ZOOM mode was used to scan the deepest area of the tooth abutment; with the same purpose, the scan depth was set to 23 mm for Medit i700.

A

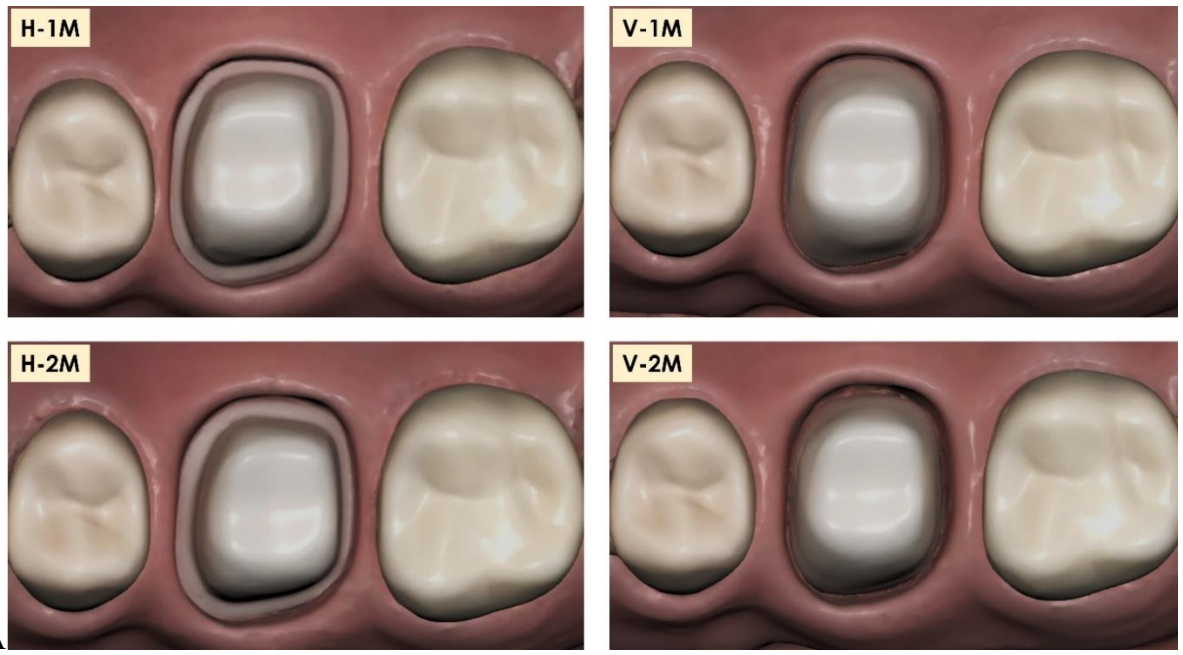

B

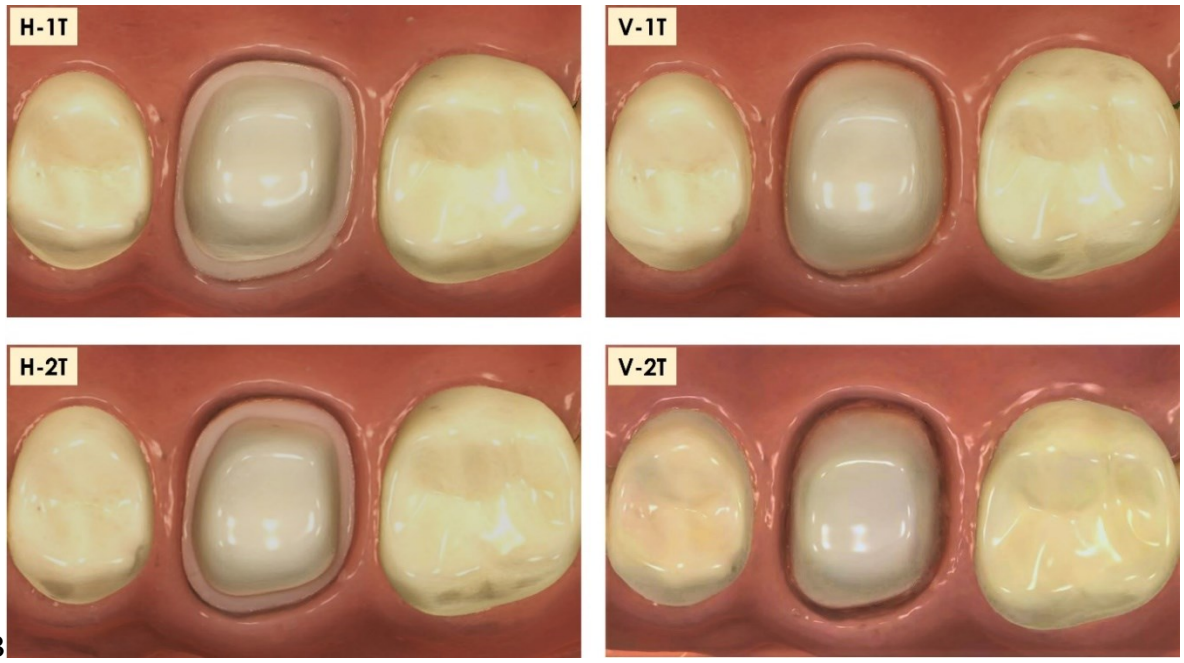

Fig. 3. IOS' scans of each abutment and tested IOS. A, Medit i700 scans: H-1M, Horizontal -1 mm; H-2M, Horizontal -2 mm; V-1M, Vertical -1 mm; V-2M, Vertical -2 mm. B, TRIOS 4 scans: H-1T, Horizontal -1 mm; H-2T, Horizontal -2 mm; V-1T, Vertical -1 mm; V-2T, Vertical -2 mm.

Each scan was made by the same experienced prosthodontist (G.R.), on the same day and in the same room, under comparable illumination and climatic settings with a temperature of 22°C, air pressure of 760 mmHg, and 45% relative humidity. The scanning sequence was randomized using a random sequence generator (Random Number Generator Pro v.1.72, Segobit Software) to reduce the effects of operator fatigue and prevent related bias, as well as with a 12-minute interval to allow the operator to rest and the device to cool properly. The number of shots

per scan varied between 1836 and 4651 and the time for a complete arch scan was comprised between 1 and 2 minutes.

All Standard Tessellation Language (STL) files acquired with the IOSs were imported into a dedicated software (Meshlab v2016.12; ISTI-CNR) where each scan was cut to isolate the prepared abutment with its marginal geometry and the surface beyond it. In the case of vertical preparations, the finish area was set through the overlapping of vertical experimental scans and the horizontal reference scan that had the same preparation depth (Supplementary Video 1). Eight experimental groups were made (n = 10): about Medit i700, they were named “H-1M” for horizontal preparation at 1 mm from the gingival margin and “H-2M” for the same at 2 mm, while “V-1M” for vertical preparation at 1 mm and “V-2M” for the same at 2 mm; about TRIOS 4, with the same criteria, they were named “H-1T”, “H-2T”, “V-1T”, and “V-2T”.

Both the reference scans and, subsequently, the 8 groups of .stl files (n = 10) were imported into Geomagic Control X (3D SYSTEMS, software v2018.0.1) (Fig. 4) and the accuracy of each one was evaluated by calculating trueness and precision, measured in µm. The 4 digital reference abutments were imported as "reference data" in the software [39].

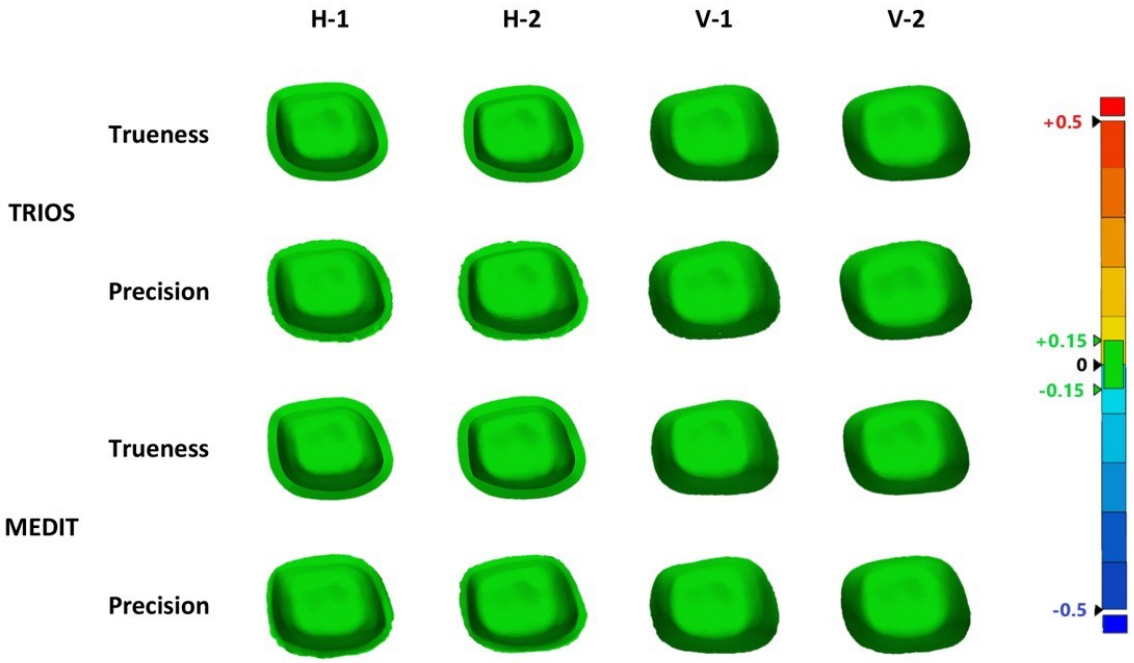

Fig. 4. Analyses of trueness and precision: Best superimposition for each experimental scan. Green areas indicate minimum displacement of experimental scan compared to the reference model.

An "initial alignment" was performed by the software, followed by a "best fit alignment". After aligning the 2 digital models, the "3D compare" function was activated. The parameters in

the "color bar option" were max/min range = 1.0 mm and specific tolerance = ±0.1 mm. The standard deviation (SD) measure was selected from the "tabular view-3D compare". This measure (SD) is a mean between positive and negative deviations resulting from each superimposition of digital surfaces, as calculated by Geomagic. Therefore, the mean of the SD values was selected to measure trueness and precision [7,40]. With this method, a "color map" was generated for visual examination of the displacements between the surfaces of the overlapped digital models. The green areas indicated a minimum displacement of ±0.1 mm of the digital model compared to the "reference data"; differently, the red and blue areas indicated outward and inward displacements respectively of +1.0 mm and -1.0 mm (Fig. 4).

According to ISO-5725, the accuracy of a measurement method is defined by 2 parameters: "trueness" and "precision". "Trueness" indicates the closeness of agreement among the arithmetic mean of a large number of test results and the reference value; "precision" represents the closeness of agreement between intragroup data collected by repetitive measurements [41,42]. In other terms, trueness defines how a measurement matches the actual value while precision describes the consistency of repeated measurements.

For each experimental group, the trueness was evaluated as the mean of the SD values resulting from the superimposition between each experimental scan and the corresponding digital reference abutment.

The precision was measured as the mean of the SD values for each experimental scan and the scan that achieved the best value of trueness after the overlapping on the corresponding digital reference abutment in each of the 8 experimental groups. In this way, the scans of the same group were overlapped on this selected scan and the precision of each test group was measured as the mean of SD values registered by each of these overlaps [7,40].

Statistical analyses were performed with dedicated software (IBM SPSS v25; IBM). To evaluate both trueness and precision, descriptive statistics (i.e., mean, standard error, median, interquartile range, 95% Confidence Interval) and additional calculations to evaluate the overall statistical significance of the differences between the groups (p=.05) were performed. Particularly, the Kolmogorov-Smirnov test was used to check data normality, the Levene test was run to evaluate the homogeneity of variances.

The Welch's robust test of equality of means, the Games-Howell and Bonferroni tests were run to analyze differences between groups. To consider only clinically motivated comparisons, all the possible pairwise comparisons between the 4 experimental groups were not performed. Consequently, it was evaluated whether differences existed between preparation geometries (vertical or horizontal) within a specific depth (1 or 2 mm) and between preparation

depths within a particular geometry. Furthermore, differences were investigated even for each abutment geometry between the 2 tested IOSs.

A post hoc power analysis was made with G*Power (v. 3.1.9.7, Universität Kiel, Germany) to estimate the sample size effect. The partial eta squared (η^2) is the effect size measure for the interaction between the within and between-subject variables, and it was used to determine the effect size. Approximate η^2 conventions are large = 0.14, medium = .06, and small = .02. For the present analysis, a large effect size was estimated.

Results

There was a 92.65% possibility of correctly rejecting the null hypothesis of no significant effect of the within-between interaction, with 10 measurements for each experimental group, for a total of 20 assessments per abutment geometry (Figure 5).

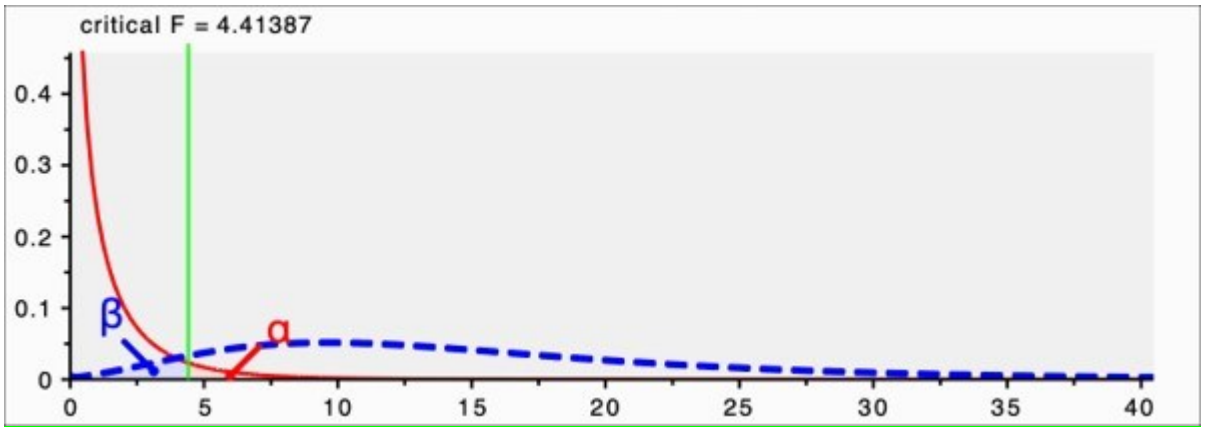

Figure 5. Power Analysis for the evaluation of the Sample Size Effect.

The ΔS of the horizontal preparations was 0.971 mm^2 while for the vertical preparations it was 0.968 mm^2.

The descriptive statistics for trueness (C.I. 95%) with upper-lower bounds, means, and standard errors are summarized in Table 1 and shown in Figure 6.

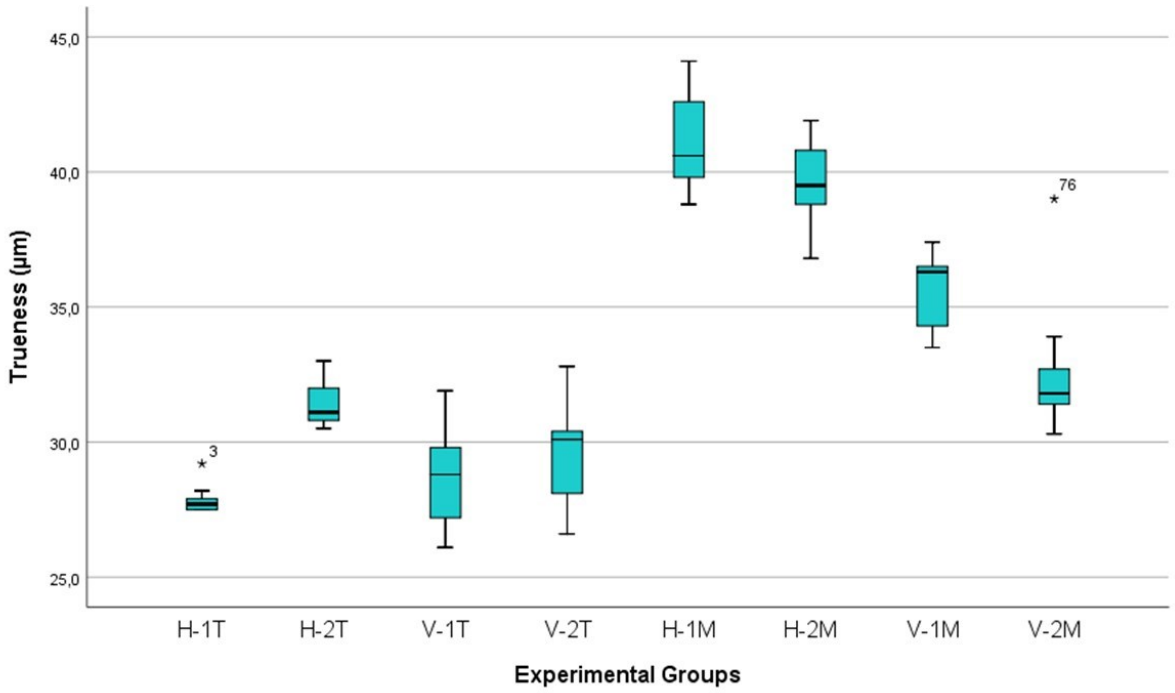

Fig. 6. Box plot chart of trueness' descriptive statistics. Whiskers above and below boxes show minimum and maximum, while box spans exhibit first quartile to third quartile. Median is displayed by segments inside box. Possible outliers are unfilled circles.

Table 1. Descriptive statistics for trueness (µm) with 95%-confidence intervals (CI95)

	Experimental Group	Upper-Lower bound (95% CI)	Mean	Standard Error
TRIOS	H-1T	27.4-28.2	27.8	.182
	H-2T	30.7-32.0	31.3	.280
	V-1T	27.2-30.2	28.7	.644
	V-2T	27.8-30.9	29.4	.669
MEDIT	H-1M	39.7-42.4	41.1	.575
	H-2M	38.2-40.7	39.4	.550
	V-1M	34.6-36.8	35.7	.486
	V-2M	30.6-34.6	32.6	.874

The mean values were normally distributed for all the groups, as reported by the Kolmogorov-Smirnov test ($p>.05$). The Levene test showed homogeneity of the variances ($p =$

.051) for the experimental groups. Due to the normal distribution and the homogeneity of variances, the Bonferroni post hoc test was used to detect the statistically significant differences between the means of the experimental groups. The values of the post hoc comparisons are shown in table 2.

As regards the analysis of precision, the descriptive statistics (C.I. 95%) with upper-lower bounds, means, and standard errors are shown in table 3 and displayed in Figure 7.

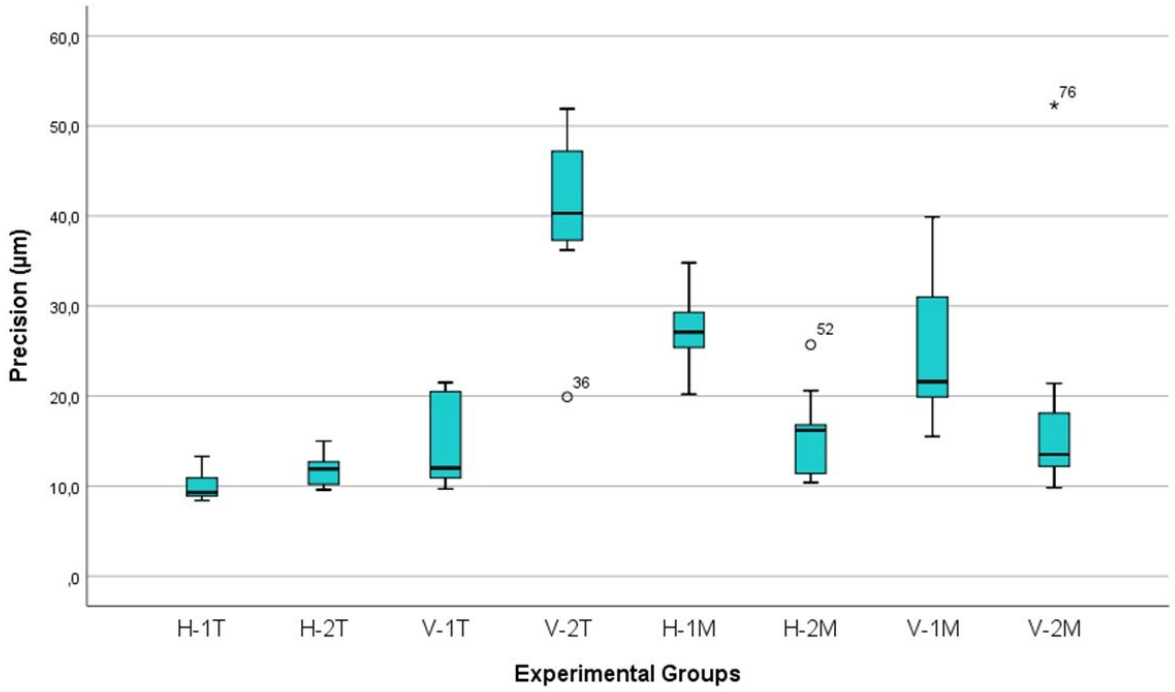

Fig. 7. Box plot chart of precision's descriptive statistics. Whiskers above and below boxes show minimum and maximum, while box spans exhibit first quartile to third quartile. Median is displayed by segments inside box. Possible outliers are unfilled circles.

The mean values were not normally distributed for all the groups, as reported by the Kolmogorov-Smirnov test ($p<.05$). Moreover, the Levene test showed no homogeneity of the variances ($p = .010$) for the experimental groups. A $\log_{10}$ transformation of the data was made because the assumptions on the normal distribution and the homogeneity of the variances were violated to evaluate differences among the experimental groups. After the data transformation, the Kolmogorov-Smirnov test reported a normal distribution ($p>.05$), whereas the Levene test did not show homogeneity of the variances ($p = .021$). Welch's robust test of equality of means was significant ($p<.001$) and the Games-Howell post hoc test was run to detect statistically significant differences between the experimental groups. P-values of post hoc comparisons are shown in table 2.

Table 2. *P*-values of post hoc comparisons

	Experimental Group	Trueness	Precision
TRIOS	H-1T vs H-2T	.002*	388
	H-1T vs V-1T	1.0	.161
	H-2T vs V-2T	.424	<.001*
	V-1T vs V-2T	1.0	<.001*
MEDIT	H-1M vs H-2M	1.0	.004*
	H-1M vs V-1M	<.001*	.952
	H-2M vs V-2M	<.001*	1.0
	V-1M vs V-2M	.03*	.535
TRIOS vs MEDIT	H-1T vs H-1M	<.001*	<.001*
	H-2T vs H-2M	<.001*	.269
	V-1T vs V-1M	<.001*	.086
	V-2T vs V-2M	.008*	.008*

*=Statistically significant differences (*P*<.05).

Table 3. Descriptive statistics for precision (μm) 95%-confidence intervals (CI95)

	Experimental Group	Upper-Lower bound (95% CI)	Mean	Standard Error
TRIOS	H-1T	8.8-11.1	10.0	.514
	H-2T	10.3-12.9	11.6	.581
	V-1T	11.0-19.0	15.0	1.738
	V-2T	33.5-48.7	41.1	3.295
MEDIT	H-1M	23.9-30.9	27.4	1.520
	H-2M	12.1-19.6	15.9	1.640
	V-1M	18.3-31.6	24.9	2.885
	V-2M	8.2-28.5	18.4	4.416

About the analysis of trueness and precision, the color bar map of the best superimposition for each group of scans did not show outward and inward displacements greater than 150 μm (Fig. 4).

Figure 3 showed that the finish lines/areas of the preparations were visible both in the horizontal (H-1 and H-2) and vertical (V-1 and V-2) preparations at the different depths (1 and 2 mm subgingivally).

Conversely, the surface area beyond the finish margins was only visible for vertical preparations at both 1 (V-1) and 2 (V-2) mm below the free gingival margin and is about 1 mm (Fig. 8), whereas this area was not detected on the horizontal preparations (H-1 and H-2) (Fig. 8).

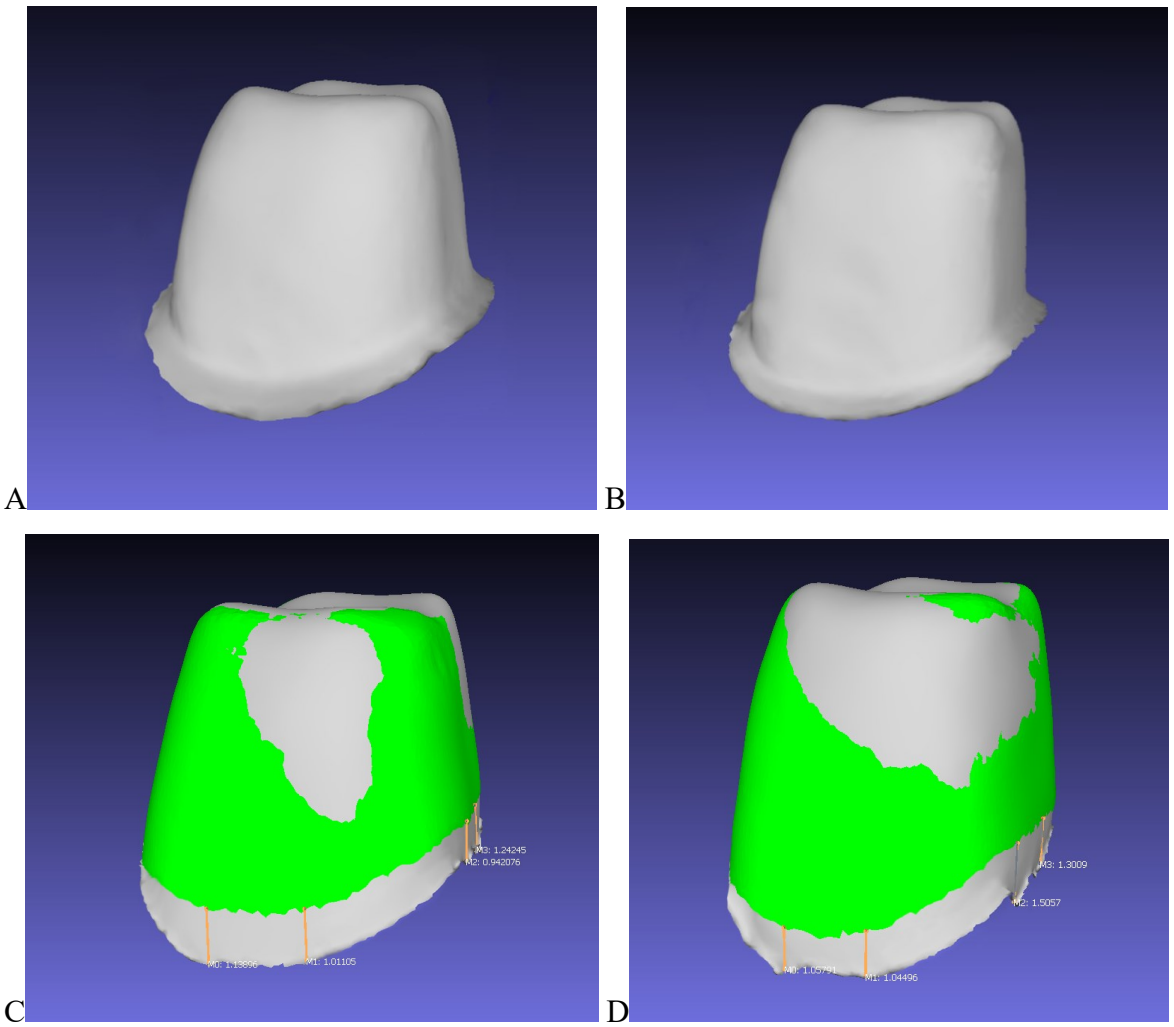

Fig. 8. Detection of area over finish line with both horizontal and vertical preparations at 1 and 2 mm below free gingival margin. A, H-1; B, H-2; C, V-1; D, V-2. About vertical preparations (C, D), the displayed segments show some linear measurements between the apical line detected by IOSs and the set finish line cut for three-dimensional analysis.

Discussion

The present study aimed to compare the accuracies of 2 IOSs (TRIOS 4 and Medit i700) on models of tooth abutments prepared with vertical and horizontal finish geometries at both 1 and 2 mm under the free gingival marginal.

The first null hypothesis, stating that there is no difference within the accuracies of scans made on tooth abutments with the 2 tested geometries at different depths, was rejected. Besides, the second null hypothesis was partially rejected because IOSs were able to detect the surface beyond the set vertical finish area, but not the ones under the horizontal finish lines.

The descriptive statistics showed mean values of the accuracy of <150 μm that were in the clinically accepted threshold [43], for both the tested geometries at 1 and 2 mm below the gingival margin, as reported in tables 1 and 3, for the tested IOSs.

The trueness and precision values of the Medit i700 ranged between 32.6-41.1 μm and 15.9-27.4 μm respectively; these values are comparable to those reported for the same IOS by Jivanescu et al. (trueness: 25.55 ±1.85 μm; precision: 9.1 ±3.8 μm) [44] for short-span fixed dental prostheses [44]. About TRIOS 4, the values of trueness (27.8-31.3) and precision (10-41.1 μm) are not comparable to the few studies available in the literature, because they did not focus on tooth abutments, but on full arches with linear measurements [28,45] and on scan bodies [46].

It is not possible to provide a range of values for the accuracy of IOS scans on a single tooth abutment, because of the heterogeneity and possible confounders of different research protocols used in the literature. Indeed, various IOS were examined, scans were performed by several operators on different reference models or environmental conditions, and various parameters were investigated, such as the root mean square, standard deviation, and mean absolute distance of the superimposed surfaces [20,29,47,48]. Nevertheless, a study with a research protocol similar to that shown in the present investigation was made by Lee et al. [49] on a single molar abutment, reporting comparable trueness values in the range of 24-34.1 μm [49].

The surface beyond the finish area/line was detectable for vertical preparations but not for horizontal ones, as displayed in Figure 8. In this regard, it should be mentioned that the finish border of the vertical preparations was set at the same depths as the horizontal ones by superimposing each other and then removing the surface excess (Supplementary Video 1). The reason on the basis for the impossibility to detect the area beyond the finish line, in horizontal preparations is shown in Figure 9. Due to their geometry, horizontal preparations do not allow the scanner light beam to pass easily beyond the finish line for the presence of geometrical undercuts that can create possible shadow areas (Fig. 9A); conversely, this phenomenon usually does not occur for vertical preparations (Fig. 9B). According to previous studies, the angle of the scanner light beam is an important factor in detecting the surface beyond the finish area [29,36], as if there was too much angulation between the coronal-apical axis of the tooth and the light beam, then the gingiva itself would favor the formation of shadow cones (Fig. 9).

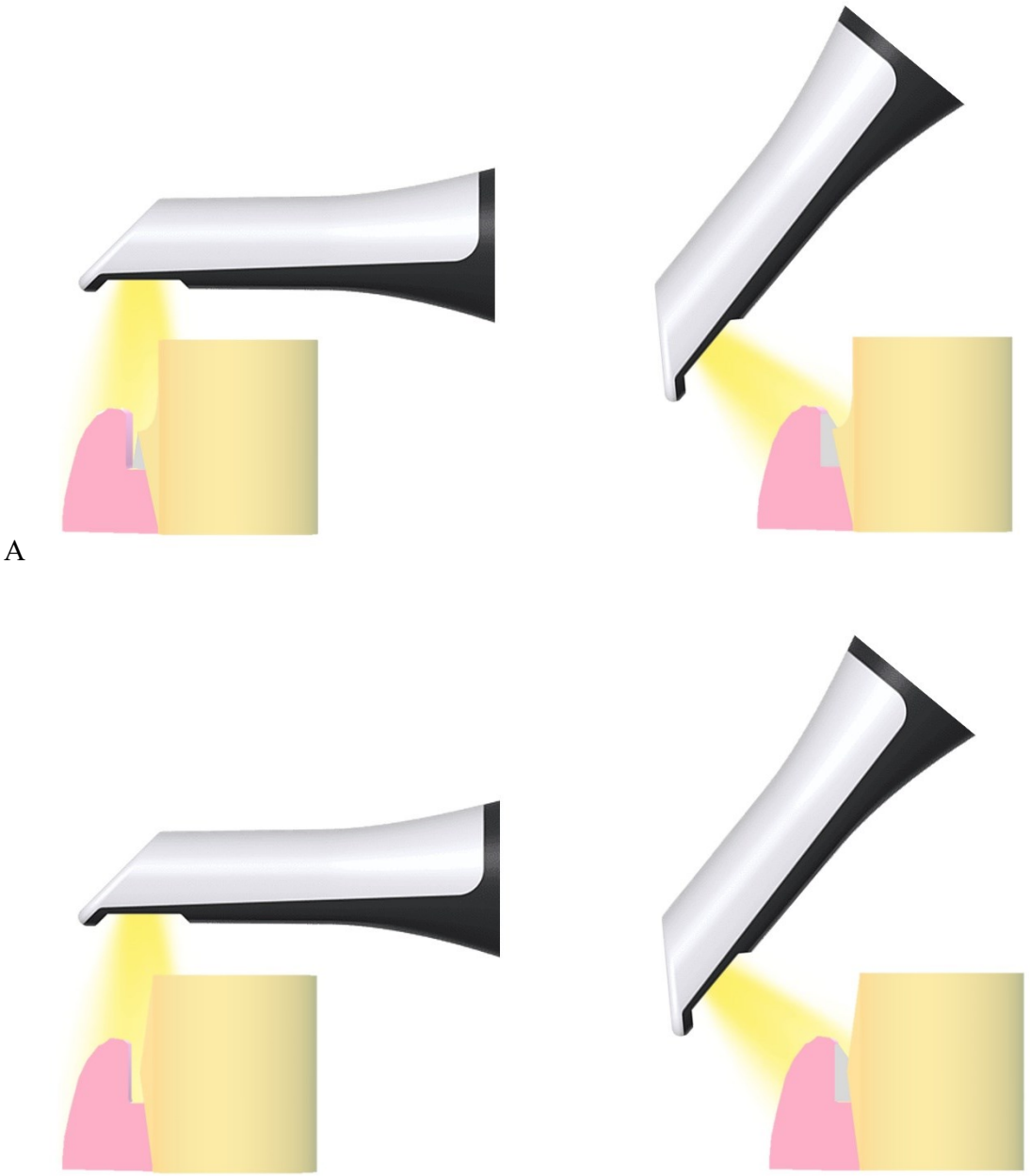

Fig. 9. Limitations to scanner light beam on surface beyond finish line due to presence of undercuts. A, different angulations of the IOS on horizontal margin. B, different angulations of IOS on vertical margin.

As regards the depth of tooth preparations, TRIOS 4 seems to be negatively influenced by geometries with deep finish lines (tables 1 and 3). Also, significant differences reported that the trueness for the horizontal geometry ($p = .002$) and precision of the vertical ones ($p<.001$) were better at 1 mm than at 2 mm. On the contrary, Medit i700 showed better results for deeper preparations (tables 1 and 3). Furthermore, significant differences reported that the precision of H-1M is worse than that of H-2M ($p = .002$), and the trueness of V-2M is better than V-1M ($p = .03$). An explanation of the presented results might be found in the technologies of the tested

IOSs. TRIOS 4 is based on confocal laser scanning microscopy (CLSM) [50,51], while Medit i700 is based on three-dimensional in-motion video technology and three-dimensional full-color streaming capture [52]. As reported in the literature, the CLSM has a controlled and limited depth of focus [53], in particular, objects behind and in front of the focus plane are shown out of focus, so, they could not be detected [54]. Moreover, as resulted in previous investigations, the ZOOM mode did not enhance the detection of smaller details of margin areas for TRIOS [45,55]. Therefore, the ZOOM mode of TRIOS seems to be not as efficient as the max depth scan setting of Medit i700.

About the preparations designs, TRIOS 4 did not result to be influenced by this variable at 1 mm neither for trueness nor precision; at 2 mm, despite no differences being found in the trueness, TRIOS 4 made more precise scans on horizontal preparations than on vertical ones ($p<.001$). In the Medit i700 scenario, vertical preparations reported better trueness and precision than horizontal ones at both the tested depths ($p<.001$); furthermore, significant differences were found in the trueness at 1 mm and the precision and 2 mm. The reason behind these results might be understood considering the bending or distortions discussed in previous studies for TRIOS in the case of steep inclines of tooth surfaces [28,45], like the vertical abutments that do not have clearly identifiable planes as the horizontal ones. Moreover, the vertical preparations could be favored in the Medit scenario, due to the presence of a 45-degree angulated mirror. Indeed, with this angulation, it is possible to obtain a perpendicular reflection of the light beam from the surface of the vertical preparation than from the 0.8 mm chamfer of the horizontal one. Therefore, the software did not need to redesign drastically the image detected on the sensor, so, there will be a reduced cumulative error for its algorithm.

Regarding the comparison between the tested IOSs, TRIOS 4 showed better trueness than Medit i700, as supported not only by descriptive statistics but also by statistically significant differences (Table 2), both for vertical and horizontal preparations, at 1 and 2 mm below the gingival margin (H-1T vs H-1M: $p<.001$; H-2T vs H-2M: $p = .001$; V-1T vs V-1M: $p<.001$; V-2T vs V-2M: $p = .008$). On one hand, TRIOS 4 showed a significantly better precision at 1 mm for horizontal preparations ($p<.001$), but, on the other one, Medit i700 is more precise in the case of deeper preparations (2 mm) with a vertical design ($p = .016$).

To sum up, the overall geometries, the preparation depths, and the IOSs are variables that affect the scanning accuracy. Moreover, the presented results would suggest that the behavior of such systems can be somehow associated with myopia and hyperopia, where Medit i700 appears to be farsighted and more able to read deep preparations when compared to TRIOS 4.

To date, there are no studies that can explain this different behavior related to the optics and technologies of the tested IOSs, also because they were introduced on the market very recently.

Regardless of what was discussed, it must be considered that both IOSs achieved clinically acceptable values for both trueness and precision, showing their suitability for scanning these tooth abutments geometries.

The present study had some limitations, primarily due to its *in vitro* nature; specifically, the experimental scans were made with the IOSs on resin models of tooth abutments, so, clinically relevant factors such as humidity, temperature, optical features, intraoral anatomic limitations, and - mainly - mobility and resilience of soft tissues were not factored. Particularly, a proper clinical displacement of gingival tissues or particular anatomical conformation of every single tooth could influence the present results, particularly in the case of horizontal preparations. Moreover, despite the presumed occlusal surface variation being numerically negligible, it was calculated on the morphology of a truncated cone, which does not reproduce the perfect morphology of the model abutments.

In order to corroborate the findings of the present investigation, further studies should be done, including clinical trials with larger sample sizes.

Conclusions

As regards the scans made with the tested IOSs, based on the findings of the present *in vitro* comparative investigation, the following conclusions can be drawn.

1) At both 1 and 2 mm below the free gingival margin:

- it is possible to scan tooth abutments with detectable vertical and horizontal finishing geometries;
- the mean values of the accuracy are in the clinically accepted threshold for both the tested geometries;
- the surface beyond the finish area/line is detectable for vertical preparations but not for horizontal ones;
- about TRIOS 4, the trueness for the horizontal geometry is better at 1 mm than at 2 mm, while for vertical ones they were comparable. Regarding the precision, the results were comparable for horizontal designs and better for vertical ones at 1 mm than at 2 mm.
- about Medit i700, the precision for the horizontal geometry is better at 2 mm than at 1 mm, while for vertical ones they were comparable. As regards the trueness, the results

were comparable for horizontal designs and better for vertical ones at 2 mm than at 1 mm.

2) Only at 1 mm below the gingival margin:

There was no difference in trueness and precision between vertical and horizontal designs for TRIOS 4;

About Medit i700, the trueness is better for vertical geometry and no difference was found between horizontal and vertical preparations regarding the precision.

3) Only at 2 mm below the gingival margin:

TRIOS 4 showed better precision for horizontal preparations and no difference for the trueness. Conversely, the precision of Medit i700 was comparable between horizontal and vertical designs, while the trueness of vertical preparations was better.

4) About the comparison between the tested scanners:

The trueness of TRIOS 4 was better than that of Medit i700 both for vertical and horizontal preparations at 1 and 2 mm below the gingival margin.

The precision of Medit i700 was better at 2 mm on the vertical preparations, while TRIOS 4 showed a significantly better result at 1 mm for horizontal preparations. No differences were found between the tested IOSs for the precision at 2 mm with the horizontal preparation and 1 mm with the vertical one.

Further *in vitro* and *in vivo* studies, and randomized controlled trials are needed to corroborate the outcomes of the present *in vitro* investigation.

References

1. Mangano F, Gandolfi A, Luongo G, Logozzo S. Intraoral scanners in dentistry: a review of the current literature. BMC Oral Health. 2017 Dec 12;17(1):149.
2. Zimmermann M, Mehl A, Mörmann WH, Reich S. Intraoral scanning systems a current overview. Int J Comput Dent. 2015;18(2):101-29.
3. Ahlholm P, Sipilä K, Vallittu P, Jakonen M, Kotiranta U. Digital versus conventional impressions in fixed prosthodontics: A review. J Prosthodont 2018;27(1):35-41.
4. Joda T, Lenherr P, Dedem P, Kovaltschuk I, Bragger U, Zitzmann NU. Time efficiency, difficulty, and operator's preference comparing digital and conventional implant impressions: a randomized controlled trial. Clin Oral Implants Res 2017;28(10):1318-23.
5. Goracci C, Franchi L, Vichi A, Ferrari M. Accuracy, reliability, and efficiency of intraoral scanners for full-arch impressions: a systematic review of the clinical evidence. Eur J Orthod. 2016;38(4):422-8.
6. Joda T, Zarone F, Ferrari M. The complete digital workflow in fixed prosthodontics: a systematic review. BMC Oral Health. 2017; 17(1): 124.
7. Imburgia M, Logozzo S, Hauschild U, Veronesi G, Mangano C, Mangano FG. Accuracy of four intraoral scanners in oral implantology: a comparative in vitro study. BMC Oral Health. 2017;17(1):92.
8. Marti AM, Harris BT, Metz MJ, Morton D, Scarfe WC, Metz CJ, Lin WS. Comparison of digital scanning and polyvinyl siloxane impression techniques by dental students: instructional efficiency and attitudes towards technology. Eur J Dent Educ. 2017;21(3):200-5.
9. Stanley M, Paz AG, Miguel I, Coachman C. Fully digital workflow, integrating dental scan, smile design and CAD-CAM: case report. BMC Oral Health. 2018;18(1):134. Published 2018 Aug 7. doi:10.1186/s12903-018-0597-0.
10. Lawson NC, Burgess JO. Clinicians reaping benefits of new concepts in impressioning. Compend Contin Educ Dent. 2015;36(2):152-3.
11. Rheude B, Sadowsky PL, Ferriera A, Jacobson A. An evaluation of the use of digital study models in orthodontic diagnosis and treatment planning. Angle Orthod. 2005;75(3):300-304. doi:10.1043/0003-3219(2005)75[300:AEOTUO]2.0.CO;2.
12. Mangano FG, Bonacina M, Mandelli F, Marchiori F. Solid index versus intraoral scanners in the full-arch implant impression: in vitro trueness evaluation. BMC Res Notes. 2020;13(1):504. doi:10.1186/s13104-020-05353-2

13. Mangano FG, Admakin O, Bonacina M, Lerner H, Rutkunas V, Mangano C. Trueness of 12 intraoral scanners in the full-arch implant impression: a comparative in vitro study. BMC Oral Health. 2020;20(1):263. doi:10.1186/s12903-020-01254-9
14. Ferrini F, Sannino G, Chiola C, Capparé P, Gastaldi G, Gherlone EF. Influence of Intra-Oral Scanner (I.O.S.) on The Marginal Accuracy of CAD/CAM Single Crowns. Int J Environ Res Public Health. 2019;16(4):544.
15. García-Gil I, Perez de la Calle C, Lopez-Suarez C, Pontevedra P, Suarez MJ. Comparative analysis of trueness between conventional and digital impression in dental-supported fixed dental prosthesis with vertical preparation. J Clin Exp Dent. 2020;12(9):e896-e901.
16. Carbajal Mejía JB, Wakabayashi K, Nakamura T, Yatani H. Influence of abutment tooth geometry on the accuracy of conventional and digital methods of obtaining dental impressions. J Prosthet Dent. 2017;118(3):392-9.
17. The Academy of Prosthodontics. The Glossary of Prosthodontic Terms: Ninth Edition. J. Prosthet. Dent. 2017;117:e1-e105.
18. Podhorsky A, Rehmann P, Wöstmann B. Tooth preparation for full-coverage restorations-a literature review. Clin Oral Investig. 2015;19(5):959-68.
19. Boening KW, Walter MH, Schuette U. Clinical significance of surface activation of silicone impression materials. J Dent. 1998;26(5-6):447-52.
20. Bernauer SA, Müller J, Zitzmann NU, Joda T. Influence of preparation design, marginal gingiva location, and tooth morphology on the accuracy of digital impressions for full-crown restorations: an in vitro investigation. J Clin Med. 2020;9(12):3984.
21. Keeling A, Wu J, Ferrari M. Confounding factors affecting the marginal quality of an intra-oral scan. J Dent. 2017;59:33-40.
22. German MJ, Carrick TE, McCabe JF. Surface detail reproduction of elastomeric impression materials related to rheological properties. Dent Mater. 2008;24(7):951-6.
23. Donovan TE, Chee WW. A review of contemporary impression materials and techniques. Dent Clin North Am. 2004;48(2):445-70.
24. Livaditis GJ. The matrix impression system for fixed prosthodontics. J Prosthet Dent. 1998;79(2):208-16.
25. Zarone F, Ruggiero G, Ferrari M, Mangano F, Joda T, Sorrentino R. Accuracy of a chairside intraoral scanner compared with a laboratory scanner for the completely

edentulous maxilla: An in vitro 3-dimensional comparative analysis. J Prosthet Dent. 2020;124(6):761.e1-761.e7.

26. Koulivand S, Ghodsi S, Siadat H, Alikhasi M. A clinical comparison of digital and conventional impression techniques regarding finish line locations and impression time. J Esthet Restor Dent. 2020;32(2):236-43.

27. Sakornwimon N, Leevailoj C. Clinical marginal fit of zirconia crowns and patients' preferences for impression techniques using intraoral digital scanner versus polyvinyl siloxane material. J Prosthet Dent. 2017;118(3):386-91.

28. Amornvit P, Rokaya D, Sanohkan S. Comparison of Accuracy of Current Ten Intraoral Scanners. Biomed Res Int. 2021;2021:2673040.

29. Nedelcu R, Olsson P, Nyström I, Thor A. Finish line distinctness and accuracy in 7 intraoral scanners versus conventional impression: an in vitro descriptive comparison. BMC Oral Health. 2018;18(1):27.

30. Nulty AB. A comparison of full arch trueness and precision of nine intra-oral digital scanners and four lab digital scanners. Dent J (Basel) 2021;9(7):75.

31. Flügge TV, Att W, Metzger MC, Nelson K. Precision of dental implant digitization using intraoral scanners. Int J Prosthodont. 2016;29(3):277-83.

32. Chochlidakis KM, Papaspyridakos P, Geminiani A, Chen CJ, Feng IJ, Ercoli C. Digital versus conventional impressions for fixed prosthodontics: A systematic review and meta-analysis. J Prosthet Dent. 2016;116(2):184-190.e12.

33. Zarone F, Ruggiero G, Ferrari M, Mangano F, Joda T, Sorrentino R. Comparison of different intraoral scanning techniques on the completely edentulous maxilla: An in vitro 3-dimensional comparative analysis. J Prosthet Dent. 2020;124(6):762.e1-762.e8.

34. Lo Russo L, Salamini A, Troiano G, Guida L. Digital dentures: A protocol based on intraoral scans. J Prosthet Dent. 2021;125(4):597-602. doi:10.1016/j.prosdent.2020.02.006.

35. Ferrari Cagidiaco E, Zarone F, Discepoli N, Joda T, Ferrari M. Analysis of the reproducibility of subgingival vertical margins using intraoral optical scanning (IOS): A randomized controlled pilot trial. J Clin Med. 2021;10(5):941.

36. Di Fiore A, Vigolo P, Monaco C, Graiff L, Ferrari M, Stellini E. Digital impression of teeth prepared with a subgingival vertical finish line: a new clinical approach to manage the interim crown. J Osseointegr 2019;11(4):XX.

37. Praça L, Pekam FC, Rego RO, Radermacher K, Wolfart S, Marotti J. Accuracy of single crowns fabricated from ultrasound digital impressions. Dent Mater. 2018;34(11):e280-e288.

38. Kim DY. Evaluation of the effect of abutment preparation angles on the repeatability and reproducibility using a blue light model scanner. J Adv Prosthodont. 2020;12(4):210-217.

39. Mandelli F, Gherlone E, Gastaldi G, Ferrari M. Evaluation of the accuracy of extraoral laboratory scanners with a single-tooth abutment model: a 3D analysis. J Prosthodont Res 2017;61:363-70.

40. Zarone F, Ruggiero G, Di Mauro MI, Spagnuolo G, Ferrari M, Sorrentino R. Accuracy of three impression materials on the totally edentulous maxilla: in vitro/in silico comparative analysis. Materials (Basel) 2020;13:515.

41. International Organization for Standardization. ISO 5725-1. Accuracy (trueness and precision) of measurement methods and results. Part 1: general principles and definitions. Berlin: International Organization for Standardization; 1994. Available at: http://www.iso.org/iso/home.html.

42. Sim JY, Jang Y, Kim WC, Kim HY, Lee DH, Kim JH. Comparing the accuracy (trueness and precision) of models of fixed dental prostheses fabricated by digital and conventional workflows. J Prosthodont Res 2019;63:25-30.

43. Boitelle P, Mawussi B, Tapie L, Fromentin O. A systematic review of CAD/CAM fit restoration evaluations. J Oral Rehabil 2014;41:853-74.

44. Jivănescu A, Bara A, Faur A-B, Rotar RN. Is There a significant difference in accuracy of four intraoral scanners for short-span fixed dental prosthesis? A comparative in vitro study. Appl. Sci. 2021;11(18):8280.

45. Amornvit P, Rokaya D, Peampring C, Sanohkan S. Confocal 3d optical intraoral scanners and comparison of image capturing accuracy. CMC. 2021;66:303-14

46. Revell G, Simon B, Mennito A, Evans ZP, Renne W, Ludlow M, Vág J. Evaluation of complete-arch implant scanning with 5 different intraoral scanners in terms of trueness and operator experience. J Prosthet Dent. 2021:S0022-3913(21)00052-4.

47. Hack GD, Patzelt SB. Evaluation of the accuracy of six intraoral scanning devices: An invitro investigation. ADA Prof Prod Rev 2015;10:15.

48. Lee JJ, Jeong ID, Park JY, Jeon JH, Kim JH, Kim WC. Accuracy of singleabutment digital cast obtained using intraoral and cast scanners. J Prosthet Dent 2017;117:2539.

49. Lee DG, Son K, Lee KB. Comparison of the accuracy of intraoral scanners based on the type of tooth preparation for a single crown. Appl. Sci. 2021; 11(20):9399. https://doi.org/10.3390/app11209399.

50. Renne W, Ludlow M, Fryml J, Schurch Z, Mennito A, Kessler R, Lauer A. Evaluation of the accuracy of 7 digital scanners: An in vitro analysis based on 3-dimensional comparisons. J Prosthet Dent. 2017;118(1):36-42.

51. Ender A, Zimmermann M, Attin T, Mehl A. In vivo precision of conventional and digital methods for obtaining quadrant dental impressions. Clin Oral Investig. 2016;20(7):1495-504.

52. Available online: https://www.medit.com/dental-clinic-i700

53. Medit i700 Specification. Link: https://www.medit.com/dental-clinic-i700 (Accessed on July 30, 2022)

54. Logozzo S, Zanetti EM, Franceschini G, Kilpelä A, Mäkynen A. Recent advances in dental optics - part I: 3D intraoral scanners for restorative dentistry. Opt. Lasers Eng. 2014;54:203-21.

55. Waldecker M, Rues S, Rammelsberg P, Bömicke W. Accuracy of complete-arch intraoral scans based on confocal microscopy versus optical triangulation: A comparative in vitro study. J Prosthet Dent. 2021;126(3):414-420.

56. Chiu A, Chen YW, Hayashi J, Sadr A. Accuracy of CAD/CAM digital impressions with different intraoral scanner parameters. Sensors (Basel) 2020;20(4):1157.

3.2 LASER SYSTEMS FOR GINGIVAL RETRACTION IN FIXED PROSTHODONTICS: A NARRATIVE REVIEW

Sorrentino Roberto, Ruggiero Gennaro, Zarone Fernando

J Osseointegr 2022;14:1-5

Introduction

The accuracy of the marginal fit of a fixed prosthesis mainly depends on the recording of the finish line of the tooth to be restored. This recording is possible by making an impression of the finish line, which, if subgingival, can be shown through the retraction of the gingiva itself. This gingival retraction must take place both apically and laterally, to allow accurate registration of all the details of the finish line through the use of impression materials or intraoral scanners.
A minimum lateral displacement of approximately 0.2 mm is mandatory to allow the impression material to flow within the sulcus with proper dimensional accuracy (1).
Furthermore, retraction procedures must take place in a way that does not injure the basal cell layer and connective tissue cells, in order to avoid tissue changes and shrinkage of the gingiva (1).
Various gingival retraction systems have been described in the literature, which are as follows:

1. mechanical systems, such as retraction cords or pastes;
2. chemomechanical systems, with cords impregnated with hemostatic solutions;
3. surgical procedures, such as gingivectomy or electrosurgery based on the use of electrotomes;
4. laser surgery involving diode lasers, neodymium-doped yttrium-aluminum-garnet (Nd:YAG), erbium-doped yttrium-aluminum-garnet (Er:YAG), erbium, chromium-doped yttrium-scandium-gallium-garnet (Er,Cr:YSGG), and CO_2 laser systems (2-4).

Several investigations confirmed the effectiveness of laser systems in gingival retraction (1,4-6), through the removal of about 200 μm epithelium thickness from the sulcus (4), as a painless, simple, and convenient procedure (5).

The characteristics of the several types of laser systems are related to waveforms and wavelength (7).

Lasers are based on a high-powered focused beam operating by photo-ablation that causes tissue vaporization at 100-150 °C and they incise the tissues without hemorrhage and by fast healing with no inflammation and pain (7-8).

A survey of 696 dentists in the USA and Canada reported that 92% of them use gingival displacement cords, while 20.2% use laser systems and 32% electrosurgery as an adjunct for gingival troughing (9).

To date, the effectiveness of laser technologies in gingival retraction is clear, but despite their use in this procedure, there are still many points to be clarified.

First, what are the disadvantages and advantages related to the use of lasers compared to other systems for gingival retraction. In addition, it should be investigated whether the laser is better than other gingival retraction methods. Finally, what is the best type of laser for gingival retraction and how to set them.

The purpose of the present narrative review is to shed light on the use of dental lasers for gingival retraction procedures, in particular, the pre-setting of laser devices, advantages and disadvantages of laser retraction devices, and the comparison with other gingival retraction systems.

Methods

Search strategy

An electronic literature search was performed using the following databases: Medline (using PubMed), Scopus, Embase, Google Scholar, Dynamed, and Open Grey. Articles published up to August 31 2021, were considered.

The electronic search was conducted using keywords and MeSH terms connected by the Boolean operators “AND”, “OR”:

- (gingiva AND displacement AND laser);
- (gingiva AND displacing AND laser);
- (gingiva AND troughing AND laser);
- (gingiva AND retraction AND laser).

Only with the Google Scholar database, the following combination was used:
(gingiva) and (retraction or displacement or displacing or troughing) and (laser).

To avoid the lack of relevant papers, the authors examined the reference lists of the identified records.

In the present literature search, no time limits were considered for the year of publication of the records.

Inclusion and exclusion criteria

Studies were deemed suitable for the present review if they met the following inclusion criteria: 1) studies in which at least one laser system was used or tested for gingival retraction, 2) studies made in vivo or in vitro, systematic reviews, or case reports, and 3) studies published in English. The following exclusion criteria were used: 1) non-human animals in vivo studies, and 2) studies published in languages other than English.

Data extraction

According to the inclusion criteria, 3 calibrated researchers independently selected the studies reading the titles, abstracts, and keywords. The full text of each identified article was read to decide if it was suitable for inclusion. A majority criterion (i.e., 2 out of 3) was used in the case of disagreement among the investigators.

Results

Study selection

The search strategy produced 344 records, many of which were duplicates, 49 from PubMed/Medline, 49 from Scopus, 44 from Embase, 202 from Google Scholar, and 0 from both Dynamed and Open Grey. All the duplicates were discarded, thereby all the selected databases produced 164 records. After evaluating titles, abstracts, and keywords, the reviewers deleted 121 papers that did not meet the inclusion criteria. After a full-text analysis of the remaining 43 papers, 18 more were omitted because they did not provide any useful information about laser systems for gingival retraction. The remaining 25 records were included in the present review. No systematic reviews were found.

The literature search was concluded in August 2021, and the papers included in the present review were published between 1995 and 2019.

Among the search investigators, no disagreement was reported.

The workflow of the paper screening process is displayed in Figure 1, following the "PRISMA 2009 Flow Diagram" (10).

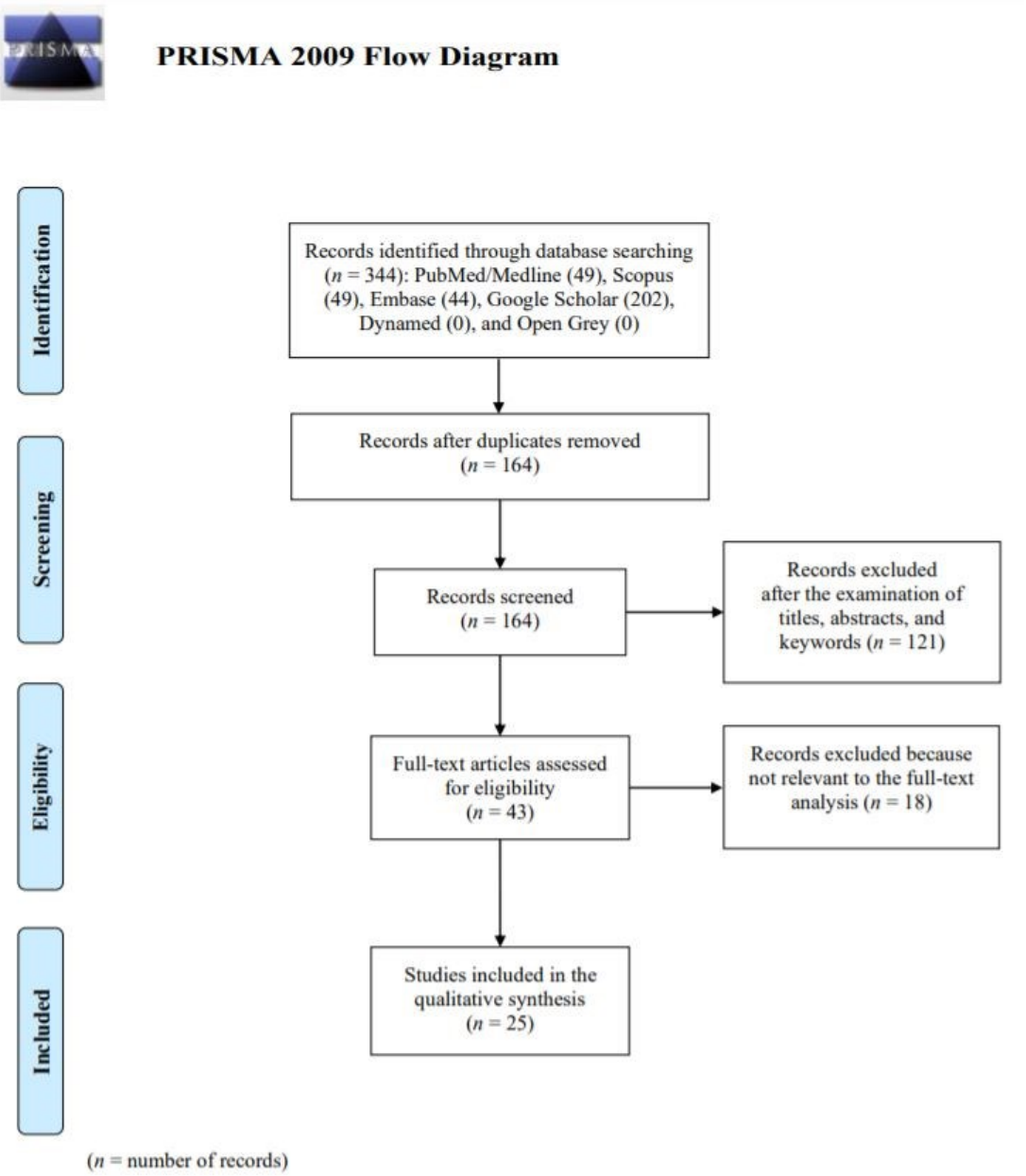

Figure 1 - Prisma search workflow.

Advantages and disadvantages, indications, and contraindications

Several advantages can be related to the use of dental laser systems for gingival retraction. First of all, the reduced bleeding during laser-surgical procedures (4,7,11-13) and postoperative hemostasis (3-4,14), both determined by coagulation through tissue vaporization, should be considered. Besides, the less intra-operative bleeding is accompanied by minor mechanical trauma (13), which favors less postoperative swelling and scarring (13). It is worth noticing that laser-induced surgical wounds heal with secondary intention, and incision lines display disorganized fibroblast alignment. This helps to preserve gingival margin heights by reducing tissue shrinkage caused by scarring (7).

The characteristic hemostasis of laser technologies facilitates the procedure for impression making on multiple abutments. This is very important because, in the case of zirconia frameworks that are becoming more and more popular (15), greater accuracy of impressions is required than those in metal alloy, as zirconia cannot be soldered to compensate for the inherent imprecision in impressions (16).

Moreover, thanks to coagulation properties, laser systems are helpful for digital scanning in order to provide a dry and clear surface for the scanning procedure (2).

Differently from electrocoagulation, lasers technology provides a lesser collateral heat generation (4) on soft and hard tissue, also with control of heat transfer to adjacent tissues (14).

Generally, the procedure of gingiva displacement seems to be relatively painless (3, 3,13,17), improving patient comfort (4,11-12).

Finally, it should be considered that laser systems could be effectively managed not requiring local anesthesia for gingival troughing, especially in the case of gingival hypertrophied tissues (8).

Despite the many advantages related to laser-mediated gingival retraction, it should be considered that this procedure is technique sensitive (13,17), without tactile feedback (18). Also, it is complicated to visualize the laser beam, due to the cooling water (18) and exposure of the prosthetic crown margins and tissue shrinkage could occur when overused (8).

Trainor et al. suggested to not use laser systems on thin gingiva in order to avoid recession (19).

Additionally, differently from the CO_2 laser, Nd:YAG systems are not recommended on peri-implant soft tissues because the implant surfaces tend to absorb heat and transport it towards bone tissues (20-21). Indeed, unlike other lasers, the technology behind CO_2 lasers has water as the prime chromophore which bounces off metal surfaces. Close to metal implant surfaces, CO_2 lasers absorb little energy, with only minimal temperature increases (<3 °C), minor collateral damage, and without altering the structure of implant surfaces. CO_2 lasers uncover the implant margins by creating a trough by excision instead of displacing soft tissue (22). Hence, if they are adopted around deeply positioned implants, significant defects may occur (17,21). Also 2.940 nm Er:YAG lasers could be considered reasonably safe because their wavelengths are reflected on metal implant surfaces also with a minimum penetration of the soft tissues, but its hemostasis is not as efficient as that of CO_2 lasers (21).

Pre-setting of laser devices

Laser devices have preset parameters based on the type of dental procedure to be performed, but at the same time, it is possible to customize these settings (2).

Several protocols were described in the literature for the various types of lasers, where the settings of the main parameters vary, as described in Table 1.

Table 1 –Laser settings used for gingival retraction as reported in the literature.

Reference	Laser system (wavelength)	Power (W)	Mode	Frequency (Hz)	Fiber tip diameter (µm)
Dawani et al. 2016 (1)	Diode Laser (810 nm)	0.8	Continuous	25.000	400
Marsch 2013 (2)	Diode laser (970 nm)	2.0	Pulsed	20	320
Krishna et al. 2013 (4)	Diode Laser (980 nm)	0.8	Continuous		
Goutham et al. 2018 (6)	Diode Laser (wavelength not specified)	0.8	Continuous	25.000	400
Gherlone et al. 2004 (23)	Diode Laser (980 nm)	2.5 to 3.5	Continuous		
Gherlone et al. 2004 (23)	Nd:YAG (1064 nm)	2.5 to 4.0		25 to 40	
Gururaj et al. 2019 (24)	Diode Laser (810 nm)	0.8	Continuous	25.000	400
Gupta et al. 2012 (25)	Diode Laser (980 nm)	1.5	Continuous		320
Stuffken and Vahidi 2016 (26)	Diode Laser (810 nm)	0.7 to 2.0	Continuous		
Melilli et al. 2018 (27)	Diode Laser (940 nm)	0.9	200 µs pulse duration	20	300
Tao et al. 2018 (28)	Diode Laser (810 nm)	2.0	Continuous	20	320
Tao et al. 2018 (28)	Nd:YAG (1064 nm)	2.0	Short pulse	15	320
Tao et al. 2018 (28)	Er:YAG (2940)	2.0	Very long pulse	15	500

Some authors suggested inserting the fiber tip to a depth of 1.0 to 1.5 mm into the crevicular sulcus (4,23) with a circular movement around the tooth (23), in the same manner of a conventional scalpel (8).

Although many authors set a continuous mode (1,4,6,23-26), Lee (16) suggests using the laser beam in a pulsed mode where possible with the addition of spray water and air for cooling during the procedure.

Comparison among lasers and other gingival retraction systems

Several clinical studies evaluated the effectiveness of laser systems in gingival retraction and focused on the biological impact of these technologies, particularly on periodontal structures, sometimes through comparisons with other gingival retraction systems or among different types of laser systems.

The results of clinical investigations are different, sometimes discordant, as they were conducted with different research protocols.

A clinical investigation reported that a diode laser produced greater gingival lateral mean displacement (0.48 ±0.10 mm) than magic foam cord, an expanding polyvinyl siloxane (Coltene Whaledent Inc, Altstätten, Switzerland) (0.31 ±0.09 mm), and retraction cord impregnated with aluminum chloride (0.44 ±0.11 mm) (6). These findings were confirmed by another study in which diode laser made a wider lateral displacement (0.62 ±0.09 mm) than magic foam cord (0.42 ±0.04 mm) (1).

Conversely, another clinical study reported that retraction cord produced a larger lateral displacement (0.33 mm) than diode laser (0.31 mm) and magic foam cord (0.19 mm).

The effectiveness of gingival retraction can be highlighted by noticing that laser systems determine a gingival troughing of about 230-670 μm, a range similar to the sulcular epithelium thickness and wider than the minimum limit of 200 μm needed for retraction (4,19).

As regards the depth of the gingival sulcus, the retraction cord showed the best value (1.43 mm), followed by diode laser (1.24 mm) and finally by magic foam cord (0.81 mm) (24).

Diode laser also seems to be the fastest gingival retraction system (mean value = 56.20 s) compared to magic foam cord (85.75 s) and retraction cord (252.15 s). Furthermore, compared to the latter troughing system, the diode laser procedure appears to be simpler (24).

One clinical study showed that the use of pulsed Nd:YAG lasers allowed faster healing and lower inflammation and hemorrhage than retraction cords impregnated with ferric sulphate or aluminum chloride (5). Furthermore, another investigation reported a better hemorrhage control of diode laser than retraction cord, although it was worse than magic foam cord (24).

As regards gingival recession, comparable but not clinically significant differences were reported for the double-cord technique impregnated with aluminum chloride cords (mean = 0.26 mm) and diode laser (0.27 mm) 8 weeks after the cementation (26).

Different authors reported a greater gingival recession with the double-cord and electro-surgery systems compared to the laser diode and Nd:YAG one (23). Furthermore, both these laser systems were found to be less aggressive also about gingival bleeding. In effect, less bleeding occurred with lasers than with the double-cord technique. Finally, the same authors observed that the diode laser has a haemostatic capacity similar to electrosurgery and superior to the Nd:YAG one (23).

According to the Visual Analog Scale (VAS) assessment system, the use of the diode laser (mean = 9.37) is significantly easier than the cord retraction technique (6.79). Furthermore, diode laser saved time (mean = 16.46 ±3.2 s) than cord (185.26 ±46.2 s) and is considered more comfortable according to VASs (mean of diode laser = 9.4; mean of cord = 5.95) (27). A clinical study did not record bleeding on the 35 tooth abutments that underwent laser system, while bleeding was observed for 10 abutments out of 39 during the retraction and 8 ones after the retraction for the cord system. No significative difference was detected between the 2 retraction systems about gingival retraction immediately after each retraction procedure (mean cord = 0.65 ±0.33 mm; mean laser = 0.66 ±0.43 mm) and 15 days after the impression session (mean cord = 0.03 ±0.27 mm; mean laser = 0.02 ±0.46 mm) (27).

Another comparative study measured the gingival width and recession occurred with the following gingival troughing systems: the retraction cord and diode, Nd:YAG, and Er:YAG laser systems (28). It resulted significant differences between lasers and retraction cords in gingival width, with the following mean values immediately after retraction: retraction cord = 0.32 ±0.09 mm, diode = 0.55 ±0.15 mm, Nd:YAG = 0.60 ±0.17 mm, Er:YAG = 0.65 ±0.14 mm. Also, regarding gingival recession, statistical differences were found between lasers and retraction cords, with the following mean values 4 weeks after the surgery: retraction cord = 0.24 ±0.08 mm, diode = 0.13 ±0.08 mm, Nd:YAG = 0.14 ±0.07 mm, Er:YAG = 0.10 ±0.06 mm. These results showed wider gingival width and less gingival recession for lasers than retraction cord. Also, the authors reported that among laser systems, Er:YAG exhibited the most uneventful and rapid wound healing when compared to diode and Nd:YAG lasers (28).

Conclusion

According to the current state of the literature, the following conclusions can be drawn:

- Laser systems provide optimal postoperative hemostasis and minor mechanical trauma that favors less postoperative swelling and scarring which preserve gingival margin heights.
- CO_2 and Er:YAG lasers could be used on peri-implant soft tissues while Nd:YAG systems are contraindicated.
- Diode laser makes a greater gingival lateral displacement than magic foam cord. Also, it seems to be the faster, more comfortable, and simpler gingival retraction system compared to magic foam cord and retraction cord.
- Nd:YAG lasers allowed faster healing, better hemostasis, and lower inflammation than retraction cords impregnated with ferric sulphate or aluminum chloride.

To date, the data concerning the lateral and vertical displacement of the gingiva are still scarce and often controversial due to the different research protocols and the few available studies. Laser technologies are efficient systems for gingival retraction and appear safe when used for thick gingival biotypes. Nevertheless, more in vitro, in vivo, and randomized controlled trial studies are mandatory to define the clinical indications around implants, the best laser gingival retraction system and the pre-setting protocol, and their effectiveness than other retraction systems.

References

1. Dawani M, Sathe S, Godbole SR. Comparative evaluation of clinical efficacy of two new gingival retraction systems - An in vivo research. Int J Sci Res 2016;5:4-10.
2. Marsch A. Use of a diode laser for gingival troughing in conservative and prosthetic dentistry. Int Mag Laser Dent 2013:30-1.
3. Martin E, Parker S. The use of lasers in fixed prosthodontics. Dent Clin North Am 2004;48:971-98.
4. Krishna CV, Gupta N, Reddy KM, Sekhar NC, Aditya V, Reddy GV. Laser gingival retraction: a quantitative assessment. J Clin Diagn Res 2013;7:1787-8.
5. Gabbar AF, Aboulazm SF. Comparative study on gingival retraction using mechanochemical procedure and pulsed Nd = YAG laser irradiation. Egypt Dent J 1995;41:1001-6.
6. Goutham GB, Jayanti I, Jalaluddin M, Avijeeta A, Ramanna PK, Joy J. Clinical assessment of gingival sulcus width using various gingival displacement materials. J Contemp Dent Pract 2018;19:502-6.
7. Parker S. The use of lasers in fixed prosthodontics. Dent Clin North Am 2004;48:971-98.
8. Kamath R, Sarandha DL, Baid GC. Advances in gingival retraction. Int J Clin Dent Sci 2011;2:64-7.
9. Ahmed SN, Donovan TE. Gingival displacement: Survey results of dentists' practice procedures. J Prosthet Dent 2015;114:81-5.e1-2.
10. Liberati A, Altman DG, Tetzlaff J, Mulrow C, Gøtzsche PC, Ioannidis JP, Clarke M, Devereaux PJ, Kleijnen J, Moher D. The PRISMA statement for reporting systematic reviews and meta-analyses of studies that evaluate health care interventions: explanation and elaboration. PLoS Med 2009;6:e1000100, https://doi.org/10.1371/journal.pmed.1000100.
11. Coluzzi DJ, Convissar RA. Lasers in clinical dentistry. Dent Clin North Am 2004;48:11-2. https://doi.org/10.1016/j.cden.2004.06.003.
12. Donovan TE, Chee WW. Current concepts in gingival displacement. Dent Clin North Am 2004;48:433-44.
13. Singh DK, Gupta P, Bhatnagar A. Gingival displacements options in prosthodontics: A critical review on recent advances. J Adv Res Dent Oral Health 2016;1:13-21.
14. Rossmann JA, Cobb CM. Lasers in periodontal therapy. Periodontol 2000 1995;9:150-64.

15. Zarone F, Di Mauro MI, Ausiello P, Ruggiero G, Sorrentino R. Current status on lithium disilicate and zirconia: a narrative review. BMC Oral Health 2019;19:134. https://doi.org/10.1186/s12903-019-0838-x.
16. Lee EA. Laser-assisted gingival tissue procedures in esthetic dentistry. Pract Proced Aesthet Dent 2006;18:suppl 2-6.
17. Prasad KD, Hegde C, Agrawal G, Shetty M. Gingival displacement in prosthodontics: A critical review of existing methods. J Interdiscip Dentistry 2011;1:80-6.
18. Albaker AM. Gingival retraction-techniques and materials: a review. Pak Oral Dent 2010;30:545-51.
19. Trainor J, Keeling A, Wassell R. Extra-Coronal Restorations. Concepts and clinical application, 2nd ed. In: Wassell R, Nohl F, Steele J, Walls A. (eds). Cham: Springer; 2019. P 363-374.
20. Scott A. Use of an erbium laser in lieu of retraction cord: a modern technique. Gen Dent 2005;53:116-9.
21. Martin E. Lasers in dental implantology. Dent Clin North Am 2004;48:999-1015.
22. Bennani V, Schwass D, Chandler N. Gingival retraction techniques for implants versus teeth: current status. J Am Dent Assoc 2008;139:1354-63.
23. Gherlone EF, Maiorana C, Grassi RF, Ciancaglini R, Cattoni, F. The use of 980-nm diode and 1064-nm Nd;YAG lasers for gingival retraction in fixed prosthesis. J Oral Laser Appl 2004;4:183-90.
24. Gururaj R, Jayesh SR, Nayar S. Comparative evaluation of four factors in gingival retraction using three different gingival retraction techniques: In vivo study. Indian J Public Health Res Dev 2019;10:1190-5.
25. Gupta A, Jain N, Makhija PG. Clinical applications of 980 nm diode laser for soft tissue procedures in prosthetic restorative dentistry. J Lasers Med Sci 2012;3:185-8.
26. Stuffken M, Vahidi F. Preimpression troughing with the diode laser: A preliminary study. J Prosthet Dent 2016;115:441-6.
27. Melilli D, Mauceri R, Albanese A, Matranga D, Pizzo G. Gingival displacement using diode laser or retraction cords: A comparative clinical study. Am J Dent 2018;31:131-4.
28. Tao X, Yao JW, Wang HL, Huang C. Comparison of gingival troughing by laser and retraction cord. Int J Periodontics Restorative Dent 2018;38:527-32.

4. DIGITAL-LINKED MATERIALS

Dental research has focused on finding novel materials that are both aesthetically pleasing and mechanically reliable in response to patient demands for enhanced esthetics and minimal invasiveness. The fast development of production technology has also caused a significant change in the operating procedures for prosthodontics. The standards of accuracy, aesthetics, and mechanical durability of metal-free materials (such as zirconia and lithium disilicate) have been elevated to extremely high levels by the development of digital hardware and software, further promoting the replacement of metal for indirect restorations.

To date, zirconia and lithium disilicate undoubtedly represent the protagonists of the new generation of prosthetic materials, and international research is strongly focused on their properties. In recent years, these materials, the former representing a pure polycrystalline core and the latter belonging to the etchable glass-ceramics, have undergone progressive improvements thanks to the modifications of production technologies, aiming, on one hand, to make them optically more appealing (like in the case of "translucent" zirconia), and, on the other hand, to increase their mechanical performances (as in the case of lithium silicate reinforced with zirconia, also known as ZLS). Furthermore, not only have CAD-CAM (Computer-Aided Design - Computer-Aided Manufacturing) processing techniques promoted a higher quality standardization of the final products with a noticeable cost and time reduction, but they have also allowed for the fabrication of monolithic prostheses, significantly reducing the occurrence of cohesive fractures (or chipping) of the veneering ceramics, broadly reported as the major complication of bi-layered restorations.

These novel ceramic materials offer a comprehensive panel of operative options to the prosthodontists, thanks to their continuous evolution. In the present chapter, several literature reviews about lithium disilicate, zirconia, and ZLS are presented.

Moreover, it is important to understand whether even different preparation designs can lead to a greater removal of enamel tissue, which is essential as it guarantees better adhesion than dentin tissue. For this reason, it was conducted a study aimed to evaluate whether there were differences in dentinal exposure between two different preparation designs for laminate veneers, Window and Butt-Joint.

Furthermore, another study analyzes the data deriving from the aesthetic, biological and mechanical results of single crowns in CAD-CAM monolithic zirconia supported by implants

and cemented on titanium abutments with dual-curing resin cement, after 6 years of function.

At the end of the chapter, it is possible to read an excerpt from a publication regarding the advantages of exploiting digital technologies such as digital scanners to reduce the risk of cross-contamination from COVID-19.

SUMMARY:

4.1 CURRENT STATUS ON LITHIUM DISILICATE AND ZIRCONIA: A NARRATIVE REVIEW

Zarone Fernando, Di Mauro Maria Irene, Ausiello Pietro, Ruggiero Gennaro, Sorrentino Roberto
BMC Oral Health. 2019;19:134.

1. Introduction

At "The Digital Dentistry Society II Consensus Conference on Digital Technologies – Marrakech 2018" the main topics of digital interest were thoroughly discussed, in order to draw clinical recommendations based on scientific evidence and, when missing, on the clinical experience shared by the scientific community. The present narrative review is focused on the technical and clinical profile of the two most popular metal-free materials, lithium disilicate and zirconia, in order to briefly shed light on their different indications, advantages and shortcomings.

2. Methods

An extensive research has been carried out in the literature available on the subject, worldwide, limiting itself exclusively to articles in english, available on the main search engines (Pubmed, Embase, Scopus) and published in the most important indexed journals of the Materials and Dental sector, with and without impact factor. The results highlighted in this narrative review were extrapolated from this literature search, with reference to the authors' clinical experience.

3. Results

LITHIUM DISILICATE

Physico-chemical features, optical and mechanical properties

Lithium disilicate (LS2) is classified as a glass-ceramic, in the class of particle-filled glass materials. Introduced on the market in the 90s with the commercial formulation named "IPS Empress 2" (Ivoclar Vivadent, Schaan, Liechtenstein), it was composed of 65 vol% lithium disilicate, small needle-shaped crystals (3–6 μm × 0.8 μm) embedded in a glass matrix, with a 1 vol% porosity [1–3], showing valuable mechanical characteristics (flexural strength: 350 MPa;

fracture toughness (KIC): 3.3 MPa√m; heat extrusion temperature: 920 °C; thermal expansion coefficient (CTE): 10.6 + 0.25 ppm/°C). At first, this material was made commercially available as ingots, to be utilized according to the "heat-pressing" fabrication procedure, similar to the classic "lost wax" technique for metal-alloy casts, aimed at producing cores, hot pressed into a mold. In order to get an appealing reproduction of the optical characteristics of natural teeth, the cores are lately veneered with a very translucent fluorapatite ceramic, containing 19–23% of fluorapatite crystals ($Ca_5(PO_4)_3F$) embedded in a glassy matrix [4].

Thanks to an optimization of the processing parameters, allowing the formation of smaller and more uniformly distributed crystals, in 2005 a new formulation of LS2 was marketed as "IPS e.max Press" (Ivoclar Vivadent), exhibiting improved mechanical properties and optical features (flexural strength: 370–460 MPa; fracture toughness (KIC): 2.8–3.5 MPa√m), much higher than the older glass-ceramics. The high mechanical performance of this material is due, on one side, to a layered, tightly interlocked distribution of the elongated disilicate crystals, hindering crack propagation across the planes and, on the other side, to a mismatch between the thermal expansion coefficients of LS2 crystals and the glassy matrix, so that the latter induces a tangential, compressive stress around the crystals [2]. Besides the production of ceramic cores for bilayered crowns, the increase of strength and toughness of IPS e.max Press has allowed to extend its clinical indication to monolithic restorations, without veneering ceramic, anatomically shaped, colored by surface stains and characterized by a higher fatigue resistance than the bilayered ones.

Besides the heat-pressed technique, the widespread, increasing implementation of computer-aided design/computer-aided manufacturing (CAD-CAM) technologies has led to the introduction of ceramic blocks aimed at the production of restorations by milling devices (IPS e.max CAD), also suitable for chairside production of restorations. Partially, pre-crystallized blocks are manufactured in a "blue state", containing 40% of metasilicates (Li_2SiO_3) in addition to lithium disilicate crystal nuclei

($Li_2Si_2O_5$). Such blocks are characterized by moderate flexural strength of ~ 130 MPa, resulting in higher cutting efficiency, easier and faster workability and lower wear of the milling tools [2, 3, 5]. The milling procedure is performed in this pre-crystallized state and, after its completion, it is followed by a heating cycle (840°-850 °C for 10 min) that turns metasilicate crystals into lithium disilicate (~ 70%), increasing the flexural strength up to values of 262 ± 88 MPa, together with a fracture toughness of 2.5 MPa·m1/2. The blocks are available in different colors, obtained by dispersing staining ions in the glassy matrix [6] and in different degrees of translucency, on the basis of the size and distribution of the crystals in the glassy matrix [4]. The

variability of flexural strength of lithium disilicate among heat-pressed and CAD-CAM blocks with different translucency is still under debate [7, 8]. Particularly, the flexural strength of IPS e.max Press and IPS e.max CAD was reported to be similar and the manufacturing process did not seem to affect the mechanical characteristics of lithium disilicate ceramics; moreover, the flexural strength was significantly influenced by translucency only for CAD-processed materials [7].

In vitro fully anatomical e.max CAD crowns have been shown to exhibit fracture resistance that is suitable for posterior, monolithic restorations [9] and to be more resistant to fatigue in cyclic loading than veneered zirconia, that is more prone to chipping [10]. For the high interest generated by its clinical versatility, further developments are expected on this material, being it influenced by different production processes, like thermal gradients, times and rates, that affect its microstructure and mechanical properties. It has been shown, for instance, that extending temperature range (750–840 °C, compared to the standard 820–840 °C) or prolonging holding time (14 min vs 7 min at 840 °C) increase elastic modulus and hardness properties, without affecting flexural strength and fracture toughness [11]. Moreover, new technologies, as spark plasma sintering, can induce a refinement and a densification of the nano-crystalline microstructure, increasing lithium disilicate and metasilicate phases and reducing lithium orthophosphate and cristobalite/quartz phases [12, 13].

As regards mechanical resistance, it has been clearly demonstrated that, in vitro, veneered LS2 crowns exhibit significantly lower fracture load values (1431.1 ± 404.3 N) compared to monolithic ones (2665.4 ± 759.2 N), the main failure mechanism being bulk fracture initiating from the occlusal surface [14]. To date, there is strong evidence from in vitro studies that, differently from bilayered restorations, monolithic ones show fracture strength and fatigue resistance suitable for use in the posterior areas, both in tooth- and implant-supported single crowns (SC) and 3-unit fixed dental prostheses (FDPs) [15–22].

Monolithic LS2, as well as Zirconia reinforced-Lithium Silicate ceramics (ZLS), offers higher fracture resistance than bilayered, hand-veneered zirconia [20], while a recent in vitro research has shown that load-to-fracture values of monolithic zirconia are higher than those of LS2; the latter, in turn, are higher than those of ZLS [23]. It has to be pointed out, however, that, particularly as regards LS2, fatigue resistance is strongly influenced by many experimental variables, like amount of cyclic loading, abutment and antagonist design and material, thermocycling parameters and test environment; for this reason, the heterogeneity and lack of standardization in research designs, tested materials and experimental conditions make a comparison of data not easily feasible [24].

Abrasiveness and wear

As to wear and abrasiveness, LS2 shows quite favourable properties, that are highly depending on the surface characteristics of the restoration. When accurately polished at its surface, the material exhibits convenient tribological behaviour in vitro, in terms of friction and wear of restorations, being its abrasiveness quite close to enamel, although more aggressive when compared to type III gold [25] or to polished monolithic zirconia in in vitro simulations [26–28]. Such favourable wear behaviour and durability have been also confirmed by some in vivo evidence [15].

On the other hand, it has been reported that grinding, glaze coating and fluorapatite ceramic veneering can increase wear, both of the antagonist teeth and of the restoration itself; at the same time, surface roughness can also be increased, besides a reduction of gloss, in the presence of basic pH environment and after toothbrushing with abrasive toothpaste [29–33]. For these reasons, when it is not crucially needed for esthetic reasons, glazing of monolithic restorations should be avoided on the occlusal surfaces in posterior sites and only limited to the esthetically relevant zones; moreover, careful polishing procedures should always follow any occlusal grinding or esthetic refinement of disilicate restorations, although in vitro evidences at scanning electron microscope (SEM) have shown that LS2 is one of the most critical materials to adjust intraorally, due to significant chip accumulation in the diamond burs, requiring higher machining forces and energy, with likely onset of intergranular and transgranular fractures, besides risks of thermal damage to tissues and restorations [32].

Biocompatibility

One of the strongest points of LS2 is the excellent quality of soft tissue response. In vitro, this material exhibits high levels of biocompatibility, not only due to low plaque retention, but also to adhesion and proliferation of human epithelial cells [34] and human gingival fibroblasts [35], particularly when its surface is polished. In vivo, in the presence of LS2 restorations no inflammatory reactions were detected, analyzing the concentration of inflammation indicators in the gingival crevicular fluid; the same results were found with zirconia restorations [36]. Such favourable tissue responses have also been confirmed by tissue culture data [34]. In clinical experience, LS2 restorations are likely to yield very natural and sound aspect of soft tissues when in contact with marginal gingiva or peri-implant mucosa, in the presence of subgingival margins.

Surface treatment and cementation

In addition to excellent biocompatibility and high mechanical properties, LS2 exhibits very good esthetic features, especially as regards translucency, that is about 30% higher than conventional zirconia [37]. Moreover, for the presence of silica, LS2 is an acid-sensitive ceramics, so that high strength of adhesion to the substrate is expected, due to both micromechanical and chemical bonding mechanisms. Micromechanical interlocking between ceramics and resin cement at the intaglio surface is based on the creation of surface microirregularities, pits and roughness by means of acid etching and/ or physical treatments like alumina particles sandblasting or diamond bur grinding. For the glass-ceramic class, to date hydrofluoric acid (HF) etching is the best-established procedure, to be performed according to validated protocols taking into account both acid concentration and etching time. For LS2, 20 s HF etching (at 5% concentration) is suggested, that is a shorter time than requested for feldspathic and leucite-based ceramics (generally 60 s). Higher HF concentrations (9–10%) and longer etching times have been shown to be too aggressive and can introduce relevant damages, not only to the surface but also to the internal microstructure of the material, negatively influencing mechanical performance (reduction of flexure strength), adhesion potential and long-term success of ceramic restorations, particularly when thickness is low [38–41]. Another system to create surface microirregularities is sandblasting LS2 with aluminum oxide particles. Nevertheless, it has been shown that this procedure, as well as laser etching, can determine excessive loss of material, with surface modifications that are less uniformly distributed than after HF etching and that can significantly reduce flexural strength [42, 43]. In addition to micromechanical interlocking, as for all silica-based materials, adhesive bonding of LS2 is efficiently increased by silane, ensuring a chemical interaction between the resin-based agent and the ceramics, obtained forming strong siloxane linkages [44–50].

Recently, it has been shown that the use of silane combined to a phosphate functional monomer, the 10- Methacryloyloxydecyl-Dihydrogen-Phosphate (10-MDP), creating an acidic environment further improves the bond strength of resin-based luting cement to lithium disilicate ceramics [51].

Clinical indications and performances

As regards clinical indications of LS2, it has to be pointed out that this is one of the most versatile metal- free materials for its high esthetic potential, good mechanical properties and favourable bonding strength to dental tissues, thanks to its silica content. Lithium disilicate

ceramics can be utilized both for tooth- and implant-supported restorations, ranging from SCs to FDPs, from anterior veneers to posterior inlays, onlays and overlays [4, 7].

To date, due to its relatively recent market introduction, there is still a lack of data about long-term outcomes of LS2 restorations, particularly as regards CAD-CAM production. Prospective, medium-term studies reported good cumulative survival rates, both for tooth-supported crowns (94.8% after 8 years [52]) and implant-supported crowns, made by CAD-CAM procedure following conventional impression (100% after 5 years [53]). A recent prospective study on implant-supported, single-unit monolithic restorations made of LS2 in a complete digital workflow has demonstrated survival rates of 100%, without any technical or biological complications, after 2 years of service [54]. Similarly, retrospective studies have shown that LS2 can yield satisfactory clinical performance with favourable survival rates and low incidence of mechanical failures, like debonding, fractures and chipping [15, 55–58]. As regards chairside procedures, monolithic LS2 crowns revealed a survival rate of 83.5% after 10 years of follow-up; the main complications were loss of retention, secondary caries and hypersensitivity [59].

In the last decade, LS2 has been proposed for producing full-contoured, monolithic SCs to be bonded to CAD-CAM zirconia full-arch frameworks supported by implants. In a mid-term study, such a restorative solution exhibited 100% survival rate, after 5 years of follow- up [60]. Recently, an in vitro study has suggested that LS2 crowns supported by ceramic-reinforced polyether ether ketone (PEEK) implant abutments may be an alternative to zirconia abutments with a titanium base for single-implant restorations in the anterior region [61].

Thanks to the high reliability of resin bond to glass-ceramics, LS2 clinical indications also include adhesively retained, tooth-supported restorations. In the anterior sites, in the authors' and in other clinicians' clinical experience, laminate veneers made of bilayered, hand-veneered LS2 are a likely choice, particularly when clinical performance and high esthetic results are expected [62]. Clinical and in vitro studies demonstrated that, in the presence of long teeth, margins positioned beyond the cemento-enamel junction (CEJ), large areas of exposed dentin or flexural tensile stresses due to high functional loads, laminate veneers are exposed to higher failure risks, being maximum enamel preservation and veneer mechanical resistance paramount success factors [63, 64]. Due to its mechanical properties, lithium disilicate can be considered a viable option to fabricate ceramic veneers in the presence of unfavorable biomechanical conditions; in fact, it was reported that more rigid ceramic materials exert a kind of shield effect onto underlying tooth structures, strengthening the restorative complex [65].

Since their introduction in 1991, all-ceramic, resin- bonded fixed dental prostheses (RBFDPs) have been increasingly utilized as minimally invasive restorations aimed at replacing one missing tooth in the anterior arch [66]. Although recording a high rate of early (1-year), unilateral retainer fractures in conventional, two retainers all-ceramic adhesive bridges, the authors noticed that the fractured, unilaterally supported restorations stayed in situ for 5 to 10 years [67–69]; for that reason, since 1997 cantilevered all-ceramic RBFDPs were proposed as a new conservative treatment modality for replacement of single anterior missing teeth, with minimal tooth preparation on the lingual side, just aimed at achieving a correct positioning during cementation [70]. Different materials have been proposed over the years, mainly, for their high strength, glass-infiltrated alumina ceramics [71] and densely sintered, bilayered zirconia, treated with a combination of moderate pressure air-abrasion and MDP, with promising medium-term outcomes [72–75]. Thanks to its advantageous optical properties and to its HF etching/silane bonding option, LS2 has also been proposed as an alternative material for such cantilevered restorations, showing comparably promising clinical results [76–78]. In a systematic review, cantilevered RBFDPs showed a lower failure rate than conventional, two-retainer, "Maryland bridge-style" ones, in which higher biomechanical stress arises for the different directions of forces acting on the adjacent supporting teeth during anterior guidance in protrusive and lateral mandibular movements [79]. In another recent review, an estimated 91.2% survival rate at 5 years was reported for all-ceramic RBFDPs, exhibiting higher debonding rate with zirconia resin-bonded restorations than with glass-ceramic ones; conversely a higher fracture rate was reported with glass-ceramics [80], even though higher level of evidence will be necessary to draw final long-term evaluations of all-ceramic RBFDPs clinical performances. RBFDPs are a suitable prosthetic solution as an alternative to implant-supported SCs, in the presence of anatomical impairment requiring costly and invasive surgical procedures, financial problems, young age of patients with congenitally or post-traumatically missing incisors; in any case, to limit the risks of mechanical failure or debonding, after an extensive esthetic, occlusal and technical evaluation of the case, a very careful treatment planning has to be defined prior to proceed with the operative phases.

In the posterior sites, LS2 can be successfully employed for resin-bonded single restorations, like inlays, onlays, non-retentive partial crowns and full coverage table-tops, in the monolithic form. The material offers undisputable advantages, like high fracture resistance, showed by high load-at-fracture values in table-tops/occlusal veneers, allowing reduced thickness of the restorations (1–1.5 mm), low wear and abrasive potential, adhesive bonding strength and high biocompatibility, properties that are very favourable when teeth are severely abraded or a heavy occlusal correction is needed (like in lateral post- orthodontic open bite) [10, 81–85]. These

restorative solutions have shown favourable clinical outcomes in the most recent literature, even though with limited follow-up [86, 87]. A recent 3-years randomized, controlled prospective trial has shown that LS2 partial crowns can be used as successful restorative solutions for endodontically treated posterior teeth, with no significant differences between premolar or molars and with or without the use of fiber posts [88].

The utilization of LS2 for FDPs is a controversial topic: literature data is quite scant and not homogeneous, with a high variability of reported survival and success rates, ranging from rather poor clinical results [89–92] to acceptable long-term serviceability both in anterior and posterior sites, similar to metal-ceramics [93]. In the opinion of the authors, from a strictly clinical point of view, taking into account the cost/benefit ratio in terms of esthetic needs and structural resistance, the material of choice for 3- or 4-unit FDPs is still zirconia, in all of its different typologies.

Marginal accuracy and internal fit

Several studies evaluated the adaptation of lithium disilicate restorations, fabricated in both conventional and digital workflow. According to the most recent literature, there is no significant difference in terms of marginal accuracy between conventional and full-digital procedures for the fabrication of monolithic lithium disilicate crowns [94–96]. Moreover, some authors reported that hot- pressed LS2 crowns made from conventional impressions with polyvinylsiloxanes exhibit better fit than CAD-CAM digitally produced ones [97].

Furthermore, centralized milling production has been reported to result in better fit compared to chairside system; in the same study, occlusal internal adaptation was better in the conventionally manufactured crowns than in the digitally fabricated ones [95]. Conversely, other studies reported that marginal and internal fit of LS2 crowns were more accurate when using digital impression technique; in any case, whatever the workflow used, the adaptation was shown to be within clinical acceptability range [98–101].

To date, drawing univocal conclusions about adaptation accuracy of lithium disilicate restorations is not easy, due to the high number of variables involved in the final prosthetic fit, like digital impression system and technique, used material and fabrication procedure, so there is still a noticeable amount of controversial debate [3, 102]. As regards fabrication techniques, hot-pressed lithium disilicate is reported to offer better internal fit and mechanical performances compared to CAD-CAM pre-crystallized blocks, even if, also about this topic, further data will

be necessary to definitely shed light on these aspects, due to the constant evolution and increasing quality of milling procedures and devices [103–108].

ZIRCONIA REINFORCED-LITHIUM SILICATE CERAMICS (ZLS)

In the last years, the continuous research and progress in prosthetic material field for dental CAD-CAM applications has led to the introduction on the market of promising materials, the ZLS, thanks to an alternative strategy to enhance translucency: a glassy matrix, containing a homogeneous crystalline structure made of lithium silicate crystals, is reinforced with tetragonal zirconia fillers (about 10% by weight) allowing higher strength values than LS2 [109]. The higher mean translucency, together with proper biaxial flexural strength values, make such material a proper choice for minimally invasive, single tooth esthetic restorations, like inlays, onlays, partial crowns, veneers, anterior and posterior crowns, both tooth- and implant-supported [109, 110], also fulfilling the “no-prep, table- top” strategy [85]. The restorations show higher translucency and ease of intraoral polishing than both feldspathic and disilicate blocks, but, at the same time, exhibit high brittleness [110–112]. In case of a dark substrate, moreover, it has to be considered that the high translucency of the material requires adequate thickness (1.5–2.0 mm) in order to get a proper chromatic masking [113].

To date, as regards mechanical properties and clinical performances of ZLS, data are still limited, often controversial and short-term; these highly promising ceramics need further studies, both in vitro and in vivo, in order to precisely define physical-mechanical properties, clinical indications, limits and long-term performance of such restorations [114–117].

ZIRCONIA

Physico-chemical features

In the ceramic classification, zirconia (ZrO2) is a heterogenous, highly-resistant, polycrystalline ceramic, characterized by favourable mechanical properties (toughness: 5–10 MPa√m, flexural strength: 500–1200 MPa, Young’s modulus: 210 GPa) and good optical characteristics [118–121]; however, differently from glass-ceramics, it is not susceptible to conventional acid etching techniques and, consequently, does not take advantage of conventional adhesive bonding procedures [122].

Both in vitro and in vivo, it shows excellent biocompatibility, lower plaque retention than titanium and good radiopacity; moreover, it is not soluble in water and its susceptibility to

corrosion in the oral environment is negligible [118–121]. Among the various metal-free, ceramic materials, after conventional finishing and polishing, monolithic zirconia exhibits the lowest wear behaviour towards opponent teeth [123].

Phase transformation toughening (PTT)

In dentistry, zirconia is usually considered an all-ceramic material but, from the physical-chemical point of view, it is a metal oxide with ceramic properties characterized by polymorphism and allotropy. In fact, it is present in nature with three different crystalline configurations at different temperatures: cubic (from the melting point at 2680 °C to 2370 °C), tetragonal (from 2370 °C to 1170 °C) and monoclinic (from 1170 °C to room temperature). These different allotropic states present with distinct mechanical and optical properties that can be exploited differently in Prosthodontics [118–121, 124].

Conventionally, zirconia is mainly used in its partially yttria-stabilized tetragonal phase (Y-TZP) as a prosthetic material for indirect restorations. Under the effect of mechanical, thermal and/or combined stresses, the adsorbed energy can break part of the atomic bonds of its polycrystalline structure turning such tetragonal crystals to a stabler monoclinic shape. This spontaneous and irreversible transformation is known as Phase Transformation Toughening (PTT) and shows a contemporary 4–5% increase in crystals volume, creating significant compressive stresses within the material [118–121, 124]. From the technological and prosthetic sides, the PTT has been advertised as a paramount advantage, since it allows a kind of self-repairability of zirconia; indeed, it permits to block or at least to hinder the propagation of micro-cracks and fractures within the material. In fact, the subsequent volumetric increment of the crystals generates comses within the material at the fracture tip, limiting crack propagation [118–121, 124–126]. It is worth noticing that at room temperature such transformation is irreversible and localized, centered at the stress bearing area (i.e. occlusal load area, traumatic impact zone, etc.): once the limiting action of the fracture propagation has occurred, in its monoclinic configuration zirconia is no longer able to limit cracks any further [119, 124, 126]. On the contrary, heating monoclinic zirconia again up to 900–1000 °C (for limited time according to manufacturers' instructions), the PTT becomes reversible: by means of a process called "regeneration" or "annealing", monoclinic crystals can be moved back to the tetragonal phase, causing the relaxation of compressive stresses within the material [125, 126]. After annealing, however, zirconia toughness tends to be reduced and, as regards the optical properties, a chromatic oversaturation can occur; consequently, thermal treatments at high temperature should be used carefully and

only after potentially aggressive mechanical procedures (i.e. relevant occlusal grinding, polishing, etc.) [126–128].

In order to profit from the positive features of the PTT intraorally, during industrial manufacturing cubic and tetragonal zirconia are stabilized with metal oxides, just like yttrium, magnesium, cerium and lanthanum; the percentage of such dopants can vary according to manufacturing techniques and clinical use. These stabilizing oxides contribute to keep zirconia in its crystalline tetragonal phase also at room temperature in a thermodynamically metastable state, preventing the spontaneous transformation in the more stable monoclinic crystals. However, such dopant oxides can get lost after traumatic events, surface modifications (i.e. occlusal adjustments, grinding, polishing, etc.) and material aging [118–121, 124–127].

Low temperature degradation (LTD) and aging

In turn, the PTT is closely related to a negative phenomenon, the so-called "Low Temperature Degradation (LTD)", responsible for zirconia aging. At room temperature, the material can undergo a spontaneous and irreversible transformation to the monoclinic phase, even in the absence of any mechanical stress. This phenomenon causes a worsening of mechanical properties, till the possible occurrence of spontaneous fractures [118–121, 124–127, 129, 130]. The LTD is a multifactorial phenomenon affected by several variables, such as crystals dimension, temperature, surface defects, manufacturing techniques, percentage and distribution of stabilizing oxides, mechanical stress and wetness; particularly, the last two factors can significantly accelerate zirconia aging. Although aging is considered a risk factor for mechanical failure, to date no univocal correlation has been evidenced between this phenomenon and the failures affecting zirconia during clinical service. Nonetheless, the LTD is known to cause a worsening of zirconia characteristics, contributing to the onset of micro-cracks, toughness reduction, increased wear, roughening and plaque accumulation, till a severe surface degradation, affecting both mechanical and optical properties [118–121, 125–127, 129, 130].

As reported in a recent in vitro study, monolithic tetragonal zirconia restorations can undergo hydrothermal degradation (i.e. aging) also after short observation times; however, such phenomenon does not reduce significantly the mechanical properties of tetragonal zirconia even in the presence of wide monoclinic transformed areas [126]. In the same research, the glassy layer used for glazing effect can act as a protective barrier against hydrothermal degradation; nonetheless, some restoration areas, particularly at the margins, can show absence of glazing protection and subsequently can be more susceptible to aging [126].

In vitro studies have clearly demonstrated that mechanical properties of zirconia, expressed by parameters like load-to-fracture values, are higher than those of LS2, which, from their part, are higher than those of ZLS; the number of fatigue loading cycles does not seem to affect the load-to-fracture of zirconia restorations [23].

Optical and mechanical properties

Laboratory investigations reported that monolithic zirconia restorations showed higher resistance to fracture than bilayered ones, even after mechanical cycling and aging [131–136]. Surface finishing techniques did not influence mechanical performance [132], neither did cementation techniques, particularly onto implants [137]; on the contrary, fracture resistance has been reported to be significantly influenced by preparation design [138, 139] and low temperature degradation [138], so it can be inferred that material and geometrical characteristics are crucial to optimize longevity of monolithic zirconia restorations [140]. The high mechanical reliability of zirconia has been confirmed by recent in vitro analyses, demonstrating that monolithic zirconia crowns with occlusal thickness of 0.5 mm exhibit sufficient fracture resistance to withstand occlusal loads in the molar regions [134, 135]. Moreover, increasing the content of yttrium oxide to improve the optical properties of zirconia can reduce mechanical properties after aging, although fracture resistance was reported to be higher than masticatory loads (3000 N) [141].

Zirconia is usually considered as an opaque restorative material with optical and esthetic properties less attractive than glassy ceramics, particularly in terms of translucency. By means of transillumination, it has been shown that tetragonal zirconia allows only about 25% of incident light to pass through; this characteristic can be advantageously used to mask dark substrates (i.e. metal posts/abutments, dark teeth, etc.) [126, 127, 142–144].

Recently, in order to enhance the esthetic properties of the material, translucent zirconia has been introduced in the market, characterized by the presence of 30–35% of cubic crystals. Besides the improved optical characteristics, in the presence of such cubic phase no hydrothermal degradation (i.e. aging) of this allotropic component is evidenced. However, apart from the better optical properties, the toughness of translucent zirconia is reduced, compared to tetragonal one, with values of flexural strength ranging between 500 and 900 MPa; as a consequence, translucent zirconia represents a suitable esthetic and mechanical compromise to be preferred in anterior areas up to the first premolars in its monolithic configuration [126, 142, 143]. As demonstrated by a recent investigation, the reduced mechanical properties of

translucent zirconia are due to the dimensions and distribution of the crystals: in fact, cubic grains present with wider dimensions than tetragonal ones and segregate a higher amount of stabilizing oxides, making the tetragonal phase more prone to aging [126].

Manufacturing procedures

Although new additive technologies are emerging from the research on dental materials, to date, zirconia is still fabricated by CAD-CAM milling, according to two different production techniques: either soft machining of pre-sintered zirconia or hard machining of fully-sintered zirconia. Both procedures can be accomplished in industrial milling centers, in dental laboratories or by chairside devices [118–121, 124, 127].

Soft machining represents the most popular manufacturing technique and is based on milling of pre-sintered zirconia blanks fabricated by cold-isostatic pressing a mixture of zirconia powder, stabilizing oxides and binding agents (the latter removed during the pre-sintering process). With this technique, zirconia is highly homogenous and easier to mill, reducing production times, machinery wear and surface flaws; furthermore, soft machining generates negligible internal porosities (about 20–30 nm). The downside is that this process requires a 25% oversizing of the framework to be milled, since following sintering a linear shrinkage of the final volume occurs; as a consequence, although milling procedures are easier, soft machining requires a precise matching of CAD oversizing and material shrinking in order to avoid dimensional inaccuracies, particularly in the presence of complex framework geometry [118–121, 125, 127].

Viceversa, hard machining requires milling of fully-sintered zirconia blanks generally produced with hot isostatic pressing (HIP) at 1400°-1500 °C. This approach eliminates the problem of post-milling shrinkage, since neither oversizing nor sintering are necessary; however, hard machining needs longer milling times and more complex manufacturing, involving higher costs due to accelerated wear of production machinery and increased risks of attrition flaws. In addition, right after hard machining, zirconia frameworks can undergo a certain amount of monoclinic transformation phase due to mechanical stress, working burs friction and overheating subsequent to machining of the hard material [118–121, 125, 127].

Literature data are still controversial about which technique is the best, being the choice mainly guided by the operator preference, according to considerations related to shape, volume and complexity of the prosthetic geometry as well as time and cost of the milling procedures [118–121, 127].

High temperature and prolonged sintering time generate bigger zirconia crystals and the dimension of such grains significantly influences the mechanical properties of the material. In fact, the critical crystal dimension is about 1 mm: above this diameter, zirconia becomes spontaneously more susceptible to PTT, while under 0.2 mm such phenomenon does not occur and the toughness of the material decreases. Consequently, fabrication procedures (particularly sintering) significantly affect mechanical properties and stability of zirconia and have to be carefully checked during the whole manufacturing process [126, 127, 129, 130, 142].

In order to get a proper color of the restorations, specific metal oxides can be used as stains within the pre-sintering zirconia powder mixture or metallic salts can be infiltrated after milling; moreover, zirconia blanks are also available in multilayered color configurations. It has been clearly demonstrated that the coloring process does not influence mechanical properties of tetragonal zirconia, whilst uncertainty still remains regarding translucent cubic crystals [118–121, 125, 127, 129, 130].

Zirconia can be fabricated in monolithic or layered configurations. The monolithic material, not veneered with any ceramic layer, shows a less attractive esthetic appearance, but is not affected by the frequent cohesive fractures of the layering ceramics, known as “chipping” [134, 145].

To date, scientific evidences support the use of monolithic zirconia in posterior regions and in not esthetically relevant areas of the anterior arch (i.e. lingual tooth surfaces), while the use of layered restorations should be mainly addressed in highly esthetic zones [134, 145–149]. The minimum thickness suitable for monolithic Y- TZP restorations is 0.5 mm [134]; as regards layered prostheses, the total thickness ranges between 1.0 and

1.5 mm [134, 145–149]. In order to optimize mechanical resistance of layered restorations, it is paramount that veneering ceramics exhibit zirconia-compatible CTE [128, 150].

Marginal accuracy and internal fit

The accuracy of zirconia prostheses can be influenced by several factors, such as manufacturing, complexity of framework geometry (i.e. marginal finish line, span length, connectors dimension, etc.) and aging. The comparison of data regarding internal precision and marginal fit of zirconia is quite difficult, as literature data are heterogeneous and study designs are different for both laboratory and clinical investigations [119, 120, 127]. To date, it is possible to state that marginal precision of zirconia restorations is better than internal fit (probably because of the shape/size of the CAD-CAM milling burs) and that, in any case,

precision values are well within the range of clinical acceptability reported in the specifications of the American Dental Association (ADA). Marginal gap values have been reported between 0 and 75 mm for SCs [151, 152] and 140 mm for FDPs, the latter showing an increasing proportional to framework span [119, 120, 127, 153]. As regards preparation geometry, the high stability and structural resistance of zirconia are compatible with both vertical and horizontal finish lines [124, 153].

Surface treatment and cementation

Due to the absence of any glassy matrix, zirconia is free from silica and, consequently, cannot be conditioned with conventional acid etching techniques, differently from glass-ceramics [119, 122]. Several surface treatments aimed at getting a reliable bond to the substrate have been reported in the literature but to date this topic is still controversial [154–163]. Aggressive sandblasting (i.e. 250 mm alumina particles at 0.4 MPa) can cause loss of the stabilizing oxides with a subsequent increased risk of accelerated PTT and aging of the material; as a consequence, it would be advisable to treat zirconia surfaces with milder sand- blasting, using 110 mm alumina particles at 0.2 MPa. Such treatment can be advantageous for partially stabilized zirconia (PSZ) while it seems to weaken the fully stabilized material (FSZ) [155, 156, 158, 159, 163].

The use of coupling agents like silane can be adopted only after a tribochemical conditioning with silica-coated alumina particles or after infiltrating the zirconia surface with a thin layer of glassy ceramics [154, 155, 161]; however, the latter approach can determine the creation of excessive ceramic thickness and the effectiveness of adhesion between the glassy matrix and the polycrystalline network still remains unclear [154, 155, 158, 161].

The combination of mechanical and chemical treatments of zirconia surface was proved to offer the best results; particularly, the use of primers and adhesion promoting agents containing acidic monomers (10-MDP) can have a synergic effect with silane, improving the effectiveness of simplified adhesive techniques [155, 160–163].

On the basis of the physical-chemical properties of zirconia, in the presence of retentive preparation geometries and full coverage prostheses, conventional water-based luting agents (i.e. glass-ionomer and zinc phosphate cements) and hybrid cements (i.e. resin- modified glass-ionomer cements) can be considered a good choice for cementation. Otherwise, in the presence of partial coverage restorations, scarcely retentive preparation geometries (e.g. abutment teeth with reduced occluso-cervical dimension) and/or high masticatory loads, besides the above mentioned conditioning treatments of zirconia surface, it is possible to use conventional resin

cement or simplified self-adhesive luting agents, so as to allow resin better adsorb, distribute occlusal forces and withstand possible micro-cracks on the inner surface of the restorations [155, 158, 162].

Clinical indication and performances

From a clinical point of view, in the last decades zirconia has more and more gained ground in the realm of metal-free, mainly utilized to restore both natural teeth and osseointegrated implants with SCs and short- and medium-span FDPs up to 5 elements [134, 145, 146, 148, 149, 164, 165]. As regards FDPs, besides the high mechanical properties of the material, fracture resistance and clinical performance are also strongly related to a proper framework architecture. In case of bilayered FDPs, in particular, an "anatomic" design has to be performed, ensuring proper support and thickness to the veneering; moreover, connectors are to be designed with adequate dimensions (minimum area of section: 9, 15 and 25 mm2 for 3-, 4- and 5-unit FDPs respectively) and with rounded interdental embrasures, in order to avoid sharp angles that can contribute to generate risky stress concentration [146]. The presence of an adequate occlusal support is a relevant factor in maintaining an efficient chewing [166]; consequently, due to the absence of veneering ceramics that could be subjected to wear over time, monolithic restorations could be helpful in keeping occlusal stability during clinical service, particularly in the presence of discrepancies in occlusal contact patterns that could influence the onset of temporo-mandibular disorders [167].

Recently, clinical investigations regarding tooth- and implant-supported full-arch restorations have been published [165]. Although short- and medium-term results were encouraging with 94.8% success rate after 3 years of clinical service for monolithic full-arch bridges [145], it is worth noticing that a systematic review of the literature has reported 5-year complication rates of 27.6 and 30.5%, respectively for tooth-supported and implant- supported full-arch restorations [168]. Moreover, layered restorations showed 5-year success rates significantly lower than monolithic prostheses (i.e. 60.4% vs 90.9%) [169]. Consequently, the use of full-arch, extended zirconia restorations should always be carefully evaluated and further long-term clinical studies are necessary to validate the effectiveness of their serviceability.

As regards zirconia implants, the literature reports controversial, short-term and mainly anecdotal data [165, 170–174]. A recent systematic review with metaanalysis has evidenced similar potentialities of hard and soft-tissue integration between zirconia and titanium implants, although with a slower initial osseointegration process detected in zirconia ones. In any case, the

use of the latter should be cautiously evaluated, until more light is shed on long term outcomes and, particularly, on the possible mechanical complications. Viceversa, zirconia abutments are to be considered widely validated today in the esthetic sites, where the clear color of zirconia contributes to achieve a natural aspect of peri- implant soft tissues, particularly when they are quite thin [127, 148, 165, 172, 173]. A retrospective clinical study on a relevant number of ceramic abutments reported that internal zirconia implant connections are much more prone to mechanical complications (i.e. unscrewing, fractures, etc.) than hybrid connections with zirconia abutments cemented onto titanium bases; moreover, the same investigation reported that the distance between the implant/abutment connection and the occlusal plane can significantly influence the onset of bending moments that can be detrimental for the long- term prognosis of metal-free restorations [172].

Table 1 Lithium disilicate and zirconia: pros and cons

LITHIUM DISILICATE	
Pros	**Cons**
Excellent optical characteristics and good mechanical properties Clinical versatility Biocompatibility Favourable abrasiveness Marginal accuracy and internal fit High strength of adhesionto to the substrate	Glaze coating and fluorapatiteceramic veneering can increase wear Critical to adjust intraorally Chipping of the veneering ceramics
ZIRCONIA	
Pros	**Cons**
Excellent mechanical characteristics and good optical properties Excellent biocompatibilityand low plaque retention Favourable wear behaviour Implant abutments for esthetic sites Crack-hindering potential (through ptt) Marginal accuracy and internal fit Monolithic and layered	Opacity Unetchable with conventional methods Low temperature degradationand aging Critical to adjust intraorally Glaze coating and fluorapatiteceramic veneering can increase wear Chipping of the veneering ceramics

4. Conclusions

At the moment, it can be stated that silicate- and zirconia-based ceramics are amongst the most versatile metal-free materials available for the “digital prosthodontic environment”. In the last years, an increasing amount of available in vitro and in vivo data is shedding precious light on the outline of guidelines for a restorative rational use, focused on specific materials advantages and limitations, taking into account mechanical, optical and biological properties in the light of a widespread clinical experience (Table 1). In the meanwhile, the world of industry is intensively working on new strategies aimed at further enhancing microstructural characteristics of these materials, together with the introduction of new production technologies, mainly based on additive processes.

References

1. Albakry M, Guazzato M, Swain MV. Influence of hot pressing on the microstructure and fracture toughness of two pressable dental glass- ceramics. J Biomed Mater Res B Appl Biomater. 2004;71(1):99–107.
2. Denry I, Holloway JA. Ceramics for dental applications: a review. Materials. 2010;3:351–68.
3. Zarone F, Ferrari M, Mangano FG, Leone R, Sorrentino R. "Digitally oriented materials": focus on lithium disilicate ceramics. Int J Dent. 2016;2016:9840594.
4. Fischer K, Bühler-Zemp P, Völkel T. Scientific Documentation IPS e.max CAD. Schaan, Liechtenstein: Ivoclar Vivadent; 2005. p. 1–30.
5. Willard A, Gabriel Chu TM. The science and application of IPS e. max dental ceramic. Kaohsiung J Med Sci. 2018;34(4):238–42.
6. Vivadent I. IPS e. max lithium disilicate: the future of all- ceramic dentistry material science, practical applications, keys to success. Amherst, NY: Ivoclar Vivadent; 2009. p. 1e15.
7. Fabian Fonzar R, Carrabba M, Sedda M, Ferrari M, Goracci C, Vichi A. Flexural resistance of heat-pressed and CAD-CAM lithium disilicate with different translucencies. Dent Mater. 2017;33(1):63–70.
8. Belli R, Geinzer E, Muschweck A, Petschelt A, Lohbauer U. Mechanical fatigue degradation of ceramics versus resin composites for dental restorations. Dent Mater. 2014;30(4):424–32.
9. Furtado de Mendonca A, Shahmoradi M, Gouvêa CVD, De Souza GM, Ellakwa A. Microstructural and mechanical characterization of CAD/CAM materials for monolithic dental restorations. J Prosthodont. 2019; 28(2):e587–94.
10. Guess PC, Zavanelli RA, Silva NR, Bonfante EA, Coelho PG, Thompson VP. Monolithic CAD/CAM lithium disilicate versus veneered Y-TZP crowns: comparison of failure modes and reliability after fatigue. Int J Prosthodont. 2010;23(5):434–42.
11. Lien W, Roberts HW, Platt JA, Vandewalle KS, Hill TJ, Chu TM. Microstructural evolution and physical behavior of a lithium disilicate glass-ceramic. Dent Mater. 2015;31:928–40.
12. Al Mansour F, Karpukhina N, Grasso S, Wilson RM, Reece MJ, Cattell MJ. The effect of spark plasma sintering on lithium disilicate glass-ceramics. Dent Mater. 2015;31(10):e226–35.
13. Kubatík TF, Lukáč F, Mušálek R, Brožek V, Stehlíková K, Chráska T. Compaction of

lithium-silicate ceramics using spark plasma sintering. Ceramics-Silikáty. 2017;61(1):40–4.

14. Zhao K, Wei YR, Pan Y, Zhang XP, Swain MV, Guess PC. Influence of veneer and cyclic loading on failure behavior of lithium disilicate glass-ceramic molar crowns. Dent Mater. 2014;30(2):164–71.

15. Silva NR, Thompson VP, Valverde GB, Coelho PG, Powers JM, Farah JW, Esquivel-Upshaw J. Comparative reliability analyses of zirconium oxide and lithium disilicate restorations in vitro and in vivo. J Am Dent Assoc. 2011; 142(Suppl 2):4S–9S.

16. Schultheis S, Strub JR, Gerds TA, Guess PC. Monolithic and bi-layer CAD/ CAM lithium disilicate versus metalceramic fixed dental prostheses: comparison of fracture loads and failure modes after fatigue. Clin Oral Investig. 2013;17(5):1407–13.

17. Kim JH, Lee SJ, Park JS, Ryu JJ. Fracture load of monolithic CAD/CAM lithium disilicate ceramic crowns and veneered zirconia crowns as a posterior implant restoration. Implant Dent. 2013;22(1):66–70.

18. Monaco C, Rosentritt M, Llukacej A, Baldissara P, Scotti R. Marginal adaptation, gap width, and fracture strength of teeth restored with different all-ceramic vs metal ceramic crown systems: an in vitro study. Eur J Prosthodont Restor Dent. 2016;24(3):130–7.

19. Dogan DO, Gorler O, Mutaf B, Ozcan M, Eyuboglu GB, Ulgey M. Fracture resistance of molar crowns fabricated with monolithic all-ceramic CAD/CAM materials cemented on titanium abutments: an in vitro study. J Prosthodont. 2017;26(4):309–14.

20. Hamza TA, Sherif RM. Fracture resistance of monolithic glass-ceramics versus bilayered zirconia-based restorations. J Prosthodont. 2019;28(1):e259–64.

21. Choi JW, Kim SY, Bae JH, Bae EB, Huh JB. In vitro study of the fracture resistance of monolithic lithium disilicate, monolithic zirconia, and lithium disilicate pressed on zirconia for three-unit fixed dental prostheses. J Adv Prosthodont. 2017;9(4):244–51.

22. Alsarani M, Souza G, Rizkalla A, El-Mowafy O. Influence of crown design and material on chipping-resistance of all-ceramic molar crowns: an in vitro study. Dent Med Probl. 2018;55(1):35–42.

23. Kashkari A, Yilmaz B, Brantley WA, Schricker SR, Johnston WM. Fracture analysis of monolithic CAD-CAM crowns. J Esthet Restor Dent. 2019. https:// doi.org/10.1111/jerd.12462.

24. Nawafleh N, Hatamleh M, Elshiyab S, Mack F. Lithium disilicate restorations fatigue testing

parameters: a systematic review. J Prosthodont. 2016;25(2):116–26.

25. Lee A, Swain M, He L, Lyons K. Wear behavior of human enamel against lithium disilicate glass ceramic and type III gold. J Prosthet Dent. 2014;112:1399–405.

26. Kim MJ, Oh SH, Kim JH, Ju SW, Seo DG, Jun SH, Ahn JS, Ryu JJ. Wear evaluation of the human enamel opposing different Y-TZP dental ceramics and other porcelains. J Dent. 2012;40(11):979–88.

27. Amer R, Kürklü D, Kateeb E, Seghi RR. Three-body wear potential of dental yttrium-stabilized zirconia ceramic after grinding, polishing, and glazing treatments. J Prosthet Dent. 2014;112(5):1151–5.

28. Zurek AD, Alfaro MF, Wee AG, Yuan JC, Barao VA, Mathew MT, Sukotjo C. Wear characteristics and volume loss of CAD/CAM ceramic materials. J Prosthodont. 2019;28(2):e510–8.

29. Preis V, Weiser F, Handel G, Rosentritt M. Wear performance of monolithic dental ceramics with different surface treatments. Quintessence Int. 2013;44: 393–405.

30. Mörmann WH, Stawarczyk B, Ender A, Sener B, Attin T, Mehl A. Wear characteristics of current aesthetic dental restorative CAD/CAM materials: two-body wear, gloss retention, roughness and martens hardness. J Mech Behav Biomed Mater. 2013;20:113–25.

31. Peng Z, Izzat Abdul Rahman M, Zhang Y, Yin L. Wear behavior of pressable lithium disilicate glass ceramic. J Biomed Mater Res B Appl Biomater. 2016; 104(5):968–78.

32. Song XF, Ren HT, Yin L. Machinability of lithium disilicate glass ceramic in in vitro dental diamond bur adjusting process. J Mech Behav Biomed Mater. 2016;53:78–92.

33. Figueiredo-Pina CG, Patas N, Canhoto J, Cláudio R, Olhero SM, Serro AP, Ferro AC, Guedes M. Tribological behaviour of unveneered and veneered lithium disilicate dental material. J Mech Behav Biomed Mater. 2016;53:226–38.

34. Forster A, Ungvári K, Györgyey Á, Kukovecz Á, Turzó K, Nagy K. Human epithelial tissue culture study on restorative materials. J Dent. 2014; 42(1):7–14.

35. Tetè S, Zizzari VL, Borelli B, De Colli M, Zara S, Sorrentino R, Scarano A, Gherlone E, Cataldi A, Zarone F. Proliferation and adhesion capability of human gingival fibroblasts onto zirconia, lithium disilicate and feldspathic veneering ceramic in vitro. Dent Mater J. 2014;33(1):7–15.

36. Ariaans K, Heussen N, Schiffer H, Wienert AL, Plümäkers B, Rink L, Wolfart S. Use of molecular indicators of inflammation to assess the biocompatibility of all-ceramic restorations. J Clin Periodontol. 2016;43(2):173–9.

37. Baldissara P, Llukacej A, Ciocca L, Valandro FL, Scotti R. Translucency of zirconia copings made with different CAD/CAM systems. J Prosthet Dent. 2010;104(1):6–12.

38. Murillo-Gómez F, Palma-Dibb RG, De Goes MF. Effect of acid etching on tridimensional microstructure of etchable CAD/CAM materials. Dent Mater. 2018;34(6):944–55.

39. Bajraktarova-Valjakova E, Grozdanov A, Guguvcevski L, Korunoska-Stevkovska V, Kapusevska B, Gigovski N, Mijoska A, Bajraktarova-Misevska C. Acid etching as surface treatment method for luting of glass-ceramic restorations, part 1: acids, application protocol and etching effectiveness. Open Access Maced J Med Sci. 2018;6(3):568–73.

40. Prochnow C, Venturini AB, Guilardi LF, Pereira GKR, Burgo TAL, Bottino MC, Kleverlaan CJ, Valandro LF. Hydrofluoric acid concentrations: effect on the cyclic load-to-failure of machined lithium disilicate restorations. Dent Mater. 2018;34(9):e255–63.

41. Sundfeld D, Palialol ARM, Fugolin APP, Ambrosano GMB, Correr-Sobrinho L, Martins LRM, Pfeifer CS. The effect of hydrofluoric acid and resin cement formulation on the bond strength to lithium disilicate ceramic. Braz Oral Res. 2018;32:e43.

42. Ataol AS, Ergun G. Repair bond strength of resin composite to bilayer dental ceramics. J Adv Prosthodont. 2018;10(2):101–12.

43. Menees TS, Lawson NC, Beck PR, Burgess JO. Influence of particle abrasion or hydrofluoric acid etching on lithium disilicate flexural strength. J Prosthet Dent. 2014;112(5):1164–70.

44. Blatz MB, Sadan A, Kern M. Resin-ceramic bonding: a review of the literature. J Prosthet Dent. 2003;89(3):268–74.

45. Carvalho AO, Bruzi G, Giannini M, Magne P. Fatigue resistance of CAD/CAM complete crowns with a simplified cementation process. J Prosthet Dent. 2014;111:310–7.

46. Fabbri G, Sorrentino R, Brennan M, Cerutti A. A novel approach to implant screw-retained restorations: adhesive combination between zirconia frameworks and monolithic lithium disilicate. Int J Esthet Den. 2014;9:490–505.

47. Frankenberger R, Hartmann VE, Krech M, Krämer N, Reich S, Braun A, Roggendorf M. Adhesive luting of new CAD/CAM materials. Int J Comput Dent. 2015;18:9–20.

48. Neis CA, Albuquerque NL, Albuquerque Ide S, Gomes EA, Souza-Filho CB, Feitosa VP, Spazzin AO, Bacchi A. Surface treatments for repair of feldspathic, leucite and lithium disilicate-reinforced glass ceramics using composite resin. Braz Dent J. 2015;26(2):152–5.

49. Carvalho AO, Bruzi G, Anderson RE, Maia HP, Giannini M, Magne P. Influence of adhesive core buildup designs on the resistance of endodontically treated molars restored with lithium disilicate CAD/CAM crowns. Oper Dent. 2016;41:76–82.

50. Swank HM, Motyka NC, Bailey CW, Vandewalle KS. Bond strength of resin cement to ceramic with simplified primers and pretreatment solutions. Gen Dent. 2018;66(5):33–7.

51. Taguchi S, Komine F, Kubochi K, Fushiki R, Kimura F, Matsumura H. Effect of a silane and phosphate functional monomer on shear bond strength of a resin-based luting agent to lithium disilicate ceramic and quartz materials. J Oral Sci. 2018;60(3):360–6.

52. Gehrt M, Wolfart S, Rafai N, Reich S, Edelhoff D. Clinical results of lithium-disilicate crowns after up to 9 years of service. Clin Oral Investig. 2013;17(1):275–84.

53. Spies BC, Pieralli S, Vach K, Kohal RJ. CAD/CAM-fabricated ceramic implant-supported single crowns made from lithium disilicate: final results of a 5-year prospective cohort study. Clin Implant Dent Relat Res. 2017;19(5):876–83.

54. Joda T, Ferrari M, Brägger U. Monolithic implant-supported lithium disilicate (LS2) crowns in a complete digital workflow: a prospective clinical trial with a 2-year follow-up. Clin Implant Dent Relat Res.

55. 2017;19(3):505–11.

56. Fabbri G, Zarone F, Dellificorelli G, Cannistraro G, De Lorenzi M, Mosca A, Sorrentino R. Clinical evaluation of 860 anterior and posterior lithium disilicate restorations: retrospective study with a mean follow-up of 3 years and a maximum observational period of 6 years. Int J Periodontics Restorative Dent. 2014;34(2):165–77.

57. Simeone P, Gracis S. Eleven-year retropective survival study of 275 veneered lithium disilicate single crowns. Int J Periodontics Restorative Dent. 2015; 35(5):685–94.

58. Valenti M, Valenti A. Retrospective survival analysis of 110 lithium disilicate crowns with feather-edge marginal preparation. Int J Esthet Dent. 2015; 10(2):246–57.

59. van den Breemer CR, Vinkenborg C, van Pelt H, Edelhoff D, Cune MS. The clinical performance of monolithic lithium disilicate posterior restorations after 5, 10, and 15 years: a retrospective case series. Int J Prosthodont. 2017; 30(1):62–5.

60. Rauch A, Reich S, Dalchau L, Schierz O. Clinical survival of chair-side generated monolithic lithium disilicate crowns:10-year results. Clin Oral Investig. 2018;22(4):1763–9.

61. Pozzi A, Tallarico M, Barlattani A. Monolithic lithium disilicate full-contour crowns bonded on CAD/CAM zirconia complete-arch implant bridges with 3 to 5 years of follow-up. J Oral Implantol. 2015;41(4): 450–8.

62. Atsü SS, Aksan ME, Bulut AC. Fracture resistance of titanium, zirconia, and ceramic-reinforced polyetheretherketone implant abutments supporting CAD/CAM monolithic lithium disilicate ceramic crowns after aging. Int J Oral Maxillofac Implants. 2019;34(3):622–30.

63. Radz GM. Minimum thickness anterior porcelain restorations. Dent Clin N Am. 2011;55(2):353–70 ix.

64. Ge C, Green CC, Sederstrom D, McLaren EA, White SN. Effect of porcelain and enamel thickness on porcelain veneer failure loads in vitro. J Prosthet Dent. 2014;111(5):380–7.

65. Ge C, Green CC, Sederstrom DA, McLaren EA, Chalfant JA, White SN. Effect of tooth substrate and porcelain thickness on porcelain veneer failure loads in vitro. J Prosthet Dent. 2018;120(1):85–91.

66. Sorrentino R, Apiucela D, Riccio C, Gherlone E, Zarone F, Aversa R,

67. Garcia-Godoy F, Ferrari M, Apicella A. Nonlinear visco-elastic finite element analysis of different porcelain veneers configuration. J Biomed Mater Res B Appl Biomater. 2009;91(2):727–36.

68. Kern M, Knode H, Strub JR. The all-porcelain, resin-bonded bridge. Quintessence Int. 1991;22(4):257–62.

69. Kern M, Strub JR. Bonding to alumina ceramic in restorative dentistry: clinical results over up to 5 years. J Dent. 1998;26(3):245–9.

70. Kern M. Clinical long-term survival of two-retainer and single-retainer all-ceramic resin-bonded fixed partial dentures. Quintessence Int. 2005; 36(2):141–7.

71. Kern M, Sasse M. Ten-year survival of anterior all-ceramic resin-bonded fixed dental prostheses. J Adhes Dent. 2011;13(5):407–10.

72. Kern M, Gläser R. Cantilevered all-ceramic, resin-bonded fixed partial dentures: a new treatment modality. J Esthet Dent. 1997;9(5):255–64.

73. Kern M. Fifteen-year survival of anterior all-ceramic cantilever resin-bonded fixed dental prostheses. J Dent. 2017;56:133–5.

74. Sasse M, Kern M. CAD/CAM single retainer zirconia-ceramic resin-bonded fixed dental prostheses: clinical outcome after 5 years. Int J Comput Dent. 2013;16(2):109–18.

75. Sailer I, Hämmerle CH. Zirconia ceramic single-retainer resin-bonded fixed dental prostheses (RBFDPs) after 4 years of clinical service: a retrospective clinical and volumetric study. Int J Periodontics Restorative Dent. 2014;34(3): 333–43.

76. Sasse M, Kern M. Survival of anterior cantilevered all-ceramic resin- bonded fixed dental prostheses made from zirconia ceramic. J Dent. 2014;42(6):660–3.

77. Klink A, Hüttig F. Zirconia-based anterior resin-bonded single-retainer cantilever fixed dental prostheses: a 15- to 61-month follow-up. Int J Prosthodont. 2016;29(3):284–6.

78. Sun Q, Chen L, Tian L, Xu B. Single-tooth replacement in the anterior arch by means of a cantilevered IPS e.max press veneer-retained fixed partial denture: case series of 35 patients. Int J Prosthodont. 2013;26:181–7.

79. Sailer I, Bonani T, Brodbeck U, Hämmerle CH. Retrospective clinical study of single-retainer cantilever anterior and posterior glass-ceramic resin-bonded fixed dental prostheses at a mean follow-up of 6 years. Int J Prosthodont. 2013;26(5):443–50.

80. Zhou T, Wang X, Zhang G. All-ceramic resin bonded fixed partial denture made of IPS hot-pressed casting porcelain restore anterior missing teeth: a three years clinical observation. Beijing Da Xue Xue Bao. 2011;43(1):77–80.

81. Wei YR, Wang XD, Zhang Q, Li XX, Blatz MB, Jian YT, Zhao K. Clinical performance of anterior resin-bonded fixed dental prostheses with different framework designs: a systematic review and meta-analysis. J Dent. 2016;47:1–7.

82. Chen J, Cai H, Ren X, Suo L, Pei X, Wan Q. A systematic review of the survival and complication rates of all-ceramic resin-bonded fixed dental prostheses. J Prosthodont. 2018;27(6):535–43.

83. Dhima M, Carr AB, Salinas TJ, Lohse C, Berglund L, Nan KA. Evaluation of fracture resistance in aqueous environment under dynamic loading of lithium disilicate restorative systems for posterior applications. Part 2. J Prosthodont. 2014;23(5):353–7.

84. Seydler B, Rues S, Muller D, Schmitter M. In vitro fracture load of monolithic lithium disilicate ceramic molar crowns with different wall thicknesses. Clin Oral Investig.

2014;18:1165–71.

85. Sasse M, Krummel A, Klosa K, Kern M. Influence of restoration thickness and dental bonding surface on the fracture resistance of full-coverage occlusal veneers made from lithium disilicate ceramic. Dent Mater. 2015;31(8):907–15.

86. Vianna ALSV, Prado CJD, Bicalho AA, Pereira RADS, Neves FDD, Soares CJ. Effect of cavity preparation design and ceramic type on the stress distribution, strain and fracture resistance of CAD/CAM onlays in molars. J Appl Oral Sci. 2018;26:e20180004.

87. von Maltzahn NF, E Meniawy OI, Breitenbuecher N, Kohorst P, Stiesch M, Eisenburger M. Fracture strength of ceramic posterior occlusal veneers for functional rehabilitation of an abrasive dentition. Int J Prosthodont. 2018; 31(5):451–2.

88. Mobilio N, Fasiol A, Catapano S. Survival rates of lithium disilicate single restorations: a retrospective study. Int J Prosthodont. 2018;31(3):283–6.

89. Politano G, Van Meerbeek B, Peumans M. Nonretentive bonded ceramic partial crowns: concept and simplified protocol for long-lasting dental restorations. J Adhes Dent. 2018;20(6):495–510.

90. Ferrari M, Ferrari Cagidiaco E, Goracci C, Sorrentino R, Zarone F, Grandini S, Joda T. Posterior partial crowns out of lithium disilicate (LS2) with or without posts: a randomized controlled prospective clinical trial with a 3-year follow up. J Dent. 2019;83:12–7.

91. Makarouna M, Ullmann K, Lazarek K, Boening KW. Six-year clinical performance of lithium disilicate fixed partial dentures. Int J Prosthodont. 2011;24:204–6.

92. Taskonak B, Sertgöz A. Two-year clinical evaluation of lithia-disilicate-based all-ceramic crowns and fixed partial dentures. Dent Mater. 2006;22:1008–13.

93. Solá-Ruiz MF, Lagos-Flores E, Román-Rodriguez JL, Highsmith Jdel R, Fons- Font A, Granell-Ruiz M. Survival rates of a lithium disilicate-based core ceramic for three-unit esthetic fixed partial dentures: a 10-year prospective study. Int J Prosthodont. 2013;26(2):175–80.

94. Teichmann M, Göckler F, Weber V, Yildirim M, Wolfart S, Edelhoff D. Ten- year survival and complication rates of lithium-disilicate (empress 2) tooth- supported crowns, implant-supported crowns, and fixed dental prostheses. J Dent. 2017;56:65–77.

95. Kern M, Sasse M, Wolfart S. Ten-year outcome of three-unit fixed dental prostheses made from monolithic lithium disilicate ceramic. J Am Dent Assoc. 2012;143:234–40.

96. Abdel-Azim T, Rogers K, Elathamna E, Zandinejad A, Metz M, Morton D. Comparison of the marginal fit of lithium disilicate crowns fabricated with CAD/CAM technology by using conventional impressions and two intraoral digital scanners. J Prosthet Dent. 2015;114(4):554–9.

97. Zeltner M, Sailer I, Mühlemann S, Özcan M, Hämmerle CH, Benic GI. Randomized controlled within-subject evaluation of digital and conventional workflows for the fabrication of lithium disilicate single crowns. Part III: marginal and internal fit. J Prosthet Dent. 2017;117(3):354–62.

98. Haddadi Y, Bahrami G, Isidor F. Accuracy of crowns based on digital intraoral scanning compared to conventional impression-a split-mouth randomised clinical study. Clin Oral Investig. 2019. https://doi.org/10.1007/ s00784-019-02840-0.

99. Anadioti E, Aquilino SA, Gratton DG, Holloway JA, Denry I, Thomas GW, Qian

100. F. 3D and 2D marginal fit of pressed and CAD/CAM lithium disilicate crowns made from digital and conventional impressions. J Prosthodont. 2014;23(8):610–7.

101. Memari Y, Mohajerfar M, Armin A, Kamalian F, Rezayani V, Beyabanaki E. Marginal adaptation of CAD/CAM all-ceramic crowns made by different impression methods: a literature review. J Prosthodont. 2019;28(2):e536–44.

102. Mostafa NZ, Ruse ND, Ford NL, Carvalho RM, Wyatt CCL. Marginal fit of lithium disilicate crowns fabricated using conventional and digital methodology: a three-dimensional analysis. J Prosthodont. 2018;27(2): 145–52.

103. Ng J, Ruse D, Wyatt C. A comparison of the marginal fit of crowns fabricated with digital and conventional methods. J Prosthet Dent. 2014;112(3):555–60.

104. Alfaro DP, Ruse ND, Carvalho RM, Wyatt CC. Assessment of the internal fit of lithium disilicate crowns using micro-CT. J Prosthodont. 2015;24:381–6.

105. Schaefer O, Decker M, Wittstock F, Kuepper H, Guentsch A. Impact of digital impression techniques on the adaption of ceramic partial crowns in vitro. J Dent. 2014;42(6):677–83.

106. Mously HA, Finkelman M, Zandparsa R, Hirayama H. Marginal and internal adaptation of ceramic crown restorations fabricated with CAD/ CAM technology and the heat-press technique. J Prosthet Dent. 2014; 112:249–56.

107. Guess PC, Vagkopoulou T, Zhang Y, Wolkewitz M, Strub JR. Marginal and internal fit

of heat pressed versus CAD/CAM fabricated all-ceramic onlays after exposure to thermo-mechanical fatigue. J Dent. 2014;42(2): 199–209.

108. Azar B, Eckert S, Kunkela J, Ingr T, Mounajjed R. The marginal fit of lithium disilicate crowns: press vs. CAD/CAM. Braz Oral Res. 2018;32:e001.

109. Neves FD, Prado CJ, Prudente MS, Carneiro TA, Zancopé K, Davi LR, Mendonça G, Cooper LF, Soares CJ. Micro-computed tomography evaluation of marginal fit of lithium disilicate crowns fabricated by using chairside CAD/CAM systems or the heat-pressing technique. J Prosthet Dent. 2014;112(5):1134–40.

110. Homsy F, Bottin M, Özcan M, Majzoub Z. Fit accuracy of pressed and milled lithium disilicate inlays fabricated from conventional impressions or a laboratory-based digital workflow. Eur J Prosthodont Restor Dent. 2019; 27(1):18–25.

111. Revilla-León M, Olea-Vielba M, Esteso-Saiz A, Martínez-Klemm I, Özcan M. Marginal and internal gap of handmade, milled and 3D printed additive manufactured patterns for pressed lithium disilicate onlay restorations. Eur J Prosthodont Restor Dent. 2018;26(1):31–8.

112. Elsaka SE, Elnaghy AM. Mechanical properties of zirconia reinforced lithium silicate glass-ceramic. Dent Mater. 2016;32(7):908–14.

113. Sen N, Us YO. Mechanical and optical properties of monolithic CAD-CAM restorative materials. J Prosthet Dent. 2018;119(4):593–9.

114. Lauvahutanon S, Takahashi H, Shiozawa M, Iwasaki N, Asakawa Y, Oki M, Finger WJ, Arksornnukit M. Mechanical properties of composite resin blocks for CAD/ CAM. Dent Mater J. 2014;33(5):705–10.

115. Vichi A, Fonzar RF, Goracci C, Carrabba M, Ferrari M. Effect of finishing and polishing on roughness and gloss of lithium disilicate and lithium silicate zirconia reinforced glass ceramic for CAD/CAM systems. Oper Dent. 2018; 43(1):90–100.

116. Passos L, Linke B, Street A, Torrealba Y. Effect of thickness, translucency, and firing protocol on the masking ability of a CAD/CAM zirconia-reinforced lithium silicate for different backgrounds. Int J Comput Dent. 2019;22(1):29–38.

117. Ramos Nde C, Campos TM, Paz IS, Machado JP, Bottino MA, Cesar PF, Melo RM. Microstructure characterization and SCG of newly engineered dental ceramics. Dent Mater. 2016;32(7):870–8.

118. Fathy SM, Swain MV. In-vitro wear of natural tooth surface opposed with zirconia reinforced lithium silicate glass ceramic after accelerated ageing. Dent Mater. 2018;34(3):551–9.

119. Zimmermann M, Koller C, Mehl A, Hickel R. Indirect zirconia-reinforced lithium silicate ceramic CAD/CAM restorations: preliminary clinical results after 12 months. Quintessence Int. 2017;48(1):19–25.

120. Saavedra GSFA, Rodrigues FP, Bottino MA. Zirconia-reinforced lithium silicate ceramic - a 2-year follow-up of a clinical experience with anterior crowns. Eur J Prosthodont Restor Dent. 2017;25(1):57–63.

121. Denry I, Kelly JR. State of the art of zirconia for dental applications. Dent Mater. 2008;24:299–307.

122. Zarone F, Russo S, Sorrentino R. From porcelain-fused-to-metal to zirconia: clinical and experimental considerations. Dent Mater. 2011;27(1):83–96.

123. Miyazaki T, Nakamura T, Matsumura H, Ban S, Kobayashi T. Current status of zirconia restoration. J Prosthodont Res. 2013;57(4):236–61.

124. Chen YW, Moussi J, Drury JL, Wataha JC. Zirconia in biomedical applications. Expert Rev Med Devices. 2016;13(10):945–63.

125. Zarone F, Sorrentino R, Vaccaro F, Traini T, Russo S, Ferrari M. Acid etching surface treatment of feldspathic, alumina and zirconia ceramics: a micromorphological SEM analysis. Int Dent South Afr. 2006;8:50–6.

126. Nakashima J, Taira Y, Sawase T. In vitro wear of four ceramic materials and human enamel on enamel antagonist. Eur J Oral Sci. 2016;124:295–300.

127. Sorrentino R, Navarra CO, Di Lenarda R, Breschi L, Zarone F, Cadenaro M, Spagnuolo G. Effects of finish line design and fatigue cyclic loading on phase transformation of zirconia dental ceramics: a qualitative micro-Raman spectroscopic analysis. Materials. 2019;12:6. https://doi.org/10.3390/ma12060863.

128. Lughi V, Sergo V. Low temperature degradation -aging of zirconia: a critical review of the relevant aspects in dentistry. Dent Mater. 2010;26(8):807–20.

129. Camposilvan E, Leone R, Gremillard L, Sorrentino R, Zarone F, Ferrari M, Chevalier

130. J. Aging resistance, mechanical properties and translucency of different yttria- stabilized

zirconia ceramics for monolithic dental crown applications. Dent Mater. 2018;34(6):879–90.

131. Ferrari M, Vichi A, Zarone F. Zirconia abutments and restorations: from laboratory to clinical investigations. Dent Mater. 2015;31:e63–76.

132. Rodrigues CDS, Aurélio IL, Kaizer MDR, Zhang Y, May LG. Do thermal treatments affect the mechanical behavior of porcelain-veneered zirconia? A systematic review and meta-analysis. Dent Mater. 2019;35(3):807–17.

133. Mota YA, Cotes C, Carvalho RF, Machado JPB, Leite FPP, Souza ROA, Özcan M. Monoclinic phase transformation and mechanical durability of zirconia ceramic after fatigue and autoclave aging. J Biomed Mater Res B Appl Biomater. 2017;105(7):1972–7.

134. Wille S, Zumstrull P, Kaidas V, Jessen LK, Kern M. Low temperature degradation of single layers of multilayered zirconia in comparison to conventional unshaded zirconia: phase transformation and flexural strength. J Mech Behav Biomed Mater. 2018;77:171–5.

135. Sun T, Zhou S, Lai R, Liu R, Ma S, Zhou Z, Longquan S. Load-bearing capacity and the recommended thickness of dental monolithic zirconia single crowns. J Mech Behav Biomed Mater. 2014;35:93–101.

136. Lameira DP, Buarque e Silva WA, Andrade e Silva F, De Souza GM. Fracture strength of aged monolithic and bilayer zirconia-based crowns. Biomed Res Int. 2015;2015:418641.

137. Lan TH, Liu PH, Chou MM, Lee HE. Fracture resistance of monolithic zirconia crowns with different occlusal thicknesses in implant prostheses. J Prosthet Dent. 2016;115(1):76–83.

138. Sorrentino R, Triulzio C, Tricarico MG, Bonadeo G, Gherlone EF, Ferrari M. In vitro analysis of the fracture resistance of CAD-CAM monolithic zirconia molar crowns with different occlusal thickness. J Mech Behav Biomed Mater. 2016;61:328–33.

139. Nakamura K, Harada A, Inagaki R, Kanno T, Niwano Y, Milleding P,

140. Örtengren U. Fracture resistance of monolithic zirconia molar crowns with reduced thickness. Acta Odontol Scand. 2015;73(8):602–8.

141. Ramos GF, Monteiro EB, Bottino MA, Zhang Y, Marques de Melo R. Failure probability of three designs of zirconia crowns. Int J Periodontics Restorative Dent. 2015;35(6):843–9.

142. Weyhrauch M, Igiel C, Scheller H, Weibrich G, Lehmann KM. Fracture strength of monolithic all-ceramic crowns on titanium implant

143. abutments. Int J Oral Maxillofac Implants. 2016;31(2):304–9.

144. Mitov G, Anastassova-Yoshida Y, Nothdurft FP, von See C, Pospiech P. Influence of the preparation design and artificial aging on the fracture resistance of monolithic zirconia crowns. J Adv Prosthodont. 2016;8(1):30–6.

145. Øilo M, Kvam K, Gjerdet NR. Load at fracture of monolithic and bilayered zirconia crowns with and without a cervical zirconia collar. J Prosthet Dent. 2016;115(5):630–6.

146. Zhang Y, Mai Z, Barani A, Bush M, Lawn B. Fracture-resistant monolithic dental crowns. Dent Mater. 2016;32(3):442–9.

147. Elsayed A, Meyer G, Wille S, Kern M. Influence of the yttrium content on the fracture strength of monolithic zirconia crowns after artificial aging. Quintessence Int. 2019. https://doi.org/10.3290/j.qi.a42097.

148. Vichi A, Sedda M, Fabian Fonzar R, Carrabba M, Ferrari M. Comparison of contrast ratio, translucency parameter, and flexural strength of traditional and "augmented translucency" zirconia for CEREC CAD/CAM system. J Esthet Restor Dent. 2016;28(Suppl 1):S32–9.

149. Shahmiri R, Standard OC, Hart JN, Sorrell CC. Optical properties of zirconia ceramics for esthetic dental restorations: a systematic review. J Prosthet Dent. 2018;119(1):36–46.

150. Bacchi A, Boccardi S, Alessandretti R, Pereira GKR. Substrate masking ability of bilayer and monolithic ceramics used for complete crowns and the effect of association with an opaque resin-based luting agent. J Prosthodont Res. 2019. https://doi.org/10.1016/j.jpor.2019.01.005.

151. Venezia P, Torsello F, Cavalcanti R, D'Amato S. Retrospective analysis of 26 complete-arch implant supported monolithic zirconia prostheses with feldspathic porcelain veneering limited to the facial surface. J Prosthet Dent. 2015;114:506–12.

152. Sorrentino R, De Simone G, Tetè S, Russo S, Zarone F. Five-year prospective clinical study of posterior three-unit zirconia-based fixed dental prostheses. Clin Oral Investig. 2012;16(3):977–85.

153. Borelli B, Sorrentino R, Goracci C, Amato M, Zarone F, Ferrari M. Evaluating residual dentin thickness following various mandibular anterior tooth preparations for zirconia full-coverage single crowns: an in vitro analysis. Int J Periodontics Restorative Dent. 2015;35(1):41–7.

154. Ferrari M, Sorrentino R, Cagidiaco C, Goracci C, Vichi A, Gherlone E, Zarone F. Short-term clinical performance of zirconia single crowns with different framework designs: 3-year clinical trial. Am J Dent. 2015;28(4):235–40.

155. Fuzzi M, Tricarico MG, Ferrari Cagidiaco E, et al. Nanoleakage and internal adaptation of zirconia and lithium disilicate single crowns with knife edge preparation. J Oss Periodont Prosthodont. 2017;9:262–74.

156. Vichi A, Sedda M, Bonadeo G, Bosco M, Barbiera A, Tsintsadze N, Carrabba M, Ferrari M. Effect of repeated firings on flexural strength of veneered zirconia. Dent Mater. 2015;31(8):e151–6.

157. Lee B, Oh KC, Haam D, Lee JH, Moon HS. Evaluation of the fit of zirconia copings fabricated by direct and indirect digital scanning procedures. J Prosthet Dent. 2018;120(2):225–31.

158. Pilo R, Folkman M, Arieli A, Levartovsky S. Marginal fit and retention strength of zirconia crowns cemented by self-adhesive resin cements. Oper Dent. 2018;43(2):151–61.

159. Riccitiello F, Amato M, Leone R, Spagnuolo G, Sorrentino R. In vitro evaluation of the marginal fit and internal adaptation of zirconia and lithium disilicate single crowns: micro-CT comparison between different manufacturing procedures. Open Dent J. 2018;12:160–72.

160. Pagniano RP, Seghi RR, Rosenstiel SF, Wang R, Katsube N. The effect of a layer of resin luting agent on the biaxial flexure strength of two all-ceramic systems. J Prosthet Dent. 2005;93(5):459–66.

161. Papia E, Larsson C, du Toit M, Vult von Steyern P. Bonding between oxide ceramics and adhesive cement systems: a systematic review. J Biomed Mater Res B Appl Biomater. 2014;102:395–413.

162. Özcan M, Bernasconi M. Adhesion to zirconia used for dental restorations: a systematic review and meta-analysis. J Adhes Dent. 2015;17(1):7–26.

163. Srikanth R, Kosmac T, Della Bona A, Yin L, Zhang Y. Effects of cementation surface modifications on fracture resistance of zirconia. Dent Mater. 2015;31(4):435–42.

164. Luthra R, Kaur P. An insight into current concepts and techniques in resin bonding to high strength ceramics. Aust Dent J. 2016;61:163–73.

165. Sulaiman TA, Abdulmajeed AA, Shahramian K, Lassila L. Effect of different treatments on the flexural strength of fully versus partially stabilized monolithic zirconia. J Prosthet

Dent. 2017;118:216–20.

166. Ebeid K, Wille S, Salah T, Wahsh M, Zohdy M, Kern M. Evaluation of surface treatments of monolithic zirconia in different sintering stages. J Prosthodont Res. 2018;62(2):210–7.

167. Dal Piva AMO, Carvalho RLA, Lima AL, Bottino MA, Melo RM, Valandro LF. Silica coating followed by heat-treatment of MDP-primer for resin bond stability to yttria-stabilized zirconia polycrystals. J Biomed Mater Res B Appl Biomater. 2019;107(1):104–11.

168. Pilo R, Dimitriadi M, Palaghia A, Eliades G. Effect of tribochemical treatments and silane reactivity on resin bonding to zirconia. Dent Mater. 2018;34(2): 306–16.

169. Schünemann FH, Galárraga-Vinueza ME, Magini R, Fredel M, Silva F, Souza JCM, Zhang Y, Henriques B. Zirconia surface modifications for implant dentistry. Mater Sci Eng C Mater Biol Appl. 2019;98:1294–305.

170. Poggio CE, Ercoli C, Rispoli L, Maiorana C, Esposito M. Metal-free materials for fixed prosthodontic restorations. Cochrane Database Syst Rev. 2017. https://doi.org/10.1002/14651858.CD009606.pub2.

171. Bagegni A, Abou-Ayash S, Rücker G, Algarny A, Att W. The influence of prosthetic material on implant and prosthetic survival of implant-supported fixed complete dentures: a systematic review and meta-analysis. J Prosthodont Res. 2019. https://doi.org/10.1016/j.jpor.2019.02.001.

172. Ciancaglini R, Gherlone EF, Radaelli G. Association between loss of occlusal support and symptoms of functional disturbances of the masticatory system. J Oral Rehabil. 1999;26(3):248–53.

173. Ciancaglini R, Gherlone EF, Radaelli S, Radaelli G. The distribution of occlusal contacts in the intercuspal position and temporomandibular disorder. J Oral Rehabil. 2002;29(11):1082–90.

174. Le M, Papia E, Larsson C. The clinical success of tooth- and implant- supported zirconia-based fixed dental prostheses. A systematic review. J Oral Rehabil. 2015;42(6):467–80.

175. Wong CKK, Narvekar U, Petridis H. Prosthodontic complications of metal- ceramic and all-ceramic, complete-arch fixed implant prostheses with minimum 5 years mean follow-up period. A systematic review and meta- analysis. J Prosthodont. 2019;28(2):e722–35.

176. Ferrari M, Tricarico MG, Cagidiaco MC, Vichi A, Gherlone EF, Zarone F, Sorrentino R.

3-year randomized controlled prospective clinical trial on different CAD-CAM implant abutments. Clin Implant Dent Relat Res. 2016; 18(6):1134–41.

177. Abdulmajeed AA, Donovan TE, Cooper LF, Walter R, Sulaiman TA. Fracture of layered zirconia restorations at 5 years: a dental laboratory survey. J Prosthet Dent. 2017;118(3):353–6.

178. Fabbri G, Fradeani M, Dellificorelli G, De Lorenzi M, Zarone F, Sorrentino R. Clinical evaluation of the influence of connection type and restoration height on the reliability of zirconia abutments: a retrospective study on 965 abutments with a mean 6-year follow-up. Int J Periodontics Restorative Dent. 2017;37(1):19–31.

179. Sailer I, Balmer M, Hüsler J, Hämmerle CHF, Känel S, Thoma DS. Comparison of fixed dental prostheses with zirconia and metal frameworks: five-year results of a randomized controlled clinical trial. Int J Prosthodont. 2017;30(5):426–8.

180. Roehling S, Schlegel KA, Woelfler H, Gahlert M. Zirconia compared to titanium dental implants in preclinical studies - a systematic review and meta-analysis. Clin Oral Implants Res. 2019;30(5):365–95.

4.2 ZIRCONIA-REINFORCED LITHIUM SILICATE (ZLS) MECHANICAL AND BIOLOGICAL PROPERTIES: A LITERATURE REVIEW

Zarone Fernando, Ruggiero Gennaro, Leone Renato, Breschi Lorenzo, Leuci Stefania, Sorrentino Roberto

J Dent. 2021;109:103661

Introduction

The research and development of new restorative materials aimed at getting high mechanical and esthetic performances has led to the introduction on the market of zirconia-reinforced lithium silicate ceramics (ZLS), that can be employed with Computer-aided design / Computer-aided manufacturing (CAD/CAM) technologies.

ZLS was developed by two companies, Vita (Vita Zahnfabrik, H. Rauter GmbH & Co., Bad Säckingen, Germany) and Dentsply (Dentsply Sirona, DeguDent, GmbH, Hanau-Wolfgang, Germany), in conjunction with the Fraunhofer Institute for Silicate Research (Würzburg, Germany), separately marketed as different products: Vita Suprinity PC and Celtra Duo [1-3].

These materials exhibit similar microstructures: a homogeneous glassy matrix contains a crystalline component made of round and submicrometric elongated grains of lithium metasilicates and lithium orthophosphates; in addition to these, tetragonal zirconia fillers are added, aimed at increasing strength values. After a crystallization process, lithium disilicate grains are generated. Lithium metasilicate is reported to be grown larger in Celtra Duo than in Suprinity (up to ∼1 and ∼0.5 μm in length, respectively) [2-6].

This structural typology has been developed in order to combine favorable optical properties with increased mechanical characteristics, compared to other glass-ceramics, although, to date, this assumption is still controversial [4,7-13].

ZLS blanks are available in a pre-crystallized or crystallized form. The crystallization process, inside a dental furnace, allows the nucleation of the crystals, with a subsequent improvement of their mechanical properties compared to the pre-crystallized ones [2]. Furthermore, the fracture resistance was reported to withstand physiological occlusal forces, and it increases after one firing protocol [14].

Due to its high translucency and biaxial flexural strength values, ZLS was tested for tooth- and implant-supported single partial and full restorations in both anterior and posterior regions [4,15-16], as well as for occlusal veneers [7,17]. It was also tested for endocrowns [18-19], although the reported results are not satisfactory.

Some findings showed that the machinability of ZLS is worse than the one of LS_2 [4,20], so that ZLS was defined "the most difficult to machine among glass ceramics" [20].

Also, ZLS is acid sensitive [21], and it is important to clarify what the ideal acid concentration and etching times are; moreover, the best cements polymerization (dual- or light-curing) and whether it is worth silanizing ZLS.

ZLS is also reported to be a biocompatible material [2], but to date, there is no univocal evidence about *in vitro* data regarding cell proliferation.

To date, the biological and mechanical performances of ZLS need a more in-depth look from a scientific point of view, in order to formulate a clear definition of their clinical indications and limitations. With the purpose of shedding light on the mechanical and biological properties of ZLS in CAD/CAM systems, this literature review is focused on the chemical composition, microstructure, biocompatibility, physico-mechanical properties, and marginal/internal fit of ZLS-based restorations.

Methods

2.1 Search strategy

An extensive search of the literature for papers related to ZLS was performed on the databases of PubMed/Medline, Scopus, Embase, Google Scholar, Dynamed, and Open Grey.

The literature search was performed using combinations of the keywords "zirconia-reinforced lithium silicate" or "ZLS". The following queries were used for each electronic database:

- PubMed/Medline, Google Scholar, and Open Grey = “(zirconia-reinforced lithium silicate) or (zls)” was added into each query box.
- Dynamed = ZLS; zirconia-reinforced; zirconia-reinforced lithium silicate; zirconia lithium.
- Scopus = (TITLE-ABS-KEY (zirconia-reinforced AND lithium AND silicate) OR TITLE-ABS-KEY (zls)).
- Embase = 'zirconia-reinforced lithium silicate' OR ('zirconia reinforced' AND ('lithium'/exp OR lithium) AND ('silicate'/exp OR silicate)) OR zls.

The references of the found records were imported as a Research Information Systems file into Mendeley (Mendeley Ltd., London, UK) in order to remove the duplicates.

2.2 Inclusion and exclusion criteria

Studies were considered as appropriate for the present literature review if they met the following inclusion criteria: 1) studies focused on the biocompatibility and/or mechanical properties of ZLS for CAD/CAM systems; 2) studies performed *in vitro*, *in silico,* or *in vivo*; 3) case reports; 4) systematic reviews.
The following exclusion criteria were used: 1) studies performed on non-human animals; 2) studies not addressed to the dentistry field; 3) studies referred to ZLS restorations produced by heat-pressed ceramics process.
No limitations were applied to the publication date or the language of the papers.

2.3 Data extraction

With the purpose of shedding light on the mechanical and biological characteristics of ZLS, the following variables were extracted:

1. Chemical composition and microstructure;
2. Biocompatibility;
3. Physico-mechanical values of ZLS;
4. Laboratory and post-milling manual processing;
5. Minimal thickness;
6. Fracture patterns and plastic deformation;
7. Fatigue failure load;
8. Marginal and internal fit.

According to the inclusion criteria, 3 calibrated researchers (F.Z., R.S, and G.R.) independently selected the articles reading the titles, abstracts, and keywords. The full text of each identified article was read to determine whether it was suitable for inclusion. In case of disagreement among the investigators, a majority criterion would have been used (i.e., 2 out of 3).
The workflow of the paper screening process is reported in Figure 1, according to the "PRISMA 2009 Flow Diagram" [22].

Figure 1 - Title: Search flowchart as described in the PRISMA guidelines.

Caption: (*n* = number of records).

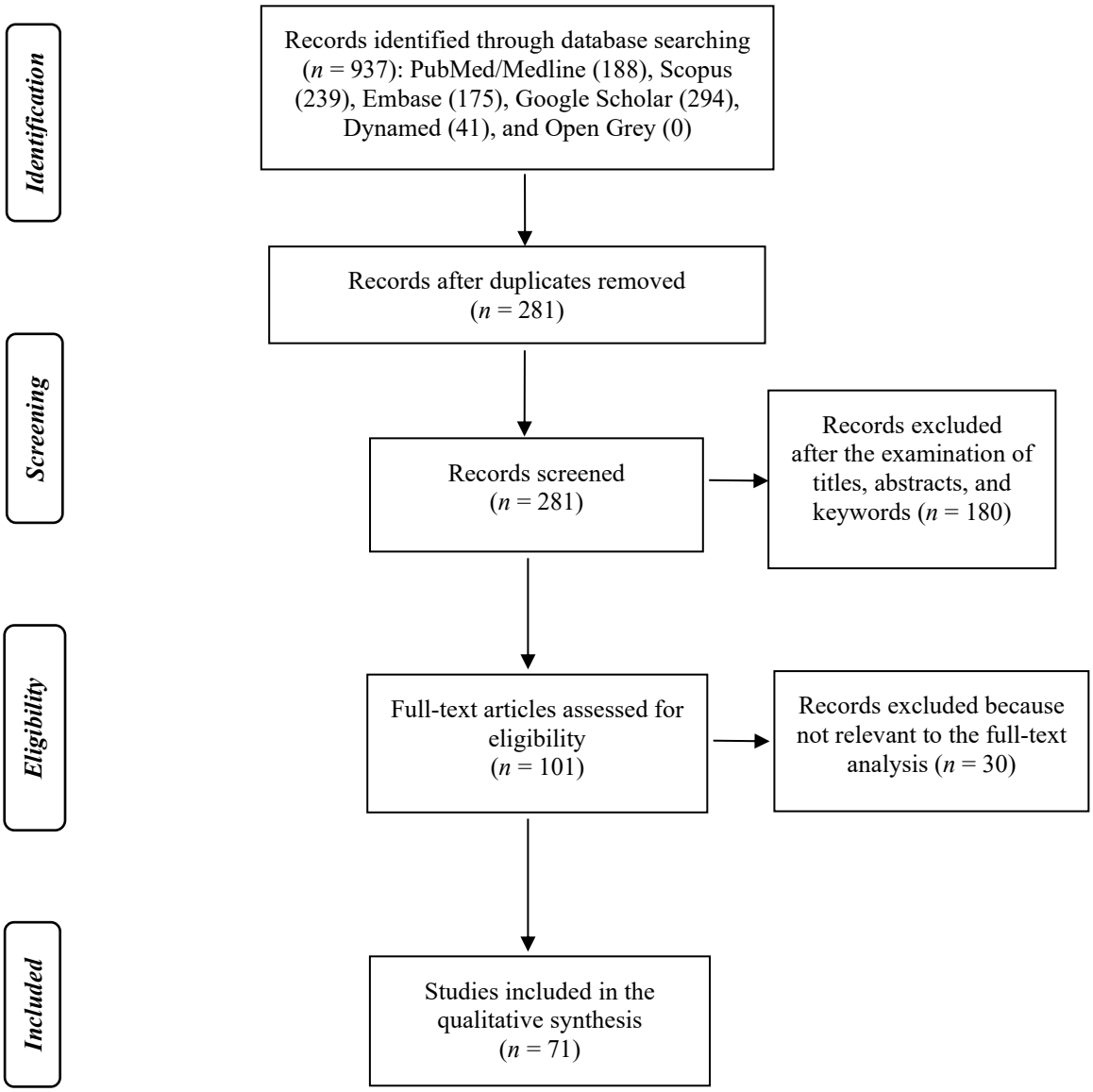

2.4 Calibration process

As regards the recorded titles and abstracts, the 3 reviewers performed pilot calibration exercises on a common random group of 20 references, applying the inclusion and exclusion criteria. After the exercise, the reviewers discussed which references were included or excluded. The reviewers

aimed to reach an agreement on at least 90% of the papers. The process would have been repeated until they had obtained the predetermined agreement level before starting the screening of the whole set of titles and abstracts collected. Also, the calibration process, with the same agreement level, was used on a random sample of 8 papers for the full-text screening of the included articles after reading titles and abstracts.

Results

3.1 Data synthesis

The literature search was completed in February 2021 and the included studies were published between 2015 and January 2021.

The search strategy produced 937 records, many of which were duplicates: 188 from PubMed/Medline, 239 from Scopus, 175 from Embase, 294 from Google Scholar, 41 from Dynamed, and 0 from Open Grey. All the duplicates were removed, thus all the selected databases produced 281 records. After the examination of titles, abstracts, and keywords, the reviewers excluded 180 records, because they did not meet the inclusion criteria. As to the remaining 101 records, 30 more were excluded after a full-text analysis because they did not provide considerable information about ZLS for dental research and clinical practice. The remaining 71 records were included in the present literature review (Table 1).

Table 1 - An overview of the 71 included records and the variables for inclusion regarding each paper

Analyzed variables	Authors (Year of publication)
Chemical composition or microstructure	Riquieri et al. (2018) [1], Vita Zahnfabrik (2019) [2], Dentsply Sirona Inc. (2016) [3], Elsaka and Elnaghy (2016) [4], Belli et al. (2018) [5], Belli et al. (2017) [6], Vasiliu et al. (2020) [12], Sen and Us (2018) [15], Wendler et al. (2017) [23], Ramos et al. (2016) [24], De Mendonca et al. (2019) [25], Traini et al. (2016) [26]
Biocompatibility	Vita Zahnfabrik (2019) [2], Rizo-Gorrita et al. (2018) [27], Rizo-Gorrita et al. (2019) [28], Dal Piva et al. (2018) [29], De Luca et al. (2018) [30], Abdalla et al. (2018) [31]
Physico-mechanical values of ZLS	Elsaka and Elnaghy (2016) [4], Belli et al. (2018) [5], Belli et al. (2017) [6], Al-Akhali et al. (2017) [7], Hamza and Sherif (2019) [8], Gomes et al. (2017) [9], Kashkari et al. (2019) [10], Schwindling et al. (2017) [11], Zarone et al. (2020) [13], Sen and Us (2018) [15], Preis et al. (2017) [16], Von Maltzahn et al. (2018) [17], Taha et al. (2018) [18], El Ghoul et al. (2019) [19], Chen et al. (2020) [20], Wendler et al. (2017) [23], Ramos et al. (2016) [24], De Mendonca et al. (2019) [25], Nishioka et al. (2018) [32], Guilardi et al. (2020) [33], Choi et al. (2017) [34], Zimmermann et al. (2017) [35], Preis et al. (2015) [36], Jassim and Majeed (2018) [37], Rosentritt et al. (2017) [38], Yeğin and Atala (2020) [39], Yilmaz et al. (2020) [40], Kermanshah et al. (2020) [41], Dartora et al. (2020) [42], Liu et al. (2021) [43], Juntanvee and Uasuwan (2020) [44], Srichumpong et al. (2019) [45], Monteiro et al. (2018) [46], Ottoni et al. (2018) [47], Lawson et al. (2016) [48]
Laboratory or post-milling manual processing	Riquieri et al. (2018) [1], Passos et al. (2019) [14], Traini et al. (2016) [26], Lawson et al. (2016) [48], Schweitzer et al. (2020) [49], Alao and Bujang (2021) [50], Badawy et al. (2016) [51], Aurèlio et al. (2017) [52], Romanyk et al. (2020) [53], Passos et al. (2018) [54], Kang et al. (2020) [55], Alves et al. (2019) [56]
Minimal thickness	Choi et al. (2017) [34], Zimmermann et al. (2017) [35], Monteiro et al. (2018) [46], Sieper et al. (2017) [57], Bergamo et al. (2019) [58], Shaik and Alfarsi (2019) [59], Tribst et al. (2018) [60], Alammari et al. (2018) [61]
Fracture patterns and plastic deformation	Ramos et al. (2016) [24], De Mendonca et al. (2019) [25], Liu et al. (2021) [43], Monteiro et al. (2018) [46], Sieper et al. (2017) [57], Bergamo et al. (2019) [58], Abu-Izze et al. (2018) [62], Diniz et al. (2020) [63]
Fatigue failure load	Von Maltzahn et al. (2018) [17], Monteiro et al. (2018) [46], Ottoni et al. (2018) [47], Alammari et al. (2018) [61], Diniz et al. (2020) [63], Al-Akhali et al. (2019) [64], Venturini et al. (2019) [65], Alves et al. (2020) [66], Schlenz et al. (2020) [67], Dal Piva et al. (2020) [68]
Marginal and internal fit	Vita Zahnfabrik (2019) [2], Gomes et al. (2017) [9], Taha et al. (2018) [18], El Ghoul et al. (2019) [19], Preis et al. (2015) [36], Alammari et al. (2018) [61], Hasanzade et al. (2020) [69], Dentsply Sirona Inc. (2017) [70], Zimmermann et al (2019) [71], Falahchai et al. (2020) [72-73]

No systematic reviews or case reports were found.

The reviewers obtained an agreement level superior to 90% after the first calibration exercise on titles and abstracts screening and an agreement level of 100% on full-text papers screening after only one exercise.

No disagreement was pointed out among the search investigators about the included records.

3.2 Chemical composition and microstructure

ZLS-based materials, to date marketed as Celtra Duo (Dentsply Sirona, DeguDent, GmbH, Hanau-Wolfgang, Germany) and Suprinity (Vita Zahnfabrik, H. Rauter GmbH & Co., Bad Säckingen, Germany), showed very similar microstructures, mainly consisting of two ~70 vol.% crystallized phases: one is made of larger, submicrometric lithium metasilicate crystallites (Li_2SiO_3) in slightly elongated shapes, more rounded than lithium disilicate ceramics (LS_2) needle-shaped ones; the other is made of smaller nanometric lithium orthophosphate crystallites (Li_3PO_4) as round granules [6]. After crystallization firing, a significant increase was observed for both phases and a new crystal phase appears, namely lithium disilicate ($Li_2Si_2O_5$), crystallized from the glassy matrix; such a crystallization is allowed by the presence of diphosphorus pentoxide (P_2O_5) as nucleation agent [6].

Lithium metasilicate crystallites in the glassy phase show different dimensions in Celtra Duo (about 1 μm) compared to Suprinity (about 0.5 μm) [6,12,23], in both cases smaller than LS_2 crystals, the latter described as elongated, needle-shaped, with length comprised between 0.5 and 4 μm [24,74]. It has been suggested that such a difference in size between the two different brand formulations could be due to discrepancies in the processing parameters, like firing temperature and time, being Suprinity treated with an additional and shorter crystallization firing process compared to Celtra Duo [5-6].

X-ray diffraction analysis on Suprinity showed crystallization peaks corresponding to lithium monosilicate, aluminum silicate, and tetragonal zirconia [24].

Raman analysis in pre-crystallized ZLS confirmed the presence of crystal phases made of lithium metasilicate and lithium orthophosphate; post-crystallization, besides an increase in intensity related to these components, the new crystal phase of lithium disilicate was also observed [6].

In a microstructural comparison, LS_2 is characterized by interlocking needle-shaped crystals embedded in a glassy matrix, while ZLS shows a homogeneous fine crystalline structure with rounded and rod-like crystals. The percentage of the crystalline phase is higher in LS_2 [4,24-25]. Actually, as found in CAD/CAM LS_2, in ZLS the presence of both lithium metasilicate and disilicate grains has been evidenced in the final stage of crystallization [5-6,75-77].

The chemical composition of ZLS-based materials is specified in Table 2, as reported by various sources in the literature.

Table 2 - Analysis of ZLS chemical composition (in weight %)

Vita Suprinity® PC. Technical and scientific documentation. 2019 [2]	Silicon dioxide (56-64); Lithium oxide (15-21); Zirconia (8-12); Phosphorus oxide (3-8); Potassium oxide (1-4); Aluminium oxide (1-4); Pigments (0-6); Cerium dioxide (0-4).
Celtra® Duo. Zirconia-Reinforced Lithium Silicate (ZLS) Block. Technical Monograph. 2016 [3]	Silicon dioxide (58.0); Lithium oxide (18.5); Zirconia (10.1); Phosphorus oxide (5.0); Cerium dioxide (2.0); Aluminium oxide (1.9); Terbium Oxide (1.0).
Traini et al. 2016 [26], about Suprinity fired	Silicon (59); Lithium (20); Zirconium (12); Phosphorus (4.2); Potassium (2.5); Aluminium (1.5); Other minor components (0.8).
Ramos et al. 2016 [24], about Suprinity fired	Oxygen (51.2); Silicon (29.6); Zirconia (15.5); Potassium (2.3); Aluminium (1.3).
Riquieri et al. 2018 [1], about Suprinity fired	Oxygen (52.60); Silicious (30.95); Zirconium (13.00); Potassium (2.06); Aluminium (1.35).
Riquieri et al. 2018 [1], about Celtra Duo fired	Oxygen (53.09); Silicious (30.85); Zirconium (12.50); Potassium (2.36); Aluminium (1.17).
Sen and Us. 2018 [15], about Suprinity fired	Oxygen (52.1); Silicon (27.52); Zirconium (15.7); Potassium (2.34); Aluminium (1.28); Carbon (1.05).

3.3 Biocompatibility

In the present state of knowledge, data regarding the biocompatibility of ZLS are scarce and controversial. Suprinity was deemed biocompatible by the "North American Science Associates Inc." (NAMSA) from specific evaluations based on cytotoxicity, sensitization, subchronic systemic toxicity, irritation, and genotoxicity [2].

Human gingival fibroblasts (HGFs) cultured onto ZLS exhibited lower cell proliferation, coverage, and spreading than onto zirconia; such a worse cellular response in ZLS could be attributed to a rougher and less homogeneous surface topography [27]. In a comparative *in vitro* study, ZLS and zirconia showed intermediate values of cell viability and collagen secretion between LS_2, which exhibited the best values, and polymethyl methacrylate (PMMA), which showed the lowest values [28].

Furthermore, polished ZLS surfaces have been reported to be less rough, accumulating less biofilm and displaying higher surface free energy than glazed surfaces; however, polished surfaces showed severe initial cytotoxicity for HGFs but were inert in the long term; such cytotoxicity (24 hours) may be related to an initial release of remnants of the polishing material, reducing its cytotoxic effect after 7 days. Over time, the cells strengthen their defense mechanisms and become able to protect themselves [29].

Another *in vitro* study showed that proliferation and viability of HGFs onto crystallized, not polished and polished ZLS, before and after crystallization, are similar to those of zirconia ceramics, with favorable biological properties suggesting an indication for use in implant-supported restorations with margins in contact with peri-implant tissues [30].

In the case of polished surfaces, ZLS demonstrated the lowest bacterial adhesion, compared to LS_2 and feldspathic ceramics (FC) [31].

3.4 Physico-mechanical properties

3.4.1 Physico-mechanical values of ZLS

According to several reports, it can be stated that in ceramic materials the lower the glassy content, the higher the dental ceramic overall strength [23-24,32-33]. In the last decade, ZLS was introduced on the market with the purpose of offering at the same time advanced esthetic properties, being a translucent glass-ceramic with silicate crystals embedded in a high content of glassy matrix, together with a favorable mechanical behavior, thanks to the addition of tetragonal zirconia fillers, exploiting a mechanism of crack interruption [4].

In the last years, several studies have proved that ZLS restorations show fracture resistance values exceeding the physiological occlusal/masticatory forces [7,9,34-36], although the concept of zirconia fillers acting as an additional toughening mechanism [20,78], at the basis of the material physico-chemical formulation, has been confuted by some authors [24]. It has always to be considered that, due to the wide heterogeneity of research designs and testing modalities, *in vitro* data are not infrequently controversial, making their comparisons very difficult and possible correlations to *in vivo* biomechanical behavior not always easy.

According to some research data, in a comparison with other restorative materials, occlusal veneers made of LS_2 and ZLS showed higher resistance to fracture than those fabricated with polymer-infiltrated ceramic networks (PICN) and PMMA [7]. In another study, the load at fracture of ZLS tabletops was found to be significantly higher than that of feldspar-based ceramic ones [17]. Besides, similar results were reported by a research conducted on monolithic, crown-shaped restorations, showing higher fracture strength of LS_2 and ZLS compared to PICN and a hybrid high-performance polymer composite resin [25].

Compared to bilayered, ceramic-veneered zirconia restorations, monolithic crowns made of LS_2 and ZLS were reported to exhibit higher fracture resistance [8].

To date, several studies have been carried out in order to compare the mechanical properties of the two most popular silicate-based materials, LS_2 and ZLS, although the reported data are not always in agreement.

According to some *in vitro* investigations [4,8,11,15,37], ZLS exhibited higher mechanical performances than LS_2, confirming the possible efficiency of the zirconia additional phase in increasing resistance thanks to a mechanism of crack interruption. In some studies, compared to LS_2, the material showed higher fracture [8,37] and flexural strength [4,15]. In another research, carried out on monolithic crowns in the anterior sites, load-to-failure values were reported to be slightly higher for glazed ZLS than for LS_2; after submitting the restorations to an extensive thermocycling test, such a fracture resistance was still maintained by ZLS specimens [11].

ZLS has also been tested *in vitro* as a material for implant-supported molar crowns, reporting high fracture forces, although lower than those shown by zirconia [16]. In any case, the insertion of a screw channel might reduce the stability of ZLS restorations [38].

On this topic, other studies report fewer positive results. In an *in vitro* investigation, high strength zirconia crowns showed the most favorable load-to-fracture values, followed by LS_2 and ZLS, the latter exhibiting significantly lower mechanical performance [10]. Also, fatigue strength, evaluated by biaxial flexural test on disc-shaped specimens, exhibited the highest values with high translucence yttrium stabilized tetragonal zirconia, followed, in decreasing order by LS_2, ZLS, PICN, and FC [32].

Other investigations reported lower values for fracture [9] and failure [39] loads in implant-supported ZLS monolithic crowns compared to LS_2 ones.
Moreover, in a recent study, no differences were detected among ZLS, PICN, LS_2, and zirconia as to strains around the implant platform, none of these materials offering a significant load absorption aimed at minimizing the strains generated at the platform level. [40].
In ceramic inlay-retained fixed partial dentures, the fracture load of zirconia was reported to be higher than that of ZLS [41].
In the last decade, the concept of endocrown has been gaining more and more popularity for the restoration of endodontically treated teeth, utilizing mechanical retention offered by the pulp chamber together with chemical/micromechanical adhesion provided by bonding procedures. In posterior endocrowns, LS_2 resistance to fracture was reported to be higher compared to ZLS, both under axial [19] and lateral forces [18-19]. According to a recent *in vitro* and finite element analysis (FEA) study, the highest fracture strength resistance values were exhibited by monolithic endocrowns made of zirconia, compared to LS_2, ZLS, and leucite reinforced ceramics, although monolithic zirconia and ZLS showed worse failure modalities, with a higher rate of catastrophic fractures [42].

The physico-mechanical values collected from different studies are shown in Table 3.

Authors (Product name)	Modulus of Elasticity (GPa)	Flexural Strength (MPa)	Fracture toughness = K_{Ic} (MPa $m^{1/2}$)	Vickers' Hardness (GPa)	Characteristic Strength (MPa)	Weibull modulus (m)	Poisson's ratio	Fracture Resistance (N)	Density (g/cm^3)
Liu et al. 2020 [43] (Celtra Duo)					279	2.7			
Juntavee and Uasuwan 2020 [44] (Suprinity)		218.43 ± 38.46			234.23	6.40			
De Mendonca et al. 2019 [25] (Suprinity)		230 ± 20		6.78 ± 0.013*					
Srichumpong et al. 2019 [45] (Suprinity and Celtra Duo)			1.86 (Suprinity) 1.75 (Celtra Duo)	6.8 (Same value both for Suprinity and Celtra Duo)					
Monteiro et al. 2018 [46] (Celtra Duo)							0.30		
Von Maltzahn et al. 2018 [17] (Celtra Duo)								1,571.1 ± 297.0	
Ottoni et al. 2018 [47] (Suprinity)		179 ± 56	1.93 ± 0.32	6.67 ± 0.18	197 (158; 200)	4 (3;5)			
Nishioka et al. 2018 [32] (Suprinity)					152.1 ± 7.5				
Jassim et al. 2018 [37] (Celtra Duo)								1404.5 ± 236.51	
Sen and Us. 2018 [15] (Suprinity)		510 ± 43			532	8.8			
Belli et al. 2018 [5] (Suprinity and Celtra Duo)			1.40 ± 0.10 (Suprinity) 1.52 ± 0.05 (Celtra Duo)						
Schwindling et al. 2017 [11] (Celtra Duo)								725 ± 162	
Belli et al. 2017 [6] (Suprinity and Celtra Duo)	105.8 (Suprinity) 108.2 (Celtra Duo)						0.207 (Suprinity) 0.224 (Celtra Duo)		2.643 (Suprinity) 2.630 (Celtra Duo)
Wendler et al. 2017 [23] (Suprinity and Celtra Duo)	104.9 (Suprinity) 107.9 (Celtra Duo)				611.24 (573.80;651.58) (Suprinity) 626.84 (587.74;669.02) (Celtra Duo)	5.29 (3.96;6.45) (Suprinity) 5.19 (3.89;6.33) (Celtra Duo)	0.208 (Suprinity) 0.222 (Celtra Duo)		
Hamza et al. 2017 [8] (Suprinity)								1742.9 ± 102.7	
Ramos et al. 2016 [24] (Suprinity)	65.6 ± 4.1		1.25 ± 0.79		217.5 (151.84;238.6)	10.0 (C.I. 6.92-14.41)	0.23 ± 0.03		1.60
Lawson et al. 2016 [48] (Celtra Duo)	61.0 ± 10.0	300.1 ± 16.8		4.54 ± 0.26*					
Elsaka and Elnaghy 2016 [4] (Celtra Duo)	70.44 ± 1.97	443.63 ± 38.90	2.31 ± 0.17	6.53 ± 0.46	460.74	13.41			

Table 3 - Physico-mechanical values of ZLS (mean ± SD)

*The numerical values of Vickers' Hardness were different from the ones reported in the corresponding original papers. This change had the goal to report numerical values converted to the same unit (GPa).

It is more than evident that, in order to get a deeper insight about the mechanical properties of this material, data reported by *in vitro* studies should be furtherly corroborated by *in vivo* results of clinical, long-term, controlled and randomized trials, that are missing, at the moment, in the scientific literature.

3.4.2 Laboratory and post-milling manual processing

Several studies have been carried out on the modifications of the physico-mechanical properties of ZLS following laboratory manufacturing, particularly sintering and crystallization. In this regard, an evident increase of the following ZLS physical values was shown after the firing process: modulus of elasticity, flexural strength, fracture toughness, hardness, and characteristic strength [1,26,48-51], simultaneously with a decrease of the Weibull modulus and a significant shrinkage [1,49], as reported in Table 4. The material seemed to be brittler with a tendency to develop inner cracks at the partially crystallized state; for this reason, particular care should be taken during the manipulation process for marginal adaptation [26].

Table 4 - Physical values (mean ± SD) of unfired/fired ZLS

	Modulus of Elasticity (GPa)	Flexural Strength (MPa)	Fracture toughness = K_{Ic} (MPa $m^{1/2}$)	Vickers' Hardness (GPa)*	Weibull Modulus (m)	Characteristic Strength (MPa)
Schweitzer et al. 2020 [49] (Celtra Duo)		189.02 ± 25.5 / 252.86 ± 53.78			8.9 / 5.81	219.3 / 314.35
Alves et al. 2019 [56] (Suprinity and Celtra Duo)	89.8 ± 5 / 97 ± 6.2 (Suprinity) 92 ± 4.7 / 98.9 ± 3.8 (Celtra Duo)		1.15 ± 0.13 / 1.39 ± 0.04 (Suprinity) 1.4 ± 0.12 / 1.49 ± 0.05 (Celtra Duo)	6.34 ± 0.33/ 6.5 ± 0.11* (Suprinity) 6.64 ± 0.17 / 6.63 ± 0.14* (Celtra Duo)		
Riquieri et al. 2018 [1] (Suprinity and Celtra Duo)			2..21 ± 0.11 / 2.63 ± 0.14 (Suprinity) 2.26 ± 0.80 / 2.51 ± 0.59 (Celtra Duo)	597.533 ± 33.97 / 683.267 ± 16.07 (Suprinity) 682.400 ± 15.31 / 693.333 ± 10.85 (Celtra Duo)	7.07 / 5.38 (Suprinity) 5.86 / 5.77 (Celtra Duo)	106.95 / 191.02 (Suprinity) 163.86 / 251.25 (Celtra Duo)
Lawson et al. 2016 [48] (Celtra Duo)	61.0 ± 10.0 / 63.6 ± 3.3	300.1 ± 16.8 / 451.4 ± 58.9		4.546 ± 0.26* / 5.836 ± 0.36*		
Traini et al. 2016 [26] (Suprinity)			2.8 ± 0.9 / 4.7 ± 0.8	6.8 ± 0.5 / 7.6 ± 0.7		

*The numerical values of Vickers' Hardness were different from the ones reported in the corresponding original papers. This change had the goal to report numerical values converted to the same unit (GPa).

The increase of ZLS restoration strength after one firing protocol was confirmed by Passos et al. [14]. Moreover, an extended glaze firing protocol has been proposed, based on the same initial pre-heating time, temperature, and temperature increase rate as the conventional manufacturer-recommended glaze firing, with a difference, in that the extended glaze firing differs by slow cooling until the temperature drops to 200° C in a closed furnace for a dwell time of 15 min [52]. This extended glaze firing protocol, after hard machining of ZLS, repaired defects by generating beneficial compressive residual stress, differently from conventional glaze firings, that can create tensile stresses [52].

The surface defects related to machining procedures negatively influence the mechanical performance of ZLS fabricated with CAD/CAM technologies; in this regard, the post-machining heat treatment can partially relieve the strength-limiting damage caused by CAD/CAM procedures [53].

After the final processing of the ZLS restorations, a manual adjustment of occlusal morphology should be avoided, because it has been demonstrated that this procedure can decrease the fracture load of ZLS crowns [54].

As for the milling accuracy, ZLS showed lower mean values than LS_2; nevertheless, the milling accuracy of ZLS was within 120 µm, therefore considered clinically acceptable [55].

3.4.3 Minimal thickness

Thickness is a paramount factor in all-ceramic restorations, both from a clinical and technical point of view, in that it affects the design of the tooth preparation and, at the same time, strongly influences fracture resistance and survival rate of the prosthesis.

In ZLS, as expected, mean fracture loads of monolithic restorations were reported to increase significantly as thickness increased [34-35,57].

According to an *in vitro* study, at a thickness of 1.5 mm Suprinity exhibited a fracture resistance similar to LS_2 and higher than PICN and Celtra Duo [34]; conversely, another paper reported higher mean fracture loads for LS_2 than for ZLS at both 1.5 mm and 1.0 mm thickness [35].

Another research showed promising durability of ZLS single crowns for the thickness of 1.0 mm [57]; at such a thickness, fracture resistance values of ZLS, LS_2, and PICN were shown to be similar [34]. At 0.5 mm thickness, a substantially reduced mechanical resistance was evidenced for most metal-free, silicate-based, feldspathic, and hybrid materials [35,58]; on the contrary, another research, aimed at comparing fracture resistance of full-coverage minimally invasive crowns made of ZLS, PICN, and high translucent zirconia ceramics (HT-Z), showed that with minimal thickness of 0.6 mm restorations made of HT-Z and PICN were mechanically resistant within the range of biting forces, while ZLS exhibited the lowest load values [59].

FEA studies have been increasingly carried out in the last decade on the topic of metal-free materials, allowing an "*in silico*" reliable evaluation of mechanical behavior of dental restorations. In a research on stress distribution in occlusal veneers, a direct correlation between restoration thickness and concentration of tensile stresses was detected, in the following decreasing order for the simulated materials: HT-Z (highest stress concentration), LS_2, FC, ZLS, and PICN [60]. Moreover, the typology of restorative material differently influenced the concentration of stress on the cement layer, in the following decreasing order: PICN > HT-Z > ZLS > LS_2 > FC. In the same study, the cement layer thickness was not shown to be relevant to mechanical resistance.

In another FEA investigation, higher stress concentrations on the cement interface were detected reducing ceramic thickness [46].

As regards the influence of preparation design on ZLS mechanical resistance, it has been evidenced that an increase in total occlusal convergence from 12° to 20° resulted in higher load-to-fracture values of ZLS crowns and did not influence their internal and marginal fit [61].

3.4.4 Fracture patterns and plastic deformation

Some fractographic studies have been carried out in order to shed light on mechanical behavior and failure patterns of ZLS restorations.

Silicate-based materials like ZLS and LS_2 are showed to suffer mainly from unrepairable and catastrophic fracture patterns, differently from hybrid ceramics, in which limited chipping and type II fracture patterns (i.e., affecting less than half the crown) are more commonly found [25].

Light microscopy showed that ZLS failures consisted primarily of bulk fractures starting from the cementation surface as radial cracks propagating to the cervical area [46,58,62-63]. It has also been evidenced that both ZLS and LS_2 are susceptible to slow crack propagation, which is one of the main causes of failure in metal-free prostheses [24].

ZLS and LS_2 have been reported to show similar susceptibility to subcritical crack growth, a phenomenon more limited for zirconia thanks to its phase transformation known as transformation toughening [43]; in another study, an effective mechanism of crack interruption was confirmed in ZLS by the presence of clear semicircular arrest lines at scanning electron microscope (SEM), close to the origin of failure [57].

3.4.5 Fatigue failure load

To date, it has been demonstrated that load-at-fracture resistance of ZLS makes this material suitable for clinical purposes; cyclic loading simulating 1 year of use (i.e., 10^6 cycles at 4 Hz and a load of 88 N) did not result in ZLS crowns fatigue failure [61]. As regards the effects of thermal aging, the results reported in the literature are still controversial; in an investigation, experimental aging (i.e., 10^6 cycles at 2.5 Hz and a load of 50 N with thermal aging of 10,000 cycles at 5-55 °C) did not compromise the mechanical stability of the material [17], conversely, in another study, aging (induced according to staircase method with 100,000 cycles at 20 Hz and thermal aging of 10,000 cycles in 5-55 °C) determined a reduction in fatigue failure load [63]. Furthermore, it was reported that thermo-mechanical fatigue reduced the survival rate and fracture strength of ZLS occlusal veneers bonded to enamel using the self-etching technique [64].

Several investigations evaluated the fatigue failure load of ZLS, with different experimental designs [46-47,65]. An *in vitro* study using the boundary and staircase fatigue methods showed that, after 10^3 cycles, a degradation of 78% of the initial strength occurred for both fatigue methods; differently, when the number of cycles increased from 10^3 to 10^4, there was no further significant degradation [47].

In another research, fatigue failure loads for ZLS, determined using the staircase method (i.e., 100,000 cycles at 20 Hz) at ceramic thicknesses ranging from 1.0 to 2.5 mm, showed the

following values: Suprinity = 716.5 ± 95.5 N (at 1.0 mm) up to 1119.6 ± 241.7 N (at 2.5 mm); Celtra Duo = 404.0 ± 43.3 N (at 1.0 mm) up to 1126.8 ± 80.2 N (at 2.5 mm). From these results, it can be asserted that different ZLS thicknesses affect the fatigue failure load of the bonded system so that the thicker the ZLS, the higher the expected fatigue failure load. Moreover, the staircase experimental procedure confirmed that the firing procedures (glaze firing process or crystallization firing) improved the fatigue failure load [63].

Comparisons among the fatigue behavior of ZLS and other materials have shown conflicting results among different studies, perhaps due to the different fatigue test designs performed. Comparative *in vitro* studies between ZLS and other materials showed that CAD/CAM posterior ZLS crowns exhibited better fatigue resistance than LS_2 but worse than monolithic crowns made of translucent zirconia [66]. In a different analysis performed with the optical coherence tomography, ZLS showed the highest horizontal and vertical fatigue damages, followed by PICN, resin composites, and 5 mol% Y_2O_3- partially stabilized zirconia [67].

Another *in vitro* investigation reported that the fatigue behavior of ZLS was similar to LS_2 and leucite ceramics, better than FC and PICN but worse than resin nanoceramic (RNC); in the same study, the fatigue failure load evaluated by a step-stress approach (i.e., 400 N-2200 N; step-size of 200 N; 10,000 cycles per step; 1.4 Hz) reached 1013.33 N after 40,666 cycles for ZLS [65]. These results do not clarify whether the fatigue behavior of ZLS is better than LS_2, but it should be noted that RNC [65] and resin composites [67] expressed better fatigue performance than ZLS, due to the superior flexibility and reduced brittleness, probably determined by the resinous content in their microstructure [65]. In any case, compared to zirconia, it is clear that ZLS is less efficient even in fatigue behavior [66-67].

Surface morphology is a factor that seems to affect fatigue behavior; in fact, ZLS presented higher survival probability and fatigue strength when polished than when showing a roughened surface [68]; in support of these results, another *in vitro* study reported that higher degrees of roughness (i.e., Ra = 1.98 μm; Rz = 12.25 μm) had a negative influence on the fatigue performance of ZLS [33].

3.5 Marginal and internal fit

ZLS crowns were proved to offer clinically acceptable internal and marginal gaps (≤150 μm) [9,18-19,36,69]. This is in agreement with manufacturers' documentations reporting good edge stability at a thickness of 160-200 μm [2,70]. Nevertheless, higher levels of marginal misfit were reported for ZLS implant-supported crowns compared to LS_2 CAD/CAM ones in an *in vitro* study [9].

As regards design preparation, it has been demonstrated that marginal and internal adaptation of ZLS crowns is not significantly affected by the parameter of total occlusal convergence, in a range comprised from 12° to 20° [61]. With regard to ZLS overlay restorations, a preparation design characterized by anatomical occlusal reduction with rounded shoulder and a central groove exhibited poorer marginal adaptation than one with anatomical occlusal reduction alone [71]. This latter preparation design also showed the highest fracture resistance (2737.95 ± 409.66) [72].

As regards endocrown restorations, the following, not exciting, mean values of fit were reported for ZLS: margin = 131.0 μm, axial = 160.8 μm, and occlusal = 182.3 μm [73]; internal and marginal adaptation of endocrowns were not demonstrated to be significantly different among ZLS, LS_2, and PICN [69].

Conclusions

According to the present literature review, in the current state of knowledge, the following conclusions can be drawn for the mechanical and biological properties of ZLS CAD-CAM:

1. Despite the presence of zirconia grains in the glassy matrix, there is no undisputed evidence confirming a higher mechanical strength compared to LS_2. The fracture resistance was reported to withstand physiological occlusal forces. At 1.0 mm thickness, the durability is promising.
2. ZLS crowns can exhibit clinically acceptable internal marginal gaps (≤150 μm).
3. After the firing process, there is an increase of modulus of elasticity, flexural strength, fracture toughness, hardness, and characteristic strength, in parallel with a decrease of both the Weibull modulus and volume (shrinkage).
4. The firing and polishing procedures positively affect the fatigue failure load.
5. ZLS seems to show a certain degree of biocompatibility, allowing proliferation, coverage, and spreading of HGFs, encouraging its use in contact with peri-implant soft tissues.

Although ZLS can be considered promising hybrid ceramic materials for CAD-CAM technologies, it cannot be denied that further *in vitro* and, in particular, randomized controlled trials *in vivo* studies are needed to accurately define mechanical properties and biocompatibility of ZLS-based restorations both tooth- and implant-supported.

References

1. H. Riquieri, J.B. Monteiro, D.C. Viegas, T.M.B. Campos, R.M. de Melo, G. de Siqueira Ferreira Anzaloni Saavedra, Impact of crystallization firing process on the microstructure and flexural strength of zirconia-reinforced lithium silicate glass-ceramics, Dent. Mater. 34 (2018) 1483-91, https://doi.org/10.1016/j.dental.2018.06.010.

2. Vita Suprinity® PC. Technical and scientific documentation. Bad Säckingen, Germany: Vita Zahnfabrik; 2019. https://mam.vita-zahnfabrik.com/portal/ecms_mdb_download.php?id=82440&sprache=en&fallback=en&cls_session_id=&neuste_version=1, 2021 (accessed 20 February 2021)

3. Celtra® Duo. Zirconia-Reinforced Lithium Silicate (ZLS) Block. Technical Monograph. DeguDent GmbH, Hanau, Wolfgang, Germany: Dentsply Sirona Inc.; 2016. https://assets.dentsplysirona.com/dentsply/microsites/celtra/celtraduo-tech-monograph.pdf, 2021 (accessed 20 February 2021)

4. S.E. Elsaka, A.M Elnaghy, Mechanical properties of zirconia reinforced lithium silicate glass-ceramic, Dent. Mater. 32 (2016) 908-14, https://doi.org/10.1016/j.dental.2016.03.013.

5. R. Belli, M. Wendler, A. Petschelt, T. Lube, U. Lohbauer, Fracture toughness testing of biomedical ceramic-based materials using beams, plates and discs, J. Eur. Ceram. Soc. 38 (2018) 5533-44.

6. R. Belli, M. Wendler, D. de Ligny, M.R. Cicconi, A. Petschelt, H. Peterlik, U. Lohbauer, Chairside CAD/CAM materials. Part 1: Measurement of elastic constants and microstructural characterization, Dent. Mater. 33 (2017) 84-98, https://doi.org/10.1016/j.dental.2016.10.009.

7. M. Al-Akhali, M.S. Chaar, A. Elsayed, A. Samran, M. Kern, Fracture resistance of ceramic and polymer-based occlusal veneer restorations, J. Mech. Behav. Biomed. Mater. 74 (2017) 245-50, https://doi.org/10.1016/j.jmbbm.2017.06.013.

8. T.A. Hamza, R.M. Sherif, Fracture Resistance of Monolithic Glass-Ceramics Versus Bilayered Zirconia-Based Restorations, J. Prosthodont. 28 (2019) e259-e264, https://doi.org/10.1111/jopr.12684.

9. R.S. Gomes, C.M.C. Souza, E.T.P. Bergamo, D. Bordin, A.A. Del Bel Cury, Misfit and fracture load of implant-supported monolithic crowns in zirconia-reinforced lithium silicate, J. Appl. Oral Sci. 25 (2017) 282-9, https://doi.org/10.1590/1678-7757-2016-0233.

10. A. Kashkari, B. Yilmaz, W.A. Brantley, S.R. Schricker, W.M. Johnston, Fracture analysis of monolithic CAD-CAM crowns, J. Esthet. Restor. Dent. 31 (2019) 346-52, https://doi.org/10.1111/jerd.12462.

11. F.S. Schwindling, S. Rues, M. Schmitter, Fracture resistance of glazed, full-contour ZLS incisor crowns, J. Prosthodont. Res. 61 (2017) 344-9, https://doi.org/10.1016/j.jpor.2016.12.008.

12. R.D. Vasiliu, S.D. Porojan, M.I. Bîrdeanu, L. Porojan, Effect of Thermocycling, Surface Treatments and Microstructure on the Optical Properties and Roughness of CAD-CAM and Heat-Pressed Glass Ceramics, Materials (Basel) 13 (2020) 381, https://doi.org/10.3390/ma13020381.

13. F. Zarone, M.I. Di Mauro, P. Ausiello, G. Ruggiero, R. Sorrentino, Current status on lithium disilicate and zirconia: a narrative review, BMC Oral Health 19 (2019) 134, https://doi.org/10.1186/s12903-019-0838-x.

14. L. Passos, B. Linke, A. Street, Y. Torrealba, Effect of thickness, translucency, and firing protocol on the masking ability of a CAD/CAM zirconia-reinforced lithium silicate for different backgrounds, Int. J. Comput. Dent. 22 (2019) 29-38.

15. N. Sen, Y.O. Us, Mechanical and optical properties of monolithic CAD-CAM restorative materials, J. Prosthet. Dent. 119 (2018) 593-9, https://doi.org/10.1016/j.prosdent.2017.06.012.

16. V. Preis, S. Hahnel, M. Behr, L. Bein, M. Rosentritt, In-vitro fatigue and fracture testing of CAD/CAM-materials in implant-supported molar crowns, Dent. Mater. 33 (2017) 427-33.

17. N.F. von Maltzahn, O.I. El Meniawy, N. Breitenbuecher, P. Kohorst, M. Stiesch, M. Eisenburger, Fracture Strength of Ceramic Posterior Occlusal Veneers for Functional Rehabilitation of an Abrasive Dentition, Int. J. Prosthodont. 31 (2018) 451-2, https://doi.org/10.11607/ijp.5817.

18. D. Taha, S. Spintzyk, A. Sabet, M. Wahsh, T. Salah. Assessment of marginal adaptation and fracture resistance of endocrown restorations utilizing different machinable blocks subjected to thermomechanical aging, J. Esthet. Restor. Dent. 30 (2018) 319-28.

19. W. El Ghoul, M. Özcan, M. Silwadi, Z. Salameh, Fracture resistance and failure modes of endocrowns manufactured with different CAD/CAM materials under axial and lateral loading, J. Esthet. Restor. Dent. 31 (2019) 378-87, https://doi.org/10.1111/jerd.12486.

20. X.P. Chen, Z.X. Xiang, X.F. Song, L. Yin, Machinability: Zirconia-reinforced lithium silicate glass ceram-ic versus lithium disilicate glass ceramic, J. Mech. Behav. Biomed. Mater. 101 (2020) 103435, https://doi.org/10.1016/j.jmbbm.2019.103435.

21. B. Altan, S. Cinar, B. Tuncelli, Evaluation of shear bond strength of zirconia-based monolithic CAD-CAM materials to resin cement after different surface treatments, Niger. J. Clin. Pract. 22 (2019) 1475-82, https://doi.org/10.4103/njcp.njcp_157_19.

22. A. Liberati, D.G. Altman, J. Tetzlaff, C. Mulrow, P.C. Gøtzsche, J.P. Ioannidis, M. Clarke, P.J. Devereaux, J. Kleijnen, D. Moher, The PRISMA statement for reporting systematic reviews and meta-analyses of studies that evaluate health care interventions: explanation and elaboration, PLoS Med. 6 (2009) e1000100, https://doi.org/10.1371/journal.pmed.1000100.

23. M. Wendler, R. Belli, A. Petschelt, D. Mevec, W. Harrer, T. Lube, R. Danzer, U. Lohbauer, Chairside CAD/CAM materials. Part 2: Flexural strength testing, Dent. Mater. 33 (2017) 99-109.

24. N. de C. Ramos, T.M.B. Campos, I.S. de La Paz, J.P.B. Machado, M.A. Bottino, P.F. Cesar, R.M. Melo, Microstructure characterization and SCG of newly engineered dental ceramics, Dent. Mater. 32 (2016) 870-8.

25. A. Furtado de Mendonca, M. Shahmoradi, C.V.D. Gouvêa, G.M. De Souza, A. Ellakwa, Microstructural and Mechanical Characterization of CAD/CAM Materials for Monolithic Dental Restorations, J. Prosthodont. 28 (2019) e587-e594.

26. T. Traini, B. Sinjari, R. Pascetta, N. Serafini, G. Perfetti, P. Trisi, S. Caputi, The zirconia-reinforced lithium silicate ceramic: lights and shadows of a new material, Dent. Mater. J. 35 (2016) 748-55, https://doi.org/10.4012/dmj.2016-041.

27. M. Rizo-Gorrita, I. Luna-Oliva, M.Á. Serrera-Figallo, J.L. Gutiérrez-Pérez, D. Torres-Lagares, Comparison of Cytomorphometry and Early Cell Response of Human Gingival Fibroblast (HGFs) between Zirconium and New Zirconia-Reinforced Lithium Silicate Ceramics (ZLS), Int. J. Mol. Sci. 19 (2018) 2718.

28. M. Rizo-Gorrita, C. Herráez-Galindo, D. Torres-Lagares, M.Á. Serrera-Figallo, J.L. Gutiérre-Pérez, Biocompatibility of Polymer and Ceramic CAD/CAM Materials with Human Gingival Fibroblasts (HGFs), Polymers (Basel) 11 (2019) 1446.

29. A.M.O. Dal Piva, L.P.C. Contreras, F.C. Ribeiro, L.C. Anami, S.E.A. Camargo, A.O.C. Jorge, M.A. Bottino, Monolithic Ceramics: Effect of Finishing Techniques on Surface Properties, Bacterial Adhesion and Cell Viability, Oper. Dent. 43 (2018) 315-25.

30. P.G. De Luca, G.A.P. Carvalho, A.B.G. Franco, S. Kreve, G. Avila, S.C. Dias, Zirconia-Reinforced Lithium Silicate Biocompatibility Polished in Different Stages - An In Vitro Study, J. Int. Dent. Med. Res. 11 (2018) 759-64.

31. M.M. Abdalla, I.A.A. Ali, K. Khan, N. Mattheos, S. Murbay, J.P. Matinlinna, P. Neelakantan, The Influence of Surface Roughening and Polishing on Microbial Biofilm Development on Different Ceramic Materials, J. Prosthodont. (2020) 1-7, https://doi.org/10.1111/jopr.13260.

32. G. Nishioka, C. Prochnow, A. Firmino, M. Amaral, M.A. Bottino, L.F. Valandro, R.M. de Melo, Fatigue strength of several dental ceramics indicated for CAD-CAM monolithic restorations, Braz. Oral Res. 32 (2018) e53.

33. L.F. Guilardi, P. Soares, A. Werner, N. de Jager, G.K.R. Pereira, C.J. Kleverlaan, M.P. Rippe, L.F. Valandro, Fatigue performance of distinct CAD/CAM dental ceramics, J. Mech. Behav. Biomed. Mater. 103 (2020) 103540.

34. S. Choi, H.I. Yoon, E.J. Park, Load-bearing capacity of various CAD/CAM monolithic molar crowns under recommended occlusal thickness and reduced occlusal thickness conditions, J. Adv. Prosthodont. 9 (2017) 423-31.

35. M. Zimmermann, G. Egli, M. Zaruba, A. Mehl, Influence of material thickness on fractural strength of CAD/CAM fabricated ceramic crowns, Dent. Mater. J. 36 (2017) 778-83.

36. V. Preis, M. Behr, S. Hahnel, M. Rosentritt, Influence of cementation on in vitro performance, marginal adaptation and fracture resistance of CAD/CAM-fabricated ZLS molar crowns, Dent. Mater. 31 (2015) 1363-9.

37. Z.M. Jassim, M.A. Majeed, Comparative Evaluation of the Fracture Strength of Monolithic Crowns Fabricated from Different all-ceramic CAD/CAM Materials (an in vitro study), Biomed. Pharmacol. J. 11 (2018) 1689-97.

38. M. Rosentritt, S. Hahnel, F. Engelhardt, M. Behr, V. Preis, In vitro performance and fracture resistance of CAD/CAM-fabricated implant supported molar crowns, Clin. Oral Investig. 21 (2017) 1213-19.

39. E. Yeğin, M.H. Atala, Comparison of CAD/CAM manufactured implant-supported crowns with different analyses, Int. J. Implant Dent. 6 (2020) 69.

40. B. Yilmaz, A. Alsaery, S.H. Altintas, M. Schimmel, Comparison of strains for new generation CAD-CAM implant-supported crowns under loading, Clin. Implant Dent. Relat. Res. 22 (2020) 397-402.

41. H. Kermanshah, F. Motevasselian, S.A. Kakhaki, M. Özcan, Effect of ceramic material type on the fracture load of inlay-retained and full-coverage fixed dental prostheses, Biomater. Investig. Dent. 7 (2020) 62-70.

42. N.R. Dartora, I.C. Maurício Moris, S.F. Poole, A. Bacchi, M.D. Sousa-Neto, Y.T. Silva-Sousa, E.A. Gomes, Mechanical behavior of endocrowns fabricated with different CAD-CAM ceramic systems, J. Prosthet. Dent. S0022-3913 (2020) 30739-5, https://doi.org/10.1016/j.prosdent.2019.11.008.

43. C. Liu, A. Eser, T. Albrecht, V. Stournari, M. Felder, S. Heintze, C. Broeckmann, Strength characterization and lifetime prediction of dental ceramic materials, Dent. Mater. 37 (2021) 94-105, https://doi.org/10.1016/j.dental.2020.10.015.

44. N. Juntavee, P. Uasuwan, Flexural Strength of Different Monolithic Computer-Assisted Design and Computer-Assisted Manufacturing Ceramic Materials upon Different Thermal Tempering Processes, Eur. J. Dent. (2020), http://dx.doi.org/10.1055/s-0040-1713957.

45. T. Srichumpong, P. Phokhinchatchanan, N. Thongpun, D. Chaysuwan, K. Suputtamongkol, Fracture toughness of experimental mica-based glass-ceramics and four commercial glass-ceramics restorative dental materials, Dent. Mater. J. 38 (2019) 378-87.

46. J.B. Monteiro, H. Riquieri, C. Prochnow, L.F. Guilardi, G.K.R. Pereira, A.L.S. Borges, R.M. de Melo RM, L.F. Valandro, Fatigue failure load of two resin-bonded zirconia-reinforced lithium silicate glass-ceramics: Effect of ceramic thickness, Dent. Mater. 34 (2018) 891-900.

47. R. Ottoni, J.A. Griggs, P.H. Corazza, Á. Della Bona, M. Borba, Precision of different fatigue methods for predicting glass-ceramic failure, J. Mech. Behav. Biomed. Mater. 88 (2018) 497-503.

48. N.C. Lawson, R. Bansal, J.O. Burgess, Wear, strength, modulus and hardness of CAD/CAM restorative materials, Dent. Mater. 32 (2016) e275-e283.

49. F. Schweitzer, S. Spintzyk, J. Geis-Gerstorfer, F. Huettig, Influence of minimal extended firing on dimensional, optical, and mechanical properties of crystalized zirconia-reinforced lithium silicate glass ceramic, J. Mech. Behav. Biomed. Mater. 104 (2020) 103644.

50. A.R. Alao, M.H.D. Bujang, Load effect on the mechanical behaviour of zirconia-reinforced lithium silicate glass ceramics, Ceram. Int. 47 (2021) 1353-63.

51. R. Badawy, O. El-Mowafy, L.E. Tam, Fracture toughness of chairside CAD/CAM materials - Alternative loading approach for compact tension test, Dent. Mater. 32 (2016) 847-52, https://doi.org/10.1016/j.dental.2016.03.003.

52. I.L. Aurélio, L.S. Dorneles, L.G. May, Extended glaze firing on ceramics for hard machining: Crack healing, residual stresses, optical and microstructural aspects, Dent. Mater. 33 (2017) 226-40.

53. D.L. Romanyk, Y. Guo, N. Rae, S. Veldhuis, S. Sirovica, G.J. Fleming, O. Addison, Strength-limiting damage and its mitigation in CAD-CAM zirconia-reinforced lithium-silicate ceramics machined in a fully crystallized state, Dent. Mater. 36 (2020) 1557-65.

54. L. Passos, Y. Torrealba, B. Linke, A. Street, S. Passos, Fracture strength of CAD/CAM posterior ceramic crowns after manual enhancement of occlusal morphology, Int. J. Comput. Dent. 21 (2018) 191-200.

55. S.Y. Kang, J.M. Yu, J.S. Lee, K.S. Park, S.Y. Lee, Evaluation of the Milling Accuracy of Zirconia-Reinforced Lithium Silicate Crowns Fabricated Using the Dental Medical Device System: A Three-Dimensional Analysis, Materials (Basel) 13 (2020) E4680. https://doi.org/10.3390/ma13204680.

56. M.F.R.P. Alves, B.G. Simba, L.Q.B. de Campos, I. Ferreira, C. dos Santos, Influence of heat-treatment protocols on mechanical behavior of lithium silicate dental ceramics, Int. J. Appl. Ceram. Technol. 16 (2019) 1920-31.

57. K. Sieper, S. Wille, M. Kern, Fracture strength of lithium disilicate crowns compared to polymer-infiltrated ceramic-network and zirconia reinforced lithium silicate crowns, J. Mech. Behav. Biomed. Mater. 74 (2017) 342-8.

58. E.T.P. Bergamo, D. Bordin, I.S. Ramalho, A.C.O. Lopes, R.S. Gomes, M. Kaizer, L. Witek, E.A. Bonfante, P.G. Coelho, A.A. Del Bel Cury, Zirconia-reinforced lithium silicate crowns: Effect of thickness on survival and failure mode, Dent. Mater. 35 (2019) 1007-16, https://doi.org/10.1016/j.dental.2019.04.007.

59. S. Shaik, M.A. Alfarsi, Contemporary Ceramic Material for Fabrication of Minimally Invasive Full-Coverage Crowns: An In-Vitro Analysis of Fracture Resistance, J. Biomater. Tiss. Eng. 9 (2019) 388-94.

60. J.P.M. Tribst, A.M.O. Dal Piva, M.M. Penteado, A.L.S. Borges, M.A. Bottino, Influence of ceramic material, thickness of restoration and cement layer on stress distribution of occlusal veneers, Braz. Oral Res. 32 (2018) e118.

61. M.R. Alammari, M.H. Abdelnabi, A.A. Swelem, Effect of total occlusal convergence on fit and fracture resistance of zirconia-reinforced lithium silicate crowns, Clin. Cosmet. Investig. Dent. 11 (2018) 1-8.

62. F.O. Abu-Izze, G.F. Ramos, A.L.S. Borges, L.C. Anami, M.A. Bottino, Fatigue behavior of ultrafine tabletop ceramic restorations, Dent. Mater. 34 (2018) 1401-9.

63. V. Diniz, P.H. Condé Oliveira Prado, J.V. Meireles Rodrigues, J.B. Monteiro, C. Zucuni, L.F. Valandro, R.M. Melo, Ceramic firing protocols and thermocycling: effects on the load-bearing capacity under fatigue of a bonded zirconia lithium silicate glass-ceramic, J. Mech. Behav. Biomed. Mater. 110 (2020) 103963.

64. M. Al-Akhali, M. Kern, A. Elsayed, A. Samran, M.S. Chaar, Influence of thermomechanical fatigue on the fracture strength of CAD-CAM-fabricated occlusal veneers, J. Prosthet. Dent. 121 (2019) 644-50.

65. A.B. Venturini, C. Prochnow, G.K.R. Pereira, R.D. Segala, C.J. Kleverlaan, L.F. Valandro, Fatigue performance of adhesively cemented glass-, hybrid- and resin-ceramic materials for CAD/CAM monolithic restorations, Dent. Mater. 35 (2019) 534-42.

66. D.M. Alves, A.C. Cadore-Rodrigues, C. Prochnow, T.A.L. Burgo, A.O. Spazzin, A. Bacchi, L.F. Valandro, G.K.R. Pereira, Fatigue performance of adhesively luted glass or polycrystalline CAD-CAM monolithic crowns, J. Prosthet. Dent. S0022-3913 (2020) 30250-X, http://dx.doi.org/10.1016/j.prosdent.2020.03.032.

67. M. Amelie Schlenz, M. Skroch, A. Schmidt, P. Rehmann, B. Wöstmann, Monitoring fatigue damage in different CAD/CAM materials: A new approach with optical coherence tomography, J. Prosthodont. Res. (2020), http://dx.doi.org/10.2186/jpr.JPOR_2019_466.

68. A.M.O. Dal Piva, J.P.M. Tribst, A.B. Venturini, L.C. Anami, E.A. Bonfante, M.A. Bottino, C.J. Kleverlaan, Survival probability of zirconia-reinforced lithium silicate ceramic: Effect of surface condition and fatigue test load profile, Dent. Mater. 36 (2020) 808-15.

69. M. Hasanzade, M. Sahebi, S. Zarrati, L. Payaminia, M. Alikhasi, Comparative Evaluation of the Internal and Marginal Adaptations of CAD/CAM Endocrowns and Crowns Fabricated from Three Different Materials, Int. J. Prosthodont. (2020), http://dx.doi.org/10.11607/ijp.6389.

70. Celtra® Duo. Zirconia - Reinforced Lithium Silicate (ZLS). Developed to make a difference. Brochure for the dental laboratory. DeguDent GmbH, Hanau, Germany: Dentsply Sirona Inc.; 2017. https://www.celtra-dentsplysirona.com/doc/Download/Celtra_Duo/CD_Lab_BRO_EN_VFIN_22284_Screen.pdf, 2021 (accessed 20 February 2021)

71. M. Zimmermann, A. Valcanaia, G. Neiva, A. Mehl, D. Fasbinder, Three-Dimensional Digital Evaluation of the Fit of Endocrowns Fabricated from Different CAD/CAM Materials, J. Prosthodont. 28 (2019) e504-e509.

72. M. Falahchai, Y. Babaee Hemmati, H. Neshandar Asli, M. Neshandar Asli, Marginal adaptation of zirconia-reinforced lithium silicate overlays with different preparation designs, J. Esthet. Restor. Dent. 32 (2020) 823-30.

73. M. Falahchai, Y. Babaee Hemmati, H. Neshandar Asli, E. Rezaei, Effect of Tooth Preparation Design on Fracture Resistance of Zirconia-Reinforced Lithium Silicate Overlays, J. Prosthodont. 29 (2020) 617-22.

74. W. Höland, M. Schweiger, M. Frank, V. Rheinberger, A comparison of the microstructure and properties of the IPS Empress 2 and the IPS Empress glass-ceramics, J. Biomed. Mater. Res. 53 (2000) 297-303.

75. F. Zarone, M. Ferrari, F.G. Mangano, R. Leone, R. Sorrentino, "Digitally Oriented Materials": Focus on Lithium Disilicate Ceramics, Int. J. Dent. 2016 (2016) 9840594, https://doi.org/10.1155/2016/9840594.

76. W. Lien, H.W. Roberts, J.A. Platt, K.S. Vandewalle, T.J. Hill, T.M. Chu, Microstructural evolution and physical behavior of a lithium disilicate glass-ceramic, Dent. Mater. 31 (2015) 928-40.

77. F. Al Mansour, N. Karpukhina, S. Grasso, R.M. Wilson, M.J. Reece, M.J. Cattell, The effect of spark plasma sintering on lithium disilicate glass-ceramics, Dent. Mater. 31(2015) e226-e235.

78. E. Apel, C. van't Hoen, V. Rheinberger, W. Höland, Influence of ZrO2 on the crystallization and properties of lithium disilicate glass-ceramics derived from a multi-component system, J. Eur. Ceram. Soc. 27 (2007) 1571-7.

4.3 OPTICAL BEHAVIORS, SURFACE TREATMENT, ADHESION, AND CLINICAL INDICATIONS OF ZIRCONIA-REINFORCED LITHIUM SILICATE (ZLS): A NARRATIVE REVIEW

Sorrentino Roberto, Ruggiero Gennaro, Di Mauro Maria Irene, Breschi Lorenzo, Leuci Stefania, Zarone Fernando.

J Dent. 2021;112:103722

Introduction

The demand for minimum invasive, highly esthetic, and durable dental restorations has led to the development of various Computer-aided design / Computer-aided manufacturing (CAD/CAM) materials. Among these, two different zirconia-reinforced lithium silicate ceramics (ZLS) were introduced in the market, available in a pre-crystallized or crystallized form: Vita Suprinity PC (Vita Zahnfabrik, Bad Säckingen, Germany) and Celtra Duo (Dentsply Sirona, Hanau-Wolfgang, Germany) [1-3]. Suprinity and Celtra Duo are reported to be biocompatible materials and present similar microstructural configuration: tetragonal zirconia grains added to a homogeneous glassy matrix that consists of round and submicrometric elongated grains of lithium metasilicates and lithium orthophosphates [2-6]. Also, lithium disilicate grains are generated after a crystallization process. This structural configuration was made to offer higher optical properties and increased mechanical strength, compared to other glass-ceramics. Nevertheless, data about this topic are controversial [4,7-12].

Although the dimensions of the lithium metasilicate crystallites are different in the two materials, from about 0.5 μm for Suprinity to 1.0 μm for Celtra Duo [6], to date, no significant differences were reported about the mechanical and optical properties of these two materials.

The modulus of elasticity, flexural strength, fracture toughness, hardness, and characteristic strength increase after the ZLS firing procedure, while the Weibull modulus and volume decrease [1,13].

The fracture resistance withstands physiological occlusal forces [7,9,13] and the durability of ZLS-based restorations seems to be promising at 1.0 mm thickness [14].
The optical and mechanical properties of ZLS allow it to be used for single-unit restorations, either for partial or full coverage, tooth- or implant-supported, in both anterior and posterior regions [4,15-16], as well as for table-tops [7,17].
Nowadays, many questions remain unanswered for ZLS-based restorations, such as the proper acid etching protocol, in terms of both concentration and etching times, the choice of the ideal kinetics of cement polymerization (i.e., dual- or light-curing), and the effect of silane treatment on adhesion [18]. Furthermore, in the current state of the literature for ZLS, the wear behavior is not completely clear and there is no scientific evidence that supports one polishing system rather than another.
With the aim of assessing the esthetic properties, clinical indications, and handling procedures of ZLS, the present review was focused on the following points: optical characteristics, surface treatments and cementation, polishing procedures, wear behavior, and clinical indications.

Methods

2.1 Search strategy

An extensive search of the literature for papers related to ZLS was performed on the databases of PubMed (Medline), Scopus, Embase, Google Scholar, Dynamed, and Open Grey. Additionally, the "snowballing" approach was used to identify further papers by reading the reference lists of records that have already be found.
The literature search was performed using combinations of the following keywords: "zirconia-reinforced lithium silicate" OR “ZLS". The queries used for each database were as follows:

- PubMed (Medline), Google Scholar, and Open Grey = “(zirconia-reinforced lithium silicate) or (zls)” was added into each query box.
- Dynamed = ZLS; zirconia-reinforced; zirconia-reinforced lithium silicate; zirconia lithium.
- Scopus = (TITLE-ABS-KEY (zirconia-reinforced AND lithium AND silicate) OR TITLE-ABS-KEY (zls)).
- Embase = 'zirconia-reinforced lithium silicate' OR ('zirconia reinforced' AND ('lithium'/exp OR lithium) AND ('silicate'/exp OR silicate)) OR zls.

To exclude duplicates, the references of the identified records were uploaded as Research Information Systems files into Mendeley (Mendeley Ltd., London, UK).

2.2 Inclusion and exclusion criteria

Studies were considered appropriate if they satisfy the following inclusion criteria:
1) Studies addressing at least one of the following topics about ZLS for CAD/CAM systems:

- optical properties;
- wear behavior;
- polishing and/or glazing procedures;
- surface treatments and/or cementation procedures;
- clinical indications and/or outcomes.

2) studies performed *in vitro*, *in silico,* or *in vivo*.
3) case reports;
4) systematic reviews.
The following exclusion criteria were used: 1) animal studies; 2) non-dental studies; 3) studies only focusing on ZLS used in the traditional heat-pressed ceramics process.
No restrictions were made to the year of publication or the language of the papers.

2.3 Data extraction

For the present narrative review, the following variables were considered:

1) optical properties;
2) surface treatments;
3) cementation procedures;
4) polishing and glazing procedures;
5) wear behavior;
6) clinical indications.

According to the inclusion criteria, 3 calibrated researchers (F.Z., G.R., and R.S.) independently selected the articles reading the titles, abstracts, and keywords. The full text of each record was read to evaluate if it was eligible for inclusion. In case of disagreement among the investigators, a majority criterion was used (i.e., 2 out of 3).

2.4 Calibration process

To conduct pilot calibration exercises on the collected titles and abstracts, the three reviewers used a common and random set of 20 references, considering the inclusion and exclusion criteria. After this exercise, the reviewers debated about which references were included or not. Before screening the whole set of titles and abstracts recorded, this procedure would have repeated until they had reached an agreement on at least 90% of the articles. After reading titles and abstracts, the calibration system was also used on a random selection of 10 papers for full-text screening of the included papers, with the same agreement level.

Results

The search strategy reported 936 records, including duplicates: 184 from PubMed/Medline, 239 from Scopus, 175 from Embase, 294 from Google Scholar, 41 from Dynamed, 0 from Open Grey, and 3 with the "snowballing" approach. The duplicates were eliminated, thus all of the selected databases produced 280 records. After the analysis of titles, abstracts, and keywords, the investigators excluded 143 records since they did not meet the eligibility criteria. Among the remaining 137 records, 39 more were excluded after a full-text examination since these records did not present considerable information about ZLS for dental research and clinical practice. The remaining 98 articles were included in this narrative review.

According to the above-mentioned inclusion criteria, in this narrative review *in vitro* studies and case reports were found but no systematic reviews.

The workflow of the paper screening process is reported in Figure 1, according to the "PRISMA 2009 Flow Diagram" [19].

After just one calibration exercise, the reviewers achieved an agreement level of more than 90% on titles and abstracts screening and 100% on full-text articles screening.

No disagreement was pointed out among the search investigators.

Figure 1 - Title: Search flowchart as described in the PRISMA guidelines.

Caption: (*n* = number of records).

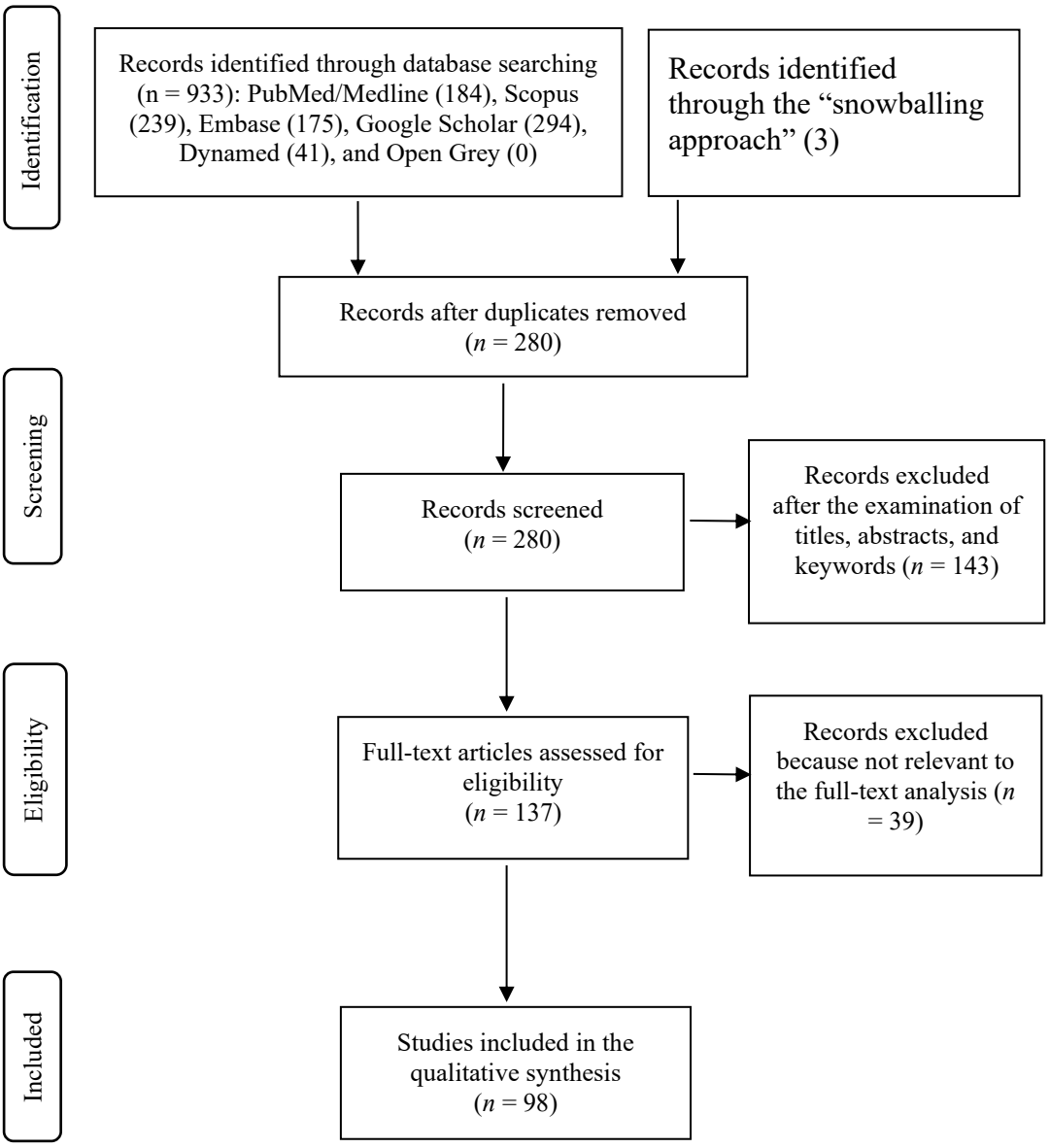

3.1 Optical properties

One of the main strong points of ZLS is, no doubt, the esthetic performance, being the material highly appreciated for its optical properties, such as the translucency. Some *in vitro* studies reported that ZLS exhibits higher translucency than resin nanoceramics (RNC), polymer-infiltrated ceramic networks (PICN), feldspathic ceramics (FC), and lithium disilicate ceramics (LS_2) [15,20-21].

In comparison with LS_2, the higher degree of ZLS translucency has been explained by the presence of smaller silicate crystals, determining a higher glassy content in the matrix [22].

It was also demonstrated that ZLS exhibits better translucency than monolithic highly translucent zirconia ceramics [23-24]. Moreover, as expected, the material showed lower substrate masking ability than zirconia [25] and LS_2 [25-26].

Conversely, other studies reported that ZLS exhibits lower translucency than LS_2 [23,27-28], both before and after thermocycling [24,29], as well as higher opalescence values [27-28], probably due to the larger crystal dimensions and the higher firing temperature of LS_2 [30]. Also, another investigation reported lower translucency and higher opacity values for ZLS than FC, LS_2, PICN, leucite reinforced ceramics (LC), hybrid ceramics (HC), RNC, and nanohybrid composite resins [29].

Various factors negatively influence the translucency in ZLS restorations, such as increased surface roughness [28], ultraviolet (UV) aging [29], and thermal aging [12]. This last factor determines a translucency reduction higher for ZLS than for FC and LS_2 [12]. Conversely, other studies reported that thermal aging improves the translucency of ZLS [24,31].

Color stability is another important element in the long-term esthetic success of ceramic restorations in the anterior sites. According to some i*n vitro* studies, ZLS color stability is higher than composite-containing materials [32], but is lower than LS_2 [21,26,33-34], PICN [21,26], and FC [35]. Color stability is enhanced by the firing technique [35] but is negatively affected by the use of staining beverages [34,36] and thermal aging [24].

Moreover, there is some evidence that, at low thickness, ZLS monolithic restorations are more prone to color changes [23,33]. In particular, at 0.5 mm thickness, the color change was clinically unacceptable for ZLS, but this drawback was not evidenced for zirconia and LS_2 [23]. At the same time, increasing thickness reduces the problem of discoloration after coffee thermocycling [33].

In some cases, it can be desirable masking with restorations dark substrates that cannot undergo or are not responsive to bleaching treatments. As regards such property, ZLS monolithic configuration can be used onto substrates of shade A3.5, in association with opaque resin-based luting agents to improve the masking ability [25]. Additionally, opaque cements exhibited

significantly higher color changes than translucent cements over substrate shade A1 for both LS_2 and ZLS (thickness of 0.8 ± 0.01 mm), resulting in whiter optical results [37]. Furthermore, to achieve the ideal masking effectiveness, the minimum thickness of ZLS should be 1.5 mm over a gold background and 2 mm over a C2 background, while it was not possible to obtain an ideal camouflage over silver-colored backgrounds [38].

Manual polishing does not seem to determine a higher color change than glazing [39]. Both the procedures do not induce significant color changes in the material [30,34,39-40], whereas extended glaze firing, providing greater crack healing than conventional glazing procedure, induces clinically unacceptable color changes in ZLS, differently from FC, LC, and LS_2 [40].

Thickness and surface roughness are the major factors affecting ZLS absolute translucency [22,28-29,41]. After thermocycling in staining beverages (i.e., coffee), the relative translucency of ZLS decreased as the thickness increased, by increasing thickness from veneer to crown [33].

The exponential increase of carbonated soft drinks consumption over the years has been demonstrated to have a significantly detrimental impact on oral and general health, not to mention economy, for the high sugar content, sparkling, and acidity [42]. From this point of view, studying the effect of such beverages on dental materials is a hot topic in the current scientific literature, particularly the possible modifications of restoration surfaces exposed to the oral environment (i.e., acid erosion, pigmentations, mechanical degradation).

In vitro investigations evaluating the effect of dark-colored beverages on ZLS restorations reported controversial results: some studies evidenced that thermocycling in cola [36] and coffee [30] decrease the translucency of both glazed and polished ZLS; conversely, other authors did not find that thermocycling in coffee affects the translucent behavior of ZLS [23].

It has been demonstrated that prolonged exposure to carbonated acidic drinks (immersion for 7 days in Coca-Cola) can also negatively influence the mechanical behavior of restorative materials. In an *in vitro* study, compared to RNC, HC, and nano-hybrid composites, ZLS showed lower micro-hardness changes after prolonged experimental exposure to Cola drinks [43].

3.2 Surface treatment and cementation

Due to the hybrid nature of ZLS, proper surface pretreatments should be performed to enhance chemical bonding and micromechanical interlocking mechanisms before cementation [44-46]. ZLS-based materials contain silica and, similarly to the other glass-ceramics, can be modified with hydrofluoric acid (HF), obtaining advantageous micromechanical retention due to the dissolution of the glassy matrix [18].

HF etching, in combination with silane primer application, represents the gold standard for bonding to lithium silicate-based glass ceramics, including ZLS [46]. HF etching produces a honeycomb-like microrough, porous surface, while particle abrasion with glass beads caused abrasion of the glassy matrix [46].

Besides surface conditioning, the bond strength between resin cements and ZLS is also significantly influenced by aging; in fact, it has been demonstrated that thermocycling decreases bond strength [47-49].

The fatigue loading of ZLS could be efficiently increased by HF etching and silane coupling, the latter ensuring an effective chemical interaction between resin-based agents and ZLS [50]. Silica coating was reported not to be effective in maintaining the bond strength over the long term [47] and sandblasting and CoJet were proved to be less effective than HF etching for Suprinity [18]. Furthermore, another *in vitro* investigation reported that acid etching with 10% HF for 20 s shows higher shear bond strength mean value (10.81 MPa) than sandblasting with 50 μm aluminum oxide for 60 s (7.76 MPa) [51].

Tribochemical silicatisation-based treatment protocols were not recommended for adhesive cementation of ZLS, because it was associated with low bond strength after long-term aging, differently from 5% HF for 30 s, which presented acceptable success as to long-term bond strength [48]. HF etching surface treatment of ZLS was more efficient than alumina blasting and erbium, chromium:yttrium-scandium-gallium-garnet (Er,Cr:YSGG) laser irradiation; the latter could not be considered as an effective surface treatment for repairing fractured restorations [52]. Some studies have investigated the possibility of repairing ZLS. From this viewpoint, in terms of microtensile bond strength after surface treatment, the use of nanohybrid composite resin is not promising either with airborne particle abrasion, tribochemical silica coating, or 5% HF for 90 s [53]. Furthermore, repair ZLS bond strength could be improved after sandblasting ZLS surfaces with CoJet sand and silanization [54].

Nowadays, HF etching appears to be the best method for conditioning ZLS surfaces, considering both acid concentration and etching time [45]. Etching with 5% HF for 20 s was characterized by small pores, whereas longer etching time exhibited wider and irregular grooves; as the etching time is prolonged (from 20 to 160 s), the glassy matrix dissolves faster than crystals and both surface roughness and wettability improve significantly [55]. Conversely, other investigations asserted that the roughness of ZLS is not influenced by different etching times, although the contact-angle analysis reveals lower values for 10% HF etching for 60 s, so suggesting protocols with longer etching times (from 40 to 60 s) [56]. Even if most literature agrees in considering HF etching as the most effective surface treatment to provide a high bond strength of ZLS [46], data are quite controversial about etching protocol, such as different values of etching duration and

acid concentration were suggested. The manufacturer of Celtra Duo recommended 5-9% HF for 30 s [57], whereas independent studies proposed 5% HF for 20 [58] or 30 s [59-60] and 10% HF for 90 s [50]. Another paper evidenced that to preserve ZLS microstructure, the best finding results from etching the surface with 4.9% HF for 20 s, while 4.9% HF for 40 s and 9.5% for 20 and 40 s cause progressive surface degradation [61]. Similar findings were obtained from another investigation, in which the most efficient etching method is achieved by using 4.9% HF for 20 s, particularly, etching time (i.e., 20, 40, 60, 120 s) do not significantly affect adhesion such as HF concentration, which proves to be better at 4.9% than 9.5% [62].

It is worth noticing that conditioning glass-containing materials with aggressive etching protocols may damage their internal microstructure, negatively influencing the mechanical performances, in particular, for very thin restorations, just like veneers and table-tops [63].

An *in vitro* bond-strength study indicated the application of self-etching ceramic primers containing polyfluoride for etching and trimethoxypropyl methacrylate for silanization, as a new viable alternative to conditioning the internal surface of ZLS restorations [64].

The high translucency of ZLS allows for proper polymerization of light-cured resin cements. Nonetheless, dual polymerization of resin cements results in higher Vickers hardness and depth of cure values than using light polymerization [20]. The biaxial flexural strength values improve increasing etching times from 20 to 60 s at 10% HF, followed by the application of resin cements [56]. Moreover, additional firings allow bond strength maintenance after aging, when ZLS was conditioned with 5% HF for 30 s [49] and the fracture toughness of ZLS crowns could be enhanced by using self-adhesive resin cements rather than glass-ionomer luting agents [65]. Furthermore, higher bond strength in ZLS cementation to dentin was reported by using resin cement with an etch-and-rinse and a universal adhesive agent than a self-adhesive resin cement [66].

To improve the biomechanical behavior of ZLS restorations, it is advisable to use low elastic modulus resin cements due to a reduced stress concentration in the cement layer that could be transmitted to ceramics [67].

Nonetheless, conventional adhesive resin cements are highly recommended especially for occlusal veneers; furthermore, self-etching techniques are not recommended for luting thin and minimally invasive occlusal veneers to enamel, as in this case the long-term survivability was reported to be questionable [68].

3.3 Polishing and wear behavior

Finishing of ZLS restorations can be obtained by both the glaze-firing cycle and the surface mechanical polishing [69].

In a study on the efficacy of different techniques for controlling roughness of ZLS and LS_2, it has been shown that manual finishing plus polishing for 60 s and the use of a glazing paste obtain the best results; moreover, ZLS exhibits higher polishability than LS_2 (namely IPS e.max CAD) [70].

To date, about refining and intraoral adjustments, LS_2 remains one of the most difficult materials to polish [45,71].

As regards the influence of professional dental prophylaxis protocols, it has been shown that the glossy surface of ZLS is only slightly affected by the conventional oral hygiene treatments, differently from resin composite blocks, that undergo a significant increase in surface roughness [72].

Machinability of CAD/CAM materials is an important mechanical property because it strongly affects the final quality of the restoration. Some studies reported that, in its crystallized form, ZLS is characterized by a higher machinability index than in the pre-crystallized one [73]. Consequently, after crystallization, it is more difficult to be machined and polished for the harder microstructure and improved strength [73].

Contrary to these findings, in another investigation, the brittleness index analysis estimates greater machinability after the crystallization process than in the pre-crystallized form [74].

Although mechanical polishing has been addressed as a very effective method to reduce ZLS surface roughness [28,30,70], for this purpose LS_2 has been shown to take better advantage using glaze firing (i.e., glaze powder and liquid in a vacuum furnace) [28].

As regards the resistance to wear, glaze-fired ZLS exhibits a wear depth and a volume loss statistically similar to those of type III gold alloy; such resistance is reduced when the material is milled and unglazed. Wear depth and volumetric loss of glaze-fired ZLS do not differ statistically from human enamel [75-76]. These *in vitro* results seem to emphasize the importance of the glaze-firing process to improve the wear resistance of ZLS.

Moreover, ZLS was reported to be more resistant to wear than LS_2 [77] and PICN [78].

According to an *in vitro* study, ZLS can induce a significant amount of enamel tooth wear after 1 year of intraoral function [79]. Additionally, a higher amount of wear onto ZLS is caused by zirconia ceramics rather than tested steatite and acrylic resin [80].

Machinability is one of the weak points of high strength silicate-based glass-ceramics, exhibiting both ZLS and LS_2 high machinability indexes and brittle fracture mechanisms induced by high grinding forces and energy with diamond tools. In particular, in an *in vitro* investigation, ZLS machinability was reported to be poorer than LS_2, ranked as the most difficult to machine among glass-ceramics, due to the materials' tendency to edge chipping damage [81].

Finally, as regards ZLS wear resistance, an in vitro study reported better results with the use of microwave energy during firing procedures rather than conventional firing processes [82].

3.4 Clinical indications and outcomes

To date, the available studies regarding the clinical performance of ZLS are quite scarce and mainly limited to case reports. ZLS was employed for monolithic full-contour crowns [58], monolithic partial crowns [58-59], laminate veneers [83], and screw-retained implant-supported monolithic crowns in the anterior sites [84].

Some authors recommended the use of ZLS for tooth-supported monolithic anterior [11] and posterior crowns [14,16,85-87], thanks to the advantageous mechanical and optical characteristics of such materials, showing fracture strength values above the clinically expected loading forces [14]. Indeed, according to ISO-6872:2015, the mechanical properties of ZLS enable the use of such hybrid materials for anterior and posterior single-unit adhesive crowns, but not in the case of fixed partial dentures [88-89].

Furthermore, ZLS has been advised for molar no-prep occlusal veneers [7,17] and implant-supported single crowns [90-91], although the insertion of a screw channel might reduce the stability of ZLS restorations [92].

As regards endodontically treated molars, mean fracture loads of 886.9 ± 195.7 N were reported for ZLS endocrowns [93]. Other investigators showed that the fracture resistance of monolithic ZLS endocrowns (1859 N) was worse than that of zirconia ceramics (6333 N) [94]. However, the high number of irreparable failures occurring in ZLS endocrowns has to be taken into account for their use onto posterior teeth [95].

To date, a small number of clinical studies were performed to evaluate the clinical success and survival rates of ZLS.

ZLS-based restorations onto the posterior tooth, for inlays or partial crowns, showed a high clinical success rate (96.7%) after 1 year of clinical service and a failure rate of 3.3% as a result of bulk fractures [96]. In a short-term clinical study, a survival rate of 100% was reported with ZLS partial coverage restorations onto 23 premolars and molars after 1 year of observation [97]. Similarly, a promising 3-year success rate of 98% was noticed onto 88 premolars and molars partial crowns [98]. In 2-year follow-up examinations of 61 partial crowns made on vital premolars and molars, it was observed that, out of 31 restorations made with a thickness of 0.5-0.74 mm, two failures were detected due to ceramic fracture (survival rate = 94.0%), while for the other 30 restorations with a thickness of 0.75-1.0 mm no losses were recorded (survival rate = 100%) [99].

Moreover, ZLS anterior crowns were reported to be a safe and valid restorative solution after 2 years of service [100].
Finally, a clinical study evaluated the esthetic outcomes of ZLS full coverage restorations, showing very positive results, according to the modified United States Public Health Service (USPHS) criteria, as to shade matching (100% alpha ranking) and patients' satisfaction (100%, according to Visual Analogue Scales - VAS) [101].

3.5 Limitations of the search methodology

The present paper is a narrative review. This approach offers a summary of the current literature rather than a synthesized finding or response to a particular question.
With the narrative review, the presence of statements about the formal synthesis and the quality of evidence is excluded. Moreover, the narrative reviews are susceptible to bias from a variety of sources since a critical assessment of the risk of bias is not needed in this type of paper.
Therefore, the present article does not provide any statistically proven findings such as a systematic review or meta-analysis. Differently, it qualitatively summarized evidence, displaying a synthesis of optical properties, surface treatment, adhesion, and clinical indications about ZLS in CAD/CAM systems.

Conclusions

According to the present narrative review, the following conclusions can be drawn:

- there is no indisputable evidence demonstrating the improved optical properties compared to LS_2, notwithstanding the peculiar microstructural configuration, that is characterized by a glassy matrix and the presence of zirconia grains;
- ZLS presents clinically acceptable color changes when it is treated with conventional glazing or polishing, whilst extended and/or repeated glaze firing cycles can affect negatively the final color of restorations; no significant differences in color stability were pointed out between manual polishing and glazing;
- ZLS exhibits lower color stability than LS_2 and FC but higher than composite-based materials;
- ZLS shows poorer machinability than LS_2. After crystallization, mechanical polishing is the most effective method to reduce its surface roughness;

- ZLS can be conditioned with conventional acid etching techniques. However, to date what is the best etching protocol is still under debate; in any case, silane coupling and dual-curing polymerization of resin cements are strongly recommended;
- ZLS can be used for anterior and posterior single-unit adhesive crowns, molar table-tops, monolithic partial crowns, laminate veneers, and implant-supported single crowns. It does not seem to be a viable option for endocrowns onto posterior teeth or fixed partial dentures;

Although ZLS can be considered a highly promising hybrid ceramic material for CAD/CAM technologies, further *in vitro* and *in vivo* studies are needed to define accurately the optical properties, the operative procedures for surface treatment and cementation, as well as the clinical indications and the long-term performance of ZLS-based, both tooth- and implant-supported restorations.

References

1. H. Riquieri, J.B. Monteiro, D.C. Viegas, T.M.B. Campos, R.M. de Melo, G. de Siqueira Ferreira Anzaloni Saavedra, Impact of crystallization firing process on the microstructure and flexural strength of zirconia-reinforced lithium silicate glass-ceramics, Dent. Mater. 34 (2018) 1483-91, https://doi.org/10.1016/j.dental.2018.06.010.

2. Vita Suprinity® PC. Technical and scientific documentation. Bad Säckingen, Germany: Vita Zahnfabrik; 2019. https://mam.vita-zahnfabrik.com/portal/ecms_mdb_download.php?id=82440&sprache=en&fallback=en&cls_session_id=&neuste_version=1, 2021 (accessed 20 February 2021)

3. Celtra Duo®. Celtra block for cerec and inlab. DeguDent GmbH, Hanau, Wolfgang, Germany: Dentsply Sirona Inc; 2018. https://www.celtra-dentsplysirona.com/doc/Download/Celtra_Duo/GA_Celtra_Duo_multilingual_50539985h_0315.pdf, 2021 (accessed 20 February 2021).

4. S.E. Elsaka, A.M Elnaghy, Mechanical properties of zirconia reinforced lithium silicate glass-ceramic, Dent. Mater. 32 (2016) 908-14, https://doi.org/10.1016/j.dental.2016.03.013.

5. R. Belli, M. Wendler, A. Petschelt, T. Lube, U. Lohbauer, Fracture toughness testing of biomedical ceramic-based materials using beams, plates and discs, J. Eur. Ceram. Soc. 38 (2018) 5533-44.

6. R. Belli, M. Wendler, D. de Ligny, M.R. Cicconi, A. Petschelt, H. Peterlik, U. Lohbauer, Chairside CAD/CAM materials. Part 1: Measurement of elastic constants and microstructural characterization, Dent. Mater. 33 (2017) 84-98, https://doi.org/10.1016/j.dental.2016.10.009.

7. M. Al-Akhali, M.S. Chaar, A. Elsayed, A. Samran, M. Kern, Fracture resistance of ceramic and polymer-based occlusal veneer restorations, J. Mech. Behav. Biomed. Mater. 74 (2017) 245-50, https://doi.org/10.1016/j.jmbbm.2017.06.013.

8. T.A. Hamza, R.M. Sherif, Fracture Resistance of Monolithic Glass-Ceramics Versus Bilayered Zirconia-Based Restorations, J. Prosthodont. 28 (2019) e259-e264, https://doi.org/10.1111/jopr.12684.

9. R.S. Gomes, C.M.C. Souza, E.T.P. Bergamo, D. Bordin, A.A. Del Bel Cury, Misfit and fracture load of implant-supported monolithic crowns in zirconia-reinforced lithium silicate, J. Appl. Oral Sci. 25 (2017) 282-9, https://doi.org/10.1590/1678-7757-2016-0233.

10. A. Kashkari, B. Yilmaz, W.A. Brantley, S.R. Schricker, W.M. Johnston, Fracture analysis of monolithic CAD-CAM crowns, J. Esthet. Restor. Dent. 31 (2019) 346-52, https://doi.org/10.1111/jerd.12462.

11. F.S. Schwindling, S. Rues, M. Schmitter, Fracture resistance of glazed, full-contour ZLS incisor crowns, J. Prosthodont. Res. 61 (2017) 344-9, https://doi.org/10.1016/j.jpor.2016.12.008.

12. R.D. Vasiliu, S.D. Porojan, M.I. Bîrdeanu, L. Porojan, Effect of Thermocycling, Surface Treatments and Microstructure on the Optical Properties and Roughness of CAD-CAM and Heat-Pressed Glass Ceramics, Materials (Basel) 13 (2020) 381, https://doi.org/10.3390/ma13020381.

13. F. Zarone, G. Ruggiero, R. Leone, L. Breschi, S. Leuci, R. Sorrentino, Zirconia-Reinforced Lithium Silicate (ZLS) mechanical and biological properties: a literature review, J. Dent. (2021) 103661, https://doi.org/10.1016/j.jdent.2021.103661.

14. K. Sieper, S. Wille, M. Kern, Fracture strength of lithium disilicate crowns compared to polymer-infiltrated ceramic-network and zirconia reinforced lithium silicate crowns, J. Mech. Behav. Biomed. Mater. 74 (2017) 342-8, https://doi.org/10.1016/j.jmbbm.2017.06.025.

15. N. Sen, Y.O. Us, Mechanical and optical properties of monolithic CAD-CAM restorative materials, J. Prosthet. Dent. 119 (2018) 593-9, https://doi.org/10.1016/j.prosdent.2017.06.012.

16. V. Preis, M. Behr, S. Hahnel, M. Rosentritt, Influence of cementation on in vitro performance, marginal adaptation and fracture resistance of CAD/CAM-fabricated ZLS molar crowns, Dent. Mater. 31 (2015) 1363-9, https://doi.org/10.1016/j.dental.2015.08.154.

17. N.F. von Maltzahn, O.I. El Meniawy, N. Breitenbuecher, P. Kohorst, M. Stiesch, M. Eisenburger, Fracture Strength of Ceramic Posterior Occlusal Veneers for Functional Rehabilitation of an Abrasive Dentition, Int. J. Prosthodont. 31 (2018) 451-2, https://doi.org/10.11607/ijp.5817.

18. B. Altan, S. Cinar, B. Tuncelli, Evaluation of shear bond strength of zirconia-based monolithic CAD-CAM materials to resin cement after different surface treatments, Niger. J. Clin. Pract. 22 (2019) 1475-82, https://doi.org/10.4103/njcp.njcp_157_19.

19. A. Liberati, D.G. Altman, J. Tetzlaff, C. Mulrow, P.C. Gøtzsche, J.P. Ioannidis, M. Clarke, P.J. Devereaux, J. Kleijnen, D. Moher, The PRISMA statement for reporting systematic

reviews and meta-analyses of studies that evaluate health care interventions: explanation and elaboration, PLoS Med. 6 (2009) e1000100, https://doi.org/10.1371/journal.pmed.1000100.

20. Y.O. Caprak, P. Turkoglu, G. Akgungor, Does the Translucency of Novel Monolithic CAD/CAM Materials Affect Resin Cement Polymerization with Different Curing Modes?, J. Prosthodont. 28 (2019) e572-e579, https://doi.org/10.1111/jopr.12956.

21. A.S. Alayad, A. Alqhatani, M.S. Alkatheeri, M. Alshehri, M.A. AlQahtani, A.E.B. Osseil, R.A. Almusallam, Effects of CAD/CAM ceramics and thicknesses on translucency and color masking of substrates, Saudi Dent. J. (2020), https://doi.org/10.1016/j.sdentj.2020.03.011.

22. D. Awad, D. Stawarczyk, A. Liebermann, N. Ilie, Translucency of esthetic dental restorative CAD/CAM materials and composite resins with respect to thickness and surface roughness, J. Prosthet. Dent. 113 (2015) 534-40, https://doi.org/10.1016/j.prosdent.2014.12.003.

23. M.G. Subaşı, G. Alp, W.M. Johnston, B. Yilmaz, Effect of thickness on optical properties of monolithic CAD-CAM ceramics, J. Dent. 71 (2018) 38-42, https://doi.org/10.1016/j.jdent.2018.01.010.

24. G. Aljanobi, Z.H. Al-Sowygh, The Effect of Thermocycling on the Translucency and Color Stability of Modified Glass Ceramic and Multilayer Zirconia Materials, Cureus 12 (2020) e6968, https://doi.org/10.7759/cureus.6968.

25. A. Bacchi, S. Boccardi, R. Alessandretti, G.K.R. Pereira, Substrate masking ability of bilayer and monolithic ceramics used for complete crowns and the effect of association with an opaque resin-based luting agent, J. Prosthodont. Res. 63 (2019) 321-6, https://doi.org/10.1016/j.jpor.2019.01.005.

26. A.F. Alfouzan, H.N. Al-Otaibi, N. Labban, S.M. Al Taweeld, S. Al-Tuwaijri, A.S. AlGazlan, E. Tashkandi, Influence of thickness and background on the color changes of CAD/CAM dental ceramic restorative materials, Mater. Res. Express (2020), https://doi.org/10.1088/2053-1591/ab9348.

27. B. Gunal, M.M. Ulusoy, Optical properties of contemporary monolithic CAD-CAM restorative materials at different thicknesses, J. Esthet. Restor. Dent. 30 (2018) 434-41.

28. M. Kurt, M. Bankoğlu Güngör, S. Karakoca Nemli, B. Turhan Bal, Effects of glazing methods on the optical and surface properties of silicate ceramics, J. Prosthodont. Res. 64 (2020) 202-9, https://doi.org/10.1016/j.jpor.2019.07.005.

29. Y.S. Choi, K.H. Kang, W. Att, Evaluation of the response of esthetic restorative materials to ultraviolet aging, J. Prosthet. Dent. S0022-3913 (2020) 30471-6, https://doi.org/10.1016/j.prosdent.2020.09.007.

30. G. Alp, M.G. Subasi, W.M. Johnston, B. Yilmaz, Effect of surface treatments and coffee thermocycling on the color and translucency of CAD-CAM monolithic glass-ceramic, J. Prosthet. Dent. 120 (2018) 263-8, https://doi.org/10.1016/j.prosdent.2017.10.024.

31. L. Porojan, R.D. Vasiliu, M.I. Bîrdeanu, S.D. Porojan, Surface Characterization and Optical Properties of Reinforced Dental Glass-Ceramics Related to Artificial Aging, Molecules 25 (2020) 3407, https://doi.org/10.3390/molecules25153407.

32. N. Aydın, S. Karaoğlanoğlu, E.A. Oktay, M.A. Kılıçarslan, Investigating the color changes on resin-based CAD/CAM Blocks, J. Esthet. Restor. Dent. 32 (2020) 251-6, https://doi.org/10.1111/jerd.12561.

33. R. Arif, B. Yilmaz, W.M. Johnston, In vitro color stainability and relative translucency of CAD-CAM restorative materials used for laminate veneers and complete crowns, J. Prosthet. Dent. 122 (2019) 160-6, https://doi.org/10.1016/j.prosdent.2018.09.011.

34. B. Kanat-Ertürk, Color Stability of CAD/CAM Ceramics Prepared with Different Surface Finishing Procedures, J. Prosthodont. 29 (2020) 166-72, https://doi.org/10.1111/jopr.13019.

35. A.M.O. Dal Piva, J.P.M. Tribst, A. Werner, L.C. Anami, M.A. Bottino, C.J. Kleverlaan, Three-body wear effect on different CAD/CAM ceramics staining durability, J. Mech. Behav. Biomed. Mater. 103 (2020) 103579, https://doi.org/10.1016/j.jmbbm.2019.103579.

36. F. Firouz, A. Izadi, F. Fotovat, S. Ghorbani Gholiabad, The effect of different solutions on optical behavior of polished and glazed zirconia-reinforced lithium silicate ceramics, J. Kerman Univ. Medical Sci. 25 (2018) 428-40.

37. B. Yildirim, D. Recen, A. Tekeli Simsek, Effect of cement color and tooth-shaded background on the final color of lithium disilicate and zirconia-reinforced lithium silicate ceramics: An in vitro study, J. Esthet. Restor. Dent. (2020), https://doi.org/10.1111/jerd.12611.

38. L. Passos, B. Linke, A. Street, Y. Torrealba, Effect of thickness, translucency, and firing protocol on the masking ability of a CAD/CAM zirconia-reinforced lithium silicate for different backgrounds, Int. J. Comput. Dent. 22 (2019) 29-38.

39. F. Ozen, N. Demirkol, O. Parlar Oz, Effect of surface finishing treatments on the color stability of CAD/CAM materials, J. Adv. Prosthodont. 12 (2020) 150-156, https://doi.org/10.4047/jap.2020.12.3.150.

40. I.L. Aurélio, L.S. Dorneles, L.G. May, Extended glaze firing on ceramics for hard machining: Crack healing, residual stresses, optical and microstructural aspects, Dent. Mater. 33 (2017) 226-40, https://doi.org/10.1016/j.dental.2016.12.002.

41. F. Nejatidanesh, K. Azadbakht, O. Savabi, M. Sharifi, M. Shirani, Effect of repeated firing on the translucency of CAD-CAM monolithic glass-ceramics, J. Prosthet. Dent. 123 (2020) 530.e1-530.e6, https://doi.org/10.1016/j.prosdent.2019.10.028.

42. J.F. Tahmassebi, A. BaniHani, Impact of soft drinks to health and economy: a critical review, Eur. Arch. Paediatr. Dent. 21 (2020) 109-17, https://doi.org/10.1007/s40368-019-00458-0.

43. M. Colombo, C. Poggio, A. Lasagna, M. Chiesa, A. Scribante, Vickers Micro-Hardness of New Restorative CAD/CAM Dental Materials: Evaluation and Comparison after Exposure to Acidic Drink, Materials (Basel) 12 (2019) 1246, https://doi.org/10.3390/ma12081246.

44. T. Strasser, V. Preis, M. Behr, M. Rosentritt, Roughness, surface energy, and superficial damages of CAD/CAM materials after surface treatment, Clin. Oral Investig. 22 (2018) 2787-97, https://doi.org/10.1007/s00784-018-2365-6.

45. F. Zarone, M.I. Di Mauro, P. Ausiello, G. Ruggiero, R. Sorrentino, Current status on lithium disilicate and zirconia: a narrative review, BMC Oral Health 19 (2019) 134, https://doi.org/10.1186/s12903-019-0838-x.

46. M.N. Aboushelib, D. Sleem, Microtensile bond strength of lithium disilicate ceramics to resin adhesives, J. Adhes. Dent. 16 (2014) 547-52, https://doi.org/10.3290/j.jad.a33249. PMID: 25516886.

47. T.P. Sato, L.C. Anami, R.M. Melo, L.F. Valandro, M.A. Bottino, Effects of Surface Treatments on the Bond Strength Between Resin Cement and a New Zirconia-reinforced Lithium Silicate Ceramic, Oper. Dent. 41 (2016) 284-92, https://doi.org/10.2341/14-357-L.

48. W. Bömicke, P. Rammelsberg, J. Krisam, S. Rues, The Effects of Surface Conditioning and Aging on the Bond Strength Between Composite Cement and Zirconia-reinforced Lithium-Silicate Glass-Ceramics, J. Adhes. Dent. 21 (2019) 567-76, https://doi.org/10.3290/j.jad.a43650.

49. V. Diniz, J.B. Monteiro, J.V.M. Rodrigues, P.H.C.O. Prado, R.M. Melo, Impact of Acid Concentration and Firing on the Long-term Bond Strength of a Zirconia-Lithium Silicate Ceramic Following Adhesive Cementation, J. Adhes. Dent. 21 (2019) 355-63, https://doi.org/10.3290/j.jad.a42998.

50. J.B. Monteiro, M.G. Oliani, L.F. Guilardi, C. Prochnow, G.K.R. Pereira, M.A. Bottino, R.M. de Melo, L.F. Valandro, Fatigue failure load of zirconia-reinforced lithium silicate glass ceramic cemented to a dentin analogue: Effect of etching time and hydrofluoric acid concentration, J. Mech. Behav. Biomed. Mater. 77 (2018) 375-82, https://doi.org/10.1016/j.jmbbm.2017.09.028.

51. K.F. Abdulkader, G.A.E. Elnaggar, L.S. Kheiralla, Shear bond strength of cemented zirconia-reinforced lithium silicate ceramics (Celtra Duo) with two surface treatments (in vitro study), J. Adhes. Sci. Technol. (2020) 1-17, https://doi.org/10.1080/01694243.2020.1785082.

52. A.S. Ataol, G. Ergun, Effects of surface treatments on repair bond strength of a new CAD/CAM ZLS glass ceramic and two different types of CAD/CAM ceramics, J. Oral Sci. 60 (2018) 201-11, https://doi.org/10.2334/josnusd.17-0109.

53. L. AL-Turki, Y. Merdad, T.A. Abuhaimed, D. Sabbahi, M. Almarshadi, R. Aldabbagh, Repair bond strength of dental computer-aided design/computer-aided manufactured ceramics after different surface treatments, J. Esthet. Restor. Dent. 32 (2020) 726-33, https://doi.org/10.1111/jerd.12635.

54. R. Al-Thagafi, W. Al-Zordk, S. Saker, Influence of Surface Conditioning Protocols on Reparability of CAD/CAM Zirconia-reinforced Lithium Silicate Ceramic, J. Adhes. Dent. 18 (2016) 135-41, https://doi.org/10.3290/j.jad.a35909.

55. R. Ramakrishnaiah, A.A. Alkheraif, D.D. Divakar, J.P. Matinlinna, P.K. Vallittu, The Effect of Hydrofluoric Acid Etching Duration on the Surface Micromorphology, Roughness, and Wettability of Dental Ceramics, Int. J. Mol. Sci. 17 (2016) 822, https://doi.org/10.3390/ijms17060822.

56. N.F. Barchetta, M. Amaral, C. Prochnow, F.P. Rodrigues, M.A. Bottino, L.F. Valandro, R.M. de Melo, Strength of a Zirconia-Reinforced Lithium Silicate Ceramic: Acid-Etching Time and Resin Cement Application Effects, Int. J. Periodontics Restorative Dent. 39 (2019) 431-7, https://doi.org/10.11607/prd.4117.

57. Celtra® Duo. Zirconia - Reinforced Lithium Silicate (ZLS). Guidelines for processing Celtra Duo. DeguDent GmbH, Hanau, Germany: Dentsply Sirona Inc; 2018. https://www.dentsplysirona.com/content/dam/dentsply/pim/manufacturer/Prosthetics/Fixed/High_strength_glass_ceramic/Celtra_Duo/GA%20Celtra%20Duo%20Processing%20Guidelines%20EN.pdf, 2021 (accessed 20 February 2021)

58. S. Rinke, M. Rödiger, D. Ziebolz, A.K. Schmidt, Fabrication of Zirconia-Reinforced Lithium Silicate Ceramic Restorations Using a Complete Digital Workflow, Case Rep. Dent. 2015 (2015) 162178, https://doi.org/10.1155/2015/162178.

59. S. Rinke, A.K. Pabel, M. Rödiger, D. Ziebolz, Chairside Fabrication of an All-Ceramic Partial Crown Using a Zirconia-Reinforced Lithium Silicate Ceramic, Case Rep. Dent. 2016 (2016) 1354186, https://doi.org/10.1155/2016/1354186.

60. K.P.P.R. Thiesen, M.D.B. de Souza, V.L. Schmitt, F.P.S. Nahsan, F.S. Naufel, Bond strength to ZLS ceramics at different etching times and cementation protocols after aging, Braz. Dent. Sci. 22 (2019) 488-96.

61. T. Traini, B. Sinjari, R. Pascetta, N. Serafini, G. Perfetti, P. Trisi, S. Caputi, The zirconia-reinforced lithium silicate ceramic: lights and shadows of a new material, Dent. Mater. J. 35 (2016) 748-55, https://doi.org/10.4012/dmj.2016-041.

62. R. Fabian Fonzar, C. Goracci, M. Carrabba, C. Louca, M. Ferrari, A. Vichi, Influence of Acid Concentration and Etching Time on Composite Cement Adhesion to Lithium-silicate Glass Ceramics, J. Adhes. Dent. 22 (2020) 175-82, https://doi.org/10.3290/j.jad.a44282.

63. F. Murillo-Gómez, R.G. Palma-Dibb, M.F. De Goes, Effect of acid etching on tridimensional microstructure of etchable CAD/CAM materials, Dent. Mater. 34 (2018) 944-55, https://doi.org/10.1016/j.dental.2018.03.013.

64. M.M. Awad, Z.A. Al Jeaidi, N. Almutairi, F. Vohra, M. Özcan, A. Alrahlah, Effect of self-etching ceramic primer on bond strength of zirconia-reinforced lithium silicate ceramics, J. Adhes. Sci. Technol. 34 (2020) 91-101.

65. G. D'Addazio, M. Santilli, M.L. Rollo, P. Cardelli, I. Rexhepi, G. Murmura, N. Al-Haj Husain, B. Sinjari, T. Traini, M. Özcan, S. Caputi, Fracture Resistance of Zirconia-Reinforced Lithium Silicate Ceramic Crowns Cemented with Conventional or Adhesive Systems: An In Vitro Study, Materials (Basel) 13 (2020) 2012, https://doi.org/10.3390/ma13092012.

66. N. Itthipongsatorn, S. Srisawasdi, Dentin microshear bond strength of various resin luting agents to zirconia-reinforced lithium silicate ceramics, J. Prosthet. Dent. S0022-3913 (2020) 30135-9, https://doi.org/10.1016/j.prosdent.2020.02.004.

67. M.M. Penteado, J.P. Mendes Tribst, A.M. Dal Piva, K.C. Archangelo, M.A. Bottino, A.L. Souto Borges, Influence of different restorative material and cement on the stress distribution of ceramic veneer in upper central incisor, Indian J. Dent. Res. 31 (2020) 236-40.

68. M. Al-Akhali, M. Kern, A. Elsayed, A. Samran, M.S. Chaar, Influence of thermomechanical fatigue on the fracture strength of CAD-CAM-fabricated occlusal veneers, J. Prosthet. Dent. 121 (2019) 644-50, https://doi.org/10.1016/j.prosdent.2018.07.019.

69. R. Badawy, O. El-Mowafy, L.E. Tam, Fracture toughness of chairside CAD/CAM materials - Alternative loading approach for compact tension test, Dent. Mater. 32 (2016) 847-52, https://doi.org/10.1016/j.dental.2016.03.003.

70. A. Vichi, R. Fabian Fonzar, C. Goracci, M. Carrabba, M. Ferrari, Effect of Finishing and Polishing on Roughness and Gloss of Lithium Disilicate and Lithium Silicate Zirconia Reinforced Glass Ceramic for CAD/CAM Systems, Oper. Dent. 43 (2018) 90-100, https://doi.org/10.2341/16-381-L.

71. X.F. Song, H.T. Ren, L. Yin, Machinability of lithium disilicate glass ceramic in in vitro dental diamond bur adjusting process, J. Mech. Behav. Biomed. Mater. 53 (2016) 78-92, https://doi.org/10.1016/j.jmbbm.2015.08.003.

72. T. Sugiyama, A. Kameyama, T. Enokuchi, A. Haruyama, A. Chiba, S. Sugiyama, M. Hosaka, T. Takahashi, Effect of professional dental prophylaxis on the surface gloss and roughness of CAD/CAM restorative materials, J. Clin. Exp. Dent. 9 (2017) e772-e778, https://doi.org/10.4317/jced.53826.

73. Z.X. Xiang, X.P. Chen, X.F. Song, L. Yin, Responses of pre-crystallized and crystallized zirconia-containing lithium silicate glass ceramics to diamond machining, Ceram. Int. 46 (2020) 1924-33.

74. A.R. Alao, M.H.D. Bujang, Load effect on the mechanical behaviour of zirconia-reinforced lithium silicate glass ceramics, Ceram. Int. 47 (2021) 1353-63, https://doi.org/10.1016/j.ceramint.2020.08.257.

75. C. D'Arcangelo, L. Vanini, G.D. Rondoni, F. De Angelis, Wear properties of dental ceramics and porcelains compared with human enamel, J. Prosthet. Dent. 115 (2016) 350-5, https://doi.org/10.1016/j.prosdent.2015.09.010.

76. F. De Angelis, C. D'Arcangelo, N. Malíšková, L. Vanini, M. Vadini, Wear Properties of Different Additive Restorative Materials Used for Onlay/Overlay Posterior Restorations, Oper. Dent. 45 (2020) E156-E166, https://doi.org/10.2341/19-115-L.

77. J.P.M. Tribst, L.M.M. Alves, A.M.D.O.D. Piva, R.M.D. Melo, A.L.S. Borges, T.J.A. Paes-Junior, M.A. Bottino, Reinforced glass-ceramics: parametric inspection of three-dimensional wear and volumetric loss after chewing simulation, Braz. Dent. J. 30 (2019) 505-10.

78. C.S. Silva, B. Henriques, A.P.N. de Oliveira, F. Silva, J.R. Gomes, J.C. Souza, Micro-scale abrasion and sliding wear of zirconium-lithium silicate glass-ceramic and polymer-infiltrated ceramic network used in dentistry, Wear 448 (2020) 203214.

79. S.M. Fathy, M.V. Swain, In-vitro wear of natural tooth surface opposed with zirconia reinforced lithium silicate glass ceramic after accelerated ageing, Dent. Mater. 34 (2018) 551-9, https://doi.org/10.1016/j.dental.2017.12.010.

80. L.M.M. Alves, L.P.C. Contreras, T.M.B. Campos, M.A. Bottino, L.F. Valandro, R.M. Melo, In vitro wear of a zirconium-reinforced lithium silicate ceramic against different restorative materials, J. Mech. Behav. Biomed. Mater. 100 (2019) 103403, https://doi.org/10.1016/j.jmbbm.2019.103403.

81. X.P. Chen, Z.X. Xiang, X.F. Song, L. Yin, Machinability: Zirconia-reinforced lithium silicate glass ceramic versus lithium disilicate glass ceramic, J. Mech. Behav. Biomed. Mater. 101 (2020) 103435, https://doi.org/10.1016/j.jmbbm.2019.103435.

82. A.B.G. de Carvalho, A.M.D.O. Dal Piva, J.P.M. Tribst, A. Werner, G.D.S.F.A. Saavedra, C.J. Kleverlaan, Effect of microwave crystallization on the wear resistance of reinforced glass-ceramics, J. Mech. Behav. Biomed. Mater. 111 (2020) 104009.

83. R.M. Maenosono, L.F.F. Brianezzi, S.K. Ishikiriama, A.Y. Furuse, Clinical perceptions of zirconia-reinforced lithium silicate ceramic: a case report and 6-month follow-up, Gen. Dent. 67 (2019) 47-50.

84. J. Conejo, M.B. Blatz, Simplified Fabrication of an Esthetic Implant-Supported Crown With a Novel CAD/CAM Glass Ceramic, Compend. Contin. Educ. Dent. 37 (2016) 396-9.

85. S. Choi, H.I. Yoon, E.J. Park, Load-bearing capacity of various CAD/CAM monolithic molar crowns under recommended occlusal thickness and reduced occlusal thickness conditions, J. Adv. Prosthodont. 9 (2017) 423-31, https://doi.org/10.4047/jap.2017.9.6.423.

86. A. Furtado de Mendonca, M. Shahmoradi, C.V.D. Gouvêa, G.M. De Souza, A. Ellakwa, Microstructural and Mechanical Characterization of CAD/CAM Materials for Monolithic Dental Restorations, J. Prosthodont. 28 (2019) e587-e594, https://doi.org/10.1111/jopr.12964.

87. E.T.P. Bergamo, D. Bordin, I.S. Ramalho, A.C.O. Lopes, R.S. Gomes, M. Kaizer, L. Witek, E.A. Bonfante, P.G. Coelho, A.A. Del Bel Cury, Zirconia-reinforced lithium silicate crowns: Effect of thickness on survival and failure mode, Dent. Mater. 35 (2019) 1007-16, https://doi.org/10.1016/j.dental.2019.04.007.

88. R. Ottoni, J.A. Griggs, P.H. Corazza, Á. Della Bona, M. Borba, Precision of different fatigue methods for predicting glass-ceramic failure, J. Mech. Behav. Biomed. Mater. 88 (2018) 497-503, https://doi.org/10.1016/j.jmbbm.2018.09.004.

89. ISO 6872. International Organization for Standardization. Dentistry - Ceramic materials; 2015. https://www.iso.org/standard/59936.html, 2021 (accessed 20 February 2021)

90. E. Yeğin, M.H. Atala, Comparison of CAD/CAM manufactured implant-supported crowns with different analyses, Int. J. Implant Dent. 69 (2020), https://doi.org/10.1186/s40729-020-00267-x.

91. V. Preis, S. Hahnel, M. Behr, L. Bein, M. Rosentritt, In-vitro fatigue and fracture testing of CAD/CAM-materials in implant-supported molar crowns, Dent. Mater. 33 (2017) 427-33, https://doi.org/10.1016/j.dental.2017.01.003.

92. M. Rosentritt, S. Hahnel, F. Engelhardt, M. Behr, V. Preis, In vitro performance and fracture resistance of CAD/CAM-fabricated implant supported molar crowns, Clin. Oral Investig. 21 (2017) 1213-9, https://doi.org/10.1007/s00784-016-1898-9.

93. D. Taha, S. Spintzyk, A. Sabet, M. Wahsh, T. Salah, Assessment of marginal adaptation and fracture resistance of endocrown restorations utilizing different machinable blocks subjected to thermomechanical aging, J. Esthet. Restor. Dent. 30 (2018) 319-28.

94. N.R. Dartora, I.C. Maurício Moris, S.F. Poole, A. Bacchi, M.D. Sousa-Neto, Y.T. Silva-Sousa, E.A. Gomes, Mechanical behavior of endocrowns fabricated with different CAD-CAM ceramic systems, J. Prosthet. Dent. S0022-3913 (2020) 30739-5, https://doi.org/10.1016/j.prosdent.2019.11.008.

95. W. El Ghoul, M. Özcan, M. Silwadi, Z. Salameh, Fracture resistance and failure modes of endocrowns manufactured with different CAD/CAM materials under axial and lateral loading, J. Esthet. Restor. Dent. 31 (2019) 378-87, https://doi.org/10.1111/jerd.12486.

96. M. Zimmermann, C. Koller, A. Mehl, R. Hickel, Indirect zirconia-reinforced lithium silicate ceramic CAD/CAM restorations: Preliminary clinical results after 12 months, Quintessence Int. 48 (2017) 19-25, https://doi.org/10.3290/j.qi.a37017.

97. H. Nassar, C.H. Halim, H.A. Katamish, Clinical outcomes of zirconia-reinforced lithium silicate partial coverage crowns compared to lithium disilicate partial coverage crowns. A randomized controlled split-mouth clinical study, F1000Research 8 (2019) 305, https://doi.org/10.12688/f1000research.18274.1.

98. S. Rinke, T. Pfitzenreuter, A. Leha, M. Roediger, D. Ziebolz, Clinical evaluation of chairside-fabricated partial crowns composed of zirconia-reinforced lithium silicate ceramics: 3-year results of a prospective practice-based study, J. Esthet. Restor. Dent. 32 (2020) 226-35, https://doi.org/10.1111/jerd.12542.

99. S. Rinke, A. Brandt, T. Hausdoerfer, A. Leha, D. Ziebolz, Clinical Evaluation of Chairside-Fabricated Partial Crowns Made of Zirconia- Reinforced Lithium Silicate Ceramic - 2-Year-Results, Eur. J. Prosthodont. Restor. Dent. 28 (2020) 36-42, https://doi.org/10.1922/EJPRD_2001Rinke07.

100. G.S.F.A. Saavedra, F.P. Rodrigues, M.A. Bottino, Zirconia-Reinforced Lithium Silicate Ceramic - A 2-Year Follow-up of a Clinical Experience with Anterior Crowns, Eur. J. Prosthodont. Restor. Dent. 25 (2017) 57-63, https://doi.org/10.1922/EJPRD_01528Saavedra07.

101. S. Abou-Steit, J. Elguindy, A. Zaki, Evaluation of patient satisfaction and shade matching of Vita Suprinity versus lithium disilicate (E-max) ceramic crowns in the esthetic zone: a randomized controlled clinical trial, F1000Research 8 (2019) 371, https://doi.org/10.12688/f1000research.18337.1.

4.4 DENTIN EXPOSURE AFTER TOOTH PREPARATION FOR LAMINATE VENEERS: A MICROSCOPICAL ANALYSIS TO EVALUATE THE INFLUENCE OF OPERATORS' EXPERTISE

Roberto Sorrentino, Gennaro Ruggiero, Bruna Borelli, Alberta Barlattani and Fernando Zarone
Materials 2022, 15, x.

1. Introduction

In recent decades, laminate veneers (LVs) have become a widespread treatment option for the possibility of meeting the demand for long-lasting, highly aesthetic, and minimally invasive restorations [1–3].

An LV is defined as a superficial or attractive display in multiple layers that restores a tooth at the incisal, buccal, and/or part of palatal and interproximal surfaces [4]. It could be made of porcelain-based or porcelain-free materials, such as feldspar ceramics, lithium disilicate, zirconia, or zirconia-reinforced lithium silicate [5–7]. This type of restoration allows for the restoring of dental aesthetics, in cases of misalignment, wear, discoloration, fractures, and morphological alterations [8,9]. Moreover, additional partial veneers, "minimal preparation" and even "no-preparation (or prepless)" laminate veneers can be used in situations involving a minimum ceramic application, with a thickness of 0.3–0.5 mm, such as in the closure of diastemas, limited reshaping of front teeth, treatment of microcracks, enamel defects, and minor discolorations [9–11].

With LVs, the teeth are considerably preserved, thanks to the reduced thickness required by the new biomimetic ceramic materials and by the efficient bond with enamel [1]. The survival rate of LVs is negatively affected by veneer preparations extending into dentin, allowing enamel an optimal adhesion [1–3,12–14].

Four typologies of tooth preparation designs are mostly used for LVs: window (WI), feather edge, butt joint (BJ) ("incisal bevel"), and palatal chamfer ("overlapped") [15]. The first two configure the "non-overlap" class, the other two the "overlap" class [16,17].

Besides, high survival rates were reported in the literature for the different preparation designs [17]. The incisal-covered preparation designs for LVs show an increased risk of failure compared to those without incisal coverage [18]. Among incisal-covered designs, the BJ is a type of preparation that affects the tooth strength less than the palatal chamfer, while the latter is more prone to ceramic fractures [16,19]. It is worth noting that the location of LVs is also a relevant factor in the risk of failure. Particularly, maxillary central and lateral incisors prepared with a palatal chamfer exhibited greater fracture strength than those prepared with a WI preparation [18,20]. Conversely, maxillary canines prepared with the WI design were more resistant to fracture than those prepared with a palatal chamfer [20]; however, it has to be pointed out that the preparation of designs with an incisal covering yield better aesthetic results than designs without incisal coverage [2].

In the present study, the BJ and WI geometries were selected as the most scientifically validated and clinically used preparation designs for laminate veneers [16,18]. Given that the thickness of enamel is not homogenous and can vary both in the mesio-distal and apico-coronal directions [21], designs limited to the buccal surface (i.e., window) are somehow more conservative than preparations involving the incisal margin reduction (i.e., feathered, butt joint, palatal chamfer) [2]; therefore, the more dental tissue is removed, the greater the risk of exposing dentin [22,23].

Moreover, several clinical investigations proved that different operative approaches could significantly affect dentin exposure; nevertheless, a correlation between particular preparation designs and the amount of exposed dentin has not yet been defined [22,23]; therefore, freehand preparation was chosen in the present study to simulate the worst clinical scenario.

In any case, detecting the exposition of dentin structure during tooth preparation is not easy, affecting the effectiveness of bonding. In this regard, optical magnification systems can be helpful to better visualize dental tissues [24]. Furthermore, there could be inter- and intra-individual variability in the recognition of tooth hard tissues and, therefore, of exposed dentin. In particular, the inter-individual variability could be relevant in the case of operators with different clinical expertise.

To date, to the authors' knowledge, there are no investigations evaluating possible differences in the identification of hard tissues in prepared teeth with different preparation designs, using magnification systems, between operators with different clinical expertise.

The purpose of the present in vitro investigation was to assess the areas of dentin exposure with the use of a stereomicroscope in 2 different designs of tooth preparations (WI and BJ) for LVs.

For this purpose, two null hypotheses were formulated:

there is no association among different designs of tooth preparation for LVs and the amount of dentin exposure;

there is no difference both intra- and inter-individual in the discrimination under magnification between prepared enamel and dentin for operators with different clinical expertise.

2. Materials and Methods

2.1. Specimen Selection

Twenty maxillary central incisors extracted for periodontal pathologies, free of caries and restorations, were collected among the discarded teeth extracted at the Department of Oral Surgery of the University Hospital "Federico II" of Naples. Also, teeth with wear were excluded. Any plaque, calculus, and periodontal ligament residues were removed using ultrasonic instruments, curettes, and silicone rubber polishers. The collected teeth were extracted from patients with an age range of 35 to 50 years. The maxillary central incisors were included in the study if fulfilling the anatomical parameters described by Nelson and Ash [25] (Figure 1):

crown length: 10–10.5 mm;

root length: 12–13 mm;

mesiodistal diameter of crown: 8.5–9 mm;

mesiodistal diameter of crown at cervix: 6.3–7 mm;

buccopalatal diameter of crown: 7 mm;

buccopalatal diameter of crown at cervix: 6 mm [25].

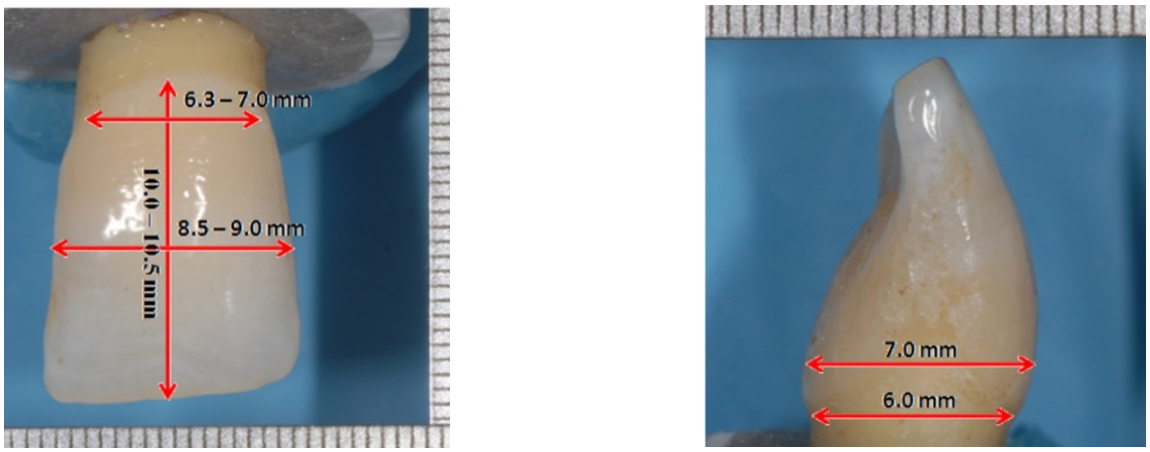

(**a**) (**b**)

Figure 1. Reference scale and selected anatomical dimensions according to the parameters described by Nelson and Ash. (**a**) crown length and mesiodistal diameters; (**b**) buccopalatal diameters. Each dash is spaced half a millimeter apart.

Therefore, all the selected specimens presented a total length of 22 ± 1 mm, buccopalatal and mesiodistal crown lengths of 7 ± 1 mm and 9 ± 1 mm, respectively.

Only the average dimensions of sample teeth but not the variation in enamel thickness were considered, so as to simulate a real clinical scenario, in which enamel thickness can vary according to the anatomy of each tooth.

The specimens were stored in a 1% solution of thymol at 25 °C immediately after extraction and for a maximum period of 4 weeks.

Subsequently, they were placed into cylinders filled with autopolymerizing resin (Orthojet Lang, Ravelli S.p.a., Milan, Italy) leaving at least 2 mm of the root exposed apically to the cemento–enamel junction, in order to make finish lines visible. The specimens were randomly numbered in ascending order to be identified individually.

2.2. Tooth Preparation

One experienced prosthodontist performed 2 different tooth preparation designs for LVs at sight under magnification of 16×, with a dedicated medical stereomicroscope (OPMI PROergo, Carl Zeiss AG, Oberkochen, Germany). According to the preparation designs, the specimens were divided into 2 experimental groups (n = 10), named WI and BJ.

For each specimen, a silicone index was made before preparation with silicone material (Platinum 85, Zhermack S.p.a., Rovigo, Italy) to check the thickness of the dental tissues removed during tooth preparation. Each silicone index was created by sectioning the index vertically through the maximum longitudinal axis of each tooth, along the buccopalatal plane. All the sectioned indexes were numbered according to the corresponding tooth.

Each preparation was performed with dedicated diamond-coated burs (801.314.006 and 837KR.314.012, Komet, Gebr. Brasseler GmbH & Co. KG, Lemgo, Germany) mounted on a contra-angle handpiece 1:5 for micromotor (WK-99 LT, Synea, W&H Dentalwerk GmbH, Bürmoos, Austria) at 200.000 min^{-1}/rpm under spray water. The specimens were prepared with a mini-chamfer cervical finish line of 0.3 mm and buccal depth of 0.6 mm. The preparation thicknesses were carefully checked with the silicone index and a millimeter-periodontal probe (Offset Williams Probe, Hu-Friedy Mfg. Co., Chicago, IL, USA), under magnification. For BJ preparations, the incisal margin was removed to a length of 2 mm (Figure 2a), while for WI preparations the incisal margin was preserved (Figure 2b). Arkansas burs (661-204-420, Komet, Gebr. Brasseler GmbH & Co. KG, Lemgo, Germany) were used for finish line polishing and surface smoothing. The polishing burs were mounted on a contra-angle handpiece 1:1 for micromotor (WK-56 LT, Synea, W&H Dentalwerk GmbH, Bürmoos, Austria), at 20.000 min^{-1}/rpm under spray water.

(**a**) (**b**)

Figure 2. The tested preparation designs for LVs: (**a**) butt joint (BJ); (**b**) window (WI).

2.3. Analysis of Prepared Surfaces

Immediately after tooth preparation, the dried surfaces were analyzed following a protocol similar to the one of Blunck et al. [1]. The specimens were photographed through the stereomicroscope (OPMI PROergo, Carl Zeiss AG) to better evidence enamel from dentin. A camera (Nikon F-Mount DK-10, Tokyo, Japan) was mounted on a dedicated arm of the stereomicroscope and each sample was placed onto a stable support surface, in order to obtain a repeatable and standardized focal distance. The teeth were placed so that the buccal surface was perpendicular to the optical system of the stereomicroscope.

A raster graphics editor software (Adobe Photoshop CS4 Extended v11.0, Adobe Inc., San Jose, CA, USA) was used to analyze the pictures made for each specimen. A measurement scale (1 mm = 129 px) was set referring to a known distance of the picture, displayed in Figure 1 as a reference millimeter scale.

To assess the quantity of exposed dentin, the full prepared area of the tooth was selected with the "Quick Selection Tool", setting a diameter of 3 px and recording the number of pixels from the "Histogram" function after clicking on "click for histogram with uncached data". This operation was made to obtain the percentage of exposed dentin area on the full prepared tooth area, according to the following formula:

% of exposed dentin area compared to the full prepared area = (exposed dentin area (px))/(prepared tooth area (px)) × 100.

In the same software, a square was drawn with a 1 mm side, according to the millimetric scale (Figure 1). Subsequently, the square was selected with the "Rectangular Marquee Tool (M)", to obtain the number of pixels corresponding to the square area through the "Histogram" function. Finally, to know the surface area in mm^2 of exposed dentin, the following formula was used:

Area of exposed dentin (mm^2) = (exposed dentin area (px))/(reference square area (px)) × 1 mm^2.

This procedure was repeated for each picture by 3 operators with different expertise: a trainee undergraduate student (ST), a general practitioner (GP), and an experienced prosthodontist (PR) (Figure 3). Operators with different clinical expertise were considered in order to report if there might be inter- and intra-individual variability in the detection of exposed dentin. Before performing the measurements, all the operators were trained to use the software with a few representative dummy pictures.

Nowadays, it is possible to accurately discriminate between enamel and dentin only through instrumental or histological investigations [26–28]. With regards to the operative procedures, during tooth preparation clinicians could discriminate between enamel and dentin visually, since enamel can be kept dry while dentin is characterized by a shiny appearance due to intrinsic humidity [29], and thanks to patients' sensitivity, typically subsequent to dentin exposure if anesthesia was not injected [23]; however, to date, no clear and univocal parameters to clinically distinguish enamel and dentin have been established yet.

Although the study specimens were kept hydrated until the execution of the microscopical analysis, dehydration could occur due to environmental conditions and microscopic light; consequently, discrimination due to intrinsic moisture could not be used for the investigation.

Study operators were trained accordingly, and some specific optical and morphological features of dental tissues were considered [29]. Particularly, enamel presents with greater translucency and value, while dentin shows a more intense chroma, opacity, and more polished appearance. Also, the grooves left by burs were more pronounced and appeared like whitish stripes onto the enamel (Figure 3). Besides, the operators used the intact interproximal enamel tissue surrounding the prepared area as a reference for comparison.

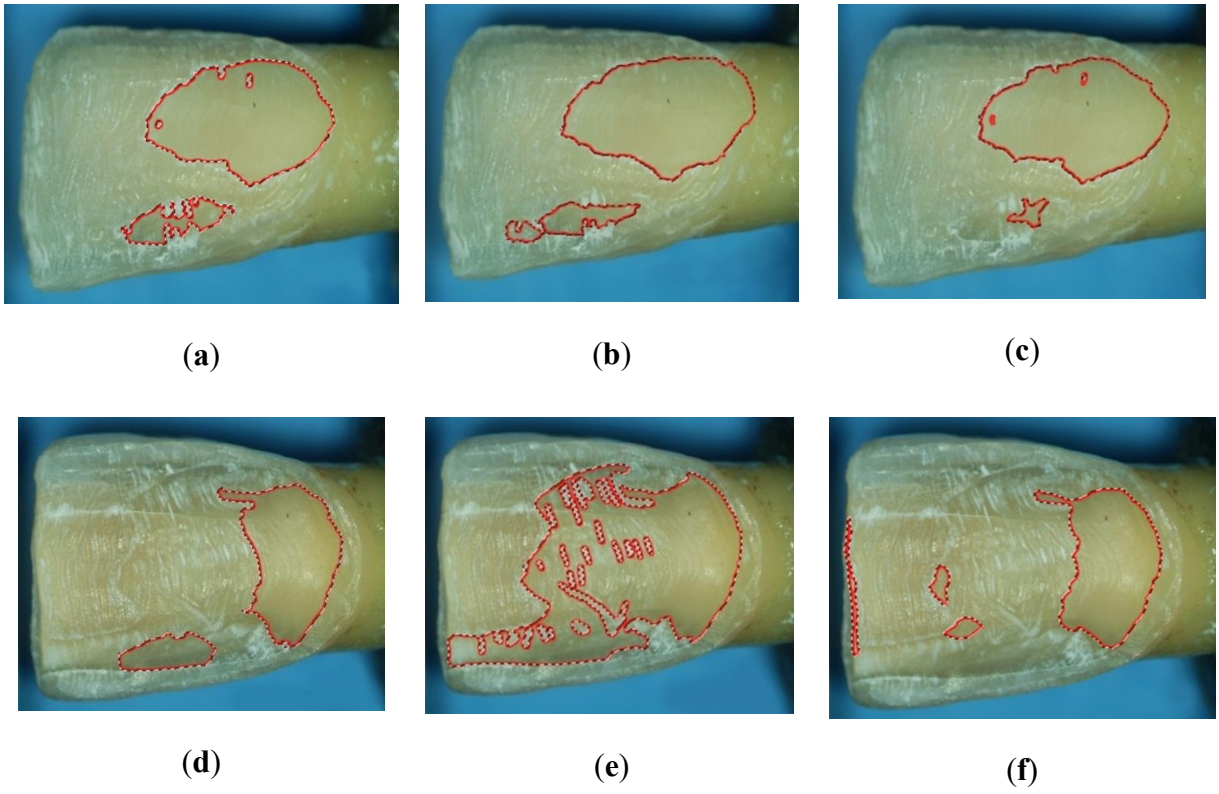

Figure 3. Exposed dentin surfaces were detected through digital analysis and the use of a stereomicroscope by 3 operators with different clinical expertise for 2 preparation designs. ST, undergraduate student; GP, general practitioner, PR, prosthodontist; WI, window; BJ, butt joint. (**a**) ST/WI; (**b**) GP/WI; (**c**) PR/WI; (**d**) ST/BJ; (**e**) GP/BJ; (**f**) PR/BJ. After tooth preparation, the prepared surfaces were first dried and then photographed with the stereomicroscope. A raster graphics software was used to analyze the pictures taken and to draw the perimeter of dentin tissue.

With this procedure, 6 experimental groups were made: ST/WI, GP/WI, PR/WI, for the WI preparation design and ST/BJ, GP/BJ, and PR/BJ for the BJ design.

The evaluation of each operator on the prepared teeth was made by alternating the two preparation designs and observing a blue paper surface on which to rest the eyes [30], in order to minimize the impact of operators' fatigue and avoid the related bias.

2.4. Statistical Analysis

The statistical analysis was performed with a statistical software program (IBM SPSS Statistics, v25; IBM Corp, New York, NY, USA) on data concerning the percentage and the mm^2 of exposed dentin areas. Descriptive statistics (i.e., mean, standard deviation, lower- and upper-bounds with 95% confidence interval—CI) and specific tests were run to determine the overall statistical significance of the differences between the experimental groups. Particularly, the

Shapiro–Wilk and the Levene tests were run, respectively, to assess the normality of the distribution of the statistical variables and to evaluate the variance homogeneity. The 2-way analysis of variance (ANOVA) was used to identify interactions among operators and preparation designs.

The Bonferroni post hoc test or the Welch test followed by the Games–Howell post hoc test were used to analyze differences among groups ($\alpha = 0.05$). To consider only clinically relevant comparisons, all the possible pairwise comparisons among the 6 experimental groups were not performed; consequently, it was evaluated whether differences existed among operators within a preparation design and between preparation designs within an operator.

Moreover, a power analysis was performed with the software G*Power (v. 3.1.9.6, Universität Kiel, Germany) to determine the sample size effect. To determine the effect size, partial eta squared (η^2) is the effect size measure for the interaction between the within and between subject variables. Approximate partial eta squared conventions are small = 0.02; medium = 0.06; large = 0.14. A medium effect size was assumed.

3. Results

There was a 99.1% of correctness in rejecting the null hypothesis of no significant effect of the interaction with 30 WI and 30 BJ measurements for a total of 60 assessments (Figure 4).

Table 1. Results in percentage of exposed dentin areas: mean, standard deviation, and lower-upper bound (95% confidence interval).

Operators	Mean (%)	Standard Deviation	Lower-Upper Bound
ST/WI	22.82	9.23	16.21–29.42
ST/BJ	28.99	15.45	17.93–40.04
GP/WI	58.05	21.58	42.61–73.49
GP/BJ	40.56	21.25	25.35–55.76
PR/WI	10.55	10.16	3.27–17.82
PR/BJ	23.42	9.56	16.58–30.26

ST, undergraduate student; GP, general practitioner, PR, prosthodontist; WI, window; BJ, butt joint.

Table 2. Results in mm^2 of exposed dentin areas: mean, standard deviation, and lower-upper bound (95% confidence interval).

Operators	Mean (mm^2)	Standard Deviation	Lower-Upper Bound
ST/WI	16.44	7.19	11.29–21.58
ST/BJ	20.83	11.94	12.29–29.38
GP/WI	40.64	12.91	31.41–49.88
GP/BJ	28.32	14.78	17.74–38.89
PR/WI	7.63	7.86	2.01–13.25
PR/BJ	16.75	7.45	11.42–22.09

ST, undergraduate student; GP, general practitioner, PR, prosthodontist; WI, window; BJ, butt joint.

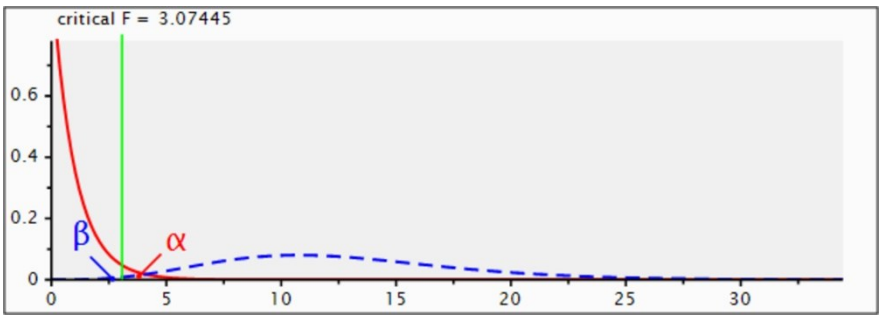

Figure 4. Power Analysis to define the Sample Size Effect.

The results of the descriptive statistics about the measurements of exposed dentin (in percentage and mm^2) are summarized in Tables 1 and 2, while the box-plot chart of the 6 experimental groups is shown in Figure 5. The means in percentage and mm^2 of exposed dentin for WI preparations were 30.48% and 21.57 mm^2, while for BJ preparations were 30.99% and 21.97 mm^2.

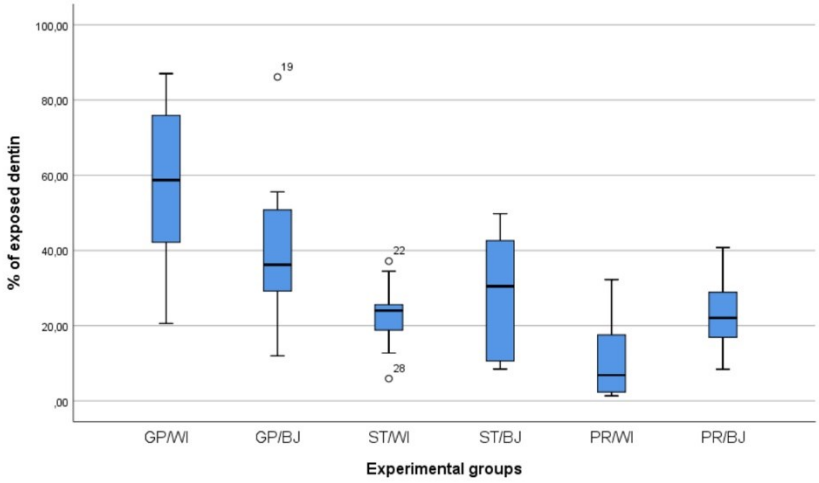

Figure 5. Box-plot chart showing values of the percentage of exposed dentin. Whiskers below and above box exhibit positions of minimum and maximum, whereas box spans show the first quartile to the third quartile. The median is represented by segments inside the box and suspected outliers are shown as unfilled circles. ST, undergraduate student; GP, general practitioner; PR, prosthodontist; WI, window; BJ, butt joint.

The 2-way ANOVA (Table 3) detected statistically significant differences between the evaluations of individual operators (ST, GP, and PR) ($p < 0.001$) but not between the 2 types of tested tooth preparation designs (WI and BJ) ($p = 0.898$). Nonetheless, the mutual interaction between the study variables showed a statistically significant difference ($p = 0.008$).

Table 3. Results of 2-way ANOVA.

Source	SS	df	MS	F	*p*
Corrected Model	13,694.17	5	2738.83	11.43	<0.001
Intercept	56,675.34	1	56,675.34	236.67	<0.001
Operator	11,144.83	2	5572.41	23.27	<0.001
Preparation	3.97	1	3.97	0.01	0.898
Operator × Preparation	2545.36	2	1272.68	5.31	0.008
Error	12,931.04	54	239.46		
Total	83,300.56	60			
Corrected Total	26,625.22	59			

ANOVA, analysis of variance; SS, sum of squares; df, degree of freedom (n − 1); MS, mean squares. Significant at $p < 0.05$.

Among the operators, the Shapiro–Wilk test reported that the values were normally distributed ($p > 0.05$) for all the groups and the Levene test showed that the variances were homogeneous ($p = 0.005$).

The Bonferroni post hoc test recorded statistically significant differences between the evaluations of ST and GP ($p < 0.001$) and between GP and PR ($p < 0.001$); differently, no statistically significant difference was detected between ST and PR ($p = 0.277$) (Table 4).

Among the 6 experimental groups, the Shapiro–Wilk test reported that the values were normally distributed ($p > 0.05$) for all the groups and the Levene test showed that the variances were not homogeneous ($p = 0.012$).

Since there was a normal distribution but no homogeneity of the variances, the robust Welch test of equality of means was used and reported a significant value [$p < 0.001$ with F (5, 24.84 = 8.96)]. After the Welch test, the Games–Howell analysis was performed to evaluate whether there were any statistically significant differences between preparation designs within an operator and among operators within a preparation design. Significant differences were detected among operators within the means of the WI preparation design, particularly between ST and GP ($p = 0.005$) and between GP and PR ($p < 0.001$) (Table 4).

Table 4. *p* values of post hoc comparisons.

Comparison	*p*
ST/WI-ST/BJ	0.880
GP/WI-GP/BJ	0.475
PR/WI-PR/BJ	0.083
ST/WI-GP/WI	0.005 *
ST/WI-PR/WI	0.099
GP/WI-PR/WI	<0.001 *
ST/BJ-GP/BJ	0.731
ST/BJ-PR/BJ	0.921
GP/BJ-PR/BJ	0.254
ST-GP	<0.001 *
ST-PR	0.277
GP-PR	<0.001 *

* Statistically significant differences ($p < 0.05$). ST, undergraduate student; GP, general practitioner, PR, prosthodontist; WI, window; BJ, butt joint.

4. Discussion

LV is an efficient restorative option, offering a reliable treatment that preserves the structure of teeth while providing outstanding esthetic outcomes and patient acceptance [1–3,14,15].

This restorative system exhibited high longevity and low complication rates, as supported by many systematic reviews with follow-up periods ranging between 5 and 21 years, showing survival rates ranging from 87% to 96% [31–34]. Several factors affect the survival of LVs, such as cementation materials [35], quality of dental substrates (enamel vs. dentin) and mechanical properties of restorations [36], presence of previous fillings, occlusal forces, and preparation design [9,32–34,37].

Tooth preparation for LVs can be performed by evaluating the following aspects: buccal surface preparation (no preparation, minimal preparation, conservative, or conventional preparation), incisal preparation (overlapping or non-overlapping), proximal finish (slice or chamfer), and cervical preparation (chamfer or knife-edge) [16].

In this study, considering the different preparation designs as statistical variables and since no statistically significant differences were detected between the 2 experimental groups, WI and BJ, the first null hypothesis (no association between the 2 types of tooth preparation design and the quantity of exposed dentin) was accepted. Instead, considering the statistically significant differences detected between the 3 operators with different expertise (ST, GP, and PR), the second null hypothesis (no difference, both intra- and inter-operator) was partially rejected.

The descriptive statistics reported lower values of exposed dentin for the WI preparation than for BJ (WI = 30.48% and 21.57 mm^2; BJ = 30.99% and 21.97 mm^2); however, this difference was not statistically significant (p = 0.898), therefore, the association between the type of tooth preparation (WI and BJ) and the amount of exposed dentin was not found. It can thus be asserted that the choice between BJ and WI designs should take into consideration factors like the risk of fracture and aesthetic needs, instead of dentin exposure; therefore, the advantages and disadvantages of these preparation geometries should be considered (Table 5).

Table 5. Advantages and disadvantages between window and butt joint designs for laminate veneers.

Preparation Design	Advantages	Disadvantages
Window	-Decreased failure risk [18]. -Conservative [16,19]. -Does not interfere with incisal guidance [16].	-More than one path for insertion [2]. -Lower aesthetic [2,16].
Butt joint	-Better aesthetic [2,16]. -Precise seat and stop for cementation [2]. -Possibility to restore incisal guidance [2]	-Increased failure risk [18]. -Not conservative as the window design [19]. -Interfere with incisal guidance [16].

In the comparison between the means of ST, GP, and PR groups, a statistical significance was found ($p < 0.001$), in particular, between GP and the other 2 operators in the WI scenario (ST/WI-GP/WI, $p = 0.005$; GP/WI-PR/WI, $p < 0.001$). These differences show that proper training may be paramount in discriminating between prepared enamel and exposed dentin. These findings were mainly observed in the WI preparation, where the amount of dental tissue to be evaluated was wider than in the BJ preparation, with its 2-mm incisal reduction. Therefore, since the evaluated surface area was wider, then the cumulative error was higher, leading to a statistical difference only in the WI scenario.

Therefore, the recorded results show that no difference was found within the operator between preparation designs, demonstrating that, even if there is an inter-operator difference for the WI design, an intra-operator difference was not detected both in WI and BJ.

Furthermore, the mean values of exposed dentin found in the 2 different preparation designs (WI and BJ) were approximately 30%, with a 70% of exposed enamel. This value is above the minimally acceptable for the enamel exposure (40%) required to obtain an efficient bond strength [38,39].

Finally, this investigation confirms that the use of magnification devices is a useful system for discriminating between enamel and dentine and therefore to standardize the preparation procedures [1,24,40].

The present study has some limitations, mainly related to its in vitro nature. Only two preparation designs for LVs were tested, WI and BJ. The samples consisted of extracted teeth, so, clinically relevant factors related to the oral environment, in particular temperature, humidity, and optical features, were not considered; moreover, the surface analysis was two-dimensional, using images taken under magnification, so the surface shape of prepared teeth was not considered. Besides, only one operator for each level of clinical expertise was considered.

Further in vitro and in vivo investigations involving a larger sample size are needed to confirm that the various preparation designs for LVs do not determine a different amount of exposed dentin. Moreover, a larger number of operators would be advisable to confirm that there are inter-individual variabilities in the discrimination of hard tissues in prepared teeth to optimize subsequent adhesive cementation procedures [22,23].

5. Conclusions

Within the limitations of the present in vitro study, the following conclusions can be drawn about LVs:

1. the quantity of exposed dentin is not associated with the two considered preparation designs, namely window and butt joint;
2. the expertise of clinical operators represents a discriminating factor in identifying prepared hard dental tissues, as both an undergraduate student and an expert prosthodontist showed statistically different values from a general practitioner as to the window preparation;
3. in the butt joint preparation, no differences were found between the different operators;
4. variability was found in the inter-individual evaluation of exposed dentin following different preparation designs for LVs;
5. no intra-operator variability was detected both in window and butt joint preparations;
6. magnification tools were useful to discriminate between prepared enamel and dentin.

Further in vivo and in vitro studies would be helpful to confirm and validate the findings of the present investigation.

References

1. Blunck, U.; Fischer, S.; Hajtó, J.; Frei, S.; Frankenberger, R. Ceramic laminate veneers: Effect of preparation design and ceramic thickness on fracture resistance and marginal quality in vitro. *Clin. Oral Investig.* **2020**, *24*, 2745–2754. https://doi.org/10.1007/s00784-019-03136-z.
2. Alothman, Y.; Bamasoud, M.S. The success of dental veneers according to preparation design and material type. *Open Access Maced. J. Med. Sci.* **2018**, *12*, 2402–2408. https://doi.org/10.3889/oamjms.2018.353.
3. Liu, M.; Gai, K.; Chen, J.; Jiang, L. Comparison of failure and complication risks of porcelain laminate and indirect resin veneer restorations: A meta-analysis. *Int. J. Prosthodont.* **2019**, *32*, 59–65. https://doi.org/10.11607/ijp.6099.
4. The Academy of Prosthodontics. The Glossary of Prosthodontic Terms: Ninth Edition. *J. Prosthet. Dent*. **2017**, *117*, e1–e105. https://doi.org/10.1016/j.prosdent.2016.12.001.
5. Zarone, F.; Di Mauro, M.I.; Ausiello, P.; Ruggiero, G.; Sorrentino, R. Current status on lithium disilicate and zirconia: A narrative review. *BMC Oral Health* **2019**, *19*, 134. https://doi.org/10.1186/s12903-019-0838-x.
6. Saker, S.; Özcan, M. Marginal discrepancy and load to fracture of monolithic zirconia laminate veneers: The effect of preparation design and sintering protocol. *Dent. Mater. J.* **2021**, *40*, 331–338. https://doi.org/10.4012/dmj.2020-007.
7. Zarone, F.; Ruggiero, G.; Leone, R.; Breschi, L.; Leuci, S.; Sorrentino, R. Zirconia-reinforced lithium silicate (ZLS) mechanical and biological properties: A literature review. *J. Dent.* **2021**, *109*, 103661. https://doi.org/10.1016/j.jdent.2021.103661.
8. Lo Muzio, L.; Bucci, P.; Carile, F.; Riccitiello, F.; Scotti, C.; Coccia, E.; Rappelli, G. Prosthetic rehabilitation of a child affected from anhydrotic ectodermal dysplasia: A case report. *J. Contemp. Dent. Pract.* **2005**, *6*, 120–126.
9. Zarone, F.; Leone, R.; Di Mauro, M.I.; Ferrari, M.; Sorrentino, R. No-preparation ceramic veneers: A systematic review. *J. Osseointegr.* **2018**, *10*, 17–22. https://doi.org/10.23805 /JO.2018.10.01.011.
10. Malcmacher, L. No-preparation porcelain veneers-back to the future! *Dent. Today* **2005**, *24*, 86–91.
11. Strassler, H.E. Minimally invasive porcelain veneers: Indications for a conservative esthetic dentistry treatment modality. *Gen. Dent.* **2007**, *55*, 68694.
12. Cherukara, G.P.; Davis, G.R.; Seymour, K.G.; Zou, L.; Samarawickrama, D.Y. Dentin exposure in tooth preparations for porcelain veneers: A pilot study. *J. Prosthet. Dent.* **2005**, *94*, 414–420. https://doi.org/10.1016/j.prosdent.2005.08.016.

13. Peumans, M.; Van Meerbeek, B.; Lambrechts, P.; Vanherle, G. Porcelain veneers: A review of the literature. *J. Dent.* **2000**, *28*, 163–177. https://doi.org/10.1016/s0300-5712(99)00066-4.
14. Burke, F.J. Survival rates for porcelain laminate veneers with special reference to the effect of preparation in dentin: A literature review. *J. Esthet. Restor. Dent.* **2012**, *24*, 257–265. https://doi.org/10.1111/j.1708-8240.2012.00517.x.
15. Shetty, A.; Kaiwar, A.; Shubhashini, N.; Ashwini, P.; Naveen, D.; Adarsha, M.; Shetty, M.; Meena, N. Survival rates of porcelain laminate restoration based on different incisal preparation designs: An analysis. *J. Conserv. Dent.* **2011**, *14*, 10–15. https://doi.org/10.4103/0972-0707.80723.
16. Chai, S.Y.; Bennani, V.; Aarts, J.M.; Lyons, K. Incisal preparation design for ceramic veneers: A critical review. *J. Am. Dent. Asso*c. **2018**, *149*, 25–37. https://doi.org/10.1016/j.adaj.2017.08.031.
17. Albanesi, R.B.; Pigozzo, M.N.; Sesma, N.; Laganá, D.C.; Morimoto, S. Incisal coverage or not in ceramic laminate veneers: A systematic review and meta-analysis. *J. Dent.* **2016**, *52*, 1–7. https://doi.org/10.1016/j.jdent.2016.06.004.
18. Hong, N.; Yang, H.; Li, J.; Wu, S.; Li, Y. Effect of preparation designs on the prognosis of porcelain laminate veneers: A systematic review and meta-analysis. *Oper. Dent.* **2017**, *42*, E197–E213. https://doi.org/10.2341/16-390-L.
19. da Costa, D.C.; Coutinho, M.; de Sousa, A.S.; Ennes, J.P. A meta-analysis of the most indicated preparation design for porcelain laminate veneers. *J. Adhes. Dent.* **2013**, *15*, 215–220. https://doi.org/10.3290/j.jad.a29587.
20. Zarone, F.; Epifania, E.; Leone, G.; Sorrentino, R.; Ferrari, M. Dynamometric assessment of the mechanical resistance of porcelain veneers related to tooth preparation: A comparison between two techniques. *J. Prosthet. Dent.* **2006**, *95*, 354–363.
21. Ferrari, M.; Patroni, S.; Balleri, P. Measurement of enamel thickness in relation to reduction for etched laminate veneers. *Int. J. Periodontics Restor. Dent.* **1992**, *12*, 407–413.
22. Gresnigt, M.M.M.; Cune, M.S.; Schuitemaker, J.; van der Made, S.A.M.; Meisberger, E.W.; Magne, P.; Özcan, M. Performance of ceramic laminate veneers with immediate dentine sealing: An 11 year prospective clinical trial. *Dent. Mater.* **2019**, *35*, 1042–1052. https://doi.org/10.1016/j.dental.2019.04.008.
23. Gurel, G.; Morimoto, S.; Calamita, M.A.; Coachman, C.; Sesma, N. Clinical performance of porcelain laminate veneers: Outcomes of the aesthetic pre-evaluative temporary (APT) technique. *Int. J. Periodontics Restor. Dent.* **2012**, *32*, 625–635.

24. Hegde, R.; Hegde, V. Magnification-enhanced contemporary dentistry: Getting started. *J. Interdiscip. Dent.* **2016**, *6*, 91–100.
25. Nelson, S.; Ash, M.M. *Wheeler's Dental Anatomy, Physiology, and Occlusion*, 9th ed.; Saunders Elsevier: St. Luis, MO, USA, 2009; p. 13.
26. Schneider, H.; Park, K.J.; Häfer, M.; Rüger, C.; Schmalz, G.; Krause, F.; Schmidt, J.; Ziebolz, D.; Haak, R. Dental applications of optical coherence tomography (OCT) in cariology. *Appl. Sci.* **2017**, *7*, 472.
27. Wilmers, J.; Bargmann, S. Nature's design solutions in dental enamel: Uniting high strength and extreme damage resistance. *Acta Biomater.* **2020**, *107*, 1–24.
28. Ohazama, A. Histological analysis of the embryonic and adult tooth. *Methods Mol. Biol.* **2012**, *887*, 1–13.
29. Hoffmann, L.; Feraric, M.; Hoster, E.; Litzenburger, F.; Kunzelmann, K.H. Investigations of the optical properties of enamel and dentin for early caries detection. *Clin. Oral Investig.* **2021**, *25*, 1281–1289.
30. Shillingburg, H.T.J.; Sather, D.A.; Wilson, E.L.J.; Cain, J.R.; Mitchell, D.L.; Blanco, L.J.; Kessler, J.C. *Fundamentals of Fixed Prosthodontics*, 4th ed.; Quintessence Publishing: Hanover Park, IL, USA, 2014; p. 422.
31. Morimoto, S.; Albanesi, R.B.; Sesma, N.; Agra, C.M.; Braga, M.M. Main of feldspathic porcelain and glass-ceramic laminate veneers: A systematic review and meta-analysis of survival and complication rates. *Int. J. Prosthodont.* **2016**, *29*, 38–49.
32. Beier, U.S.; Kapferer, I.; Burtscher, D.; Dumfahrt, H. Clinical performance of porcelain laminate veneers for up to 20 years. *Int. J. Prosthodont.* **2012**, *25*, 79–85.
33. Petridis, H.P.; Zekeridou, A.; Malliari, M.; Tortopidis, D.; Koidis, P. Survival of ceramic veneers made of different materials after a minimum follow-up period of five years: A systematic review and meta-analysis. *Eur. J. Esthet. Dent.* **2012**, *7*, 138–152.
34. Layton, D.M.; Walton, T.R. The up to 21-year clinical outcome and survival of feldspathic porcelain veneers: Accounting for clustering. *Int. J. Prosthodont.* **2012**, *25*, 604–612.
35. Perillo, L.; Sorrentino, R.; Apicella, D.; Quaranta, A.; Gherlone, E.; Zarone, F.; Ferrari, M.; Aversa, R.; Apicella, A. Nonlinear visco-elastic finite element analysis of porcelain veneers: A submodelling approach to strain and stress distributions in adhesive and resin cement. *J. Adhes. Dent.* **2010**, *12*, 403–413.
36. Sorrentino, R.; Apicella, D.; Riccio, C.; Gherlone, E.; Zarone, F.; Aversa, R.; Garcia Godoy, F.; Ferrari, M.; Apicella, A. Nonlinear visco-elastic finite element analysis of

different porcelain veneers configuration. *J. Biomed. Mater. Res. B Appl. Biomater.* **2009**, *91*, 727–736.

37. Layton, D.; Walton, T. An up to 16-year prospective study of 304 porcelain veneers. *Int. J. Prosthodont.* **2007**, *20*, 389–396.
38. Zhu, J.; Gao, J.; Jia, L.; Tan, X.; Xie, C.; Yu, H. Shear bond strength of ceramic laminate veneers to finishing surfaces with different percentages of preserved enamel under a digital guided method. *BMC Oral Health* **2022**, *22*, 3.
39. Gresnigt, M.M.M.; Braeckmans, A.; van der Made, SAM.; Naves, L.Z. Partial anterior indirect restorations in cases with dentin exposure. *Int. J. Esthet. Dent.* **2021**, *16*, 554–569.
40. Bud, M.; Jitaru, S.; Lucaciu, O.; Korkut, B.; Dumitrascu-Timis, L.; Ionescu, C.; Cimpean, S.; Delean, A. The advantages of the dental operative microscope in restorative dentistry. *Med. Pharm. Rep.* **2021**, *94*, 22–27.

4.5 CLINICAL EVALUATION OF CEMENT-RETAINED IMPLANT-SUPPORTED CAD/CAM MONOLITHIC ZIRCONIA SINGLE CROWNS IN POSTERIOR AREAS: RESULTS OF A 6-YEAR PROSPECTIVE CLINICAL STUDY

Roberto Sorrentino, Gennaro Ruggiero, Eralda Toska, Renato Leone and Fernando Zarone
Prosthesis 2022, 4,383-93

1. Introduction

To date, dental implants represent a predictable treatment for full or partially edentulous patients, with high success rates for both function and aesthetics [1,2]. In the last decades, the application of dental implants has become more and more widespread and, at the same time, many different types of fixtures and restorative materials have been introduced for use in different clinical situations [3].

To date, there is no univocal consensus in the scientific literature regarding the ideal retention system: some authors suggest the use of cement-retained implant restorations, while others prefer screw-retained implant prostheses. Both typologies exhibit advantages and drawbacks [3-6]

The main advantages of cement-retained restorations are good biomechanical stability, passive fit, absence of screw access holes, better occlusal design, and adaptation for implant prosthetic malposition. Moreover, the cement layer can compensate for dimensional discrepancies between abutment and restoration and work as a shock absorber, transferring occlusal loads to implant-restoration-bone complex [4,6,7].

The downside is the difficulty of removing cement excess, that has always been considered the major issue [8], in that it may increase the risk of peri-implant mucositis [9,10], peri-implantitis [9], and marginal bone loss [11,12].

Introduced in the early years of implantology as an integral part of the “Toronto” full-arch bridge concept, screw-retained prosthesis, for its part, offers easier retrievability, particularly advantageous in the case of long-span and cantilevered restorations [6,13]. Moreover, it is to be preferred in case of limited interocclusal space, when the height of the abutment should be ≤ 4 mm, not offering sufficient retention. Another indication for screw-retained restorations is the use

of temporary prostheses aimed at soft tissue conditioning and customization of emergence profile [6].

Compared to cemented restorations, screw-retained systems are reported to be more frequently prone to technical complications, like screw loosening and components/restoration fractures [14-16]. Moreover, the presence of an occlusal hole can impair the occlusal design, especially in the case of implant malposition. Last, but not least, screw-retained prostheses are more expensive, due to the higher cost of the components [6].

As regards cemented prostheses, they can ease the restoration design when the fixture location is not ideal and when a screw-retained solution should face the problem of a screw hole emergence in a critical position (e.g., incisal margin, buccal surface in anterior and cusp tip in posterior sites). In these cases, a proper cement-retained restoration design, together with a correct selection of the implant abutments, are paramount since they allow to customize and compensate the emergence profile, to limit micromovements and consequent bacterial contamination at the implant-prosthetic micro gap [17,18].

Titanium abutments are reported to show significantly higher fracture strength than zirconia abutments, reducing the incidence of clinical complications; consequently, they represent the first choice in posterior areas subjected to heavy occlusal forces [19,20]. Very high survival rates were reported by clinical investigations for titanium abutments that showed reliable clinical behavior and can be safely used in daily practice [21,22]

As regards prosthetic crowns, different restorative materials are currently available as clinical options. Conventional metal-ceramic restorations and bilayered all-ceramic prostheses showed high rates of technical complications mainly due to cohesive fractures of veneering ceramics (i.e., chipping) [23-27]; consequently, in the last decade, all-ceramic crowns in the monolithic configuration were proposed in posterior sites to reduce mechanical drawbacks, thanks to the excellent mechanical resistance to fracture and biocompatibility [28].

CAD/CAM monolithic zirconia was developed to limit the incidence of mechanical complications due to chipping of veneering ceramics, reduce production times, and improve cost-effectiveness [23,29]. However, different CAD/CAM zirconia milling procedures may produce discrepancies in cementation space, which eventually influence final crown retention [30]. Besides providing retention of prostheses, cementation techniques and mechanical properties of luting agents can affect the fracture strength and leakage of all-ceramic crowns [31]. Some investigations reported that zirconia should be submitted to specific mechanical and chemical surface treatments to develop durable bond strength to resin cements, just like mild sandblasting and application of primers containing 10-Methacryloyloxydecyl dihydrogen phosphate (MDP) [32,33].

The primary aim of the present prospective clinical study was to evaluate the survival and success rates of CAD/CAM monolithic zirconia single crowns (ZrSCs) cemented onto titanium implant abutments with a dual-curing resin cement containing MDP. The secondary aim was to assess possible biological and technical complications during function and the patients' aesthetic and functional satisfaction.

2. Materials and Methods

2.1 Participants

Fifty consecutive patients (18 females and 32 males) in need of 1 single crown in posterior regions of either maxilla or mandible replacing a missing premolar or molar (Table 1) were enrolled as participants in the present prospective clinical study. The age of patients ranged between 21 and 70, with a mean age of 45.6 (±14.3 y). All patients presented at the Department of Prosthodontics of the University "Federico II" of Naples (Italy) from October 2015 to March 2016 (baseline).

Table 1. Anatomical distribution of monolithic zirconia single crowns.

	Maxilla (*n*=10)		Mandible (*n*=40)	
	n	%	*n*	%
1st premolar	1	2%	9	18%
2nd premolar	4	8%	12	24%
1st molar	5	10%	19	38%

n = number of implant-supported restorations.

The patients received comprehensive explanations regarding the clinical protocol and signed written informed consent forms. Each patient was provided with only 1 ZrSC.

The patients were recruited according to the following inclusion criteria:

- age ≥18 years;
- good general health;
- ASA I (healthy) or ASA II (mild systemic disease) according to the American Society of Anesthesiologists (ASA);
- good oral hygiene;
- Angle class I occlusal relationship;
- no evident signs of occlusal parafunction and/or temporomandibular disorders;

- no pregnancy or lactation;
- smoking ≤10 cigarettes/day;
- Pocket Probing Depth ≤4 mm, no Bleeding on Probing, and Plaque Index ≤20%;
- single missing tooth, being a premolar or a molar in the maxilla or mandible, with a minimum post-extraction healing of 3 months;
- absence of infection at the implant site;
- adequate bone volume to place an implant (length 8.5-10 mm, diameter 4.1 mm, class I to III bone quality according to Lekholm and Zarb) [34];
- adequate prosthetic space to receive an anatomic restoration.

Conversely, patients fulfilling at least one of the following exclusion criteria were excluded from the study:

- general and medical contraindication for surgical procedures;
- poor oral hygiene;
- reduced prosthetic space at the edentulous site (≤5 mm);
- severe wear facets, clenching, and bruxism;
- heavy smokers (>10 cigarettes/day);
- severe or not controlled periodontal disease;
- poor compliance.

2.2 Surgical procedures

The surgical and prosthetic treatments were carried out at the Departments of Implant Surgery and Prosthodontics of the University "Federico II" of Naples. One experienced oral surgeon performed the surgical procedures and 2 skilled prosthodontists carried out the restorative treatments.

The patients presented an edentulous site with a single missing tooth for more than 3 months, showing sufficient bone volume to achieve implant primary stability. One hour before surgery, antibiotic prophylaxis (i.e., 1 gr amoxicillin or, if allergic to penicillin, 600 mg clindamycin) was given and a 0.2% chlorhexidine mouthwash for oral disinfection (twice a day for 10 days) was prescribed.

In the surgical session, a crestal incision was made under local anesthesia, followed by the preparation of a mucoperiosteal flap to expose the alveolar bone. Each patient received 1 endosseous dental implant (Outlink^2, Sweden&Martina; Padova, Italy) in the posterior regions. The implant diameter was 4.1 mm and length varied from 8.5 to 10 mm, dependent on available bone height at the implant site. A 2-stage surgical technique with submerged fixtures and no additional soft or hard tissue grafts was planned for all the patients. One week after implant placement, patients were recalled at the follow-up to remove sutures and control the healing process.

Three months after implant placement, osseointegration was verified clinically and radiographically; then, surgical re-entry was performed and a trans-mucosal healing abutment (Healing Abutment, Sweden&Martina; Padova, Italy) was screwed onto the fixture. This second surgical stage was performed by the same surgeon that placed the implants.

2.3 Prosthetic and laboratory procedures

Two weeks after surgical re-entry, a precision pick-up impression was made with the "open tray – pick-up technique" [35-37] using polyether materials (Impregum, 3M ESPE; Seefeld, Germany). The color of the final restorations was determined using a conventional shade scale (VITA Linearguide 3D-MASTER, VITA Zahnfabrik; Bad Sackingen, Germany).

All the prostheses were fabricated in a single dental laboratory. Master casts with implant analogs were poured and then digitized with a laboratory scanner (DScan 3, EGS S.R.L.; Bologna, Italy).

CAD/CAM titanium abutments (Titanium Abutment, Sweden&Martina; Padova, Italy) (Fig. 1) were selected and customized strictly following the manufacturer's instructions. Each titanium abutment was scanned and 50 monolithic ZrSCs were designed using a dedicated CAD software (Exocad DentalCAD, Exocad GmbH; Darmstadt, Germany). Then, the zirconia blocks (Katana Zirconia HT, Kuraray Noritake; Aichi, Japan), were milled with a 5-axis milling system (Plus Mill S5, Dental Plus; Gyeonggi, South Korea). Finally, each crown was polished manually without any veneering or glazing layer.

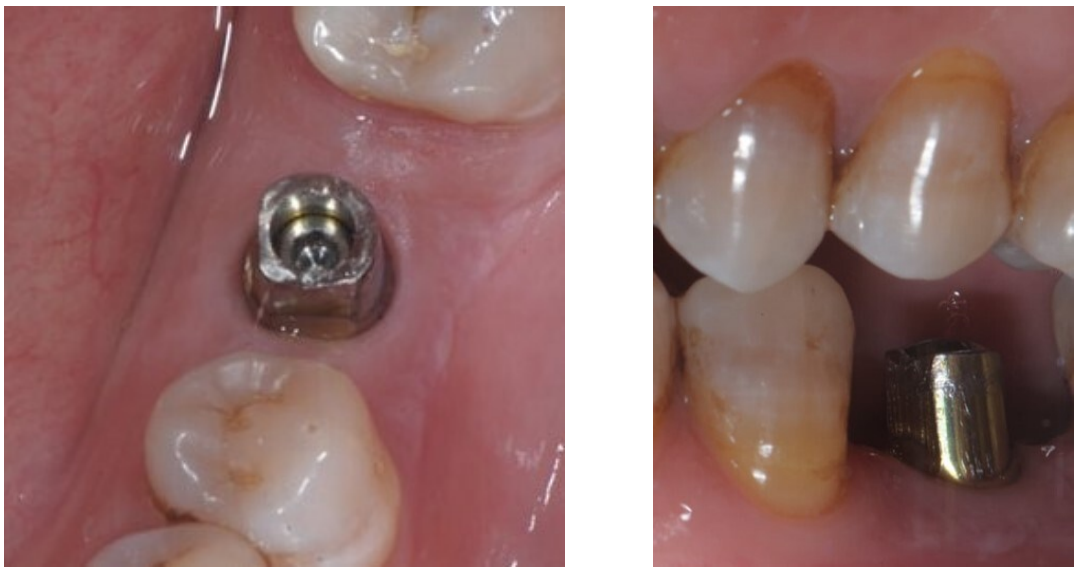

(**a**) (**b**)

Figure 1. Titanium implant abutment on the mandibular first molar area: (**a**) occlusal view; (**b**) buccal view.

2.4 Delivery of restorations

After a total healing time of 4 months, the titanium abutments were screwed onto the implants and torqued at 35 N/cm with a dynamometric wrench, according to the manufacturer's recommendations; screwing channels were protected and filled with polytetrafluoroethylene (PTFE) tape.

The internal surface of each ZrSC was sandblasted with 50 μm aluminum oxide (Al_2O_3) powder at 1 bar; then, the ZrSCs were cleaned with steam for 60 s. The monolithic ZrSCs were luted onto titanium abutments with a dual-curing resin cement (Panavia V5, Kuraray Noritake; Okayama, Japan); an MDP-containing ceramic primer (Ceramic Primer Plus, Kuraray Noritake; Okayama, Japan) was applied with a microbrush onto the intaglio surface of each ZrSC for 20 s and dried. The cement was dispensed into each restoration with an automating tip and the crowns were initially seated onto the titanium abutments with finger pressure; the excess cement was tack-cured with a curing light (Elipar™ S10, 3M ESPE; St. Paul, Minnesota, USA) for 5 s to reach a gel stage and then cleaned away with plastic tips and dental floss; the patients were asked to clench onto a wooden stick for 5 more minutes to ensure complete seating of the restorations. Finally, each surface was further light-cured for 10 s, according to the manufacturer's instructions. Postoperative radiographs were taken to detect possible cement remnants.

The occlusion was checked with 8 μm thick articulating foil (Shimstock foil, Bausch; Köln, Germany), to allow correct occlusal contacts, avoiding occlusal precontacts and interferences onto the restorations. If necessary, occlusal adjustments were made using fine-grit diamond burs; then, the adjusted surfaces were meticulously polished with a polishing system dedicated to zirconia

(Komet nos. 9425, 9426, and 9547; Brasseler; Savannah, Georgia, USA). Finally, scrupulous oral hygiene instructions were provided to all patients.

2.5 Baseline evaluations

Two experienced calibrated and trained clinicians made the baseline evaluations, that were recorded 7 days after cementation of the ZrSCs.

Furthermore, the static and dynamic occlusal contacts were carefully checked and adjusted if necessary, as previously described.

Standardized periapical radiographs and clinical photographs of the restorations were taken.

The evaluation of technical complications was performed following the modified USPHS criteria [38-40], classified on the basis of the clinical serviceability of the restorations (Table 2). The following parameters were evaluated: fracture behavior, decementation, anatomical form, and marginal adaptation.

Table 2. United States Public Health Service modified criteria for evaluation of restorations at 6-years follow-up.

USPHS criteria	Alpha	Bravo	Charlie	Delta
Fracture behavior	No fracture of zirconia	Fracture but polishing possible	Fracture but polishing not possible	New restoration is needed
Decementation	No decementation between crown and abutment	-	-	Decementation between crown and abutment
Anatomical form	Ideal Anatomical shape, good proximal contacts	Slightly over- or under-contoured, weak proximal contacts	Highly over- or under-contoured, open proximal contacts	New restoration is needed
Marginal adaptation	No probe catches	Slight probe catches but no gap	Gap with abutment exposure	New restoration is needed

The biological parameters were evaluated referring to modified Plaque Index (mPI), modified Sulcus Bleeding Index (mSBI), hypertrophy/hyperplasia of soft tissue, and peri-implantitis.

The mPI was scored from 0 to 3, as follows:

- 0 = no plaque and no inflammation;
- 1 = mild inflammation and a film of plaque adhering to free soft tissues margin which cannot be seen with the naked eye but only with probes;
- 2 = moderate inflammation with moderate glazing, redness, bleeding on probing and moderate accumulation of deposits within the soft tissue pocket and on the margin, which can be seen with the naked eye;

- 3 = abundance of soft matter within the soft tissue pocket, on the margin and/or on the restoration; severe inflammation with redness, hypertrophy, and tendency to spontaneous bleeding [41-44].
- The mSBI was scored from 0 to 3, as follows:
- 0 = no bleeding when a periodontal probe is passed along the peri-implant soft tissue;
- 1 = isolated bleeding spots visible;
- 2 = blood forms a confluent red line on the margin;
- 3 = heavy or profuse bleeding [41,44,45].

VASs were used to allow patients to rate the overall functional and aesthetic results of the restorations (0=scarce, 10=excellent).

2.6 Follow-up recalls

All the patients were recalled at follow-up after 6 months from the baseline and then yearly, for a total prospective observational period of 6 years. The baseline assessments were repeated, and their results were recorded, as previously described.

Furthermore, standardized periapical radiographs were made to evaluate possible marginal bone resorption at implant sites; moreover, clinical photographs of the restorations were taken to record peri-implant soft tissue morphology and conditions.

3. Results

After 6 years of clinical service, no patient was lost at follow-up or censored, consequently, all the restorations were available for follow-up examinations.

As to the technical problems, neither fractures nor decementations were observed (Fig. 2); as a consequence, both the survival and success rates were 100%, considering zirconia ceramic fractures and/or loss of retention as events.

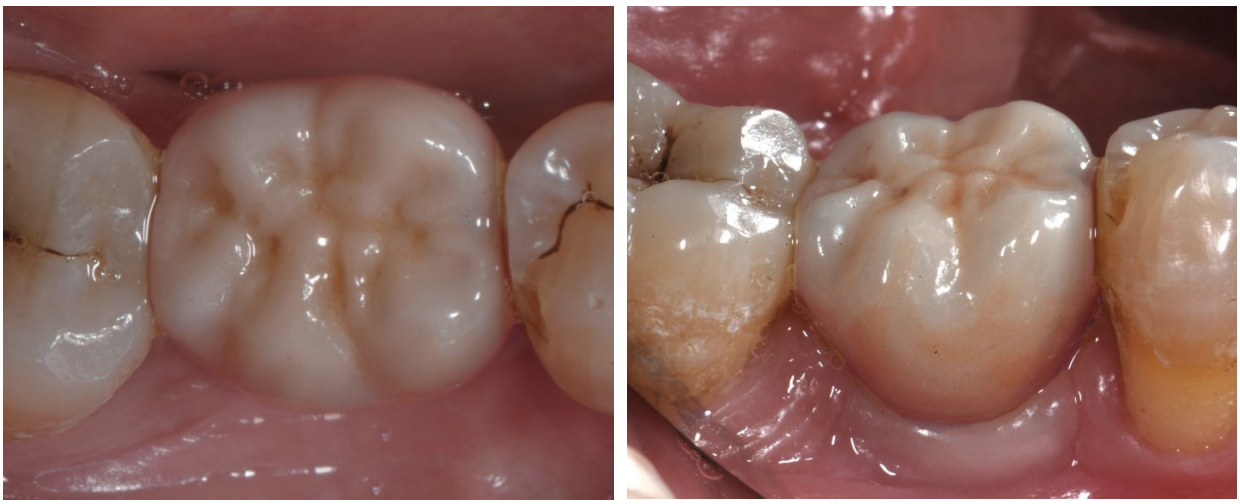

(**a**) (**b**)

Figure 2. Six-year recall evaluation. Healthy condition of monolithic zirconia single crown cemented onto titanium implant abutment: (**a**) occlusal view; (**b**) buccal view.

During the entire follow-up period, neither radiographic evidence nor signs and symptoms of peri-implant pathology nor marginal bone resorption were noticed.

The technical evaluation using the USPHS criteria showed very good clinical performances of the ZrSCs cemented onto titanium abutments. In terms of fracture behavior and decementation, all the ZrSCs rated Alpha. As regards anatomical form, 46 ZrSCs rated Alpha and 4 ZrSCs rated Bravo; differently, for the marginal adaptation, 47 ZrSCs rated Alpha and 3 ZrSCS rated Bravo.

According to the patients' VASs assessments, the overall function of the ZrSCs reported a mean value of 8.4 (±2.1), whereas the overall aesthetics rated an average value of 8.7 (±0.7). The statistical results of the VASs for gender, age, and jaw are reported in table 3.

Table 3. Statistical results for gender, age, and jaw with VASs.

Groups	VAS aesthetics score (mean)	VAS function score (mean)
Male (*n*=32)	8.9	8.7
Female (*n*=18)	8.2	7.9
21-40 years old (*n*=17)	8.6	8.4
41-70 years old (*n*=33)	8.8	8.4
Maxilla (*n*=10)	8.3	8.0
Mandible (*n*=40)	8.8	8.5

n = number of implant-supported restorations.

As regards mPI and mSBI, the score 0 was rated by 32 and 31 ZrSCs, the score 1 was rated by 16 and 17 ZrSCs, the score 2 was rated by 2 and 0 ZrSCs, the score 3 by 0 and 2 ZrSCs respectively.

No peri-implantitis or hypertrophy/hyperplasia of soft tissues was detected.

4. Discussion

Among the ideal retention systems, some authors prefer the use of cement-retained prostheses, while others suggest screw-retained restorations [3-6]. On one hand, the main advantages of cement-retained prostheses are passive fit, good biomechanical stability, absence of screw access holes, better occlusal design, and adaptation for implant prosthetic malposition. Moreover, the cement layer can compensate for dimensional discrepancies between restoration and abutment and work as a shock absorber [4,6,7]. Nevertheless, a cement excess not removed may increase the risk of peri-implantitis [9], peri-implant mucositis [9,10], and marginal bone loss [11,12]. On the other hand, screw-retained prosthesis allows easier retrievability [6,13] and is preferable for limited interocclusal space, but is prone to technical complications, like components/restoration fractures and screw loosening [14-16].

In the present study, the clinical performance of cement-retained implant-supported restorations was analyzed. Such restorative solutions offer passive fit of crowns, absence of screw access holes, easier control of occlusion, and compensation of possible implant-prosthetic malposition [4]. The restorative system made up of monolithic ZrSCs cemented onto titanium abutments with a dual-curing resin cement reported survival and success rates of 100% at 6 years, considering the loss of retention and/or fractures of zirconia as events for the cumulative survival, and excellent scores according to the USPHS criteria. Particularly, the parameters “fracture behavior” and “decementation” scored Alpha in 100% of restorations; this means that, in the medium-term of clinical service, neither fractures of the ZrSCs nor decementation between zirconia crowns and titanium abutments were observed. According to such evidence, it can be concluded that the use of dual-curing MDP-containing resin cements is a reliable choice for the cementation of zirconia monolithic crowns onto titanium abutments as well as a viable clinical option to strengthen the restorative complex. This statement is in accordance with a previous investigation where MDP monomer showed the ability to increase the bond strength between zirconia and resin-based luting agents [33].

Moreover, for a whole observation period of 6 years, no hypertrophy/hyperplasia of soft tissue or peri-implantitis was detected, indicating a complete absence of inflammation in the peri-implant tissues surrounding the ZrSCs; such occurrence confirmed the outstanding biocompatibility of

zirconia, particularly in its monolithic configuration, and the optimal mechanical coupling and biological integration of zirconia/titanium restorative complex.

As regards the parameter “anatomical form”, 46 ZrSCs rated Alpha, meaning that ideal anatomical shape and proximal contacts were achieved. Differently, 4 ZrSCs rated Bravo, because of the modifications of buccal peri-implant soft tissues over time resulting in slightly over- or under-contoured restorations; this occurrence could be due to a less than ideal position of fixtures in buccal-lingual direction and/or thin peri-implant biotype [46]. Furthermore, Bravo scores for "anatomical form" were also reported because of weak proximal contacts; such phenomenon is not uncommon in posterior implant-supported prostheses and should be considered a minor complication related to different associated factors, such as the anatomical position of restorations, lower alveolar bone support level and time since delivery of prosthesis [47,48].

As to “marginal adaptation", 47 ZrSCs rated Alpha, indicating excellent marginal precision, while the remaining 3 ZrSCs rated Bravo with slight probe catch but no gap between crown and abutment. Considering the optimal mechanical coupling between implant necks and milled restorations thanks to the well-known reliability of CAD/CAM technologies, it could be speculated that such occurrence was due to patients' relaxation during cementation clenching or to premature cement excess cleaning before complete gelification, resulting in voids at the prosthetic margin.

Regarding the periodontal parameters, mPI and mSBI reported respectively 32 and 31 the score 0, 16 and 17 the score 1, 2 and 0 the score 2, 0 and 2 the score 3, showing extremely satisfactory biological integration of the restorations. Particularly, these results indicated the absence of bleeding, plaque, and inflammation for at least 31 restorations, whereas a single discreet bleeding point or mild inflammation was reported for at least 16 ZrSCs. Furthermore, moderate inflammation was observed in 2 restorations and in 2 more the interdental spaces were filled with blood shortly after probing; this evidence was noticed in smokers and patients with less satisfactory compliance to supportive periodontal care and oral hygiene prescriptions. The findings of the present investigation are in agreement with those of other studies and confirm the excellent biological response of peri-implant soft tissues to zirconia restorations and the outstanding biocompatibility of this material, particularly in its polished monolithic configuration [40,49-53].

According to VASs scores of the overall function (8.4 ± 2.1) and aesthetics (8.7 ± 0.7), ZrSCs were considered fully satisfactory to restore proper chewing activity and to achieve a natural tooth-like appearance of the restorations.

The results of the present prospective clinical study were very promising, probably due to an extremely careful selection of the patients’ cohort. In any case, the investigation presented some limitations, namely an observational period limited to the medium-term and no randomization of participants. Moreover, the antagonist tooth and its restorative material were not variables taken

into consideration in the present study. Besides, the 100% success result might be explained by the limited sample size (n=50), the favorable implant diameter used (4.1 mm), and the retentive abutment height (> 2mm). Further RCTs with a wider sample population and longer observational periods will be essential to validate long-term serviceability, biomechanical effectiveness, and biological and aesthetical outcomes of the restorative system evaluated in the present clinical investigation.

5. Conclusions

Within the limitations of the present prospective clinical study, the restorative system based on the use of titanium abutments and monolithic zirconia single crowns, cemented with an MDP-based cement proved to be a viable clinical option to restore posterior missing teeth in the medium term and the following conclusions may be drawn:

- The tested restorative system is highly effective and reliable to restore occlusal function, showing 100% survival and success rates;
- Neither fracture nor loss of retention was noticed;
- The most frequent technical complications were minor marginal misfit and weak proximal contacts but none of them impaired function;
- The tested restorative system was highly biocompatible, as showed by the stability and optimal health status of surrounding peri-implant tissues;
- Patients reported being very satisfied by the overall function and aesthetics.

References

1. Pjetursson, B.E.; Thoma, D.; Jung, R.; Zwahlen, M.; Zembic, A. A systematic review of the survival and complication rates of implant-supported fixed dental prostheses (FDPs) after a mean observation period of at least 5 years. *Clin Oral Implants Res* **2012** *23*, 22-38.

2. Schwarz, S.; Schroder, C.; Corcodel, N.; Hassel, A.J.; Rammelsberg, P. Retrospective comparison of semipermanent and permanent cementation of implant-supported single crowns and FDPs with regard to the incidence of survival and complications. *Clin Implant Dent Relat Res* **2012,** *14*, e151-8.

3. Lee, A.; Okayasu, K.; Wang, H.L. Screw- versus cement-retained implant restorations: current concepts. *Implant Dent* **2010**, *19*, 8-15.

4. Nissan, J.; Narobai, D.; Gross, O.; Ghelfan, O.; Chaushu, G. Long-term outcome of cemented versus screw-retained implant-supported partial restorations. *Int J Oral Maxillofac Implants* **2011**, *26*, 1102-1107.

5. Kraus, R.D.; Epprecht, A.; Hämmerle, C.H.F.; Sailer, I.; Thoma, D.S. Cemented vs screw-retained zirconia-based single implant reconstructions: A 3-year prospective randomized controlled clinical trial. *Clin Implant Dent Relat Res* **2019**, *21*, 578-585.

6. Wittneben, J.G.; Joda, T.; Weber, H.P.; Brägger, U. Screw retained vs. cement retained implant-supported fixed dental prosthesis. *Periodontol 2000* **2017**, *73*, 141-151.

7. Zarone, F.; Sorrentino, R.; Traini, T.; Di lorio, D.; Caputi, S. Fracture resistance of implant-supported screw- versus cement-retained porcelain fused to metal single crowns: SEM fractographic analysis. *Dent Mater* **2007**, *23*, 296-301.

8. Linkevicius, T.; Vindasiute, E.; Puisys, A.; Linkeviciene, L.; Maslova, N.; Puriene, A. The influence of the cementation margin position on the amount of undetected cement. A prospective clinical study. *Clin Oral Implants Res* **2013**, *24*, 71-76.

9. Gapski, R.; Neugeboren, N.; Pomeranz, A.Z.; Reissner, M.W. Endosseous implant failure influenced by crown cementation: a clinical case report. *Int J Oral Maxillofac Implants* **2008**, *23*, 943-946.

10. Wasiluk, G.; Chomik, E.; Gehrke, P.; Pietruska, M.; Skurska, A.; Pietruski, J. Incidence of undetected cement on CAD/CAM monolithic zirconia crowns and customized CAD/CAM implant abutments. A prospective case series. *Clin Oral Implants Res* **2017**, 28, 774-778.

11. Wittneben, J.G.; Millen, C.; Bragger, U. Clinical performance of screw-versus cement-retained fixed implant-supported reconstructions - a systematic review. *Int J Oral Maxillofac Implants* **2014**, *29*, 84-98.

12. Hamed, M.T.; Abdullah, M.H.; Khalid, A.S.; Hossam, H.A.B.; Hussein, N.G. A Systematic Review of Screw versus Cement-Retained Fixed Implant Supported Reconstructions. *Clin Cosmet Investig Dent* **2020**, *12*, 9-16.

13. Shadid, R.; Sadaqa, N. A comparison between screw- and cement-retained implant prostheses. A literature review. *J Oral Implantol* **2012**, *38*, 298-307.

14. Sailer, I.; Mühlemann, S.; Zwahlen, M.; Hämmerle, C.H.; Schneider, D. Cemented and screw-retained implant reconstructions: a systematic review of the survival and complication rates. *Clin Oral Implants Res* **2012**, *23*, 163-201.

15. Chee, W.; Jivraj, S. Screw versus cemented implant supported restorations. *Br Dent J* **2006**, *201*, 501-507.

16. Michalakis, K.X.; Hirayama, H.; Garefis, P.D. Cement-retained versus screw-retained implant restorations: a critical review. *Int J Oral Maxillofac Implants* **2003**, 18, 719-728.

17. Steinebrunner, L.; Wolfart, S.; Bössmann, K.; Kern, M. In vitro evaluation of bacterial leakage along the implant-abutment interface of different implant systems. *Int J Oral Maxillofac Implants* **2005**, *20*, 875-881.

18. Kurbad, A.; Kurbad, S. CAD/CAM-based implant abutments. *Int J Comput Dent* **2013**, *16*, 125-141.

19. Apicella, D.; Veltri, M.; Balleri, P.; Apicella, A.; Ferrari M. Influence of abutment material on the fracture strength and failure modes of abutment-fixture assemblies when loaded in a bio-faithful simulation. *Clin Oral Implants Res* **2011**, *22*, 182-188.

20. Fabbri, G.; Fradeani, M.; Dellificorelli, G.; De Lorenzi, M.; Zarone, F.; Sorrentino, R. Clinical Evaluation of the Influence of Connection Type and Restoration Height on the Reliability of Zirconia Abutments: A Retrospective Study on 965 Abutments with a Mean 6-Year Follow-Up. *Int J Periodontics Restorative Dent* **2017**, *37*, 19-31.

21. Pjetursson, B.E.; Zarauz, C.; Strasding, M.; Sailer, I.; Zwahlen, M.; Zembic, A. A systematic review of the influence of the implant-abutment connection on the clinical outcomes of ceramic and metal implant abutments supporting fixed implant reconstructions. *Clin Oral Implants Res* **2018**, *29*, 160-183.

22. Ferrari, M.; Tricarico, M.G.; Cagidiaco, M.C.; Vichi, A.; Gherlone, E.F.; Zarone, F.; Sorrentino, R. 3-Year Randomized Controlled Prospective Clinical Trial on Different CAD-CAM Implant Abutments. *Clin Implant Dent Relat Res* **2016**, *18*, 1134-1141.

23. Zarone, F.; Russo, S.; Sorrentino, R. From porcelain-fused-to-metal to zirconia. Clinical and experimental considerations. *Dent Mater* **2011**, *27*, 83-96.

24. Alsarani, M.; Souza, G.; Rizkalla, A.; El-Mowafy, O. Influence of crown design and material on chipping-resistance of all-ceramic molar crowns: An in vitro study. *Dent Med Probl* **2018**, *55*, 35-42.

25. Poggio, C.E.; Ercoli, C.; Rispoli, L.; Maiorana, C.; Esposito, M. Metal-free materials for fixed prosthodontic restorations. *Cochrane Database Syst Rev* **2017**, *12*, CD009606.

26. Anusavice, K.J. Standardizing failure, success, and survival decisions in clinical studies of ceramic and metal-ceramic fixed dental prostheses. *Dent Mater* **2012**, *28*, 102-111.

27. Sadowsky, S.J. Has zirconia made a material difference in implant prosthodontics? A review. *Dent Mater* **2020**, *36*, 1-8.

28. Sorrentino, R.; Triulzio, C.; Tricarico, M.G.; Bonadeo, G.; Gherlone, E.F.; Ferrari, M. In vitro analysis of the fracture resistance of CAD-CAM monolithic zirconia molar crowns with different occlusal thickness. *J Mech Behav Biomed Mater* **2016**, *61*, 328-333.

29. Seydler, B.; Schmitter, M. Clinical performance of two different CAD/CAM- fabricated ceramic crowns: 2-year results. *J Prosthet Dent* **2015**, *114*, 212-216.

30. Patzelt, S.B.; Spies, B.C.; Kohal, R.J. CAD/CAM-fabricated implant-supported restorations: a systematic review. *Clin Oral Implants Res* **2015**, *26*, 77-85.

31. Blatz, M.B.; Alvarez, M.; Sawyer, K.; Brindis, M. How to Bond Zirconia. The APC Concept. *Compend Contin Educ Dent* **2016**, *37*, 611-618.

32. Qeblawi, D.M.; Muñoz, C.A.; Brewer, J.D.; Monaco, E.A.J. The effect of zirconia surface treatment on flexural strength and shear bond strength to a resin cement. *J Prosthet Dent* **2010**, *103*, 210-220.

33. Koizumi, H.; Nakayama, D.; Komine, F.; Blatz, M.B.; Matsumura, H. Bonding of resin-based luting cements to zirconia with and without the use of ceramic priming agents. *J Adhes Dent* **2012**, *14*, 385-392.

34. Lekholm, U.; Zarb, G.A. Patient selection and preparation. In *Tissue integrated prostheses: osseointegration in clinical dentistry*, 1st ed.; Branemark, P.I., Zarb, G.A., Albrektsson, T., Eds.; Quintessence Publishing Company: Chicago, USA, 1985; pp. 199-209.

35. Sorrentino, R.; Gherlone, E.F.; Calesini, G.; Zarone, F. Effect of implant angulation, connection length, and impression material on the dimensional accuracy of implant impressions: an in vitro comparative study. *Clin Implant Dent Relat Res* **2010**, *12*, e63-e76.

36. Moreira, A.H.; Rodrigues, N.F.; Pinho, A.C.; Fonseca, J.C.; Vilaca, J.L. Accuracy Comparison of Implant Impression Techniques: A Systematic Review. *Clin Implant Dent Relat Res* **2015**, *17*, e751-e764.

37. Calesini, G.; Zarone, F.; Sorrentino, R.; Micarelli, C.; Fabianelli, A.; Papacchini, F.; Gherlone, E. Effect of 2 impression techniques on the dimensional accuracy of working implant prosthesis models: an in vitro study. *J Craniofac Surg* **2014**, *25*, 822-827.

38. Bayne, S.C.; Schmalz, G. Reprinting the classic article on USPHS evaluation methods for measuring the clinical research performance of restorative materials. *Clin Oral Investig* **2005**, *9*, 209-214.

39. Pol, C.W.P.; Raghoebar, G.M.; Maragkou, Z.; Cune, M.S.; Meijer, H.J.A. Full-zirconia single-tooth molar implant-supported restorations with angulated screw channel abutments: A 1-year prospective case series study. *Clin Implant Dent Relat Res* **2020**, *22*, 138-144.

40. Sorrentino, R.; De Simone, G.; Tetè, S.; Russo, S.; Zarone, F. Five-year prospective clinical study of posterior three-unit zirconia-based fixed dental prostheses. *Clin Oral Investig* **2012**, *16*, 977-985.

41. Mombelli, A.; van Oosten, M.A.; Schurch, E.J.; Land, N.P. The microbiota associated with successful or failing osseointegrated titanium implants. *Oral Microbiol Immunol* **1987**, *2*, 145-151.

42. Bradley, H.; Owen, B.; Keys, W. Zirconia implants: a promising alternative to titanium?. *Evid Based Dent* **2021**, *22*, 102-103.

43. Curiel-Aguilera, F.P.; Griffiths, G.R.; Rossmann, J.A.; Gonzalez, J.A. Titanium versus zirconia complete-arch implant-supported fixed prostheses: A comparison of plaque accumulation. *J Prosthet Dent* **2021**, S0022-3913(21)00585-0. https://doi.org/10.1016/j.prosdent.2021.10.012.

44. Farrag, K.M.; Khamis, M.M. Effect of anodized titanium abutment collars on peri-implant soft tissue: A split-mouth clinical study. *J Prosthet Dent* **2021**, S0022-3913(21)00518-7. https://doi.org/10.1016/j.prosdent.2021.09.019.

45. Newbrun, E. Indices to measure gingival bleeding. *J Periodontol* **1996**, *67*, 555-561.

46. Ferrari, M.; Cagidiaco, M.C.; Garcia-Godoy, F.; Goracci, C.; Cairo, F. Effect of different prosthetic abutments on peri-implant soft tissue. A randomized controlled clinical trial. *Am J Dent* **2015**, *28*, 85-89.

47. Wong, A.T.; Wat, P.Y.; Pow, E.H.; Leung, K.C. Proximal contact loss between implant-supported prostheses and adjacent natural teeth: a retrospective study. *Clin Oral Implants Res* **2015**, *26*, e68-e71.

48. Pang, N.S.; Suh, C.S.; Kim, K.D.; Park, W.; Jung, B.Y. Prevalence of proximal contact loss between implant-supported fixed prostheses and adjacent natural teeth and its associated factors: a 7-year prospective study. *Clin Oral Implants Res* **2017**, *28*, 1501-1508.

49. Sailer, I.; Gottnerb, J.; Kanelb, S.; Hammerle, C.H. Randomized controlled clinical trial of zirconia-ceramic and metal-ceramic posterior fixed dental prostheses: a 3-year follow-up. *Int J Prosthodont* **2009**, *22*, 553-560.

50. Sorrentino, R.; Galasso, L.; Tetè, S.; De Simone, G.; Zarone, F. Clinical evaluation of 209 all-ceramic single crowns cemented on natural and implant-supported abutments with different luting agents: a 6-year retrospective study. *Clin Implant Dent Relat Res* **2012**, *14*, 184-197.

51. Zarone, F.; Di Mauro, M.I.; Ausiello, P.; Ruggiero, G.; Sorrentino, R. Current status on lithium disilicate and zirconia: a narrative review. *BMC Oral Health* **2019**, *19*, 134.

52. da Cruz, M.B.; Marques, J.F.; Fernandes, B.F.; Madeira, S.; Carvalho, Ó.; Silva, F.S.; da Mata, A.D.S.P.; Caramês, J.M.M. Peri-implant cell response on groove and pore-textured zirconia surfaces. *J Oral Biosci* **2022**, *64*, 100-107.

53. Zarone, F.; Ruggiero, G.; Leone, R.; Breschi, L.; Leuci, S.; Sorrentino, R. Zirconia-reinforced lithium silicate (ZLS) mechanical and biological properties: A literature review. *J Dent* **2021**, *109*, 103661.

4.6 A REVIEW ON RISK MANAGEMENT OF CORONAVIRUS DISEASE 19 (COVID-19) INFECTION IN DENTAL PRACTICE: FOCUS ON PROSTHODONTICS AND ALL-CERAMIC MATERIALS

Sorrentino, R.; Basilicata, M.; Ruggiero, G.; Mauro, M.I.D.; Leone, R.; Bollero, P.; Zarone, F
Prosthesis 2022, 4, x.

Regarding digital technologies and optical impressions, a significant advantage is the possibility to autoclave the latest-generation scanners' tips, and proper disinfectant commercial products can be used for other scanner items and scanning devices (i.e., implant-supported scan-bodies) to reduce the risk of cross-contamination, according to manufacturers' suggestions [1-2]. Moreover, intraoral scanner systems provide the advantage of avoiding the transfer of a conventional impression and therefore the risk of contagion to the laboratory via the physical impression or the gypsum cast.

Besides, digital technologies are also useful during the present pandemic for prosthetic planning and the manufacturing of removable or fixed prostheses. Indeed, compared to conventional procedures, the digital workflow allows the fabrication of reliable prostheses in fewer appointments and with quicker chairside times [3].

References

1. Barenghi, L.; Barenghi, A.; Cadeo, C.; Di Blasio, A. Innovation by Computer-Aided Design/Computer-Aided Manufacturing technology: A look at infection prevention in dental settings. *Biomed. Res. Int.* **2019**, *2019*, 6092018.

2. Punj, A.; Bompolaki, D.; Garaicoa, J. Dental impression materials and techniques. *Dent. Clin. North Am.* **2017**, *61*, 779–796.

3. Markarian, R.A.; da Silva, R.L.B.; Burgoa, S.; Pinhata-Baptista, O.H.; No-Cortes, J.; Cortes, A.R.G. Clinical relevance of Digital Dentistry during COVID-19 outbreak: A scoped review. *Braz. J. Oral Sci.* **2020**, *19*, e200201.

5. CONCLUSIONS

Digital technologies could improve the quality of prosthetic rehabilitations, enrich patient-clinician and interprofessional communications, enhance education, and implement practice management. The interaction among computer design, additive/subtractive manufacturing, materials science, and biology will undoubtedly contribute to designing the future as the boundaries between the physical, digital, and biological scenarios become more open. There are more restorative solutions available, increasing durability and improving the aesthetics of the restorations.

Furthermore, digital technologies can be of great social use, due to the possibility of reducing costs and working times, as in the case of the world's elderly population, which is on the rise. At the same time, they can be an efficient tool for planning and fabricating prosthetics for patients with jaws defects. We are witnessing actual paradigm shifts in prosthodontics, such as the variation of preparation thicknesses and materials, cementation procedures, as well as the manufacturing that these innovative materials require.

Also, the introduction of new generations of particle-filled high-strength ceramics and the development of novel production techniques have resulted in a significant shift in the operating paradigm in favor of minimally invasive restoration techniques. The innovative ceramics' physical-chemical characteristics enable a significant reduction in restorative thickness while still ensuring good aesthetic and therapeutic outcomes.

To date, it may be right to discuss about digital-linked materials, as the word "linked", in addition to being a synonym of "associated" or "related" (in this case to digital technologies), is also a word heavily used in IT-digital jargon, in fact just think of the concept of "Link". And it is precisely on this concept of "Link" as a string to which always only one web address is associated that we should dwell. In fact, similarly to the web string, with the pun "digital-linked", in clinical dental practice, these materials are generally considered "linked" only to digital technologies, perhaps due to the strong commercial drive. It is fair to remember that materials such as lithium disilicate or zirconia-reinforced lithium silicate can be processed also through "heat-pressed" procedures which, in addition to guaranteeing high clinical efficacy, sometimes have enhanced mechanical characteristics compared to the CAD-CAM versions of the same.

However, in order to achieve a predictable restorative success, the selection of the appropriate materials and workflow is a crucial step in the decision-making process of every prosthetic

project. Therefore, proper knowledge of the mechanical and aesthetic characteristics, indications, and limitations of the materials is required.

It is also reasonable to predict that the current technology will quickly become obsolete and be replaced by even more cutting-edge systems and applications, given the very dynamic nature of digital dentistry. To accurately comprehend the possible future evolution of digital dentistry in the next decades, it will be important to continuously update both the clinical tools and procedures as well as the experimental and clinical scientific data.

ACKNOWLEDGMENTS

This journey has been hard and intense. Among the many people who have supported me, some have been indispensable. My warmest thanks go to them.

To Prof. Fernando Zarone. My Lighthouse, my Role Model. No words will ever be able to describe his immense scientific knowledge, but if gratitude is the feeling of the day before, then I will be grateful to him for my life because he believed in me. All are teachers, few teach, He inspires.

To Prof. Roberto Sorrentino who made this work possible. His guidance and advice carried me through each phase of developing my projects. A man of few words but of great deeds. He is a "beautiful mind" that I've had the honor of living with all this time.

To my mom Katia and my dad Salvatore, for their continuous support and pure love. To you who give me strength in the most difficult moments. Your prayer is what has sustained me this far. Please don't forget that I am still the child that you raised.

To Roberta for her sweetness and clean soul. You are genuine, fair, and loyal. Above all, you understood. My life with you is colorful.

To those who have been on my side. Always.

To my granny, who cuddles my brightest star in the sky.